DEPARTMENT OF CHEMICAL ENGINEERING

UNIVERSITY OF CAPE TOWN

SYNTHESIS, CHARACTERISATION AND CATALYTIC TESTING OF PILLARED CLAYS AND LANTHANUM EXCHANGED ZSM-5 FOR HYDROCARBON CONVERSION

RADLEIGH HARTFORD

1989

SYNTHESIS, CHARACTERISATION AND CATALYTIC TESTING OF PILLARED CLAYS AND LANTHANUM EXCHANGED ZSM-5 FOR HYDROCARBON CONVERSION

Submitted to the University of Cape Town
in fulfilment of the requirements for the degree of
Master of Science (Chemical Engineering)

by

Radleigh Hartford

Department of Chemical Engineering,
University of Cape Town,
Rondebosch, Cape,
South Africa.

October 1989

ACKNOWLEDGEMENT

I would like to thank my supervisors, Prof. Cyril O'Connor and Prof. Masami Kojima, for their assistance throughout the course of this work.

To Bo Anderson, Stephan Schwartz and Alex Vogel for their friendship and good humour, Ta.

SYNOPSIS

Pillared clays present interesting possibilities for use as acid catalysts. The present research investigated the effect that pillaring has on the physical and catalytic properties of some smectite clays. The effect of using a hydroxy-Al solution to pillar a predominantly octahedrally substituted clay (montmorillonite) and a tetrahedrally substituted clay (beidellite) were compared. The effects of pillaring tetrahedrally substituted clays with different swellable properties (beidellite, SMM, and Ni-SMM) were investigated. In an attempt to enhance the acidic properties of the pillars, montmorillonite was pillared with a hydroxy-Al solution containing tetraethyl orthosilicate. Montmorillonite was also pillared with a hydroxy-Ni/Al solution in an effort to produce a clay with an increased pillar density. The pillared and unpillared clays were characterised using x-ray diffraction, surface area measurements, thermogravimetric analysis and ammonia TPD. The possible shape selective properties of the different clays for the conversion of trimethylbenzene were investigated, and the catalytic activities and product selectivities of these clays for high pressure propene oligomerisation were studied.

It was found that treating montmorillonite with a hydroxy-Al solution resulted in the generation of an extensive expanded-layer structure which significantly increased the surface area, pore volume and the number of accessible acid sites on the clay. The addition of tetraethyl orthosilicate to the hydroxy-Al solution prior to pillaring did not increase the acidity of the pillared clay significantly. No conclusion is drawn from the results of this study as to whether the incorporation of nickel into the aluminium pillaring species increases the pillar density in pillared montmorillonite.

Treating beidellite with the hydroxy-Al solution resulted in the generation of a less extensive pillared structure in the clay than in montmorillonite, as indicated by the results of surface area and pore volume measurements.

Contacting SMM with the Al pillaring solution generated an expanded-layer structure in the swellable phase of the clay. The surface area, pore volume and the number of accessible acid sites increased

significantly on pillaring. It is proposed that treating the Ni-SMM clays used for this work with the pillaring solution induces layer delamination, and generates an expanded-layer structure to a more limited extent than is the case in SMM. The pore volume and the number of accessible acid sites on these clays increased noticeably on treatment with the pillaring solution. These increases are attributed primarily to the proposed delamination process.

Unpillared montmorillonite and beidellite showed very limited activity for propene oligomerisation. Pillaring resulted in significant increases in the activities of both these clays. The propene oligomerisation activities of pillared montmorillonite and pillared beidellite were very similar. Catalyst deactivation occurred rapidly and is ascribed to hydrocarbon occlusion and subsequent coke formation in the microporous pillared structures.

Treating the SMM and Ni-SMM clays with the hydroxy-Al solution resulted in noticeable increases in propene oligomerisation activity. It is proposed that these increases do not arise solely due to the generation of microporous pillared structures in these clays, but may be a result of changes in layer morphology, such as layer delamination, induced by contact with the pillaring solution. The product selectivities of the SMM and Ni-SMM clays, in terms of carbon number distribution, do not change after treatment with the pillaring solution.

The microporous structures present in Al pillared clays are less effective in catalysing the oligomerisation of propene than exposed layer edges and faces in H^+ exchanged smectite minerals.

The results of this study suggest that it is unlikely that shape selectivity plays a role in the reaction of trimethylbenzene over pillared clays.

In a recent Mobil patent describing a method for converting olefins into gasoline and distillate using ZSM-5 (MOGD process), reference is made to a rare earth exchanged ZSM-5 catalyst. One possible reason for the incorporation of rare earth ions into MOGD catalysts could be the ability of such ions to crack heavy coke precursors at relatively low temperatures, thereby extending the life of the catalyst. Part of this

project involved an investigation into the effect of lanthanum exchange on H ZSM-5.

Trivalent lanthanum cations were partially exchanged with the acidic protons of H ZSM-5. Ammonia TPD indicated that La exchange reduces the number of strong acid sites and increases the number of weak acid sites on the catalyst, suggesting that La ions (or ionic complexes) function as weak acid sites. Hexane adsorption indicated that La exchange does not reduce the effective free pore volume of the catalyst, nor does it increase steric hindrances for the passage of linear molecules through the pores of the catalyst. The activity of the catalyst during propene oligomerisation and hexane cracking decreased with increasing lanthanum content as did selectivity towards heavier products in the former reaction. The rate of catalyst deactivation during the oligomerisation reaction was not reduced by the presence of lanthanum.

INDEX

LIST OF FIGURES

LIST OF TABLES

1 INTRODUCTION

In South Africa the oil from coal industry has developed the first commercial process whereby synthetic fuels are produced from coal via gasification using Fischer Tropsch catalysts. It started in 1943 when the American rights to the Fischer Tropsch process were purchased by South Africa. In 1950 the South African Oil, Coal and Gas corporation (SASOL) was formed. The first plant, Sasol I, went into operation in 1954. It used two types of reactors, namely, the Arge fixed bed and synthol fluidised bed reactors. Two further plants, Sasol II and Sasol III, which are enlarged and improved versions of Sasol 1, were built later. Due to the nature of the process, Sasol produces large quantities of light hydrocarbon gases. These are partly reticulated to local industry and partly converted, via a catalytic oligomerisation process, to liquid fuels, thereby increasing the overall production in terms of barrels of liquid fuel produced per ton of coal processed. Currently, Sasol I can more than satisfy the local demand for hydrocarbon gases. The light hydrocarbons produced by Sasol II and III therefore represent excess supply.

The catalytic oligomerisation process referred to above uses a conventional phosphoric acid catalyst to oligomerise the light hydrocarbons to liquid fuels. This process, however, produces poor quality petrol and diesel.

The work presented here forms part of an ongoing research project into the use of novel acid catalysts for the oligomerisation of olefins. Catalysts which have been extensively investigated by this research group for use in olefin oligomerisation reactions include ZSM-5, zeolite Y, mordenite, nickel-oxide silica alumina catalysts, and some synthetic clays (SMM, Ni-SMM).

A novel group of aluminosilicates, namely, pillared clays, present interesting possibilities for use as acid catalysts. Although the concept of pillaring clays is, itself, not new, it was not until fairly recently that the synthesis of pillared clays with hydrothermal stablility at temperatures in excess of ca. 500°C has been reported (Vaughan and Lussier, 1980). A major part of the work presented in this

study involves the synthesis and characterisation of some pillared clays, and an investigation into the suitability of these materials for use as olefin oligomerisation catalysts.

Since first being synthesised in the early seventies, ZSM-5 has been used in a number of industrial processes. The catalyst has been found to be particularly suitable for converting light olefins to gasoline and distillate (Garwood et al., 1983; Tabak et al., 1986). In a recent Mobil patent (Owen et al., 1986) describing a method for converting olefins to gasoline and distillate using ZSM-5 (MOGD process), reference is made to a rare-earth exchanged ZSM-5 catalyst. The present study investigates how ion-exchanged lanthanum affects the catalytic activity of H ZSM-5, with particular reference to propene oligomerisation.

1.1 PILLARED CLAYS

1.1.1 Smectite Minerals

1.1.1.1 Structure

Smectite clay minerals are hydrous layer silicates of the so-called phylosilicate family, in which the extremely stable SiO_4 tetrahedral structural unit has polymerised to form two-dimensional sheets. This occurs through the sharing of three of the oxygens at the corners of the tetrahedra. The oxygens, which can be imagined to be at the base of an equilateral triangle, form a repeating pattern of regular hexagons. The honeycomb pattern has the appearence of a graphite sheet, but with O-Si-O links instead of C-C. Each tetrahedron has a spare O, unshared in the sheet. These apical oxygens point normally away from the tetrahedral SiO sheet and are linked to the other main structural unit in the crystal.

This unit is an octahedral sheet formed from oxygen and metal ions. Most often the latter are Al (clay minerals are loosely described as aluminosilicates) or Mg. Like tetrahedra, octahedra can also polymerise in 2 dimensions, in this case by the sharing of four oxygens. This leaves two unshared O atoms, one of which points at right angles above and the other similarly below the sheet and gives a negative charge of two to be satisfied by the metal cation. This is why trivalent aluminium occupies only two thirds of the available octahedral "holes" in the structure (and forms dioctahedral minerals) whereas divalent cations, such as Mg, have to occupy them all (to give trioctahedral minerals). Other metals may also be found in the octahedral sites: both Fe^{2+} and Fe^{3+} are commonly found in naturally occurring clays, but other appropriately sized cations such as Ni, Ti, V, Mn, Li, Cu, and Zn are present in individual minerals.

The tetrahedral sheet of polymerised SiO_4 units and the octahedral sheet (whether dioctahedral or trioctahedral) are the basic building blocks of most clay minerals. It turns out to be geometrically possible for oxygens to be shared between the two types of sheet lying one on top of the other. The oxygens involved are the apical from the tetrahedral sheet and those unshared octahedral ions normal to the octahedral sheet.

The result is that the O of the Si-O becomes the O of the Al-OH, producing the link Si-O-Al, as shown in Figure 1.1. The octahedral sheet has spare oxygens both above it and below it, and is thus able to bond to another tetrahedral layer in the same way. It can be seen from Figure 1.1 that the two tetrahedral sheets have no further spare apical oxygens. Layer condensation is now complete, and the resultant 2:1 lamella is about 9.6 A thick and is incapable of further growth by condensation.

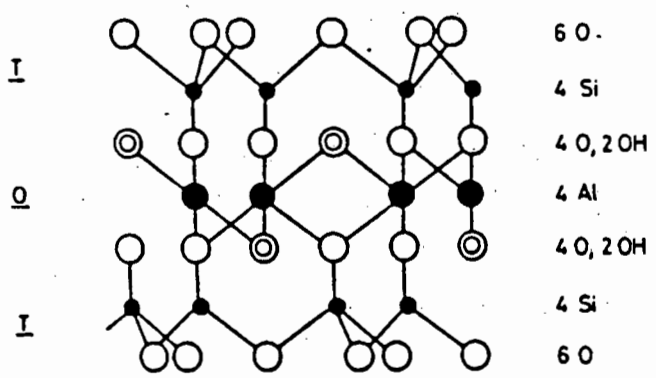

Figure 1.1: Diagramatic Representation of a 2:1 Smectite Mineral.

The lamellae of structural clays carry a net negative charge due to isomorphous substitution of lower valence cations for higher within the structure. Members of the smectite family are distinguished by the type and location of these substituted cations in the layered framework. In a unit cell formed from 20 oxygens and four hydroxyl groups there are eight tetrahedral sites and six octahedral sites. The net negative charge on the lamellae of smectite minerals, resulting from isomorphous substitution, is relatively low, typically ranging from 0.4 - 1.4 e^- per unit cell (Beson et al., 1974). The charge deficit is balanced by exchangeable cations situated on the surface of the layers. The extent of isomorphous substitution therefore determines the cation exchange capacity (CEC) of the clay.

The smectite group is divided into saponites, which are trioctahedral, and montmorillonites, which are dioctahedral. The most common example of the subgroup of saponites is saponite, which has the ideal formula

$$M_x^+(Si_{8-x}Al_x)^{iv}(Mg)_6^{vi}O_{20}(OH)_4$$

in which M^+ is the exchangeable charge balancing cation and x is the layer charge. Hectorite is also in this subgroup, but has its substitution (Li for Mg) in the octahedral layer.

Dioctahedral smectites are montmorillonites, and this plural covers a wide range of materials within this subgroup. Its two extremes are represented by compositions in which the charge is completely tetrahedral in origin, or completely octahedral. The former is beidellite:

$$M_x^+(Si_{8-x}Al_x)^{iv}(Al_4)^{vi}O_{20}(OH)_4.$$

Brown (1961) reports that an average value of x for beidellite is 0.7. The octahedral species carries the same name as the subgroup, i.e., montmorillonite:

$$M_x^+(Si_8)^{iv}(Al_{4-x}Mg_x)^{vi}O_{20}(OH)_4$$

An important property of smectites is their ability to swell by intercalation of water or alcohols. The extent of the swelling depends upon the layer charge, the interlayer cation, and the nature of the swelling agent (Mortland, 1968). When the hydration forces of the interlayer cation are strong, and the layer charge is low, the clay is most susceptible to swelling in water. Under the right conditions, the layers can be separated by hundreds of Angstroms. This swelling behaviour allows large complex ions, which can be used for catalytic purposes, to be exchanged into the interlamellar spaces. Montmorillonite and beidellite clays are particularly susceptible to swelling.

Although the 2:1 layers of these clays were described above as completed lamellae, and in chemical terms this is the case, clay minerals as a condensed phase do not usually consist of an assemblage of independent lamellae. Electrostatic forces resulting from interactions between the charge balncing cations in the interlayer spaces and the clay layers are capable, in the right conditions, of holding the individual lamellas face to face, so that assemblages of them act together. This type of face to face layer stacking occurs extensively in montmorillonite.

The dimensions of the surface of the smectite unit cell are approximately 5.2 x 8.9A (Brown, 1961). Ignoring the very small contribution from the area of the edges of the lamellae, the surface

area of smectite minerals is estimated to be 750 m^2/g. Hongdu (1981) report a BET surface area of 51 m^2/g for a naturally occurring montmorillonite sample, while Brindley and Sempels (1977) report a BET surface area of 73 m^2/g for a naturally occurring beidellite sample. These low surface areas occur as a result of the extensive face to face layer stacking in the two clays. The BET dinitrogen method involves initial degassing, and this pulls the lamellae together such that they are not subsequently intercalated by N_2.

1.1.1.2 Acidic Properties of Smectites

The proton donating ability of structural hydroxyl groups on clay minerals has been reported by Hall (1985) and Davidtz (1976). Ming-Yuan et al. (1988) used a montmorillonite sample for ammonia adsorption - infrared (IR) examination. They studied adsorption intensities at 1430 cm^{-1}, which corresponds to Bronsted acid sites, at different temperatures and found that there was a strong correlation between the number of structural hydroxyl groups present and Bronsted acidity.

Figure 1.2 shows a proposed structural model for the location of acid sites on tetrahedrally substituted (beidellite) and octahedrally substituted (montmorillonite) smectites (Ming-Yuan et al., 1988). The designations Al(VI) and Al(IV) are for octahedral and tetrahedral aluminium, respectively. Al(CUS) indicates coordinatively unsaturated Al located at the terminal octahedral sheet.

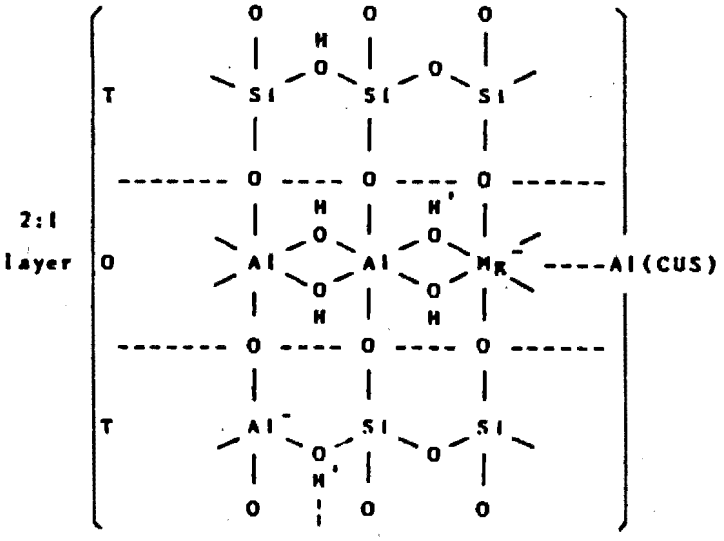

Figure 1.2.: Proposed Structural Model for the Location of Acid Sites on Smectite Minerals.

Octahedral sheet: Hall (1985) and Davidtz (1976) pointed out that the Al(CUS)-O- linkage, or octahedrally coordinated aluminium exposed at crystal edges, may become either Bronsted or Lewis acid sites. However their contributions are limited by the site density. Al(VI)-O-Al(VI) and Al(VI)-O-Mg linkages comprise most of the structural OH groups present on the clay. The strong dependence of Bronsted acidity on structural OH groups was mentioned above. A rough estimate of the amount of structural OH groups based on the idealised stoichoiometric composition of montmorillonte, $(Al_{4-x}Mg_x)Si_8O_{20}(OH)_4$, gives a number of 3.4×10^{21} OH/g. Only a small proportion of these structural hydroxyl groups can become Bronsted acid sites during adsorption of chemical species. The linkage Al(VI)-O-Mg, in Figure 1.2, compared with the linkage Al(VI)-O-Al(VI), seems more liable to donate H^+ by transferring negative charge to Mg atoms which are located in the dioctahedral sheet. In order to verify this assumption, Yuehua (1985) chose two natural montmorillonite samples to study the possible contribution of octahedral Mg to Bronsted acidity. The MgO content of the two samples was 1.82 and 3.94 %, respectively. Semi-quantitative measurements of Bronsted acid sites by IR, using NH_3 adsorption, showed that the montmorillonite sample with the higher Mg content possesed about two times more Bronsted acid sites than the other sample, within the temperature range 150 - 450°C.

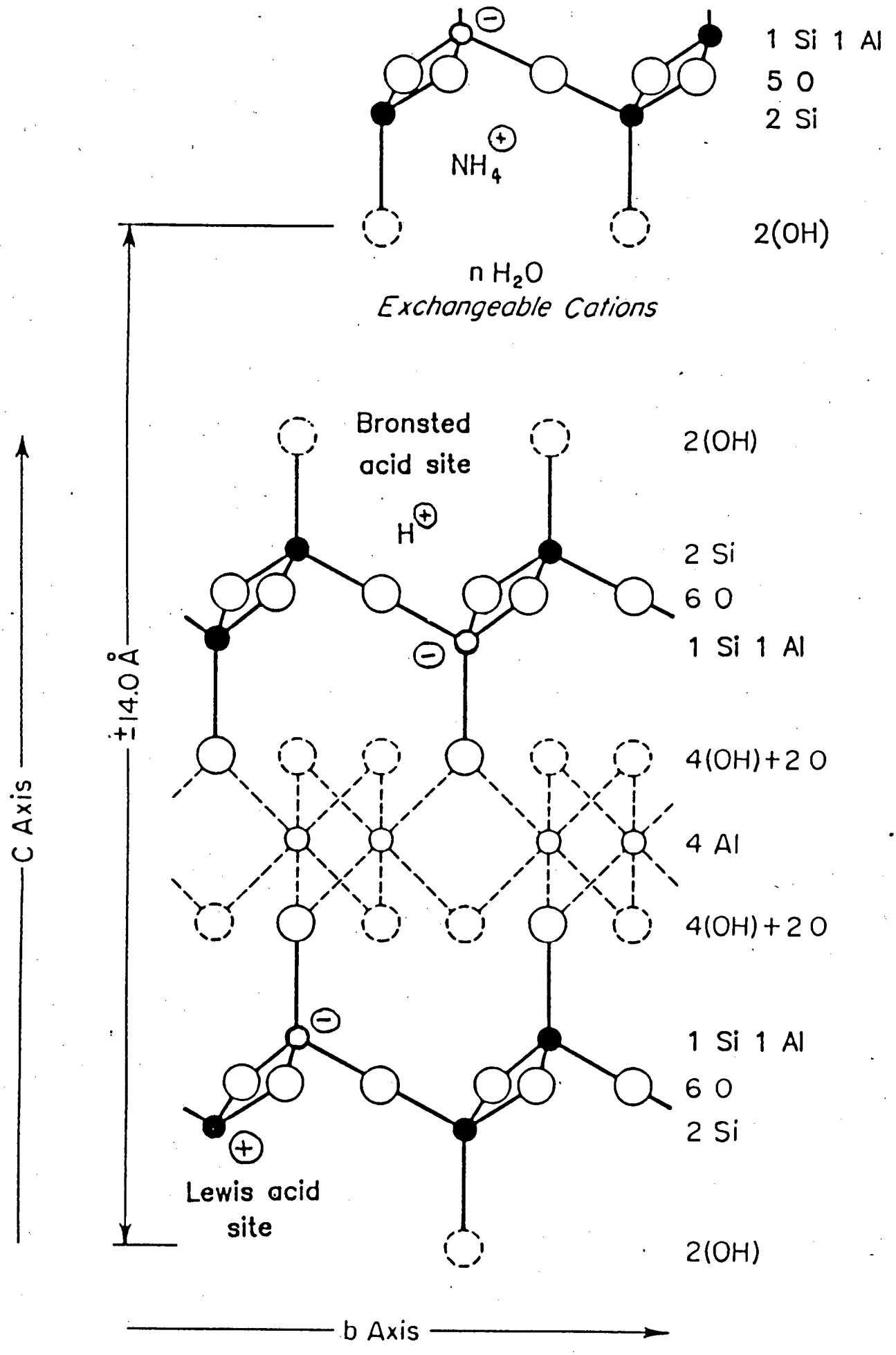

Figure 1.3: Acid Sites on Tetrahedrally Substituted Smectites.

Occelli et al. (1983) showed that a montmorillonite sample displayed both Bronsted and Lewis acidity according to the IR spectra of adsorbed pyridine. At a temperature of 400°C the acidity was mostly of the Lewis type. It seems likely that the Al(VI)-O-Mg linkage would constitute the main source of Lewis acidity in the octahedral layer.

Tetrahedral sheet: It is well established that tetrahedral aluminium in the framework of zeolites plays an important role in their acidic properties (Uytterhoven, 1965). Matsumoto (1984) demonstrated that tetrahedral aluminium atoms in 2:1 layered clays are active sites for adsorption. Figure 1.3 shows how a proton in an H^+ exchanged smectite interacts with the Si-O-Al(IV) linkage to form a Bronsted acid site . The figure also shows how the Si-O-Al(IV) linkage behaves as a Lewis acid site as a result of dehydroxylation.

1.1.2 Natural Clays as Catalysts

Clay minerals are known to catalyse numerous organic reactions. Clays were used as petroleum cracking catalysts (Voge, 1958), where reaction temperatures are in the range 673K - 773K, and for the isomerisation of hydrocarbons.

Acid clays can be used to catalyse reactions such as sucrose inversion and ester hydrolysis (Coleman and McAuliffe, 1954), and ethanol oxidation (Grim, 1968). The dehydration of organic molecules can be catalysed by a clay surface (Davidtz, 1976). Acid treated clays catalyse alkylation of aromatic rings by alcohols, alkyl chlorides and alkyl ethers (Swartzen-Allen and Matijevic, 1974). Alkylation of aromatics with olefins is enhanced by acidified clays. Acid treated clays have the ability to polymerise olefins (Solomon, 1968).

1.1.3 Synthetic Mica Montmorillonite

1.1.3.1 Synthesis

The synthesis of three-layer clays was first reported by Noll (1930) and Iiyama and Roy (1963).

The hydrothermal synthesis of a randomely interstratified layer lattice silicate (SMM) was reported by Granquist and Pollack (1967). SMM was synthesised from a slurry of diatomite (silica) and bayerite (alumina) in an aqueous solution of NaOH at 573 K. From this mixture the sodium form of SMM was obtained. The synthesis method was improved by Granquist et al. (1972a) so that the ammonium form was crystallised directly.

1.1.3.2 Structure

The structure of SMM is essentially the same as that of beidellite, and differs only in the extent of tetrahedral aluminium substitution. Like beidellite, the unit cell formula for SMM may be written

$$M_x^+Al_4(Si_{8-x}Al_x)O_{20}(OH)_4.$$

The clay consists of a randomely interstratified mixture of two clay phases. The mica-like phase, which has no swellable property, has a relatively high concentration of tetrahedrally coordinated aluminium. The montmorillonite-like or, more appropriately, beidellite-like phase has a similar concentration of tetrahedrally coordinated aluminium to beidellite and is therefore swellable. Granquist and Pollack (1967) report that in the unit cell formula of SMM, x takes the following values:

$0 < x < 1$ beidellite-like layers

$1 < x < 2$ mica-like layers

Average x approximately 1.

Electron microscopy studies (Wright et al., 1972) showed the bulk of the material to have a platelike structure, having platelets of an average diameter of 1000 A. Based on a BET surface area of 160 m^2/g, and assuming a density of 2.55 g/cm^3 derived from x-ray unit cell measurements, and inaccessibility of the interlamellar space to the N_2 molecule, the average number of layers per platelet was calculated to be about 5. This value corresponds to an average platelet thickness of 50 A (Wright et al., 1972).

The surface area of SMM was observed to drop from 160 m^2/g to 135 m^2/g after calcination at 923 K. The loss in surface area was ascribed to increased platelet to platelet association (Wright et al., 1972).

From the results of thermal analysis, Wright et al. (1972) and Kojima et al. (1986) found that deammoniation and dehydroxylation of ammonia exchanged SMM occurred concurrently. Wright et al. (1972) suggested that the presence of ammonium, as opposed to other charge balancing cations, promoted dehydroxylation of the clay layers.

X-ray diffraction studies of SMM (Wright et al., 1972) gave a non-integral 001 sequence and irregularly shaped peaks which are indicative of mixed layering. Wright et al. (1972) found basal spacings of 10.4 and 12.5 A to occur in the proportion 2:1. Upon the addition of ethylene glycol, the 10.4 A spacings persisted (mica-like material), whilst the 12.5 A spacings swelled to 17.3 A, exhibiting beidellite-like behaviour. Calcining SMM at 923 K caused an irreversible collapse of basal spacing to 9.4 A.

1.1.3.3 Acidic Properties of SMM

Due to their very similar structures, the acidic centres on SMM should be very similar to those on beidellite.

The nature of acid sites present on SMM was investigated by solid state IR studies (Kojima et al., 1986; Wright et al., 1972) and temperature programmed desorption studies (Kojima et al., 1986) using pyridine as the probe molecule.

Wright et al. (1972) reported values of 2.5 meq Bronsted and 1.5 meq Lewis bound pyridine per 100 grams of calcined NH_4^+ SMM, giving a total acidity of 4 meq/100g. Kojima et al. (1986) found that the amount of Bronsted acidity decreased as the calcination temperature increased. At a calcination temperature of 770 K there was no longer evidence of Bronsted acidity.

Upon addition of water to dehydroxylated SMM, Lewis acid sites were observed to convert to Bronsted sites. Quantitative measurements suggested a reversible one to one interconversion of these acid sites. Using the integrated adsorbance coefficients of Hughes and White (1967), Kojima et al. (1986) computed the number of Lewis acid sites per gram of

SMM after calcination at 773 K to be 2.4 x 10^{19}. The findings of the pyridine adsorption - IR studies indicated that Lewis acid sites held pyridine to higher temperatures than Bronsted acid sites. Kojima et al. (1986) found that calcination at 923 K resulted in the generation of only Lewis acid sites which existed at particle edges and faces. Wright et al. (1972) attributed the Lewis acidity to trigonal aluminium at the edges of the tetrahedral layers. The actual amount of Lewis acidity versus the theoretical amount (approx. 20 meq/100 g) indicated that only a fraction of the acid sites were accessible. This was attributed to the elimination of interlayer spaces during calcination.

Temperature programmed desorption (TPD) experiments were carried out with SMM to investigate the acid site strength and distribution (Kojima et al., 1986). At a low calcination temperature of 521 K, the acidity was due mainly to polarised water and ammonium ions. As the calcination temperature was increased, there was a shift to a higher peak desorption temperature. The effect of the calcination medium (air, hydrogen, nitrogen) on the TPD spectrum was shown to be negligible.

1.1.3.4 Catalytic Activity of SMM

Although SMM has a much lower acid site density than many zeolite catalysts, it has comparable catalytic activity. A possible explanation is that because of the platelike nature of SMM, the measured acidity is representative of accessible acidity, whereas, due to difusional limitations, only a fraction of the measured acidity of zeolites is actually catalytically active under reaction conditions (Thomas and Barmby, 1968).

The catalytic activity of SMM for cracking was first reported by Capell and Granquist (1966). SMM was observed to be twice as active as a sulphur resistant natural clay, and 1.5 times more active than a synthetic alumina catalyst.

Hattori et al. (1973) investigated the isomerisation of hydrocarbons over SMM. They reported that with silica alumina, the H^+ ions do not undergo easy exchange with the hydrocarbon molecules during isomerisation, whereas with SMM there was a high degree of exchange.

Fletcher et al. (1986) investigated the activity of SMM for the oligomerisation reaction. They studied the effect of varying the calcination and reaction conditions on the oligomerisation of propene over SMM in a fixed bed reactor at 51 atm and WHSV = 1.5. They reported that the presence of Lewis acidity gave high activity and long catalyst lifetime. The catalyst deactivated rapidly in the presence of water and this was attributed to the conversion of Lewis to more active Bronsted sites. Calcining at low temperatures (520 K), which caused the formation of mainly Bronsted acid sites, resulted in poor catalyst lifetime. The sites formed by polarised water were shown to be inactive for propene oligomerisation. The optimal condition for propene oligomerisation was found to be a calcination temperature of 770 K and a reaction temperature of 420 - 460 K.

1.1.4 Nickel Substituted SMM

The structure of Ni-SMM is similar to that of SMM except that nickel substitutes for aluminium in the octahedral layer. Like SMM, Ni-SMM consists of a randomely interstratified mixture of non-swellable and swellable phases. Ni-SMM clays readily crystallise, for varying amounts of nickel added, to form a trioctahedral smectite that may or may not contain aluminium. Therefore, a mixed dioctahedral - trioctahedral clay will be formed from mixtures of NiO, Al_2O_3 and SiO_2 that contain less than the required amount of nickel for six nickel atoms per unit cell (Granquist, 1976). Black et al. (1976) found the maximum weight percentage Ni that could be incorporated in SMM to be 36%. Gaaf et al. (1983) report a method for the hydrothermal synthesis of a 100% swellable Ni-SMM clay with a Ni content of 23%.

X-ray diffraction was used by the above workers to characterise the different Ni-SMM samples. Basal spacings were observed to vary between 10 and 13.5 A. Generally, as the number of Ni atoms/unit cell increased, the interlayer space increased.

Swift and Black (1974) reported that the incorporation of nickel into the SMM lattice via synthesis resulted in a significant increase in the stable surface area of the clay. The synthetic clay containing no nickel

had a surface area of 145 m^2/g, while the clay with a nickel content of 36% had a surface area of 332 m^2/g.

Robschlager et al. (1984) compared the Bronsted acidity of unreduced Ni-SMM and SMM and found that there was no significant difference in acid site strength. The activity of beidellite and unreduced Ni-SMM was found to be similar for n-pentane hydroisomerisation.

It has been reported that upon reduction of Ni-SMM in flowing hydrogen at elevated temperatures, a highly active catalyst for hydroisomerisation and hydrocracking was formed (Heinerman et al., 1983, Robschlager et al., 1984). Heinerman et al. (1983) investigated the acidic sites of Ni-SMM by IR analysis using NH_3 as a probe. They found that on reduction of Ni-SMM (20 wt% Ni) the number of Bronsted acid sites increased four times while the Lewis acid sites decreased by a quarter.

Bercick et al.(1978) showed that Ni-SMM is an active catalyst for oligomerising C_3 - C_4 olefins. O'Connor et al. (1988) reported that a Ni-SMM clay containing 7% nickel was significantly more active during high pressure propene oligomerisation than SMM. The product selectivities of the two clays were similar.

1.1.5 Pillaring of Clays

Clays and layered silicate minerals have a long history of use as petroleum cracking catalysts (Ryland et al., 1960). These were largely replaced in the mid sixties by zeolites (Flanigen, 1980). The greater acidity, reactivity and selectivity of zeolite catalysts allowed for closer control of cracking reactions and higher yields of desired products (Gary and Handwerk, 1975). To date, more than 100 zeolites have been synthesised, but of these only about a dozen are utilised on an industrial scale. Zeolites A, X, Y, mordenite, erionite and ZSM-5 represent more than 95% of the total worldwide usage. However, the limited pore size range of zeolites and the relatively high cost of those used in the petroleum industry have given impetus to the search for other types of porous compounds. The former limitation is a serious impediment for the possible use of zeolite catalysts for the conversion

of synthetic and heavy crude oils to give commercially desireable products. More specifically, molecular sieves with pore sizes of 8 - 40 A are required for such purposes.

The properties of clay minerals, as described above, make these materials suitable for use as acid catalysts. Clay minerals such as montmorillonite and beidellite have an extensive face to face layered structure with individual sheets separated by an interlayer space. Such clay minerals readily expand, and numerous organic reactions catalysed by clays take place within the interlamellar space. On calcination of a clay mineral, however, collapase of the layer structure occurs and, as a consequence, the interlayer space is virtually eliminated. Therefore, clay catalysts lose much of their activity at elevated reaction temperatures, and spent clay catalysts cannot be regenerated by calcination in air to burn off carbonaceous deposits.

In the preceding two decades, a new class of two-dimensional molecular sieves has been synthesised from certain types of aluminosilicate clay minerals. The general procedure is to incorporate large cations between the clay layers to prop them open. The removal of water from such "pillared" clays on heat treatment would then not result in the collpase of the interlayer spaces, provided the props or "pillars" are thermally stable. It has long been known that various organic molecules such as amines and alkylammonium ions readily intercalate between clay layers and form pillared complexes (Barrer, 1978). In general, these organically pillared structures suffer from the instability of the organic component, although relatively stable compounds have been formed with cage-like amines (Shabtai et al., 1976; Mortland and Berkheiser, 1976; Bailey, 1980).

In the late seventies, the problem of thermal stability was tackled using large inorganic polymeric oxy-hydroxy cationic species (Vaughan and Lussier, 1980). These polycationic species are set in position within the clay as a result of ion exchange with the existing charge balancing cations in the interlayer spaces. Due to the size of these pillaring species, the ion exchange process leading to pillaring can take place only in clays with a swellable property. Calcination of clays exchanged with these pillaring species results in the formation of

permanent oxide/hydroxide props which hold the layers apart and so generate a large proportion of zeolite-like pore space (Vaughan and Lussier, 1980). Such pillared clays are defined by expanded lattice basal spacings.

Many pillared clays have been prepared using polycationic species of Al, Mg, Fe, Cr, Ni, Bi, Si, and Zr. Of these, the clays pillared with aluminium(III) and zirconium(IV) species have been found to be the most stable. It has been reported that these materials are thermally stable at temperatures in excess of 500°C (Occelli, 1983).

Vaughan and Lussier (1980) reported that the major aluminium pillaring species was the Al_{13} polymer described by Johansson (1960), while the zirconium polymer was the square planar complex described by Clearfield and Vaughn (1956), or species formed by crosslinking these through oxygen across the plane to give cube-like Zr_8 polymers, and similarly formed pillars of Zr_{12} and Zr_{16}.

Jones (1988) reported that certain factors had an important influence on the interlayer spacing and pore width in pillared clays. These included the molecular dimensions of the pillaring cation, the charge on the cation, which was dependent on the degree of hydrolysis, the orientation of the pillaring cation between the clay layers, and the charge density and distribution of the clay layers.

1.1.6 Chemistry of the Aluminium Pillaring Species

An aluminium salt such as $AlCl_3 \cdot 6H_2O$ readily hydrolyses when dissolved in water (Fig. 1.4a). As the OH^- concentration of the solution is increased, dimers (Fig. 1.4b) condense to chain structures until a stable Al_6 complex is formed (Fig. 1.4c). As the OH/Al ratio is increased up to or slightly less than 2.5, the solutions have been reported to contain polynuclear species with 6 to 400 aluminium atoms per structural unit (Hem and Robertson, 1967). The exact form of these species is unknown. Some of the proposed species are illustrated in Figures 1.4d and 1.4e (Hsu and Bates, 1964; Occelli et al., 1985). From the results of NMR data (Pinnavia et al., 1984), it has now been shown that the major polymeric species in these solutions is the Keggin ion,

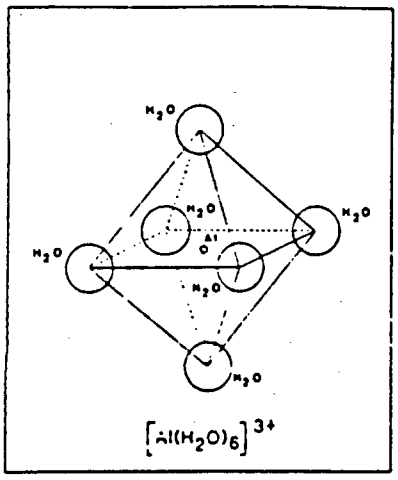

(a)

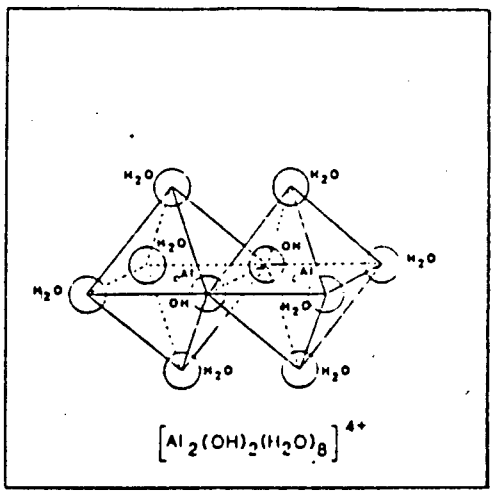

(b)

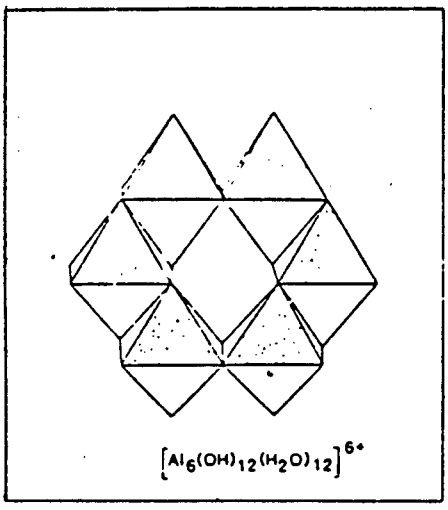

(c)

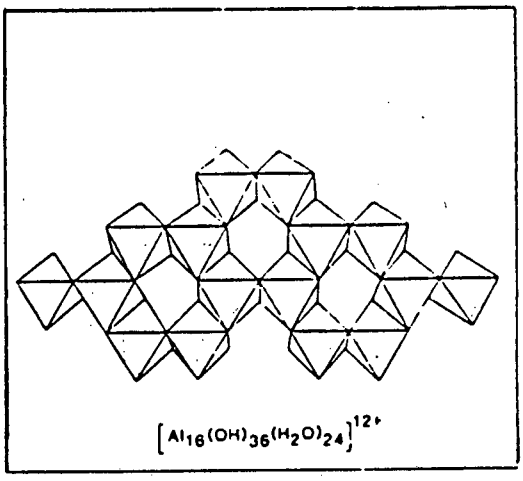

(d)

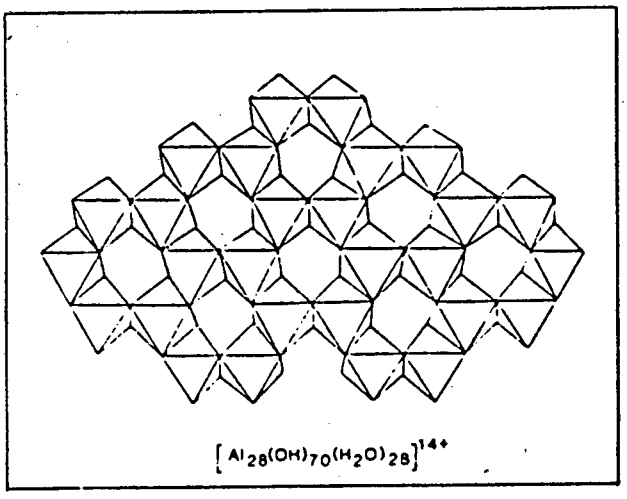

(e)

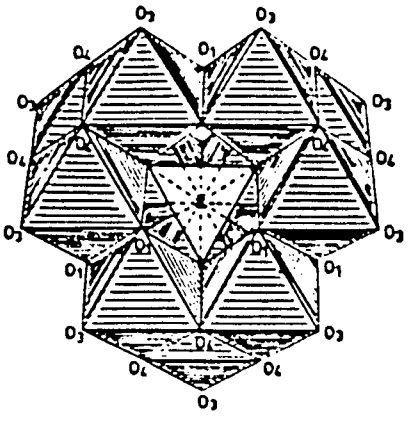

(f)

Figure 1.4: Some Polymeric Species Present in Hydroxy-Al Solutions.

$[Al_{13}O_4(OH)_{24}.12H_2O]^{7+}$, having the structure shown in Figure 1.4f. The ion consists of one tetrahedrally coordinated Al atom and twelve octahedrally coordinated Al atoms.

In preparing these aluminium solutions, seemingly trivial aspects of solution preparation can have a significant effect on the nature of the solution. This point is supported by the work of Akitt and Farthing (1978) and Bertsch et al. (1986). Usually, the hydroxy-Al solutions are prepared in one of the following ways:

(a) Na_2CO_3 addition to $AlCl_3$ solution;
(b) NaOH addition to $AlCl_3$ solution;
(c) Al metal dissolution in HCl;
(d) Electrolysis of $AlCl_3$ solution.

The hydrolysis of aluminium chloride solution using sodium carbonate has been described by Akitt and Farthing (1981). These authors studied the effect of Na_2CO_3 (solid or solution), time, anions, temperature, and OH/Al (r) values (1 or 2.5) on the nature of the solution species. The principal technique used for these studies was ^{27}Al NMR, and the solution concentrations were in the region of 1 M. For example, the rapid addition (over 30 min.) of solid sodium carbonate to a 1 M solution of $AlCl_3$ at 100°C (r=2.5) produced a solution containing about 75% Al_{13} and 25% unobservable species, as detected by NMR. Immediate purification using gel permeation chromatography resulted in pure Al_{13} of reasonable stability. The use of other bases such as MgO, $MgCO_3$, ZnO and $ZnCO_3$ has also been studied by Akitt and Farthing (1978).

Bottero et al. (1980) and Bertsch et al. (1986) have studied the solution state of aluminium(III) as a result of the addition of NaOH to $AlCl_3$ solution. Bottero et al. studied 0.1 M aluminium(III) solutions with r in the range 0.5 to 2.5. Bertsch et al., on the other hand, considered aluminium concentrations in the range 3.4×10^{-3} to 1.0 M for r values between 0 and 2.5. Base injection rates were controlled at 0.6 or 1.2 cm^3/min using 0.1 M NaOH. At high r values, for example 2.5, the base injection rate was a critical factor. The work also suggested that for higher aluminium(III) concentrations, even slower base injection rates would be required to maximise Al_{13} formation. Bertsch et al.

emphasised the sensitivity of the system towards preparation conditions.

The reaction of aluminium metal with $AlCl_3$ solution has been studied in detail by Akitt and Farthing (1981). One benefit of this method of preparation is the absence of interfering cations. Also, hydrolysis takes place at lower temperatures than with Na_2CO_3. Practical matters that were considered were the form of the metal (wire, foil, powder), the initiator concentration, time and temperature. Solution concentrations were in the range 1 - 5 M with r fixed at 2.5. Measurements were undertaken at 27°C or 80°C using ^{27}Al NMR. Other than at high concentrations and temperatures, 80 - 90% of the aluminium present could be detected. A complex picture of the solution state emerged, and the authors suggested that the species may consist of partial Al_{13} units with octahedral units dispersed as flexible chains and forming cross-links. At 27°C no Al_{13} was present in freshly prepared solutions, but the resonance associated with this species appeared on heating at 80°C, and remained on cooling. However, it eventually disappeared. The spectra were also sensitive to concentration.

Electrolytic hydrolysis of an $AlCl_3$ aqueous solution has been described by Akitt and Farthing (1981). Their preparative conditions produced a solution (r=2.4) which contained effectively only Al_{13} as judged by ^{27}Al NMR.

Vaughan and Lussier (1980) reported that when preparing hydroxy-Al solutions for pillaring, it was important to "age" the solutions prior to use. This ageing process resulted in significant improvements in the hydrothermal stabilities of the pillaring species when incorporated into the interlayer spaces of clays. Tokarz and Shabtai (1985) prepared pillared smectites from hydrothermally (reflux conditions) treated, base hydrolysed aluminium solutions. They found that the most stable compounds were prepared with solutions treated for 24 - 28 hours but that even a six hour treatment was sufficient to produce products which were stable to 500°C. Their results indicated that a hydrothermal treatment of the solution for 6 - 48 hours resulted in products with higher thermal stability and higher porosity as compared with those prepared from solutions aged at room temperature for two weeks.

1.1.7 Hydroxy-Al Pillared Clays

1.1.7.1 Characterisation

X-ray diffraction analysis can be used to measure the interlayer spacings of clay minerals (Brown, 1961). The position of the first order basal peak is a measure of the basal spacings of the clay. These basal spacings represent the centre to centre distance between clay layers which stack in the basal direction. By subtracting the thickness of one 2:1 layer (ca. 9.6 A) the interlayer spacing is obtained.

The basal spacings of clays pillared with the hydroxy-Al solution (Al PILC's) vary according to the procedures used to prepare the pillaring solutions. Lahav and Shani (1978) pillared montmorillonite with Al solutions containing different OH/Al ratios, aged for different periods of time. Basal spacings of the pillared clays varied between 14.4 and 18 A. Sterte (1988) reported that, in many cases, ageing of the hydroxy-Al solution resulted in pillared clays with slightly larger interlayer spacings. In general, basal spacings of Al PILC's reported in the literature vary between 18 and 19.5 A. Increased calcination temperature results in a progressive decrease in the interlayer spacing of Al PILC's (Tennakoon et al., 1986). Occelli and Innes (1985) reported a basal spacing of 17.5 A for Al pillared montmorillonite (Al PILMont) calcined at 500°C. This value is typical of those reported in much of the available literature.

Plee et al. (1987) reported the basal spacings of beidellite pillared with hydroxy-Al solutions prepared with OH/Al ratios varying between one and two. Spacings varied from 18.1 to 18.6 A. Calcination of the pillared clay at 300°C resulted in basal spacings of between 17 and 17.6 A.

Shabtai et al. (1984) pillared montmorillonite to different extents by varying the ratio (mmol Al present in pillaring solution)/(g clay) used in the pillaring process. Ratios of 1.25, 1.6, and 2 were used. The ratio of 2 mmol Al/g clay was estimated to be sufficient to fully satisfy the charge deficit on the clay lattice. The different ratios resulted in basal spacings of 17.2, 18.8, and 18.4 A, respectively, for

clays calcined at 300°C.

Surface areas of pillared clays are generally estimated from the results of N_2 adsorption experiments. Occelli and Tindwa (1983) reported that if the nitrogen data obtained from Al PILMont was plotted using the Langmuir and BET isotherms, the Langmuir isotherm gave a linear plot. These researchers therefore concluded that the surface area of the clay was due predominantly to micropores in the interlayer spaces. They reported a surface area for Al PILMont of 280 m^2/g which decreased gradually to approximately 240 m^2/g on heat treatment up to 540°C. Above 540°C, the pillars began to decompose, and the surface area showed a strong dependence on temperature.

Shabtai et al. (1984) reported the Langmuir surface areas of Al PILMont clays pillared with different ratios of mmol Al/g clay. They found that, up to the point where sufficient Al was used to fully satisfy the lattice charge deficit, the clay surface area increased. The surface areas of clays calcined at 400°C varied from 262 m^2/g for a ratio of 1.25, to 329 m^2/g for a ratio of 2.

Brindley and Sempels (1977) reported a Langmuir surface area of 214 m^2/g for a naturally occurring beidellite clay pillared with an hydroxy-Al solution prepared using an OH/Al ratio of 2.4. Calcination of the clay at 325°C reduced the surface area to 195 m^2/g.

Gaaf et al. (1983) reported that treatng a 100% swellable Ni-SMM clay with a hydroxy-Al solution increased the basal spacing of the clay (dried at 110°C) from 12.6 to 17.3 A. The BET surface area of the clay after calcination at 350°C had increased from 170 to 230 m^2/g.

From the results of adsorption of polycyclic compounds of various critical diameters onto Al PILMont, Shabtai et al. (1984) concluded that the lateral (interpillar) pore sizes of the pillared clay had a narrow distribution, with predominant sizes depending on the extent of pillaring. The interpillar pore sizes were mainly in the range 11 - 19 A, with some pores wider than 19 A.

From an analysis of the results of sorption of C_6 - C_{10} n-paraffins onto

Al PILMont at different partial pressures and temperatures, Occelli et al. (1984) suggested that an average interpillar spacing in the clay was in the region of 14 A.

Schutz et al. (1987) reported that upon calcination of Al PILMont, the pillars underwent dehydration followed by dehydroxylation. The dehydroxylation process occurred in the range 300 - 400°C and led to the formation of alumina-like pillars according to the equation

$$2[Al_{13}O_4(OH)_{24}.12H_2O]^{7+} \longrightarrow 13Al_2O_3 + 14H^+ + 41H_2O.$$

This equation shows that during the decomposition of the Al_{13} species, and the formation of alumina-like pillars, protons are released. These protons will migrate to the origins of the lattice charge deficit, namely, the tetrahedral layer in beidellite, and the octahedral layer in montmorillonite. This migration of protons into the clay lattice was confirmed by Tennakoon et al. (1986) who used IR and NMR to study calcined and uncalcined Al PILMont. Jones (1988) suggested that the generation of these protons enhanced Bronsted acidity of the clay, although, in the case of Al PILMont, high temperatures were required for these protons to become available for reaction due to the fact that they were small enough to migrate into the octahedral layer.

Tennakoon et al. (1986) reported that although the basal spacing of Al PILMont decreased progressively upon heating to 400°C, this did not prevent re-expansion of the interlayer spaces on exposure to moist air. The pillared clay obtained by calcination at 500°C, however, showed no tendency to expand, suggesting that pillars became anchored to the clay layers at temperatures in exess of 400°C. From this observation, and from the results of an IR and NMR study of calcined and uncalcined Al PILMont, Tennakoon et al. (1987) concluded that in the temperature range 400 - 500°C, condensation of residual hydroxyl groups on the pillars with octahedral lattice hydroxyls anchored the pillars to the octahedral sheets above and below.

Plee et al. (1985) reported the possible bonding between the tetrahedral sheet of the clay and the Al_{13} pillars through an MAS NMR examination of pillared beidellite calcined at 300 - 400°C. The existence of the Al(IV)-O-Si linkage in the tetrahedral sheets is a prerequisite for this type of bonding. The reaction would therefore not occur in pillared

montmorillonite which is theoretically free from tetrahedral substitution. During calcination, the Al_{13} ion transfers protons to the layers. The most likely point of attack in beidellite is at an Al(IV)-O-Si linkage, with the formation of a silanol group. The protonated Al(IV)-OH-Si structure in the tetrahedral sheet may react with the pillar to form either Si-O-Al_p or Al(IV)-O-Al_p linkages, where Al_p represents aluminium present in the pillar. The MAS NMR spectral changes accompanying this process gave evidence for the latter type linkage. This Al(IV)-O-Al_p linkage induces an inversion of an aluminium tetrahedron of the tetrahedral sheet. This leads to a different Al(IV)-O-Si linkage in the tetrahedral sheet in which the negative charge of the Al tetrahedron is no longer buried in a continuous tetrahedral network but is exposed in the interlamellar space.

The acidic properties of PILC's have been studied by many authors using several well established techniques such as pyridine or ammonia adsorption followed by infra red spectroscopy, ammonia temperature programmed desorption, and n-butylamine titration.

Occelli and Tindwa (1983) and Occelli and Lester (1985) indicated that Al PILMont contained both Lewis and Bronsted acid sites according to the infra red spectra of adsorbed pyridine. At 400°C, the ratio of Lewis to Bronsted acid sites was estimated to be about four. The spectra of Al PILMont in the O-H stretching region showed the presence of a doublet indicating the existence of two types of hydroxyls: one vibrating at 3650 cm^{-1} was assigned to lattice OH, and the other, vibrating at 3700 cm^{-1}, was believed to be associated with the hydroxy-Al oligomer used in pillaring the clay.

Shabtai et al. (1984) investigated the acidity of Ce exchanged Al PILMont. From measurements of NH_3 adsorption in a flow microbalance at atmospheric pressure they concluded that acidity generally decreased with a decrease in the extent of pillaring. Using the IR spectra of adsorbed pyridine they estimated the ratio of Lewis to Bronsted acid sites on Ce Al PILMont calcined at 673 K to be about 1.4.

Ming-Yuan et al. (1988) measured the acid strength of Al PILMont by n-butylamine titration. The results were compared with those of amorphous

silica alumina and calcined rare earth exchanged zeolite Y and indicated that, compared with these two catalysts, Al PILMont was a weak solid acid.

Guida (1982) investigated the acidity of Al PILMont using the IR specra of adsorbed pyridine. They found that the acidity of the sample calcined at 500°C was mainly of the Lewis type.

Using the n-butylamine titration method, Ming-Yuan et al. (1988) measured the acidity of Na montmorillonite pillared by various amounts of Al polycations. They found that the acidity increased almost in proportion to the pillar/montmorillonite ratio used when this ratio was lower than that required to fully satisfy the lattice charge deficit. The acidity was observed to level off when the pillar/montmorillonite ratio attained the stoichiometric value. They concluded from these results that pillars are a major source of Lewis acidity for Al PILC's.

Ming-Yuan et al. (1988) studied the source of Bronsted acidity on PILC's. Since the proton donating ability of structural hydroxyl groups had already been reported for clay minerals (Hall, 1985; Davidtz, 1976), they investigated the relationship between structural hydroxyl groups and Bronsted acidity on montmorillonite and Al PILMont. The IR spectra of structural OH groups of Al PILMont subjected to pretreatment at various temperatures indicated that, as compared with the parent clay, the OH groups of Al PILMont diminished rapidly with increasing temperature. The spectra of the parent and pillared samples in the O-H stretching region were very similar at lower pretreatment temperatures. These researchers concluded from their results that the contribution of OH groups on the pillars in Al PILMont was not significant. The Al PILMont samples were also used for IR examination of adsorbed ammonia. The adsorption intensities at 1430 cm^{-1}, which correspond to Bronsted acid sites, attenuated as the temperature was increased, especially above 350°C. There was fairly good agreement of the changes of both structural OH groups and Bronsted acidity with temperature.

Zhinqun et al. (1987) investigated the dependence of the amount of Lewis acidity on temperature using both infrared and ultra violet (UV) spectroscopy. The results of the IR and UV measurements agreed with each

other and indicated that the amount of Lewis acidity monotonically decreased with pretreatment temperature slowly.

Zhinqun et al. (1986) varied the extent of pillaring in Al PILMont by using different pillar/montmorillonite ratios during the pillaring process. Subsequent TG/DTA of the pillared samples indicated that progressively increasing the extent of pillaring reduced the temperatures required for lattice dehydroxylation. These researchers explained this in terms of the removal of Na^+ cations which may block structural OH groups of the octahedral layer located towards the six membered Si tetrahedra. This would facilitate the elimination of the OH groups on heating.

1.1.7.2 Catalytic Activity of Hydroxy-Al Pillared Clays

Shabtai et al. (1980) have reported that Al PILC's are more active for dealkylation and cracking of large organic molecules than Y type zeolite, which has the largest pores among the zeolites. The high activity of these PILC's has been attributed to the large pore size, which allows bulky hydrocarbon molecules to reach the interior active sites. It has also been pointed out by Shabtai et al. (1984) that higher activity is obtained when rare-earth exchanged clays are pillared rather than ion exchanged subsequent to crosslinking.

An interesting outlook on the commercial application of PILC's has been provided in recent papers by Occelli and co-workers (Occelli and Finseth, 1986; Occelli et al., 1986; Occelli, 1985). They showed that gas oil cracking, catalysed by Al PILC's, gave high and selective yields of gasoline under moderate conditions. The activity and selectivity were affected by the nature of the clays: hectorite exhibited a high gasoline selectivity and minimized light gas production, although it was not as active as montmorillonite. However, they pointed out some problems using PILC's as catalysts: high coke formation and a lack of hydrothermal stability at the high temperatures required for catalyst regeneration.

The constraint index, defined as the ratio of the cracking rate for n-hexane to 3 methylpentane, has been extensively employed as a parameter to represent the shape selectivity of zeolites. Kikuchi and Matsuda

(1985) measured the constraint indices of Al PILC's having different interlayer distances. The constraint indices of the pillared clays were similar, in spite of a large variation in interlayer distance from 4 to 9 A, and were close to those of large pore zeolites. Thus, cracking of these hydrocarbons is not a suitable reaction to evaluate the shape selectivity of pillared clays. Cracking of bulky hydrocarbons has been suggested. Kikuchi and Matsuda (1985) found that the ratio of the cracking rate of cumene to that of triisopropylbenzene over Al PILC's decreased sharply with increasing interlayer distance.

Zhinqun (1985) used cumene cracking as a test for Bronsted acidity on Al PILMont. The reactions were conducted at 250°C on samples pretreated at various temperatures. The results showed that conversion fell rapidly after treatment at or above 400°C, which is in agreement with the loss of structural hydroxyls and Bronsted acidity. The same authors found that when n-heptane cracking was conducted on dried Al PILMont, cracking was initiated at 120°C and the conversion level increased to a maximum at about 240°C, and then decreased with further increase in the reaction temperature. This behaviour was attributed to the loss of Bronsted acidity on Al PILMont upon heating during reaction.

Zhinqun (1985) compared the n-C_7 cracking activities of Al PILMont and calcined rare earth exchanged zeolite Y (REY). They found that cracking of n-C_7 occurred on Al PILMont at a temperature approximately 120°C lower than that on REY for a conversion level of 22%. However, the activity of Al PILMont decreased while the cracking activity of REY increased to much higher conversion levels with the increase in reaction temperature. The high cracking activity of Al PILMont at lower temperatures was ascribed to the fact that Al PILMont posesses abundant structural hydroxyls which may create a high density of Bronsted acid sites under suitable conditions.

Huisheng and Ying (1986) studied the alkylation of benzene with 1-octene and 1-dodecene on dried Al PILMont. They found that Al PILMont was about half as active as HY zeolite for alkylation with 1-octene, and equally as active for alkylation with 1-dodecene.

Gaaf et al. (1983) reported that pillaring a 100% swellable Ni-SMM clay

with a hydroxy-Al pillaring solution significantly increased the activity of the clay for the hydroisomerisation of n-pentane at 250°C. The catalyst was reduced at 343°C prior to reaction.

Urabe et al. (1986) showed that Al PILMont having a layer distance of 8 A yielded more p-xylene than the thermodynamically attainable fraction during the alkylation of toluene with methanol. The selectivity of the pillared clay was, surprisingly, higher than that of ZSM-5. An opposite result was reported by Occelli et al. (1985). Alkylation of toluene with ethylene produced p-ethyltoluene in equilibrium amounts by use of a pillared clay which had a similar structure to that of the catalyst used by Urabe et al. The molecular dimension of p-ethyltoluene is larger than that of p-xylene. Consequently, if methylation of toluene is shape selectively controlled, ethylation of toluene should also be. Kikuchi and Matsuda (1988) suggested that this apparent contradiction could be due to the preferential adsorption of methanol, rather than aromatic hydrocarbons, on acid sites during the alkylation of toluene with methanol. This could retard the isomerisation of p-xylene, leading to the selective formation of this isomer.

The disproportionation of trimethylbenzene (TMB) is a possible route to the production of durene, or 1245 tetramethylbenzene (TetMB). Durene can be oxidised to pyromellitic anhydride which is used as a raw material for heat resistant polymers. Kikuchi et al. (1984; 1985) reported that disproportionation of TMB can be catalysed by Al PILMont. They found that when Al PILMont having an interlayer distance of 8 A was used to convert 124 TMB, 1245 TetMB and o-xylene were produced more abundantly than expected from thermodynamic equilibrium calculations. They ascribed the formation of the specified isomers to shape selective properties of the pillared clay. Since isomerisation of TMB is a major side reaction, Ming-Yuan et al. (1988) investigated the type of acid site required for the two parallel reactions on Al PILMont. The pillared clay was dried at 120°C without further calcination. They observed that when reaction temperature was increased, increasing the ratio of Lewis/Bronsted acidity, the selectivity for disproportionation increased. In contrast, the selectivity for isomerisation was well correlated to Bronsted acidity.

From the results of a spectroscopic study of adsorbed pyridine and pilot plant data, Occelli et al. (1985) indicated that propene oligomerisation can be catalysed by Lewis acid sites on Al PILMont. These researchers used Al PILMont to oligomerise propene in a fixed bed isothermal reactor operating at 30 - 50 atm. They found that the pillared clay was less active for this reaction than zeolite omega and an amorphous aluminosilicate, but had a higher selectivity for gasoline production. At 149°C (40.8 atm and 1.0 WHSV) Al PILMont converted 16.7% of the propene fed. Raising the temperature to 204, 371, and 426°C had little effect on conversion. At 482°C conversion increased to 58.8%; however, severe coking ocurred at this temperature. The liquid product contained 80.3% gasoline.

Yuying (1986) used Al PILMont to oligomerise propene in a pulse reactor at 240°C and atmospheric pressure. They found that the activity of dried Al PILMont was lower than that of H ZSM-5 and other molecular sieves for this reaction. The deactivation rate of the pillared clay was the highest among the catalysts tested. The selectivity for producing the higher carbon number oligomers was distinctly higher in the case of Al PILMont than in the case of H ZSM-5. This was ascribed to the larger pore size of Al PILMont than that of H ZSM-5.

1.1.8 Clays pillared with Other Hydroxy-Metal Cations

1.1.8.1 Zirconium Pillared Clays

Vaughan et al. (1979) reported the synthesis of Zr PILC's using hydroxy-zirconium cations prepared using different preparation parameters. Basal spacings of the pillared clays varied from 16.8 to 22 A, while BET surface areas varied in the range 262 - 309 m^2/g.

Lussier et al. (1980) compared the activity and selectivity of Zr PILC's with that of amorphous silica alumina and a zeolite in the cracking of gas oils. The product yields reported were similar to those of the amorphous catalyst, but with increased C_5^+ gasoline selectivity and reduced coke yield. It was suggested that the difference between the PILC and the amorphous catalyst was related to the pore size of the PILC. Occelli and Finseth (1986) compared the cracking activity of Zr-

PILC's with that of analogous Al and mixed Al-Zr PILC's. From their results they concluded that cracking activity was independent of the nature of the pillar which was present. They found that pillared hectorites were less active than pillared montmorillonites, but that the products of the hectorite catalysts contained greater gasoline fractions and lower C_2 - C_4 fractions. They ascribed these differences to the lack of metal contaminants in the hectorite clay.

Kikuchi et al. (1983) studied the activities of a range of PILC's in the conversion of methanol to hydrocarbons. Of all the materials tested only Al and Zr PILC's showed good activity and stability. They found that the proportion of C_2 - C_4 olefins was quite high, at about 49 mol%. Zr PILC's were shown to produce less aromatic hydrocarbons than Al PILC's and this was attributed to narrower layer spacing of the Zr PILC's.

Burch and Warburton (1986) studied the activity of various Zr PILC's in the methanol dehydration reaction and found that the activities of the clays followed an inverse relationship with surface area. Differences in acidity were not thought to be responsible for this effect. Instead these researchers suggested that the dimensions of the PILC's are important, to the extent that large cavities are less able to activate the dimethyl ether intermediate formed in the dehydration reaction. In contrast to the activity, the selectivity was less dependent on the method of preparation, or on the dimensions of the PILC's. C_2 - C_4 olefins comprised up to 65% of the hydrocarbon products.

Bartley and Burch (1986) studied the activity and selectivity of various copper impregnated Zr PILC's for the direct synthesis of olefins from a Co/H_2 gas mixture. The intention was to use the copper to produce methanol in contact with the Zr PILC which would then dehydrate the methanol to give hydrocarbon products. The activities observed were very low, but the results showed that the direct synthesis of olefins from CO/H_2 mixtures was possible using Cu/Zr PILC's.

1.1.8.2 Chromia Pillared Clays

Tzou and Pinnavia (1988) reported that smectites can be pillared with large polyoxochromium cations. The x-ray basal spacings of the pillared

products depended in part on the extent of metal ion hydrolysis and the overall metal ion/clay ratio used in the pillaring reaction. In general, basal spacings varied from 18 - 28 A. Thermal dehydration/ dehydroxylation of smectite clays pillared with polyoxochromium cations resulted in their conversion to chromia pillared clays.

Pinnavia et al. (1985) investigated the use of chromia pillared clays as catalysts for the dehydrogenation of cyclohexane to benzene. They compared the activities of the pillared clays with a commercially used catalyst (Cr_2O_3 dispersed on alumina) and found that, depending on the chromia pillar preparation method used, the pillared clays were more active or less active than the commercial catalyst.

Carrado et al. (1986) reported alternative approaches to chromium containing pillared clays. These workers prepared "heteroionic" species in which Al_{13} oligomers served as the pillaring precursor and Cr(III) was doped into the pillar structure or onto the gallery surface between alumina pillars. The former species was prepared by doping Cr(III) into the Al_{13} ion prior to use in pillaring. This led to a kind of hybrid "chromalumina" pillared clay in which the transition metal was believed to be an integral part of the pillar structure. The reaction of a pre-exchanged Cr^{3+} montmorillonite with Al_{13} oligomers yielded a "Cr^{3+} - alumina" pillared clay in which the transition metal was thought to reside on the gallery surface between pillaring alumina aggregates. Both the chromalumina and Cr^{3+} - alumina pillared clays exhibited higher activity than alumina pillared clays for hydrocracking of n-decane at 400°C.

1.1.8.3 Iron Oxide Pillared Clays

The hydrolysis behaviour of Fe^{3+} is similar to that of Al^{3+} and Cr^{3+} ions in forming polymeric cations . Herrera and Peech (1970) investigated the uptake of hydrolysed Fe^{3+} by montmorillonite. They found that exchanged hydroxy-Fe cations were easily removed from the clay upon washing with water. Yamanaka et al. (1984) successfully prepared iron oxide pillared montmorillonite using the trinuclear acetate iron(III) ion, $[Fe_3(OCOCH_3)_7OH]^+$. The basal spacing of the pillared clay was found to be 21.5 A. Upon heating at 500°C, the basal

spacing decreased to 16.7 A. Dhar et al. (1986) also attempted to prepare iron oxide pillared clays in a similar manner. They obtained iron oxide pillared clays having smaller basal spacings of around 14 A and BET surface areas of ca. 150 m^2/g. These discrepancies have been attributed to differences in temperatures at which crosslinking took place.

Kiyozumi et al. (1984) studied the catalytic activities of hydrogen reduced iron oxide pillared clays in the conversion of a synthetic gas (CO/H_2 = 1) to olefins. The reactions were performed at a pressure of 10 kg/cm^2 and at temperatures ranging from 290 to 360°C. The selectivity for the formation of lower hydrocarbons C_1 - C_5 reached 84 - 100% among the products other than CO_2. A selectivity for lower olefins (ethene and propene) of between 16 and 38% was attained. These workers concluded that the iron oxide pillared clay catalyst possessed remarkable shape selectivity. This molecular shape selectivity was attributed to steric factors originating in the micropores of the pillared clay.

1.1.8.4 Silica Alumina Pillared Clays

Sterte and Shabtai (1988) have reported a method for preparing hydroxy-Si/Al oligocations for use as pillaring species. The method involves the addition of tetraethyl orthosilicate to a hydroxy-Al solution. It was proposed that, in so doing, $Si(OH)_3$ groups are incorporated onto the pillaring cation according to the equation

$$[Al_{13}O_4(OH)_{23}(H_2O)_{12}]^{7+}\text{—}OH + Si(OH)_4 \longrightarrow$$
$$[Al_{13}O_4(OH)_{23}(H_2O)_{12}]^{7+}\text{—}O\text{—}Si(OH)_3 + H_2O.$$

In theory, all OH groups present on the cation can be replaced by silanol groups. These researchers reported that ion exchange of montmorillonite with the hydroxy-Si/Al oligocations yielded a pillared clay with a basal spacing of 19.5 A and significantly higher acidity when compared with Al PILMont. It was proposed that calcination of the Si/Al PILMont clay led to the formation of stable silica alumina pillars.

Gaaf et al. (1983) reported that treating a 100% swellable Ni-SMM clay with a hydroxy-Si/Al solution decreased the BET surface area of the clay from 170 m^2/g to 125 m^2/g. XRD indicated only a weak signal

corresponding to the basal spacing of an expanded layer structure. The original 001 peak was still present. They attributed the decrease in the surface area of the clay to the agglomeration of Ni-SMM particles in the basal direction.

1.1.8.5 Mixed Metal Oxide Pillared Clays

Shabtai and Fijal (1986) and Vaughan (1987) reported methods for preparing pillared clays with multimetallic pillars. The basic structure of the polycationic pillaring species is similar to that of the Al_{13}^{7+} Keggin ion and may be written

$$N^{IV}(Al_{12-x}M_x)^{VI}O_4(OH)_{24}^{+a}$$

where N may be Al^{3+}, Si^{4+}, Ga^{3+}, Ge^{4+}, As^{5+}, Cr^{3+}, Fe^{3+}, V^{5+}, Ru^{3+}, Ru^{4+}, or Ni^{3+}; M may be one or more of the elements of Groups 5B, 6B, 7B and 8 of the fourth, fifth, or sixth periods of the Periodic Table. The value of x may be from about one to six and the value of a depends on the nature of the metal substitutions.

1.2 LANTHANUM EXCHANGED H ZSM-5

The zeolite ZSM-5 was first synthesised in the early seventies (Argauer and Landolt, 1972). The catalyst belongs to a group of zeolites called pentasils. It is built of five membered rings, eight of which form a building unit. These units are linked through edges to form chains. The chains are connected into sheets, which then link to form the three dimensional framework. The channel structure contains two intersecting channel systems, one sinusoidal (5.4 A x 5.6 A) and the other straight (5.1 A x 5.5 A), which are believed to be responsible for shape selective catalysis. The catalyst has been used in a number of important industrial processes. These include disproportionation of toluene, xylene isomerisation, and alkylation reactions. It has also been found to be particularly suitable for converting methanol to gasoline and olefins (Chang and Silvestri, 1977; Derouane et al., 1978; Chang et al., 1984), and for conversion of olefins to gasoline and distillate (Garwood et al., 1983; Tabak et al., 1986). Although a number of zeolites are reported in the literature as being active for olefin oligomerisation, at present by far the most promising method for the oligomerisation of light olefins is the MOGD process (Garwood et al., 1972; Garwood and Lee, 1980; Tabak, 1984). This process has been tested using commercial scale equipment in a Mobil refinery (Tabak, 1984) and makes use of ZSM-5 type catalysts.

In attempting to modify the activity and selectivity of H ZSM-5 for various reactions, much research has been carried out on ion exchanging the acidic protons within the channels of the catalyst with various metal cations. This ion exchange may cause a redistribution of the relative number of Bronsted and Lewis acid sites on the catalyst and may also alter the effective pore sizes.

Large pore rare earth zeolites are frequently referred to in the patent literature for use as cracking catalysts (Chiang and Staniulis, 1986; Miller and Bishop, 1982; Lindsley, 1978). In such catalysts, alkali metal cations, such as sodium, are exchanged with rare earth and ammonium cations in order to reduce alkali metal content. This process improves the thermal stability and catalytic activity of the zeolite.

In a recent Mobil patent (Owen et al., 1984) describing a method for converting olefins into gasoline and distillate using ZSM-5 (MOGD process), reference is made to a rare-earth exchanged ZSM-5 catalyst. It is unlikely that the reason for incorporating rare earth ions into such a catalyst is the enhancement of thermal stability since ZSM-5 is known to be stable up to temperatures far in excess of those encountered in the MOGD process (Buckley and Tallon, 1986). Chen et al. (1988) report that rare earth exchanged Zeolite X, calcined at 540°C, still exhibits considerable cracking activity when contacted with various heavy crude oil fractions at temperatures as low as 250°C. One possible reason for the incorporation of rare earth ions into MOGD catalysts, therefore, may be the ability of such ions to crack heavy coke precursors at relatively low temperatures, thereby extending the life of the catalyst.

1.3 MECHANISM AND THERMODYNAMICS OF PROPENE OLIGOMERISATION

1.3.1 Mechanism of Polymerisation

The most widely accepted mechanism for the polymerisation of olefins involves the formation of a carbonium ion (Whitmore, 1932). Acid catalysts can generate carbonium ions in alkenes by adding a proton to the extra electron pair in the double bond. Alkenes may undergo different types of polymerisation, namely, true polymerisation, conjunct polymerisation, and co-polymerisation. In true polymerisation, the products consist of alkenes having molecular weights which are integral multiples of the monomer alkene. Conjunct polymerisation yields a complex mixture of alkanes, alkenes, alkadienes, cyclo-alkenes and cyclo-alkanes, and aromatics. The number of carbon atoms in these products are not integral multiples of the monomer. Co-polymerisation involves the interpolymerisation of two different alkenes. The term oligomerisation is used in this report to describe the process occurring during the reaction of olefins over acid catalysts. This process is largely true polymerisation with some conjunt polymerisation.

1.3.1.1 Propene Oligomerisation

Solid phosphoric acid is the most widely used catalyst for propene oligomerisation. This process is known as the CATPOLY process.

The carbonium ion true polymerisation mechanism for propene oligomerisation is shown below.

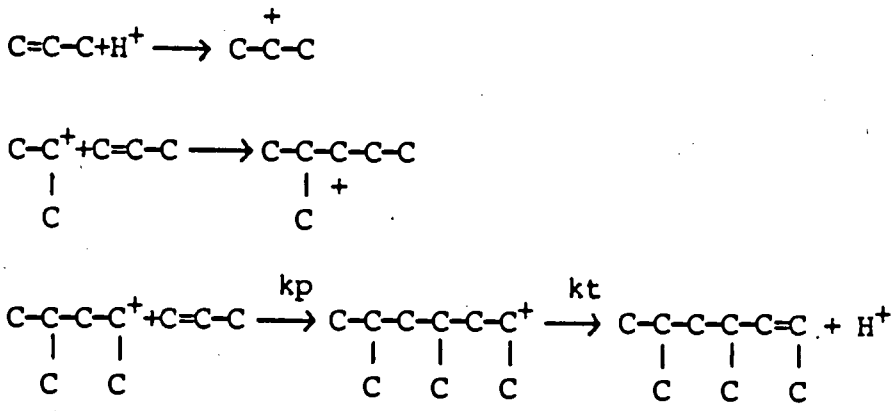

where kp = rate of further alkene addition (polymerisation)
kt = rate of proton expulsion to form an alkene (termination)

According to Germain (1969) the dimer should have the following structure:

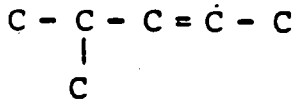

However, skeletal isomers will be present under most reaction conditions (Schmerling and Ipatieff, 1950).

The individual reaction steps for polymerisation have been proposed by Flory (1964): Let M represent the monomer, A the catalyst, SH the co-catalyst, and A.SH the catalyst / co-catalyst complex.

$$A.SH + M \longrightarrow HM^+ + AS^-$$

$$M_x^+ + AS^- + M \xrightarrow{kp} M^+_{x+1} + AS^-$$

$$M_x^+ + AS^- \xrightarrow{kt} M_x + A.SH$$

$$M_x^+ + AS^- + M \xrightarrow{ktr} M_x + HM^+ + AS^-$$

where ktr is the rate of carbonium ion transfer.

It was further shown by Flory (1964) that the average degree of polymerisation is given by:

i) $X = (kp/kt) \times [M]$ if chain termination dominates over chain transfer;

ii) $X = kp/ktr$ if chain transfer dominates over termination.

The carbonium ion mechanism does not hold for all acid catalysts. Hassan et al. (1977) found that the primary product (3-methylpentane) of propene dimerisation over zeolite catalysts could not be explained by a carbonium ion mechanism. Examination of the results suggested that a mechanism of dimerisation similar to that proposed by Imai et al. (1968) occurred. This mechanism assumes the formation of an intermediate of a cyclobutane derivative. The compounds are formed when a propene molecule reacts with one adsorbed on the zeolite surface as follows:

$$2CH_3 - CH = CH_2 \rightleftharpoons \begin{cases} CH_2\text{------}CH_3 - CH \\ \quad\vdots\qquad\quad\vdots \\ CH - CH_3\text{------}CH_2 \end{cases} \quad (I)$$

$$\rightleftharpoons \begin{cases} CH_2\text{------}CH - CH_3 \\ \quad\vdots\qquad\quad\vdots \\ CH_2\text{------}CH - CH_3 \end{cases} \quad (II)$$

The dimethyl cyclobutanes formed, I and II, are unstable complexes and are either converted to the initial molecules or undergo bond rupture. The bond rupture of the two complexes leads to the formation of extremely unstable complexes which undergo rearrangement and hydrogen redistribution. The rearranged structure desorbs as a propene dimer. If the rate of desorption is relatively slow, the dimer can adsorb another propene molecule forming a similar unstable complex which, again, is converted either to the initial state or undergoes bond rupture and hydrogen redistribution to form propene trimers. Similarly, tetramers and pentamers, etc., can be formed.

1.3.2 Thermodynamics of Polymerisation

Oblad et al. (1958) have studied the thermodynamics of olefin oligomerisation. They investigated the free energy changes accompanying the dimerisation of ethene, propene and hexene in the temperature range 300 - 900 K and found that lower temperatures favour polymerisation. The results also indicated that, at any given temperature, the dimerisation of ethene is more favourable than that of other light olefins. They found that the dimerisation of terminal bond olefins to isomers of the corresponding higher olefins at a given temperature is more favourable than the dimerisation to higher terminal olefins.

The same researchers studied the effect of pressure and temperature on the equilibrium condition of the dimerisation reaction

$$2C_3^{=} \longrightarrow \text{1-hexene.}$$

They found that the dimerisation reaction is favoured by low temperatures and high pressures. These researchers also investigated the free energy changes taking place during the polymerisation of propene to higher molecular weight polymers as a function of temperature (300 - 800 K). They found that at higher temperatures (> 550 K) free energy changes favoured the formation of low molecular weight oligomers, whereas at low temperatures, the higher molecular weight polymers were favoured. At temperatures above 550 K, free energy changes favoured the cracking, rather than the formation, of polymerised products.

1.4 OBJECTIVES OF RESEARCH

The objectives of the present research were as follows:

(i) To investigate the effect that pillaring has on the physical and catalytic properties of some smectite clays. The effects of using a hydroxy-Al solution to pillar a predominantly octahedrally substituted clay (montmorillonite) and a tetrahedrally substituted clay (beidellite) were compared. The effects of pillaring tetrahedrally substituted clays which have different swellable properties (beidellite, SMM, and Ni-SMM) were investigated. In an attempt to enhance the acidic properties of the pillars, montmorillonite was pillared with a hydroxy-Si/Al solution. Montmorillonite was also pillared with a hydroxy-Ni/Al solution in an effort to produce a clay with a higher pillar density. The pillared and unpillared clays were characterised using x-ray diffraction, surface area measurements, thermogravimetric analysis, and ammonia temperature programmed desorption. The possible shape selective properties of the different clays for the conversion of trimethylbenzene were investigated, and the catalytic activities and product selectivities of these clays for high pressure propene oligomerisation were studied.

(ii) To investigate how ion-exchanged lanthanum affects the catalytic activity of H ZSM-5. The ZSM-5 catalysts were characterised using x-ray diffraction, scanning electron microscopy, thermogravimetric analysis, and ammonia temperature programmed desorption. The catalytic activities and product selectivities of the catalysts were studied for two reactions, namely, high pressure propene oligomerisation and atmospheric hexane cracking.

2 EXPERIMENTAL

2.1 Catalyst Synthesis and Preparation

2.1.1 Clay minerals

2.1.1.1 Clay Sources

Montmorillonite was supplied by Boland Base Minerals (Pty) Ltd. The sample was a naturally occurring clay. The chemical composition and cation exchange capacity of the sample, as provided by the suppliers, were as follows (composition in mass %):

SiO_2	:	65.1
Al_2O_3	:	20.4
Fe_2O_3	:	4.8
Cao	:	2.1
MgO	:	4.4
K_2O	:	0.3
Na_2O	:	2.8
moisture	:	12% max
CEC	:	96 meq/100g

SMM and Ni-SMM were obtained from the Harshaw/Filtrol Corporation. The nickel content of the Ni-SMM clay (as reported by the suppliers) was 7% by mass. This clay will be referred to as Ni-SMM(7) hereafter.

2.1.1.2 Clay Synthesis

2.1.1.2.1 Beidellite

Beidellite was synthesised according to a slightly modified version of a nitrate decomposition method described by Diddams (1989). Diddams' synthesis procedure was found to result in very low product yields. Less than 15% of solids present in the reactor had a crystalline clay structure after the specified synthesis period. In an effort to increase product yields, a number of syntheses were carried out using slight

variations of the gel preparation technique described by Diddams. These variations included:

(i) The order in which the reactants were mixed (dropwise addition of aluminium source to silica source as opposed to the reverse process);

(ii) The effect of "ageing" the gel for a period of three days prior to calcination; and

(iii) Increasing the pH of the gel (three times more NaOH was used than was specified).

The synthesis procedure which was found to give the greatest product yield is described below. It differed from Diddams' procedure only in the order in which reactants were mixed.

21.09 g of colloidal silica (40% by mass silica) were dissolved in 100 ml of deionised water and stirred at room temperature for ten minutes. The solution was then heated to 80°C with stirring (solution A). 600 ml of deionised water was heated to 80°C and 1.406 g NaOH and 26.38 g $Al(NO_3)_3.9H_2O$ were added (solution B). Solution A was then added to solution B, dropwise, over a period of one hour with vigorous stirring. The resulting gel was stirred for a further two hours at 80°C before being evaporated to dryness at 110°C. The dried material was calcined at 700°C for four hours and was then ground to a fine powder before being redispersed in 250 ml of deionised water. The suspension was transfered to a high pressure autoclave where crystallisation took place at 300°C under water vapour pressure (85 atm) for five days. The product was centrifuged and washed before being dried at room temperature. The as-synthesised beidellite clay was in the sodium exchanged form.

2.1.1.2.2 Ni-SMM

In an attempt to synthesise a 100% swellable Ni-SMM clay, the following procedure was used (Gaaf and Van Santen, 1983): 19.93 g of nickel acetate.4aq. was dissolved in 300 ml of deionised water. To this was added 10g of dried silica (Aerosil supplied by Degussa), 11.75 g of

aluminium isopropoxide, and 0.205 g of ammonium fluoride. The resulting mixture was heated at 90°C for 20 hours with stirring, after which 2 ml of ammonia (25% by mass ammonia) was added. The gel was transferred to a high pressure autoclave where crysatllisation took place at 300°C under water vapour pressure for 40 hours. The resulting product was filtered, washed with deionised water, and dried at room temperature. This clay will be referred to as Ni-SMM(21) hereafter (subsequent Ni analysis indicated that the clay contained 21% Ni by mass). The as-synthesised Ni-SMM(21) clay was in the ammonium exchanged form.

2.1.1.3 Ammonium Ion Exchange of Montmorillonite and Beidellite

The following procedure was used to exchange the existing charge balancing cations on montmorillonite and beidellite with NH_4^+ cations: 5 grams of clay was dispersed in a solution containing 40 ml of a 25% NH_3 solution and 150 ml of deionised water. The suspension was stirred for 24 hours before being filtered and washed. Samples were dried at room temperature.

2.1.1.4 Preparation of Pillaring Solution

2.1.1.4.1 Hydroxy-Aluminium Solution

A hydroxy-Al pillaring solution was prepared following the method described by Lahav et al. (1978): 9.658 g $AlCl_3.6H_2O$ was dissolved in 200 ml H_2O. 370 ml of 0.2 M NaOH was added to this, dropwise with stirring, over a period of two hours. This results in a OH/Al ratio of 1.85. The solution was aged at between 90 and 100°C under reflux for seven hours. After ageing, the solution was allowed to cool to room temperature and was used, without further delay, to pillar 20 g of clay. (2 mmol of Al in the pillaring solution were added for each gram of clay).

2.1.1.4.2 Hydroxy-Si/Al Solution

A hydroxy-Si/Al pillaring solution was prepared according to a procedure reported by Shabtai and Sterte (1988): a hydroxy-Al solution was prepared and aged as described above. For a pillaring solution with a

Si/Al ratio of one, 570 ml of the hydroxy-Al solution was diluted with 2.28 litres of deionised water. 8.00 g of tetraethyl orthosilicate, dissolved in 100 ml of ethanol, was added to this, dropwise with stirring, over a period of five hours. For a Si/Al ratio of two, 570 ml of the hydroxy-Al solution was diluted with 4.56 litres of deionised water. Twice as much tetraethyl orthosilicate and ethanol was used, while the rate of addition to the Al solution was the same. In both cases, solutions were used to pillar 20 g of clay without further ageing (2 mmol Al/g clay).

2.1.1.4.3 Hydroxy-Ni/Al Solution

A hydroxy-Ni/Al pillaring solution was prepared according to a method outlined by Shabtai and Fijal (1986): A hydroxy-Al solution was prepared and aged as described in Section 2.1.1.4.1. 54 ml of a 0.1 M aqueous solution of $NiCl_2$ and $AlCl_3$, having a Ni/Al molar ratio of 21, and 93 ml of 0.1 M NaOH were added simultaneously to 257 ml of the Al solution. This solution was used to pillar 9 g of clay without further ageing.

2.1.1.5 Pillaring Procedure

Before pillaring the montmorillonite, which was a naturally occurring mineral, the > 2 um fraction of the clay was removed using a sedimentation procedure described by Brown (1961). This was done in order to remove impurities such as SiO_2 which are generally present as > 2 um particles. The clay was dispersed in water (15 g/litre) and stirred for two hours before being allowed to sediment for 230 minutes (depth = 5 cm). In the case of the beidellite, SMM and Ni-SMM clays, particles were crushed to below 75 um prior to pillaring.

Two different methods were used for pillaring the clays:

Method 1 (Shabtai et al., 1984)

The apparatus used for pillaring clays via this method is shown in Figure 2.1.

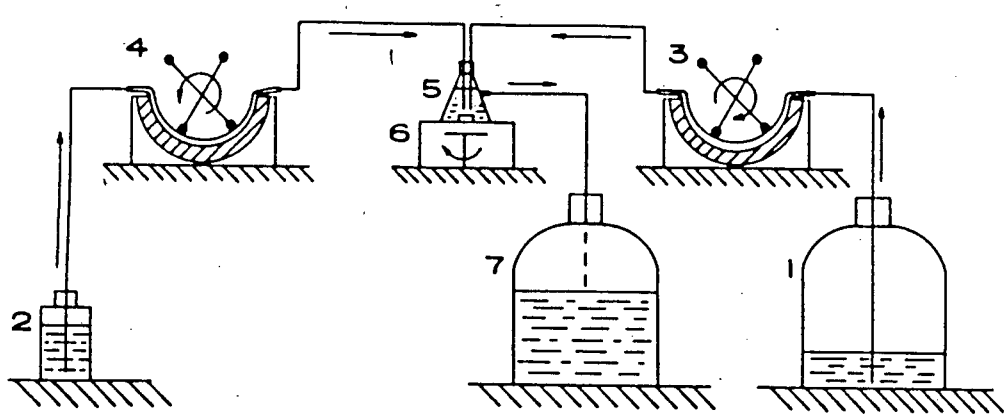

Figure 2.1: Schematic of Pillaring Apparatus (Method 1). {1 = smectite dispersion; 2 = pillaring solution; 3 and 4 = peristaltic pumps; 5 = mixing chamber; 6 = magnetic stirrer; 7 = product receiver}

Prior to pillaring, the clay was dispersed in water (2.5 g/litre) and stirred overnight. Pillaring was carried out by pumping the clay suspension and pillaring solution, at the appropriate flowrates, into a mixing chamber where pillaring took place. The residence time in the mixing chamber was ten minutes. The pillared product was allowed to stand in the product receiver for 15 hours before being removed for washing.

Method 2

Prior to pillaring, the clay was dispersed in water (5 g/litre) and stirred overnight. The pillaring solution was rapidly added to the clay suspension which was then stirred for four hours before being allowed to stand for 20 hours.

After treatment with the pillaring solutions using either of the above methods, the clays were repeatedly filtered and washed until the addition of $AgNO_3$ to the filtrate did not indicate the presence of chloride ions. The pillared clays were dried at room temperature before being crushed and sieved to the appropriate size fractions.

Montmorillonite was pillared with the hydroxy-Al solution using both methods 1 and 2. From the results of x-ray diffraction analysis of the two pillared clays, it did not appear as if method 1 held any advantage over the more straight forward method 2. All other clays used for this work, therefore, were pillared using method 2.

When treating the SMM, Ni-SMM(7) and Ni-SMM(21) clays with the hydroxy-Al solution, a montmorillonite sample was treated, in each case, with the same pillaring solution under identical conditions. This was done due to the fact that the nature of the pillaring solution is highly sensitive to preparation procedure. A comparison of the pillared montmorillonite samples would be expected to reveal any major differences in the three Al solutions used.

The following abbreviations will be used to denote the various pillared clays:

Al PILMont: Montmorillonite treated with the hydroxy-Al solution.
Si/Al PILMont(1) & (2): Montmorillonite treated with the hydroxy-Si/Al solution, with (1) and (2) denoting Si/Al ratios of one and two, respectively, in the pillaring solution.
Ni/Al PILMont: Montmorillonite treated with the hydroxy-Ni/Al solution.
Al PILBeid: Beidellite treated with the hydroxy-Al solution.
Al PILSMM: SMM treated with the hydroxy-Al solution.
Al PILNi-SMM(7): Ni-SMM(7) treated with the hydroxy-Al solution.
Al PILNi-SMM(21): Ni-SMM(21) treated with the hydroxy-Al pillaring solution.

2.1.2 ZSM-5

2.1.2.1 Synthesis

ZSM-5 was synthesised according to the method of Argauer and Landolt (1973). Aluminium hydroxide was dissolved in an aqueous sodium hydroxide solution, thus forming sodium aluminate. This was added to a solution of tetrapropylammonium bromide. Ludox (40% by mass colloidal silica) was then added to the reactant mixture, forming a thick gel. The Si/Al ratio charged to the synthesis mixture was 40. The gel was transferred to an

autoclave where crystallisation took place at 160°C for a period of three days. After allowing the autoclave to cool, the catalyst was filtered, washed repeatedly with deionised water, and dried at 80°C. The catalyst was detemplated by heating it in flowing nitrogen up to 500°C and then switching the carrier to air.

2.1.2.1 Preparation of NH_4^+ and La^{3+} Exchanged ZSM-5

The ammonium form of ZSM-5 was made by ion exchanging 15 g of the detemplated catalyst with one litre of a 2 M solution of ammonium nitrate under reflux at 80°C for 24 hours.

Two lanthanum exchanged forms of the catalyst were then prepared from the ammonium exchanged ZSM-5. The exchanges were achieved as follows:

(i) 10 grams of catalyst were contacted with 200 ml of a 0.1 N $LaCl_3$ solution under reflux at 80°C for 24 hours. The catalyst was then filtered, washed thouroughly with distilled water, and dried at 80°C.

(ii) 10 grams of catalyst were contacted with a $LaCl_3$ solution, as described above, for eight hours. The catalyst was then filtered, but not washed, and calcined at 500°C in flowing air for four hours. This procedure was repeated three times. Finally, the catalyst was washed thouroughly with deionised water and dried at 80°C.

Two more catalysts were prepared for the purposes of comparison with the lanthanum exchanged samples. The ammonium ZSM-5 was contacted with a NaCl solution to effect a 5% and 25% exchange of sodium for ammonia.

2.2 Catalyst Characterisation

2.2.1 X-Ray Diffraction

X-ray diffraction was carried out on catalyst samples using a Philips diffractometer. The following settings were used:

Radiation	:	CuK_{alpha} with a wavelength of 154 pm
Slits	:	1/2" ; 1/2" ; 1"
Current	:	30 mA
Voltage	:	40 kV

When examining the basal spacings (001 diffraction peaks) of clay minerals, Brown (1961) suggests that samples for analysis be prepared by drying a small amount of an aqueous solution of < 2 um clay particles on a glass slide. This ensures a well ordered orientation of particles on the surface of the sample and increases the intensity of the first order basal peaks. It was found, however, that packing < 75 um clay powder into a perspex holder 1 mm deep and orienting the sample surface by applying pressure with a glass slide gave good results. As it proved difficult to obtain a < 2 um size fraction from some of the clay samples, the latter procedure was used for sample preparation. Samples were scanned in the range $2\theta = 2^{\circ} - 15^{\circ}$.

In the case where XRD was used to characterise the structures of the synthesised clays, samples were prepared by packing < 75 um clay powder into a 1 mm deep sample holder using a "backloading" technique. This results in a more random orientation of particles on the sample surface which leads to the supression of basal peaks and the enhancement of structural peaks. Samples were scanned in the range $2\theta = 2^{\circ} - 65^{\circ}$.

Similarly, when characterising the synthesised ZSM-5 catalyst, samples for XRD analysis were prepared using the backloading technique. The scan range used was $2\theta = 7^{\circ} - 25^{\circ}$.

2.2.2 Nickel, Sodium and Lanthanum Analysis

Nickel analysis of the synthesised Ni-SMM(21) and Ni/Al PILMont clays was carried out by the Department of Geochemistry, UCT, using x-ray fluorescence. Standards were prepared using mixtures of nickel oxide and SMM.

The sodium content of the ZSM-5 catalysts was determined by atomic absorption spectrophotometry.

Lanthanum analyses of ZSM-5 samples were carried out by Mintek.

2.2.3 Kevex and SEM Analysis

A Cambridge S180 scanning electron microscope (SEM) was used to take micrographs of the synthesised ZSM-5 catalyst. The crystallite size distribution of the catalyst on a number basis was obtained by measuring and counting all clearly visible crystals.

The Si/Al ratios of the ammonium and 25% exchanged ZSM-5 samples were obtained using the Si(Li) detector of a Kevex model 7000 energy dispersive x-ray (EDX) spectrophotometer mounted in the sample chamber of the SEM.

2.2.4 Thermogravimetric Analysis

TG and DTA studies were performed using a Stanton - Redcroft STA 780 Simultaneous Analyser. Quartz glass was used as a reference. Between 12 and 15 mg of sample were used. Other than for coke studies, samples were in the size range < 75 um. All experiments were performed at atmospheric pressure.

2.2.4.1 Calcination

Pillared and unpillared clay samples were heated from room temperature to 750°C at a rate of 3°C/min under flowing nitrogen (30ml/min.).

2.2.4.2 Propane Adsorption

Clay samples were calcined in the thermal analyser at 500°C in flowing nitrogen (60 ml/min) for four hours prior to adsorption. Propane adsorption was carried out at at a temperature of 30°C for six hours using nitrogen as a diluent (20 ml/min N_2 and 10 ml/min propane). The propane feed was passed over a 3A molecular sieve in order to remove moisture.

2.2.4.3 Hexane Adsorption

The adsorption of n-hexane onto the ZSM-5 catalysts was carried out at 35°C. Prior to adsorption, the catalyst samples were calcined at 500°C in flowing nitrogen (60 ml/min) for two hours. Nitrogen (30 ml/min) flowed through a saturator filled with n-hexane at 25 °C before being passed over the adsorbate.

2.2.4.2 Coke Studies

Coked clay samples from propene oligomerisation runs were transferred to the thermal analyser and were heated from room temperature to 500°C at a rate of 10°C/min. Samples were held at this temperature for 352 minutes. Nitrogen (60 ml/min) was passed over the catalysts for the first three hours, at which point the gas was switched to air (60 ml/min).

2.2.5 Surface Area Determination

The surface areas of the clay samples were estimated from the results of adsorption experiments performed by the Research and Development Department of AECI Limited. Experiments were carried out using a Carlo-Erba Sorptometer using nitrogen as the adsorbate. Prior to adsorption, samples were outgassed at 110°C for one hour. The volume of nitrogen adsorbed was measured at between seven and nine different relative pressures in the range 0.01 - 0.35 for all samples. Selected samples were calcined at 500°C for four hours prior to adsorption. These samples were exposed to atmospheric conditions between calcination and outgassing.

2.2.6 Ammonia Temperature Programmed Desorption (TPD)

2.2.6.1 Apparatus

Figure 2.2 shows a schematic representation of the ammonia TPD apparatus. Samples for analysis were packed in a quartz glass cell positioned in a furnace. A temperature programmer was used to control the sample temperature. A three way shut-off valve allowed either helium, air, or 4% ammonia in helium to flow through the system. Gas

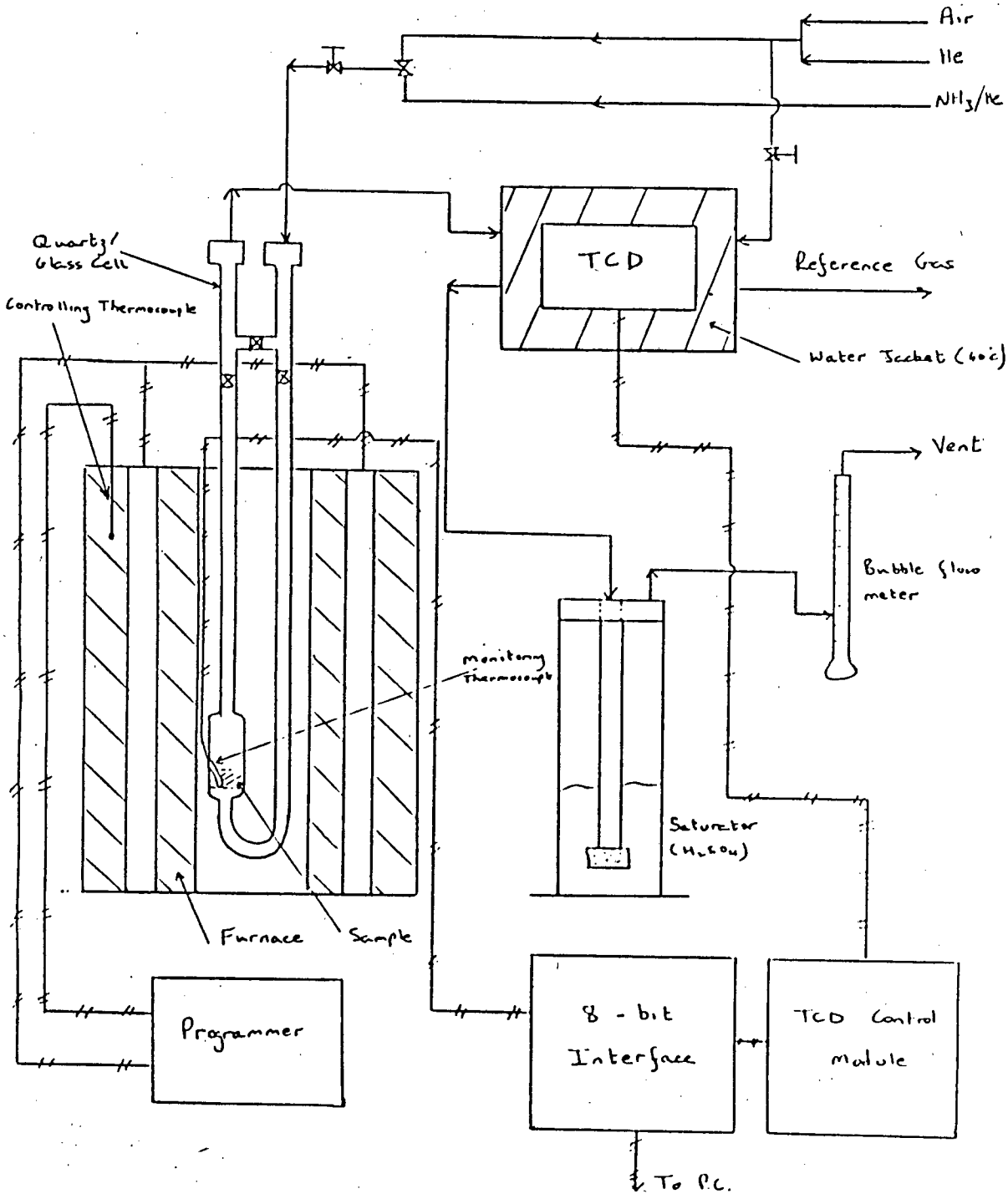

Figure 2.2: Ammonia TPD Apparatus.

flowrates were set using needle valves. Gases flowed upwards through the heated sample chamber and into a thermal conductivity detector fitted with four AuW filaments. The reference gas (helium) flowrate was 60 ml/min. From the TCD, the gases flowed into a saturator containing a 0.1 N sulphuric acid solution. Gases were then vented to the atmosphere. The TCD control module was linked to a personal computer via an eight bit interface. The interface supplied the PC with sample temperature, time, and thermal conductivity readings. A computer program was then used to convert and plot the data in the form (umol NH_3 desorbed)/g cat./°C vs. temperature. A numerical integration procedure was then used to obtain the total amount of ammonia which desorbed per gram of sample.

2.2.6.2 Experimental procedure

Clay samples for analysis were sieved to the size fraction 180 - 250 um. This relatively large size fraction was chosen to reduce the chances of bed fluidisation and the possibilty of TCD contamination by eluted particles. 500 mg of sample was packed in the quartz glass cell. Samples were calcined at 500°C for four hours in flowing air. The furnace was allowed to cool down to 100°C and was maintained at this temperature. The gas was switched to helium (60 ml/min) and the TCD reference gas was set at the same flowrate. The TCD unit was then switched on and the baseline signal was allowed to settle for a period of 30 minutes. After this time, the sample gas was switched to 4% ammonia in helium (60 ml/min) and ammonia adsorption on the catalyst sample was allowed to take place for 40 minutes at 100°C. The gas was then switched back to pure helium (60 ml/min). The temperature was maintained at 100°C for a further 40 minutes to allow desorption of weakly held ammonia molecules present on the catalyst sample to occur. At this point, the saturator was replaced with one containing a fresh H_2SO_4 solution. Temperature programming was then started. Samples were heated from 100 to 500°C at a rate of 10°C/min. The calcination temperature (500°C) was not exceeded in order to avoid the possibility of ammonia desorption and clay lattice dehydroxylation occurring simultaneously. The temperature was maintained at 500°C until the TCD indicated that no further ammonia was desorbing from the catalyst. The 0.1 N sulphuric acid solution was then titrated with 0.1 N NaOH to establish the total amount of ammonia which desorbed

from the catalyst during the experiment. This value was compared with that obtained from numerical integration of the converted TCD data.

In the case where the calcination temperature used for clay samples was lower than 500°C, "baseline" runs were performed using the identical procedure in the absence of ammonia. As the TCD is sensitive to water, dehydroxylation of the clay samples during temperature programming, which takes place when the temperature exceeds that used for calcination, will result in unrealistically high TCD readings. This is taken into account by subtracting the TCD readings recorded during the baseline run from those recorded during the run in which ammonia was adsorbed onto the catalyst.

The ammonia TPD procedure used for the ZSM-5 catalysts was the same as that used for the clay samples. Temperature programming, however, was carried out between 100 and 600°C.

2.3 Reaction Studies

2.3.1 Propene Oligomerisation

2.3.1.1 Reactor System

Figure 2.3 shows a schematic representation of the reactor system used for propene oligomerisation. The feed, which was a propane/propene mixture, was stored as a liquid in an inverted domestic gas cylinder. The feed flowed from the cylinder over a 3 A molecular sieve (used to remove moisture) and through a 30 micron filter to a high pressure diaphragm pump (Lewa Model FC-1). Ethylene glycol, at ca. -4°C, cooled the liquid feed to increase the pump head and thereby reduce the chances of cavitation. The pump head itself was also cooled by the ethylene glycol. The pump raised the system pressure to that set by the backpressure regulator. Close control of feed flowrates proved difficult and, as a result, WHSV's varied in a small range around the desired value. For example, for a reported WHSV of 5, actual space velocities generally varied in the range 4.5 - 5.5 hr^{-1}. From the pump, the feed passed through the reactor and on to a dome loaded diaphragm-type back pressure regulator, where the system pressure was reduced to

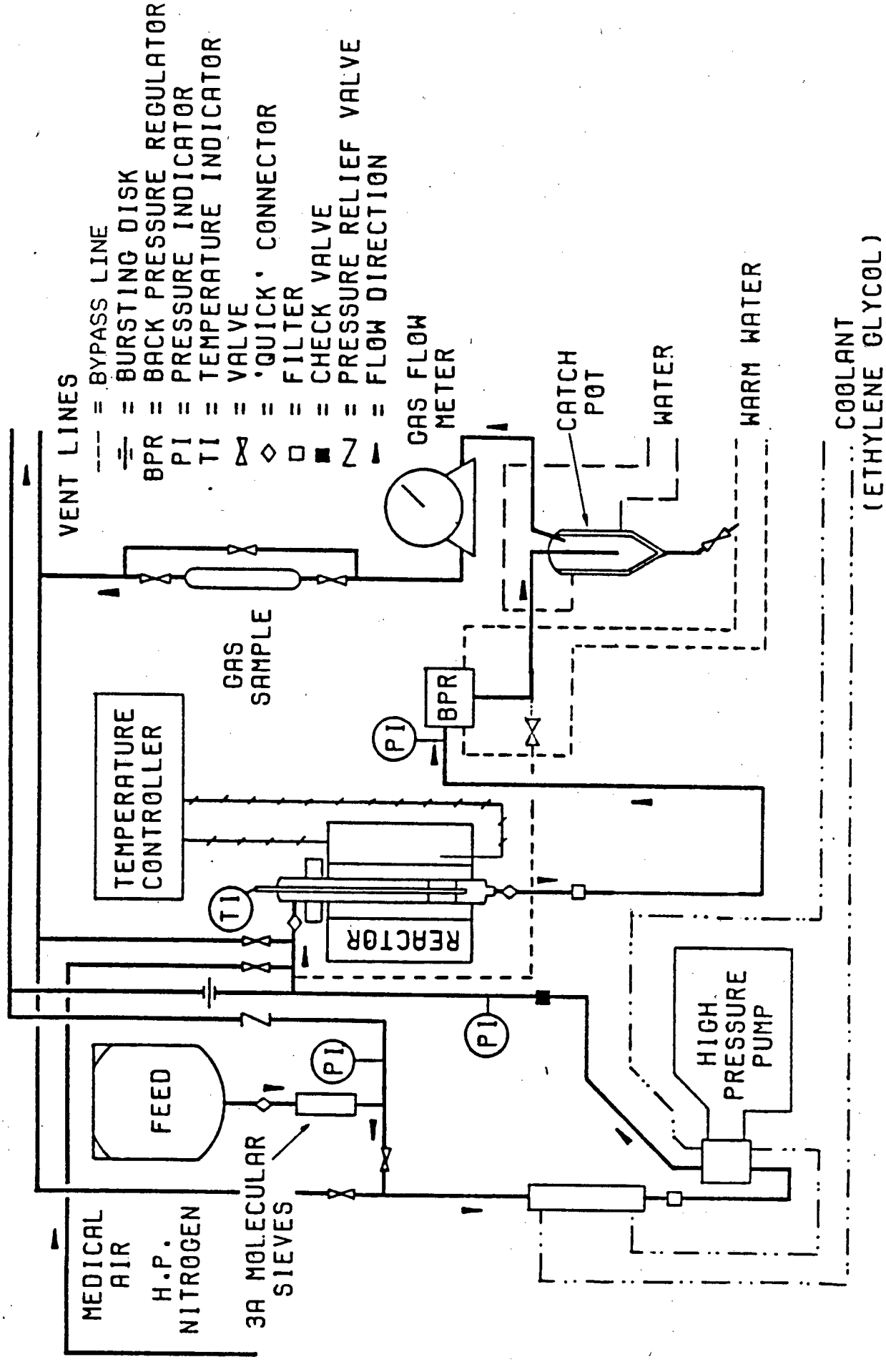

Figure 2.3: Propene Oligomerisation Reactor System

atmospheric. A filter protected the backpressure regulator against damage from eluted fine catalyst particles. The back pressure regulator was heated to ca. 60°C since the cooling which resulted from the flash vaporisation of the unreacted gases was severe enough to "freeze" the diaphragm in an open position.

A bypass line was available for use during start-up. A needle valve was present for the control of gas flowrates during calcination. Phase separation of the reactor effluent took place in a jacketed catch-pot which was maintained at around 15°C. After separation in the catch-pot, the effluent gas flow was measured using a wet gas flowmeter, sampled and, finally, vented.

All tubing upstream of the pump was 1/4" O.D., whilst downstream of the pump 1/8" tubing was used. All metallic fittings were made of 316 stainless steel.

Figure 2.4 shows the small integral reactor which was used. The reactor was made essentially of a stainless steel tube (I.D. = 1.8 cm) and was surrounded by a heating jacket fitted with four 500 W cartridge heaters. The cartridge heaters extended the full length of the heating jacket and provided a uniform reactor temperature to above 600°C. A thermocouple, situated between the reactor wall and the heating jacket, and a RKC temperature controller connected to the cartridge heaters were used to control the temperature of the heating jacket. A moveable thermocouple, situated in a thermowell which extended longitudinally through the centre of the reactor, was used to monitor temperatures in the catalyst bed and in the preheat section.

The catalyst bed rested on a plug of quartz glass wool (ca. 1 cm long) which was sandwitched between two stainless steel wire gauzes. For all experiments, 1 g of catalyst was used. In the case of the clay catalysts, particle size was in the range 106 - 212 um. This corresponded to a volume of ca. 1.1 cm^3, resulting in a bed depth of around 0.43 cm. The ZSM-5 samples used were in a fine powder form, the catalyst bed depth being slightly smaller than that of the clay samples.

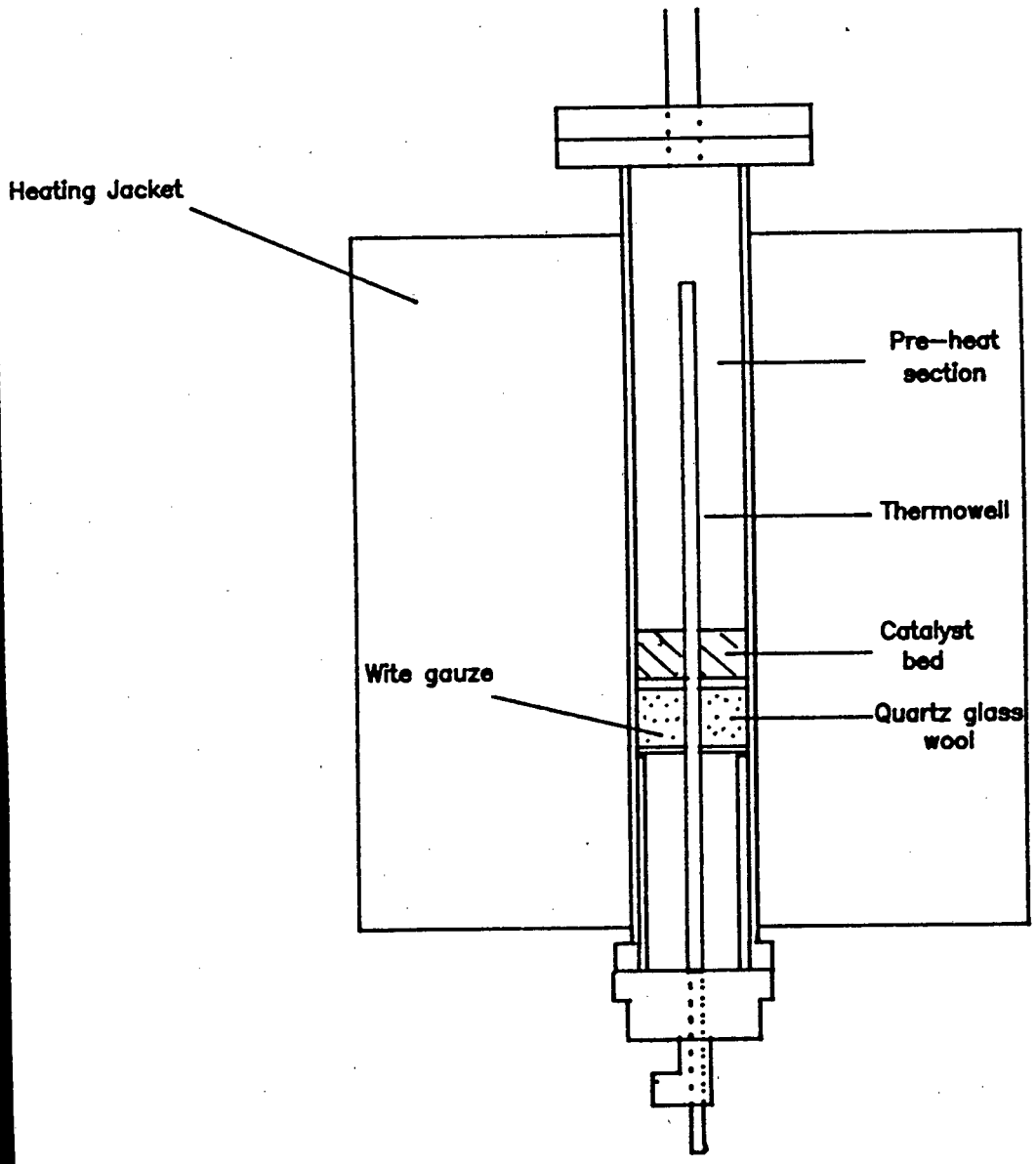

Figure 2.4: Reactor for Propene Oligomerisation.

2.3.1.2 Run Procedure

Catalyst samples were calcined at 500°C in air (60 ml/min). The bed was raised to this temperature over a period of approximately one hour and was held at that temperature for ten hours, after which time the reactor was allowed to cool down to room temperature. Air flow was maintained during the cooling period.

The feed used for all the experiments was a propane/propene mixture obtained from Sasol (see Section 2.6.3.1 for detailed feed gas analysis).

After cooling the reactor to room temperature, the backpressure regulator was set at 5 MPa using high pressure nitrogen, and the feed pump was turned on. The feed was allowed to bypass the reactor for a period of ten minutes in order to remove any residual feed from the lines which may have accumulated moisture. As the activities of the different catalysts used for this study varied considerably for this reaction, three different run procedures were used. For all the clay samples, the WHSV (based on the total feed) was maintained in the vicinity of 5 $^{-h}$, while for the ZSM-5 samples, a WHSV of 10 was used. Reaction was carried out at a pressure of 50 atm in all cases.

The montmorillonite and beidellite clays in their pillared and unpillared forms did not show appreciable activity for propene oligomerisation below 200°C. Furthermore, once reaction temperature was reached, the catalysts were seen to deactivate rapidly. On the grounds of these observations, the following run procedure was used to compare the activities of these samples: once reaction pressure was reached, and the WHSV was correctly set, the bed temperature was increased to 200°C over a period of 90 minutes and held at 200°C until the first drop of liquid appeared in the catch-pot. This time was defined as time zero for the reaction. The reaction was allowed to proceed for one hour at this temperature at which time the liquid product was removed from the catch-pot and weighed. The bed temperature was then increased to 250°C over a period of ten minutes and reaction was allowed to proceed for a furhter five minutes before the catch-pot was again emptied. This five minute period was the estimated time taken to empty the dead volume between the

catalyst bed and the back pressure regulator. The temperature was maintained at 250°C for one hour before liquid product was again collected and weighed. Reaction temperature was increased further to 300 and 350°C in a similar fashion, reaction time again being limited to one hour at each temperature. Gas samples were taken after 30 minutes at each reaction temperature.

In the case of the SMM and Ni-SMM catalysts, bed temperatures were held constant throughout the course of the reaction The reaction temperatures used for the SMM samples was 140°C, while that used for the Ni-SMM samples was 150°C. The higher temperature was used for the nickel containing clays as they were more active than the SMM samples and took longer to deactivate at the lower temperature. Bed temperature was increased to reaction temperature over a period of one hour. Five minutes after reaction temperature was reached, the catch-pot was emptied. This time was defined as time zero for the reaction. All catalysts were run for a period of twelve hours, with liquid and gas product samples being taken at regular intervals.

The ZSM-5 catalysts were run at four different temperatures, viz., 220, 250, 270 and 290°C. Reaction was allowed to proceed at each temperature until catalyst samples showed appreciable signs of deactivation, at which point bed temperature was increased. Due to the active nature of these catalysts, bed temperature was increased to reaction temperature (220°C) very slowly to avoid the possibility of a temperature runaway. The times taken to reach reaction temperature varied between two and five hours. The point at which liquid product first appeared in the catch-pot was defined as time zero for the reaction. Liquid and gas product samples were taken at regular intervals.

Whenever liquid product was collected, the wet gas flowmeter reading and exit gas temperature were recorded. For all runs, the feed cylinder was weighed at the start of reaction (time zero) and at the end of reaction for mass balance purposes.

The reaction was terminated by isolating the pump from the reactor and releasing the back pressure. The reactor was then allowed to cool down to room temperature. The catalyst sample was removed and stored in a

sealed container for coke analysis.

The conversion of propene present in the feed to liquid product, over any time interval, was calculated as follows:

$$\text{Mass\% conversion} = \frac{(\text{mass of liquid product formed})}{(\text{mass of propene fed})} \times 100$$

The mass of propene fed was calculated according to the formula

$$\text{Mass} = (P\Delta V/RT \times M + \text{mass of liquid product}) \times 0.86$$

where ΔV = [(final gas meter reading) - (initial gas meter reading)] x gas meter correction factor,

T = exit gas temperature,

P = atmospheric pressure,

and M = average molecular weight of exit gas (obtained from G.C. analysis of exit gas sample).

The term $P\Delta V/RT \times M$ represents the total weight of exit gas over the given time interval. The factor of 0.86 represents the fraction of the feed which is propene.

The mass balance over the system was calculated according to the formula

$$\%\ \text{loss} = [1 - \{(\text{Total weight of liquid product}) + (\text{Total weight of exit gas})\}/\{\text{Total weight of feed}\}] \times 100$$

The total weight of feed was obtained from the difference in the weight of the feed cylinder at the start and at the end of reaction. The total weight of liquid product was obtained by adding the weights of all the liquid samples collected. The total weight of exit gas was obtained by summing the exit gas weights calculated for the time intervals between successive gas meter readings.

2.3.1.3 Gas Analysis

The analysis of the exit gas and feed gas streams was performed using a

3 m x 6 mm stainless steel column packed with n-octane/Poracil C. The column was fitted to a Gawmac Series 750P gas chromatograph linked to a Varian 4270 integrator.

The GC settings which were used and the response factors for the compounds present in the exit gases from the propene oligomerisation runs are contained in Appendix 1.

Table 2.1 shows the typical feed gas composition.

Component	Mass %
ethane	0.3
propane	11.69
propene	85.96
iso-butane	0.08
n-butane	0.17
n-butene	1.65
iso-butene	0.15

Table 2.1. Typical Feed Gas Composition

2.3.1.4 Liquid Product Analysis

Liquid products were analysed using a 3 m by 1/8" column packed with OV-101 supported on Chromosorb WHP-SP. The column was fitted to a Varian 3400 gas chromatograph linked to a Vista 401 data system which performed the integration. The GC settings used are shown in Appendix 1.

The liquid product formed consisted of a large number of isomers of the various oligomers. It was therefore not possible to identify all peaks in the GC spectra. The liquid product analysis was thus based on carbon number groupings. The oligomer peaks in the GC spectra were clearly visible, although the exact transition points between successive oligomer peaks were not always distinct. This occurred as a result of oligomer peak overlap caused by the presence of branched hydrocarbons

which have lower boiling points and hence retention times than their straight chain counterparts. Cut off points were therefore simply estimated. Figure 2.5 shows a typical liquid product GC spectrum. The cut off points between oligomer peaks are shown. Table 2.2 shows how the oligomer groups were defined.

Oligomer	Carbon No. Grouping
Monomer	dissolved C_3
Dimer	C_6 - C_8
Trimer	C_9 - C_{11}
Tetramer	C_{12} - C_{14}
Pentamer	C_{15} - C_{17}
Hexamer	C_{18} - C_{20}
Heptamer+	C_{21}+

Table 2.2. Definition of Oligomer Groupings

Dietz (1967) showed that the relative response factors for hydrocarbons (C_5 and heavier) are approximately one. The area percentages of the oligomer peaks should thus be a reasonable representation of the mass percentage compositions of the samples.

2.3.2 Conversion of Trimethylbenzene

2.3.2.1 Reactor System

Figure 2.6 shows a schematic representation of the reactor system used for the conversion of trimethylbenzene (TMB) over pillared and unpillared clay catalysts. The liquid feed was supplied by a syringe pump, through 1/16" stainless steel tubing, to a mixing chamber made of 1/4" tubing packed with glass beads. The mixing chamber and the 1/16" tubing were heated to 220°C, a temperature high enough to vaporise the feed. The feed and carrier gas (nitrogen) were mixed in this chamber. The feed gas then flowed through the reactor and into a double stage condenser surrounded by a cooling jacket through which iced water was

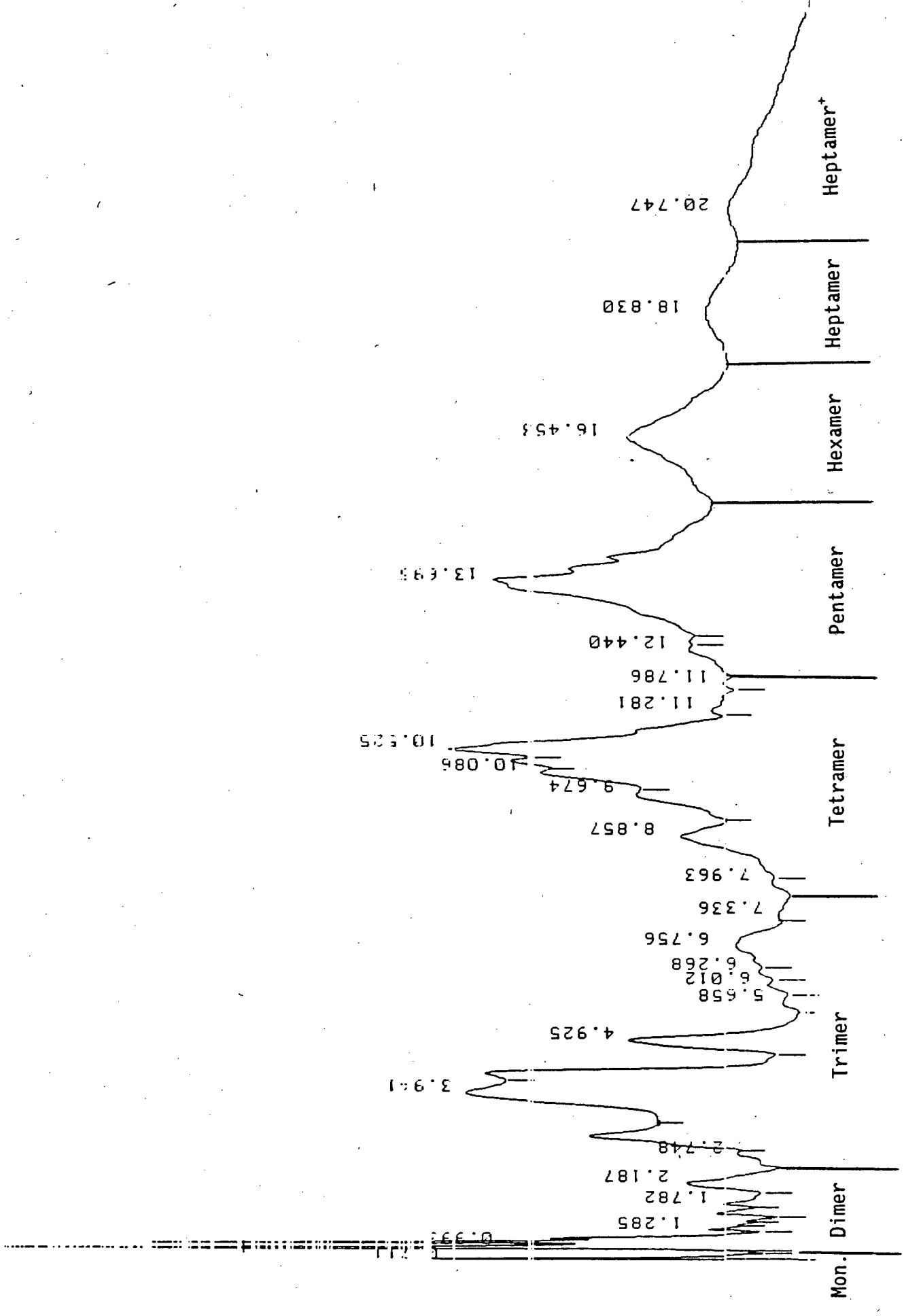

Figure 2.5: Typical Liquid Product GC Spectrum (Propene Oligomerisation). Oligomer Groupings are shown.

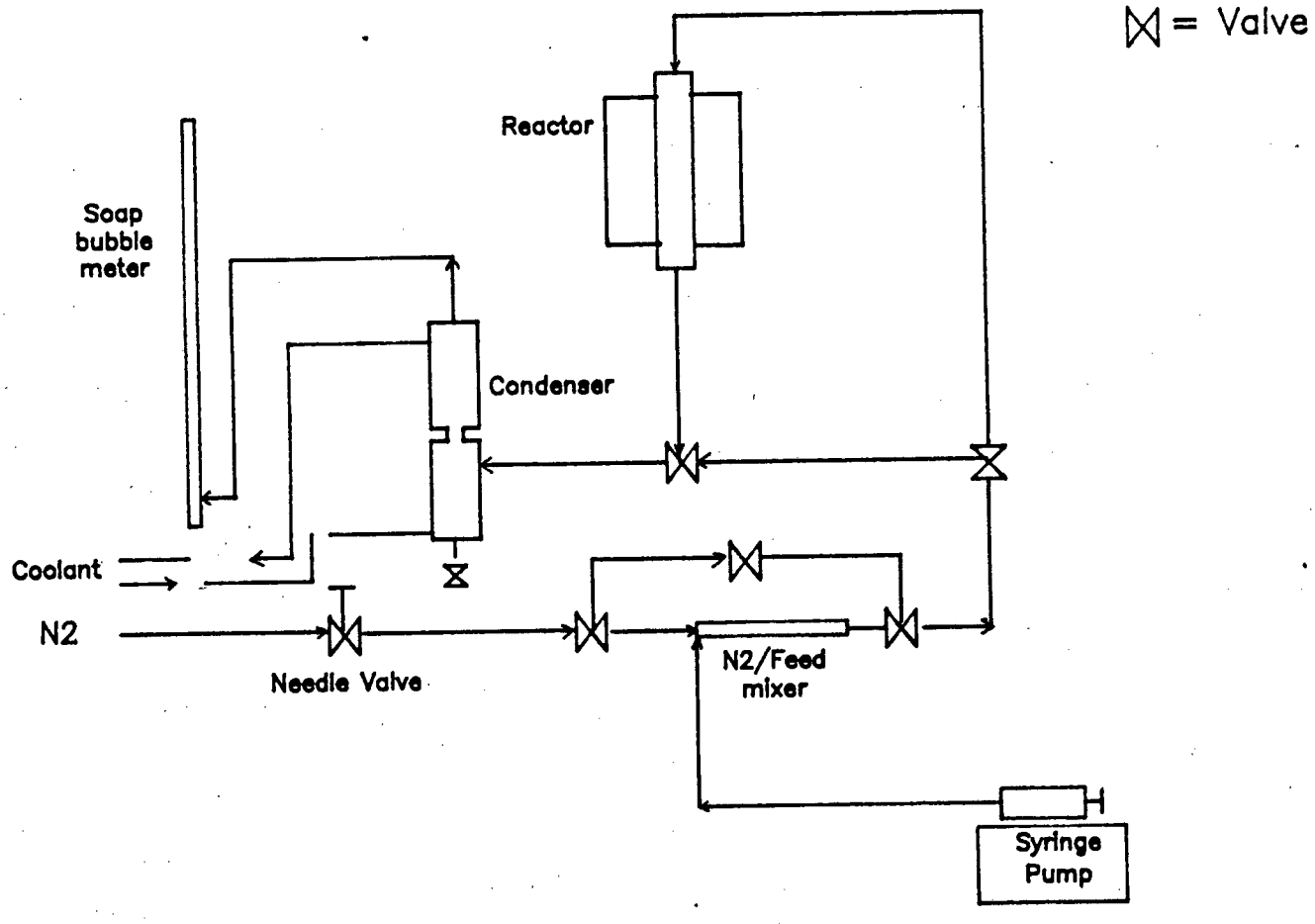

Figure 2.6: Reactor System For Conversion of Trimethylbenzene.

pumped. Essentially all of the hydrocarbon products condensed out of the carrier gas in this condenser. A line bypassing the reactor was used during start-up. Carrier gas flowrates were controlled using a needle valve and were measured using a soap bubble meter. All lines upstream of the reactor were lagged with heating tape and heated to 220°C. The integral reactor, heating jacket, and temperature control system were the same as those described in section 2.6.1. For all runs, 1 g of catalyst was packed. The size fraction used was 106 - 212 um. Reaction was carried out at atmospheric pressure.

2.3.2.2 Run Procedure

Clay samples were calcined at 500°C in air (60 ml/min) for ten hours. After calcination, the catalyst bed was allowed to cool down to 300°C. This was the reaction temperature used for all runs. The gas was then switched to N_2 and was set at the appropriate flowrate. A carrier gas/feed molar ratio of one was used. Unless otherwise indicated, a WHSV of 2.4 hr^{-1} based on the reactant was used. Once correctly set, the carrier gas was diverted through the reactor bypass line and the feed pump was switched on. The feed gas was allowed to bypass the reactor for a period of five minutes in order to clear the line or residual feed and product. The feed gas was then re-routed through the reactor. Reaction was allowed to proceed for five minutes (a time slightly greater than that required to fill the reactor volume with feed gas) before the catch-pot was emptied. This was defined as time zero for the reaction. In most cases, catalyst samples were run for a period of three hours. Liquid product samples were taken at 15 minute intervals and were analysed immediately. Conversion levels and product selectivities were calculated from the results of the liquid product analyses (see Section 3.1.3.2)

2.3.2.3 Product Analysis

Liquid product analysis was performed using an HP 5890 A gas chromatograph fitted with a Sepulcowax 10 fused silica capillary column (I.D = 0.2 mm; length = 30 m). The GC settings used are shown in Appendix 1.

The following compounds were found to be present in the product obtained from the conversion of TMB isomers over the various clay catalysts:

Benzene
Toluene
o-, m-, p-xylene
124, 123, 135 trimethylbenzene
1245, 1235, 1234 tetrametylbenzene.

The response factors of all these compounds were set equal to unity.

2.3.3 Hexane Cracking

2.3.3.1 Reactor System

The reactor system used for the cracking of n-hexane over the modified ZSM-5 catalysts was the same as that described in Section 2.3.2.1. Reaction was carried out at atmospheric pressure. A WHSV based on hexane of 2 hr^{-1} was used. The carrier gas was N_2. The concentration of hexane in the feed gas entering the reactor was 10 mol%, a concentration sufficiently low to ensure that all hydrocarbons present in the reactor effluent were in the gaseous phase. Product gases were collected in a gas sampling loop for analysis. For all runs, 1 g of catalyst was used.

2.3.3.2 Run Procedure

Catalyst samples were calcined at 500°C for ten hours in flowing air (60 ml/min). The reactor was cooled to 400°C and the gas was switched to nitrogen. Once the flowrate was correctly set, the carrier gas was diverted through the reactor bypass line and the feed pump was turned on. After five minutes, the feed gas was re-routed through the reactor and reaction was allowed to take place at 400°C for a period of three hours. Product sampling occurred after five minutes, and at half hourly intervals thereafter. Catalyst samples were then regenerated in air at 500°C for four hours before being rerun, in a similar fashion, for three hours at 500°C. Conversion levels and product selectivities were calculated from the results of the product analyses.

In order to establish the extent to which thermal cracking was taking place, a run was performed at 500°C with no catalyst in the reactor.

2.3.3.3 Product Analysis

Product analysis was carried out on the Gawmac 750 P series gas chromatograph described in Section 2.3.1.3, and on a Varian 3600 gas chromatograh fitted with a megabore column (length = 30 m, I.D = 0.53 mm) coated with DB-1. The former system was used to determine the C_1 - C_6 composition of the product gas, while the megabore system was used to determine the aromatic concentration.

3 RESULTS

3.1 Pillared Clays

3.1.1 Clay Synthesis

When the beidellite synthesis procedure described by Diddams (1989) was used, it resulted in a very low degree of crystallisation to the desired product. When the reactant mixture was removed from the autoclave, two distinct solid phases were present: one phase appeared to be very similar to the white powder which resulted from drying and calcining the synthesis gel. The second phase had a jelly-like texture, characteristic of swellable clay minerals. The two phases were separated by dispersing the mixture in one litre of water, and allowing it to stand overnight. The clay particles remained in suspension, due to their extremely small size and swellable properties, while the non-crystalline material settled out rapidly. The clay suspension was removed and centrifuged. X-ray diffraction analysis confirmed that the phase which settled out of the product dispersion had no crystalline structure. The clay phase constituted 15% by mass of the solids which were removed from the autoclave.

"Ageing" the gel for a period of three days prior to calcination did not significantly increase clay product yield. Increasing the pH of the gel, by using three times the amount of NaOH specified by Diddams, had no noticeable effect on product yield. It was found, however, that if the aluminium source was added dropwise to the silica source, as opposed to the reverse procedure, a more homogenous gel resulted. Calcination, resuspension, and reaction resulted in a slightly improved clay product yield (ca. 25%).

When the Ni-SMM synthesis mixture, prepared according to the method described by Gaaf et al. (1983), was removed from the autoclave, only one solid phase appeared to be present. This suggested that crystallisation to the clay product was extensive.

3.1.2 Catalyst Characterisation

3.1.2.1 X-Ray Diffraction

This section presents the results of XRD analyses performed on the unpillared and pillared clay samples which were used for this work.

3.1.2.1.1 Synthesised Clays

X-ray diffractogram traces were obtained from the synthesised Ni-SMM(21) and beidellite clays. For the purposes of comparison, the Ni-SMM(7) and SMM samples, obtained from the Harshaw/Filtrol Corporation, were also analysed.

Ni-SMM(21)

The XRD trace obtained from the Ni-SMM(21) sample, synthesised according to the method described by Gaaf et al. (1983), is shown in Figure 3.1. The trace obtained from the Ni-SMM(7) sample is shown in Figure 3.2. Other than the peaks at 7.2 and 3.53 A, the traces are similar. Ni-SMM clays with different Ni loadings, however, exhibit slightly different XRD patterns. Tables 3.1(a) and (b) compare the XRD peak positions of the synthesised Ni-SMM sample with those reported by Black et al. (1976) for a Ni-SMM sample with a 21% Ni loading.

Other than additional peaks at 7.2, 6.2 and 3.53 A, the results obtained from the Ni-SMM sample synthesised in this work agree well with those reported by Black et al. (1976). The peak at 6.2 A is probably the 002 basal peak which also appears in the Ni-SMM(7) trace and is therefore not significant. The peaks at 7.2 and 3.53 A are, however, not consistent with the results obtained from the Ni-SMM(7) sample or with the results reported by Black et al. (1976). The two peaks are attributed to the presence of a "clay impurity" formed during the crystallisation process. As the positions of XRD peaks associated with hk and hkl reflections of different clay minerals are generally very similar, the presence of such a clay impurity may not significantly affect the observed positions of the non-basal peaks in the XRD spectrum of the synthesised Ni-SMM clay.

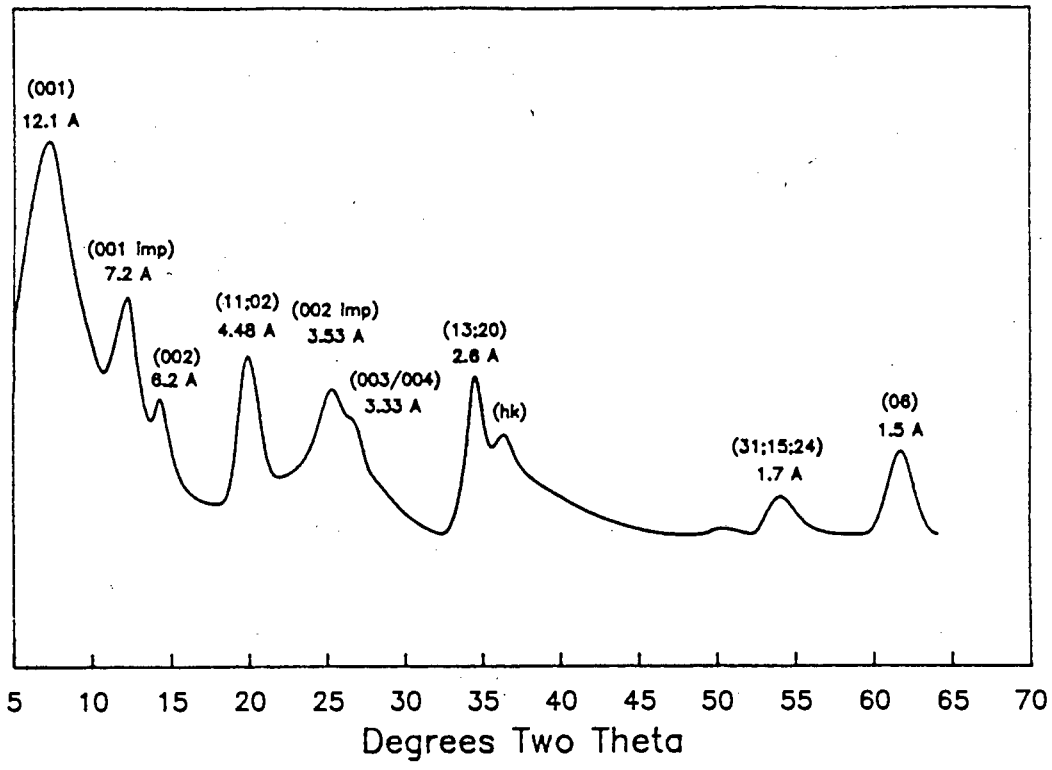

Figure 3.1. XRD : Ni-SMM(21); "imp" denotes clay impurity

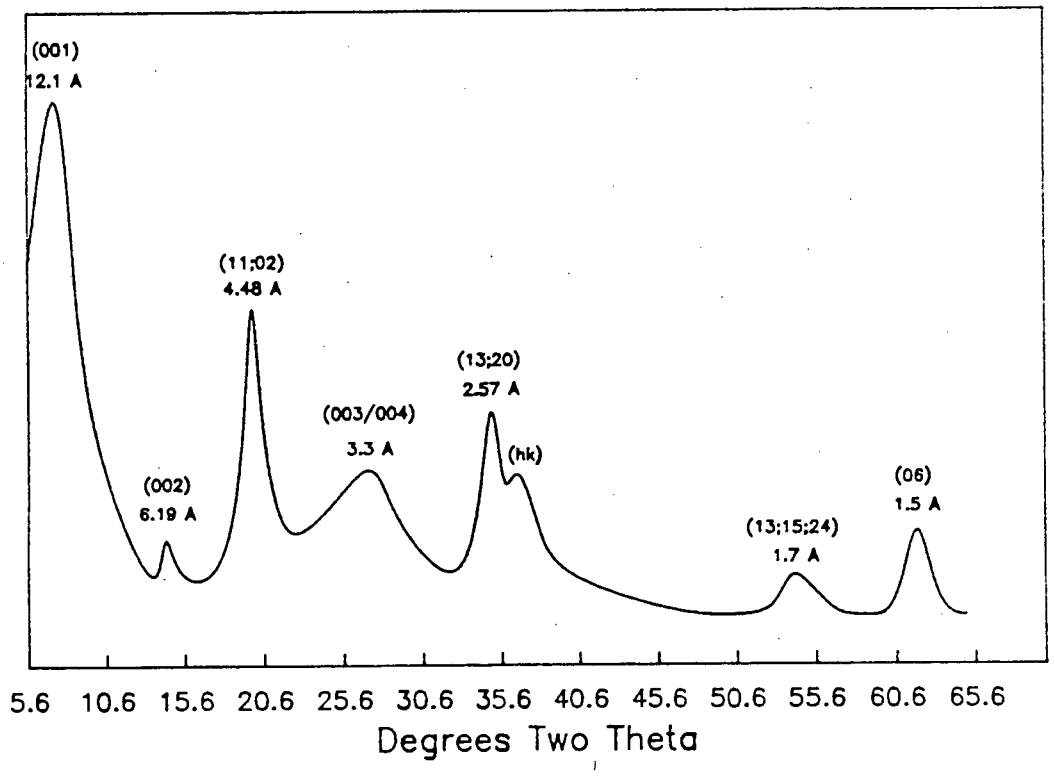

Figure 3.2. XRD: Ni-SMM(7) from Harshaw/Filtrol

Peak Position (A)	Comments	Probable Index
13	*	001
4.48		11;20
3.3	Broad	003 or 004
2.58		13;20
2.47	Ill defined	hk
1.69	Broad	31;15;24
1.5		06

* May have intercalated acetate

Table 3.1(a). XRD Peak Positions for Ni-SMM (21% Ni) (Black et al., 1976)

Peak Position (A)	Comments	Probable Index
12.1		001
7.2		001 (impurity)
6.2		002
4.48		11;02
3.53		002 (impurity)
3.33	Broad	003 or 004
2.6		13;20
2.47		hk
1.7	Broad	31;15;24
1.5		06

Table 3.1(b). XRD Peak positions for Ni-SMM(21). (This work)

Feitknecht and Berger (1942) reported the following XRD spectrum for synthetic Ni serpentine, a trioctahedral, two layered clay with Ni in the octahedral positions.

Peak Position (A)	
7.26	(001)
4.62	
3.63	(002)
2.69	
2.5	
2.16	
1.78	
1.54	

If the 12.1 and 6.2 A Ni-SMM basal peaks are not considered, the spectrum obtained from the present sample agrees well with that reported for Ni serpentine. This result suggests that the synthesised clay comprises a mixture of Ni-SMM and the above-mentioned clay. The intensity of the 7.2 A peak relative to that of the 12.1 A peak indicates that the impurity (Ni serpentine) is present in significant quantities.

The basal spacings of the synthesised Ni-SMM sample are not in agreement with those reported by the authors of the patent from which the synthesis procedure was obtained. These authors reported the presence of a single 001 peak at a value of 12.6 A and indicated that the clay was essentially 100% swellable. The difference in the position of the 001 peak (12.1 vs. 12.6 A) indicates a difference in the swellable property of the clay. Smaller fist order basal spacings generally indicate a higher percentage of non-swellable material (see Chapter 4).

Beidellite

The XRD trace of the synthesised beidellite clay is shown in Figure 3.3. The trace obtained from the Harshaw/Filtrol SMM sample is shown in Figure 3.4. As the two clays are structurally identical, their XRD traces should be very similar. This was found to be the case.

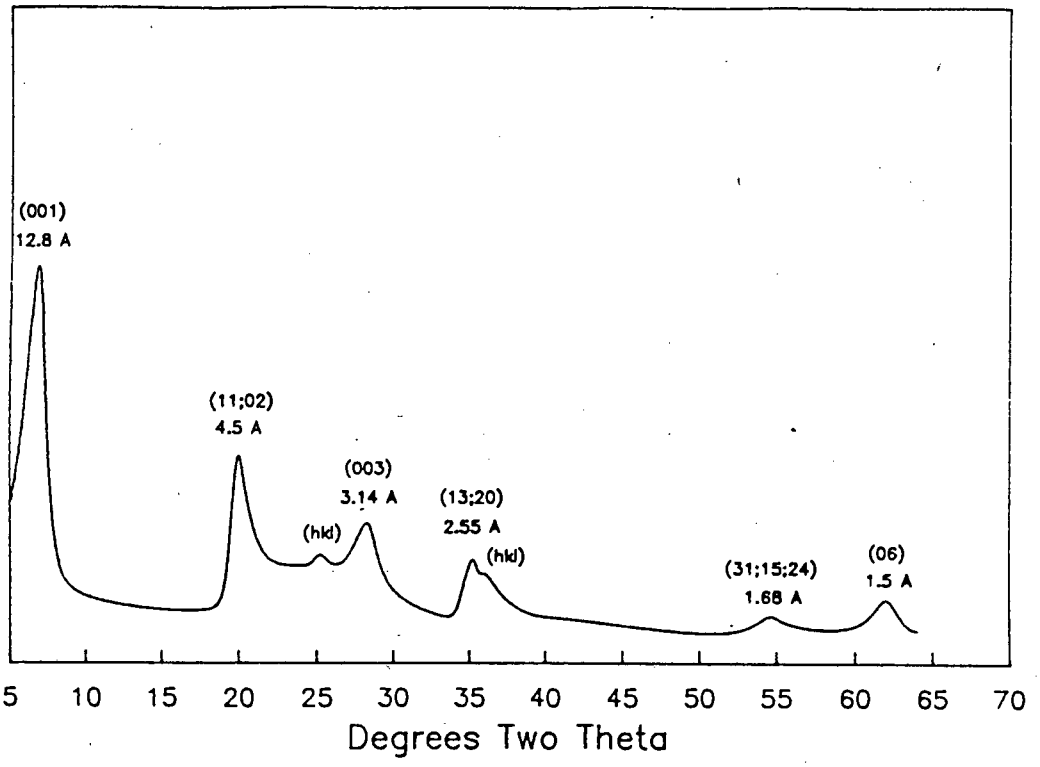

Figure 3.3. XRD: Synthesised Beidellite (This work)

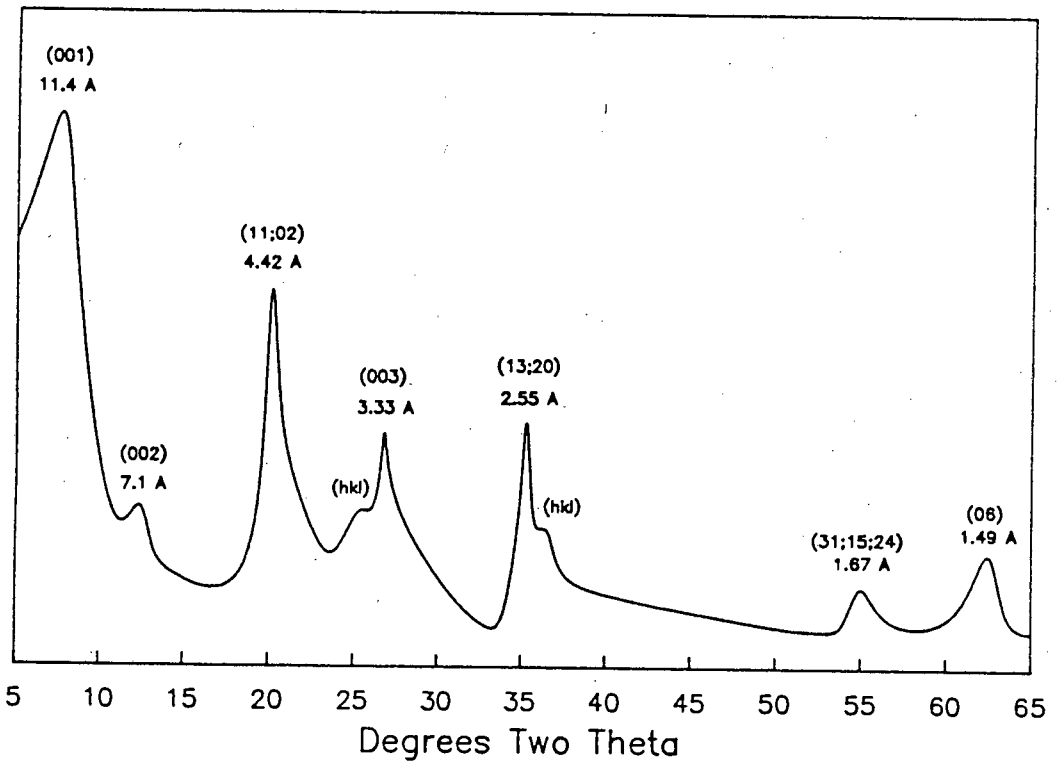

Figure 3.4. XRD: SMM from Harshaw/Filtrol

Differences in the positions of the basal peaks are attributed to different amounts of tetrahedrally co-ordinated Al in the two clays. This affects the charge deficit on the clay lattice which determines the swellability of the layers and, hence, the interlayer spacings. The results agree well with those reported for SMM by Granquist (1966).

Spacings of hk reflections for beidellite have been reported by Brown (1961). Table 3.2 compares these with the results obtained from the synthesised samples.

Peak Position (A)		Probable Index
Brown (1961)	This Work	
4.46	4.5	11;02
2.61 ; 2.5	2.55	13;20
2.24 ; 2.17 ; 2.09*	-	22;04
1.69	1.68	31;15;24
1.49	1.5	33;06
1.28	out of range	26;40

* weak

Table 3.2. XRD: Spacings of hk Reflections for Beidellite

These results confirm that the sample synthesised in this work has the beidellite structure. The position of the 001 peak (ca. 12.8 A) idicates that the clay is essentially 100% swellable (Brown, 1961; Granquist, 1966).

3.1.2.1.2 Pillaring of Montmorillonite and Beidellite

Table 3.3 shows the positions of the 001 peaks of the pillared and unpillared montmorillonite and beidellite samples.

Clay	Uncalcined Position (A)	Calcined (500°C) Position (A)
Mont.	13.3	-
Al PILMont	19.5	17.5
Si/Al PILMont	19.3	17.6
Ni/Al PILMont	19.2	17.6
Beidellite	12.8	-
Al PILBeid	19.4	18.1

Table 3.3. XRD: Pillaring of Montmorillonite and Beidellite

The 001 peak of montmorillonite was well defined and represented a basal spacing of 13.3 A. This indicates the presence of a well ordered layered struture with a dominant layer centre to layer centre distance of 13.3 A. This corresponds to an interlayer spacing of 3.7 A, since each 2:1 layer has a height of ca. 9.6 A (Brown, 1961). Treating the clay with the hydroxy-Al pillaring solution resulted in a shift in the position of the 001 peak to a lower 2θ value, indicating an expanded basal spacing of 19.5 A. This represents an interlayer spacing of 9.9 A and corresponds well to the dimensions of the polymeric cations used for pillaring. The Al_{13}^{7+} ion has the shape of a prolate spheroid with a long axis of about 9.5 A (Johansson, 1960). The original 13.3 A peak disappeared completely on pillaring. Calcination of the pillared clay at 500°C for 4 hours, which causes dehydroxylation of the Al_{13} pillaring cation to form stable Al_2O_3 pillars, resulted in a shift of the 001 peak to a position corresponding to a basal spacing of 17.5 A. This represents an interlayer spacing of 7.9 A.

Treating montmorillonite with the hydroxy-Al, hydroxy-Si/Al, and the hydroxy-Ni/Al pillaring solutions gave very similar results.

As with montmorillonite, the 001 peak of beidellite was well defined. The position of the peak corresponds to a dominant basal spacing of 12.8 A. Due to the ability of the montmorillonite and beidellite clays to

swell dramatically in aqueous solutions, the interlayer spaces of these clays may be affected by changes in humidity. This effect may be responsible for the slightly different interlayer spacings observed in the unpillared forms of the two clays. Changes in humidity, however, should not affect the basal spacings of the pillared clays, as the pillaring process largely removes the swellable property of the clays. Na^+ is the only charge balancing cation present in the unpillared beidellite sample. The presence of small quantities of Ca^{2+} and K^+ ions, in addition to the Na^+ charge balancing cations, on unpillared montmorillonite (see proposed chemical formula for montmorillonite, Chapter 4) may also be responsible for the observed differences in the interlayer spacings of the two clays (Brown, 1961).

The results of treating beidellite with the hydroxy-Al pillaring solution were similar to those of montmorillonite. Interlayer spacing increased to 9.9 A on pillaring. There was no sign of the original 001 peak. Calcination decreased the pillared interlayer spacing to 8.5 A, slightly larger than that of calcined Al PILMont.

3.1.2.1.3 Pillaring of SMM and Ni-SMM

Table 3.4 shows the 001 peak positions of the SMM and Ni-SMM samples before and after treatment with the hydroxy-Al pillaring solution.

Calcination of SMM shifted the 001 peak from 11.4 A to a position corresponding to a basal spacing of 9.8 A. Treating the clay with the hydroxy-Al pillaring solution resulted in the disappearance of the original 11.4 A peak and the appearance of two fairly weak peaks, one at 10.4 A, and the other in the region of 20.5 A. Calcination of Al PILSMM shifted the 10.4 A peak to a position corresponding to a basal spacing of 9.8 A. As was observed in the pillared montmorillonite and beidellite samples, calcination of Al PILSMM shifted the expanded-layer 001 peak to a higher 2θ value. In this case, the peak shifted from ca. 20.5 A to ca. 19 A.

As with SMM, calcination of the Ni-SMM(7) sample shifted the 001 peak of this clay from 12.1 A to 9.8 A. X-ray diffraction analysis of the Ni-SMM(7) sample treated with the hydroxy-Al pillaring solution resulted in

Clay	001 Peak Position (A)	
	Uncalcined	Calcined (500°C)
SMM	11.4	9.8
Al PILSMM	10.4 ; 20.5	9.8 ; 19
Al PILMont*	19.5	-
Ni SMM(7)	12.1	9.8
Al PILNi-SMM(7)	-	-
Al PILMont*	19.5	-
Ni-SMM(21)	12.1 ; 7.2	7 - 10
Al PILNi-SMM(21)	7.2	7.2
Al PILMont*	19.5	-

* Pillared as reference with same pillaring solution under identical conditions.

Table 3.4. XRD: Pillaring of SMM and Ni-SMM

the generation of a very diffuse spectrum in the region where the basal peaks appear. The original 12.1 A peak disappeared completely, and no low angle peak appeared to be present to indicate that an expanded-layer structure had been generated in the clay. There was also no sign of a peak in the region of 10 A to indicate the presence of non-swellable material which should remain unaffected by the pillaring process. Calcination did not significantly alter the XRD spectrum of Al PILNi-SMM(7) in the region where the first order basal peaks appeared.

Calcination of the Ni-SMM(21) sample resulted in the disappearance of the original 12.1 A 001 peak and the appearence of a broad band in the region of 7-10 A. This broad band is probably a combination of the original 001 (impurity) peak and a 9.8 A peak which appears as a result of a shift of the 001 peak of the Ni-SMM-like phase of the clay. The shape of the band suggested that the position of the 001 (impurity) peak, which represents the basal spacing of a two layered clay, is not significantly affected by calcination. This is consistent with the fact

that two layered clays, such as Ni serpentine, have essentially no interlayer spaces (Brown, 1961). As was the case with Ni-SMM(7), XRD analysis of the Ni-SMM(21) sample treated with the pillaring solution yielded a very diffuse spectrum in the region where the first order basal peaks appeared. The only clearly discernible 001 peak was the 7.2 A peak, which appeared to have been unaffected by treatment with the pillaring solution. This result is not surprising, as two layered clays of this type have no swellable property. Calcination of Al PILNi-SMM(21) did not appear to change the XRD spectrum of the clay in the region where the first order basal peaks appeared.

Table 3.4 also shows the XRD results obtained from the three montmorillonite samples which were pillared as references for the Al PILSMM, Al PILNi-SMM(7) and Al PILNi-SMM(21) clays. The positions of the 001 peaks of these samples indicate that the different effects that treatment with the pillaring solutions had on the XRD spectra of the three synthetic clays were not a result of differences in the nature of the pillaring solutions used, or the conditions under which the clays were pillared.

3.1.2.2 Nickel Analysis

The results of XRF analysis indicated that the synthesised Ni-SMM clay contained 21% Ni by mass and the Ni/Al PILMont clay contained 1.7% Ni.

A rough estimate of the Ni content of the pillars in the Ni/Al PILMont sample can be made from the Ni assay of the clay. It has to be assumed, in so doing, that the combined charge on the pillaring cations incorporated into the interlayer spaces of the clay is equivalent to the cation exchange capacity of the clay, viz., 0.96 meq/g (Boland Base Minerals). The calculation was performed as follows:

As a starting point, it was assumed that the pillaring cation contains no nickel, i.e., x takes a value of 0 in the molecular formula of the pillaring species

$$[Al^{iv}(Al_{(12-x)}Ni_x)^{vi}O_4(OH)_{24}]^{(7-x)+}.$$

(i) From the cation exchange capacity of the clay and the charge on

the pillaring species, the number of pillars per gram of unpillared clay was calculated.

(ii) Using the molecular weight of the pillaring cation, the number of pillars per gram of pillared clay was calculated.

(iii) Assuming that all nickel present in the clay is located in the pillars, the average Ni content of each pillar (x in the above formula) was calculated from the Ni assay and the number of pillars per gram of pillared clay.

(iv) Using this value of x, steps (i) - (iii) were repeated until the value of x obtained in step (iii) agreed with that used in step (i).

By using the above calculation procedure, a value of 1.82 was obtained for x, corresponding to a charge of +5.18 on the hydroxy-Ni/Al pillaring species. During the preparation of the Ni/Al pillaring solution, sufficient nickel was added to give x a value of 3.73 in the above formula.

3.1.2.3 Calcination Studies

Calcination studies were carried out on the pillared and unpillared clays using the TG-DTA apparatus described in Chapter 2. For all samples, weight loss was initially rapid, but appeared to level off in the temperature range 150 to 200°C. This initial weight loss is ascribed to the removal of water. For the purposes of comparison, a temperature of 200°C was arbitrarily chosen as a cut-off point for water removal. Weight losses observed up to this temperature were therefore used to compare the water content of the different clays.

Fig. 3.5 shows the TG curves obtained from Na Mont and Al PILMont. The microporous structure generated by pillaring increased the amount of water held by the clay. Water removal took place at a faster rate in Na Mont and was essentially complete by 150°C. Water loss was still seen to be taking place beyond this temperature in Al PILMont.

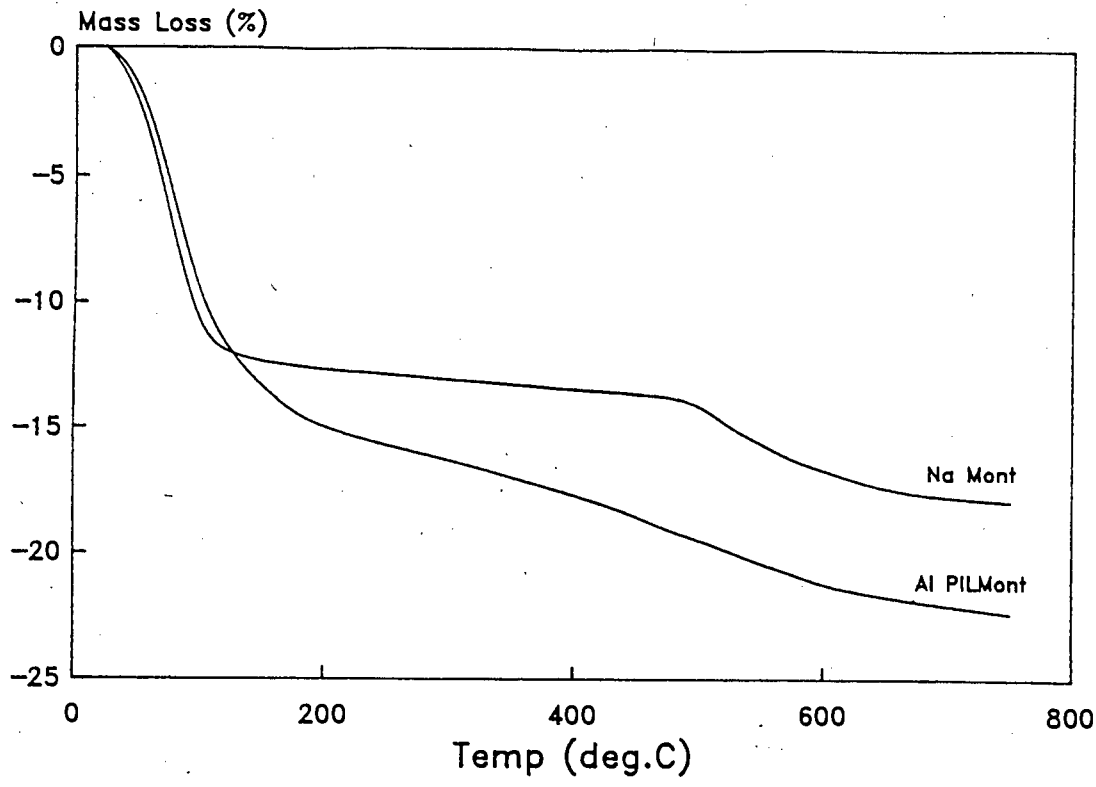

Figure 3.5. Thermal Analysis: Na Mont and Al PILMont

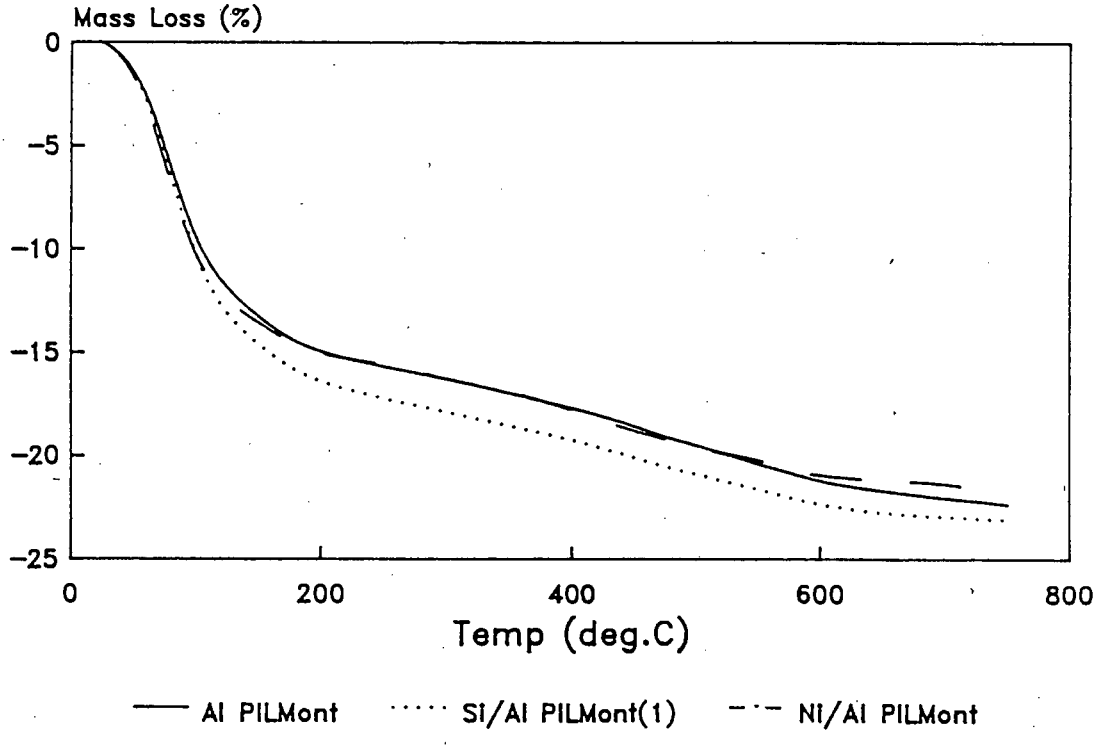

Figure 3.6. Thermal Analysis: Al, Si/Al, and Ni/Al PILMont

In Na Mont, the weight loss between 200 and 500°C was small, and is ascribed to a very gradual loss of structural hydroxyl groups. Above 500°C, weight loss increased noticeably as a result of extensive lattice dehydroxylation. These results are in agreement with those reported by Tennakoon et al. (1987) who used FTIR spectra in the region of 1600-400 cm^{-1} to study the effects of temperature on the structure of Na Mont. They found that the extent of lattice dehydroxylation was limited below 500°C.

The weight loss between 300 and 400°C for Al PILMont was 1.4% as against 0.4% for Na Mont. Schutz et al. (1985) report that dehydroxylation of the Al_{13} pillars takes place between 300 and 400°C. The increased weight loss observed in this temperature range for Al PILMont is therefore ascribed to pillar dehydroxylation.

The shoulder present in the region of 500°C in the TG curve of Na Mont, representative of the onset of extensive lattice dehydroxylation, was essentially absent in the case of Al PILMont. Instead, there was a gradual weight loss taking place between 400 and 600°C.

Fig. 3.6 shows the TG curves obtained from the Al PILMont, Si/Al PILMont(1) and Ni/Al PILMont samples. All these clays behaved very similarly on heating.

Fig. 3.7 shows the TG curves obtained from Na Beid and Al PILBeid. The changes in the TG curve observed on pillaring beidellite were consistent with those observed on pillaring montmorillonite. Pillaring of Na Beid resulted in an increase in weight loss due to water removal, while the rate of water removal appeared to be slightly slower in the pillared clay. The weight loss between 300 and 400°C was 1.3% for Al PILBeid as against 0.8% for Na Beid. This increase is once again ascribed to dehydroxylation of the hydroxy-Al species present in the pillared clay. The increase in weight loss in this temperature range, however, was not as large as that observed on pillaring montmorillonite (0.49 vs. 1.1%). The TG curve of Na Beid exhibited a shoulder in the region of 550°C. As with Na Mont and Al PILMont, this shoulder was less pronounced in Al PILBeid, the mass loss between 400 and 500°C being greater in the pillared clay.

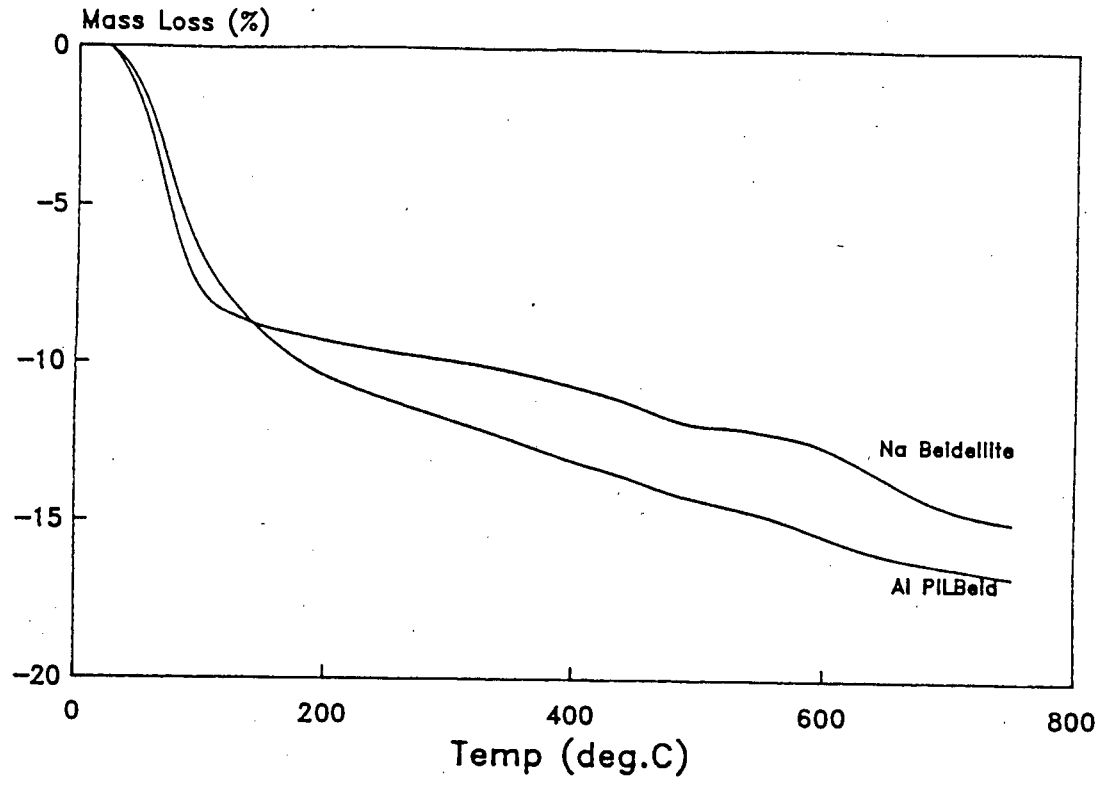

Figure 3.7. Thermal Analysis: Na Beid and Al PILBeid

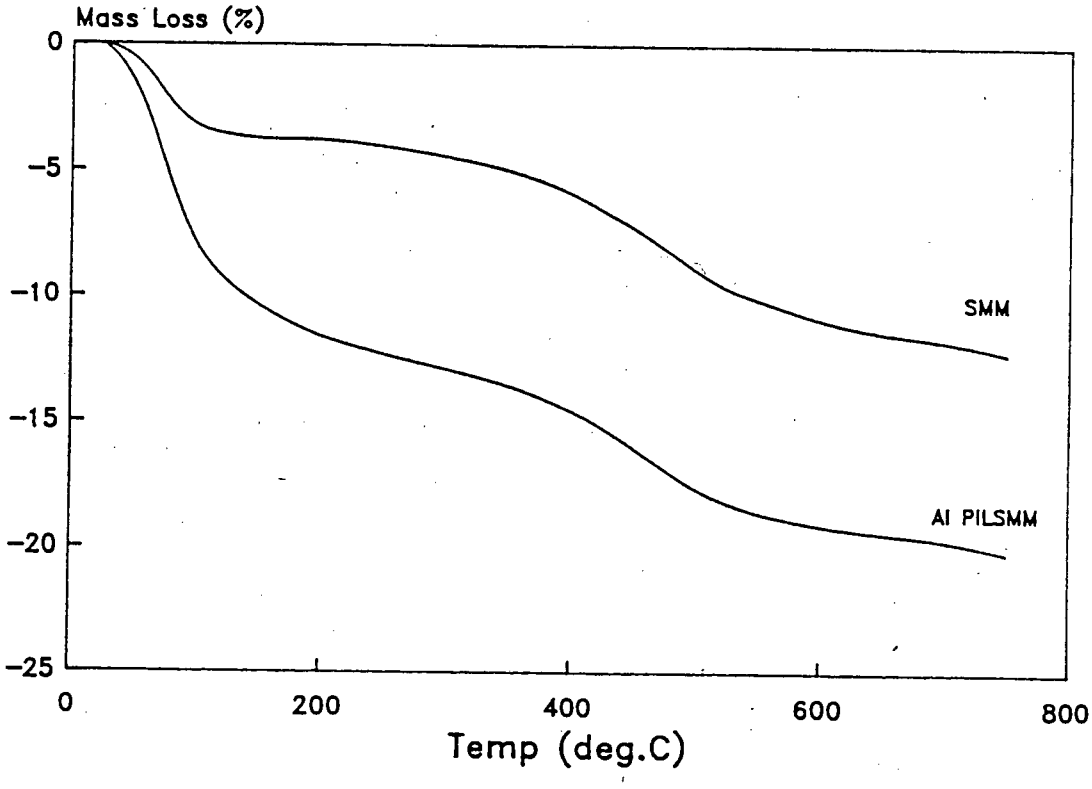

Figure 3.8. Thermal Analysis: SMM and Al PILSMM

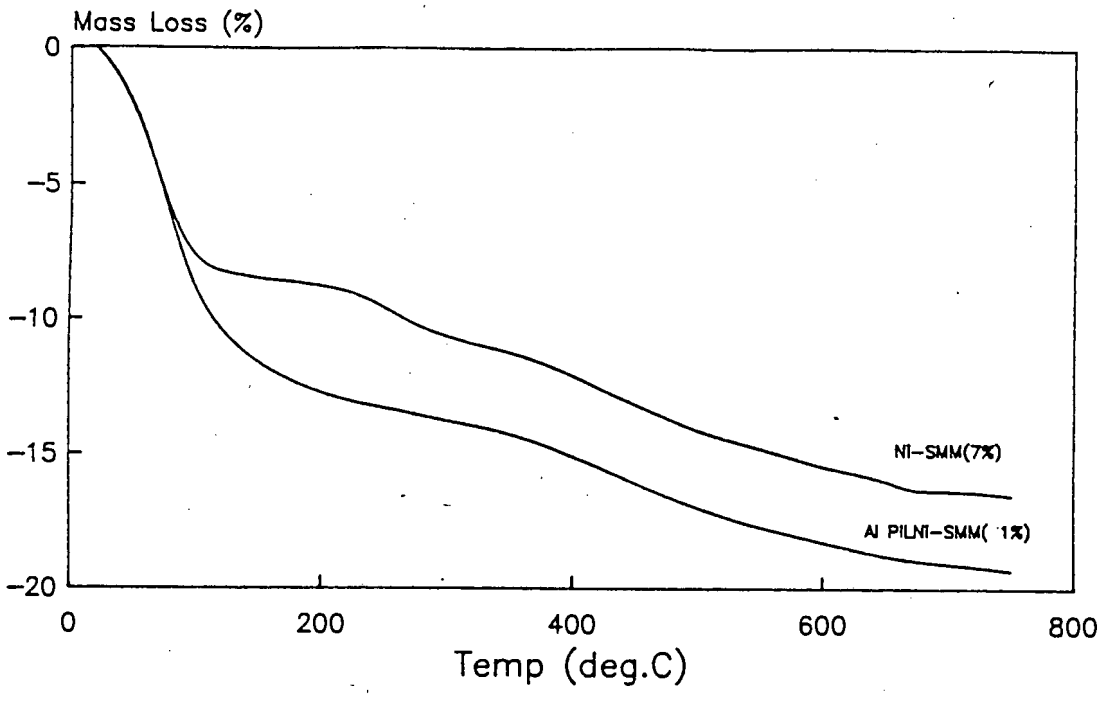

Figure 3.9. Thermal Analysis: Ni-SMM(7) and Al PILNi-SMM(7)

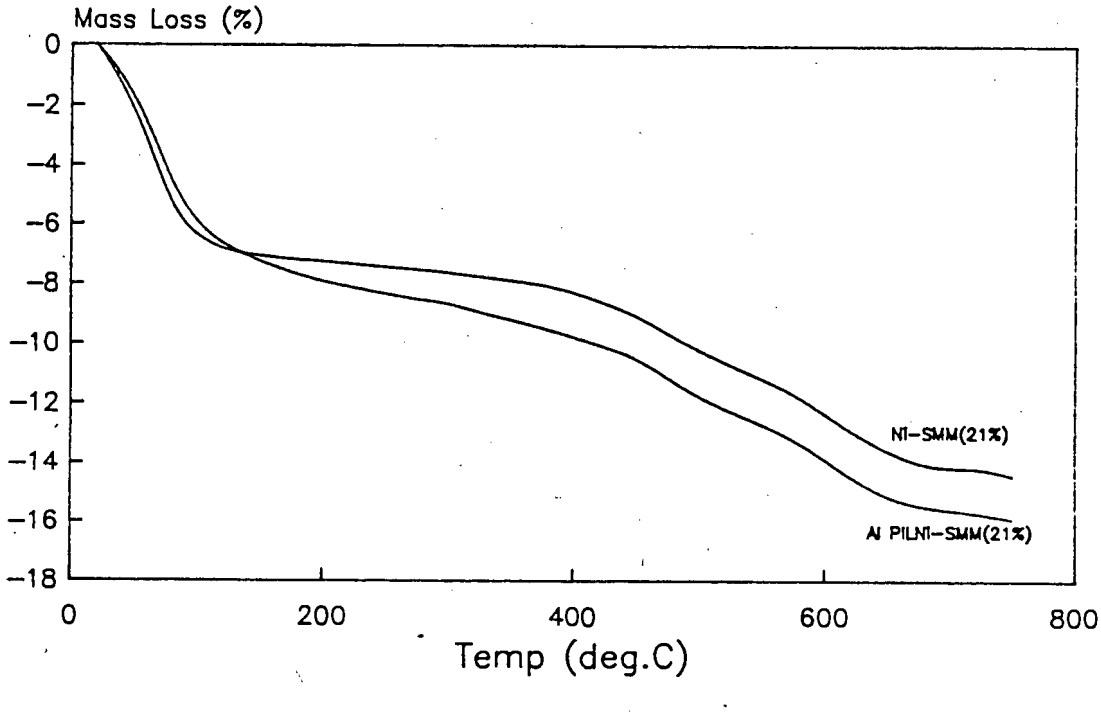

Figure 3.10. Thermal Analysis: Ni-SMM(21) and Al PILNi-SMM(21)

Figures 3.8, 3.9, and 3.10 show the TG curves obtained from SMM and Al PILSMM, Ni-SMM(7) and Al PILNi-SMM(7), and Ni-SMM(21) and Al PILNi-SMM(21), respectively. In all cases treatment with the pillaring solution resulted in an increase in the water content of the clay. Weight losses incurred on heating to 200°C increased, on pillaring, from 3.8% to 11.7% in SMM, from 8.7% to 12.7% in Ni-SMM(7), and from 7.2% to 7.9% in Ni-SMM(21). The increase in the water content of SMM and Ni-SMM(7) on treatment with the pillaring solutions was greater than that observed on pillaring Na Mont and Na Beid.

The TG curves indicate that pillaring the SMM and Ni-SMM samples does not significantly affect weight losses between 200 and 750°C. The weight losses between 300 and 400°C did not change noticeably after treatment with the pillaring solution. The shape of the TG curve also remained essentially unaffected.

3.1.2.4 Surface Area Measurements

The volume of nitrogen adsorbed was measured at between seven and nine different relative pressures (P/P_o) in the range 0.001-0.35 for all samples. Appendix 2(a) contains plots of the volume of N_2 adsorbed versus relative pressure for the different clays. In general, a greater proportion of the total N_2 uptake took place at low relative pressures on the pillared montmorillonite and beidellite clays than was the case on the parent montmorillonite and beidellite clays and the pillared and unpillared SMM and Ni-SMM samples. Nitrogen uptake levelled off more rapidly with increasing P/P_o values in the case of the former group of clays. These differences in the adsorption isotherms of the two groups of clays are consistent with differences in the isotherms proposed by Brunauer et al. (1940) for monolayer and multilayer adsorption and suggest that more monolayer (or limited-layer) adsorption is taking place on the pillared montmorillonite and beidellite samples.

For each sample, the sorption data was plotted according to the two adsorption isotherms:

Type 1: Langmuir isotherm

$$\frac{P/P_o}{V} = \frac{1}{kV_m} + \frac{P/P_o}{V_m}$$

Type 2: BET isotherm

$$\frac{1}{V(P_o/P-1)} = \frac{1}{CV_m} + \frac{P/P_o}{V_m}$$

where P/P_o is the relative vapour pressure, V is the volume of gas adsorbed, V_m is the volume of gas required for monolayer adsorption, and C and k are constants. These equations assume, respectively, (1) monolayer adsorption, and (2) multilayer adsorption on open surfaces. The former adsorption occurs when the pore dimensions approach the dimensions of the sorbate molecules. In such pores, multilayer adsorption is physically impossible.

Figures 3.11 and 3.12 show the BET and Langmuir isotherms of SMM and Al PILMont. The BET isotherm is obtained by plotting $1/V(P_o/P-1)$ vs. P/P_o, while the Langmuir isotherm is obtained by plotting P/P_oV vs. P/P_o. The isotherm which most closely approximates a straight line was used to estimate surface area. The slope of this isotherm, obtained from a linear regression analysis of the data, approximates the value of $1/V_m$. Surface area was determined from the value of V_m, taking 16.2 A^2 as the area occupied by one N_2 molecule.

For SMM (Figure 3.11), the linearity of the BET plot and the curvature of the Langmuir plot are evident. In the case of Al PILMont (Figure 3.12), the converse is true. The BET and Langmuir plots of all the samples tested are contained in Appendix 2(b). In many cases it was not possible to establish which of the two isotherms was more linear simply by visual inspection. Table 3.5 lists the correlation coefficients obtained from linear regression analyses performed on the BET and Langmuir data points for each sample.

The BET adsorption isotherms of the parent montmorillonite and beidellite clays were more linear than the Langmuir isotherms, as shown in Figures 3.13 and 3.14, respectively. This is consistent with the fact that adsorption would be expected to take place only on exposed layer edges and faces in these clays.

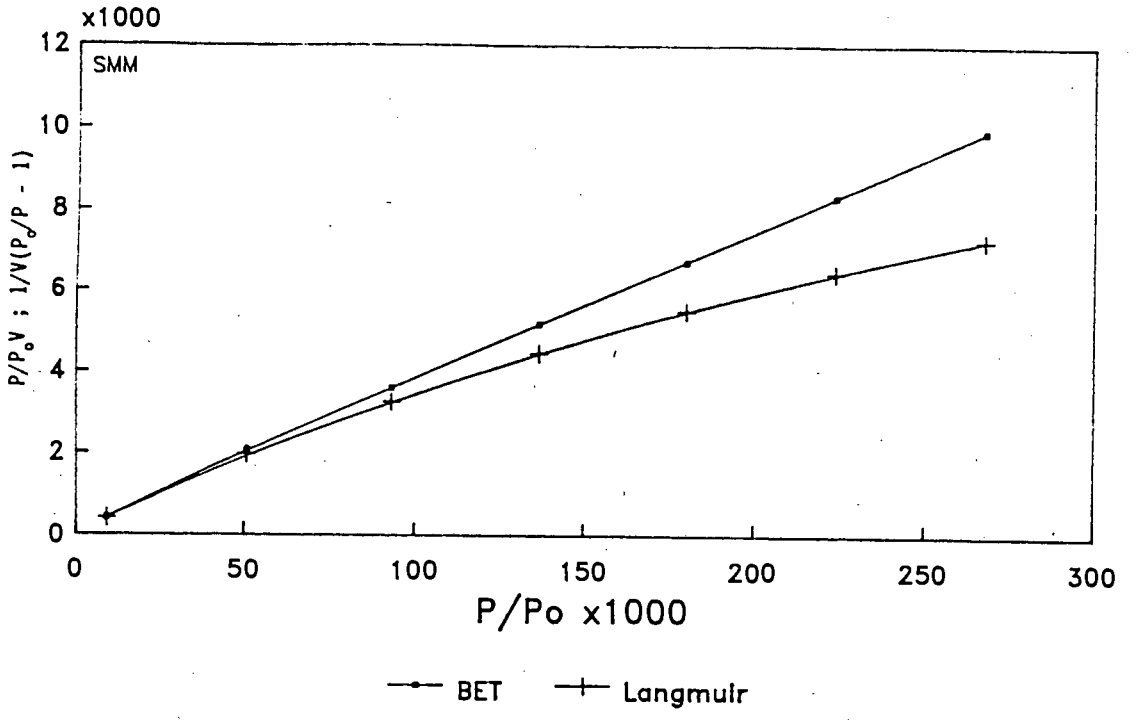

Figure 3.11. N_2 Adsorption: BET and Langmuir Isotherms of SMM

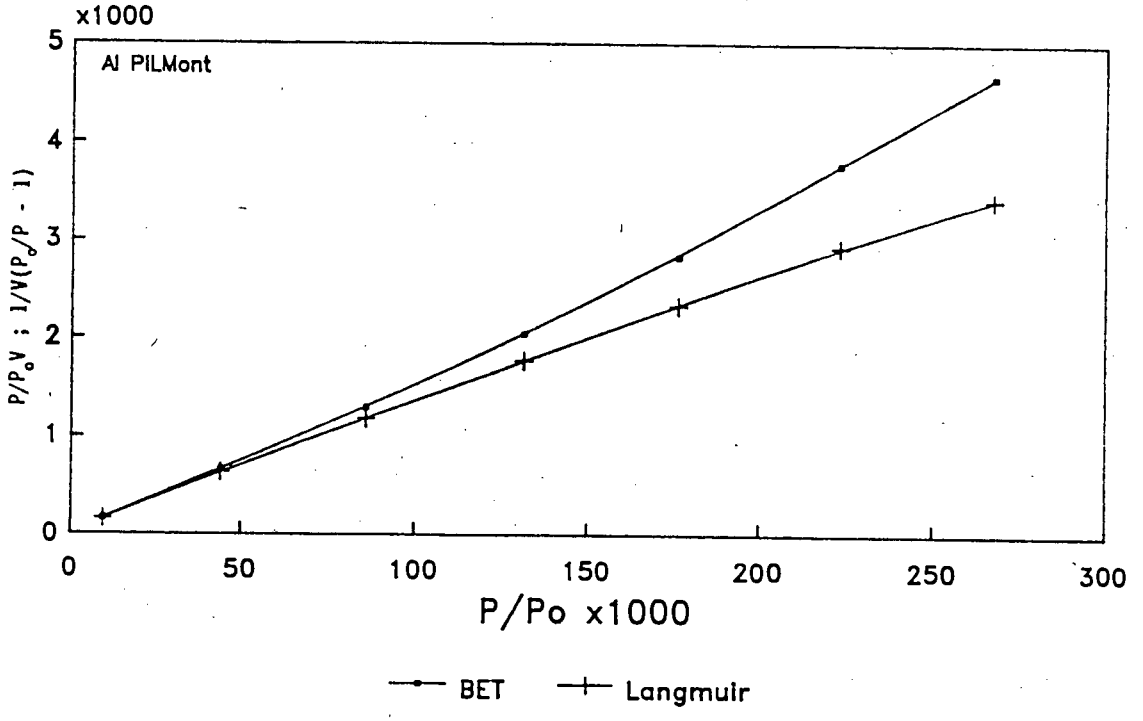

Figure 3.12. N_2 Adsorption: BET and Langmuir Isotherms of Al PILMont

Catalyst	BET		Langmuir	
	Corr. Coeff.	S.A.(m^2/g)	Corr. Coeff.	S.A.(m^2/g)
NH_4 Mont*	0.9957	23	0.9746	(31)
Al PILMont	0.9979	(250)	0.9997	343
Al PILMont*	0.9982	(189)	1.0	237
Si/Al PILMont(2)*	0.9985	(173)	0.9999	227
Ni/Al PILMont*	0.9955	(177)	0.9994	253
NH_4 Beid*	0.9998	117	0.9992	(143)
Al PILBeid	0.9985	(156)	0.9997	198
Al PilBeid*	0.9959	(132)	0.9987	163
SMM	0.9999	120	0.9930	(166)
SMM*	0.9994	101	0.9982	(135)
Al PILSMM*	0.9983	163	0.9999	215
Ni-SMM(7)	0.9996	222	0.9947	(295)
Ni-SMM(7)*	1.0	185	0.9977	(245)
Al PILNi-SMM(7)*	0.9989	190	0.9988	268
Ni-SMM(21)	1.0	163	0.9957	(220)
Ni-SMM(21)*	0.9998	151	0.9940	(211)
Al PILNi-SMM(21)*	0.9995	150	0.9950	(201)

* Calcined 500°C

Table 3.5. Surface Areas, and BET and Langmuir Isotherm Correlation Coefficients

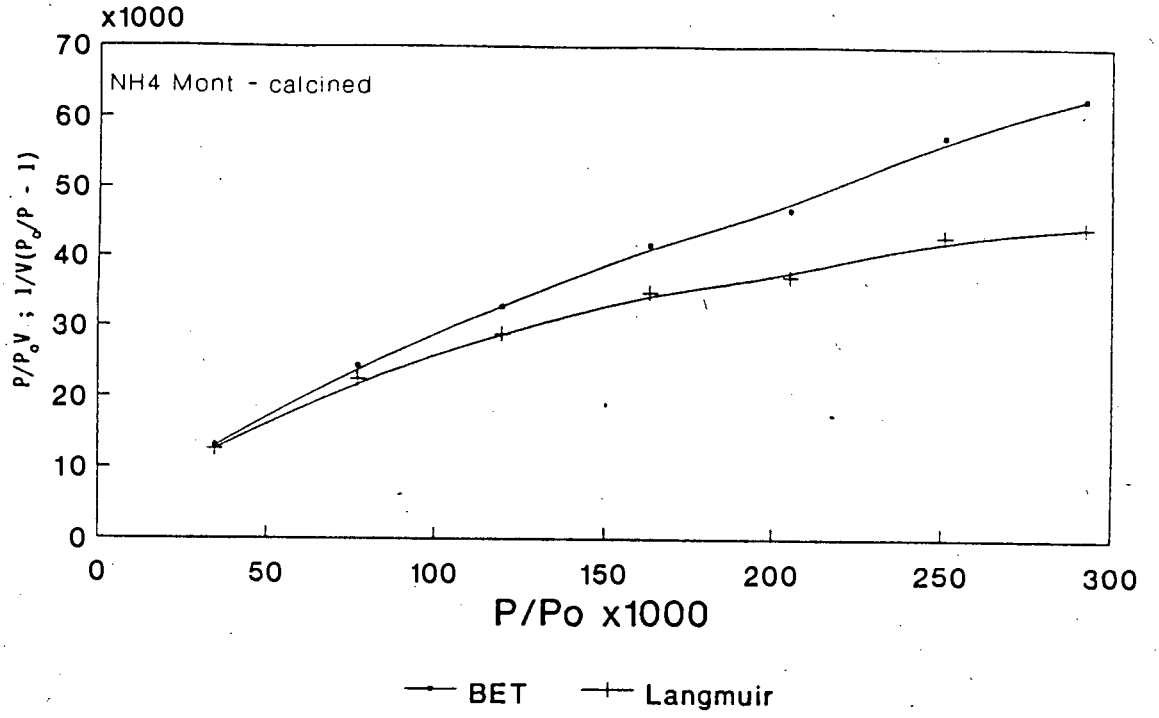

Figure 3.13. N_2 Adsorption: BET and Langmuir Isotherms of NH_4 Mont

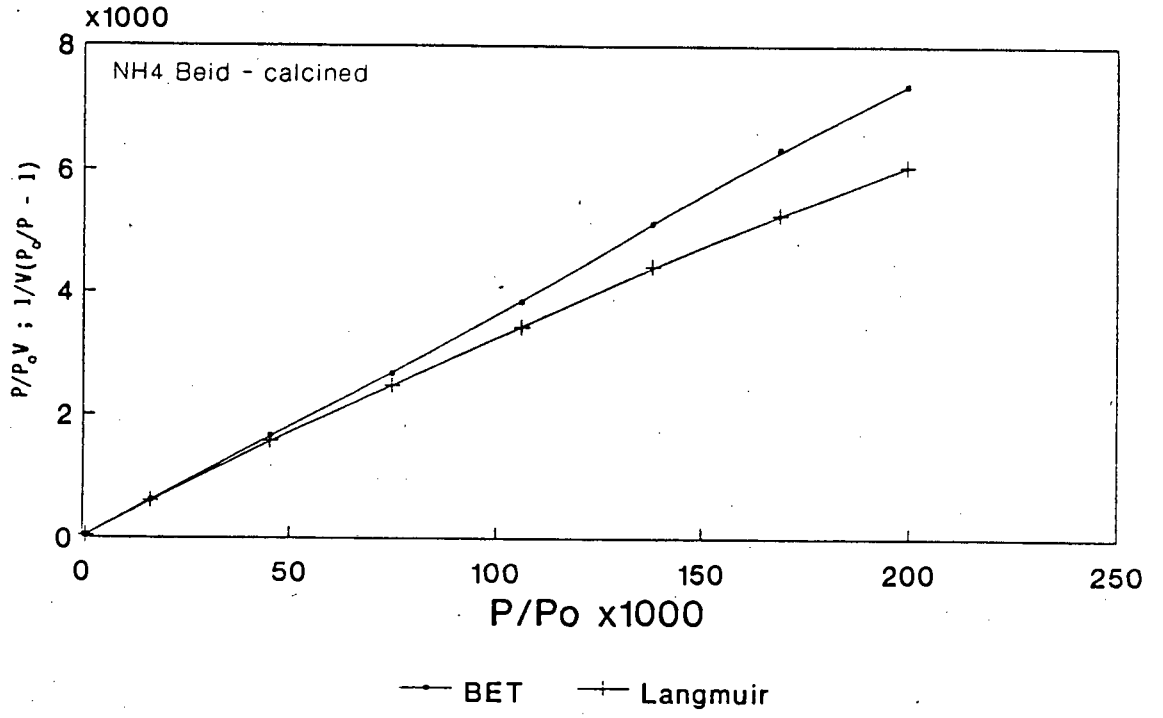

Figure 3.14. N_2 Adsorption: BET and Langmuir Isotherms of NH_4 Beid

The Langmuir isotherms of the Al PILMont, Si/Al PILMont, Ni/Al PILMont and Al PILBeid samples were all significantly more linear than the BET isotherms. These results indicate that the surface area of these samples is due predominantly to micropores in the interlayer spaces where only monolayer or limited layer adsorption can occur.

The BET isotherms of the unpillared SMM and Ni-SMM clays were significantly more linear than the Langmuir isotherms. This indicates that multilayer adsorption predominates, and is consistent with the essentially macroporous structures of these clays. Calcination did not appear to affect the type of adsorption taking place in these clays.

Treating SMM with the hydroxy-Al pillaring solution resulted in an increase in the curvature of the BET isotherm, and an increase in the linearity of the Langmuir isotherm. A similar trend was observed on treatment of the two Ni-SMM samples with the pillaring solution, although the changes in the linearity of the two isotherms were less pronounced. After pillaring, the Langmuir isotherm of SMM provided a better approximation to a straight line than the BET isotherm.

Table 3.5 contains the estimates of the surface areas of all the clays. The surface areas quoted are those calculated from the more linear of the two adsorption isotherms, although both figures are reported.

The measured surface area of the calcined montmorillonite clay was 23 m^2/g. Hongdu (1981) reported a BET surface area of 51 m^2/g for a naturally occurring montmorillonite clay. The surface area of the montmorillonite clay after treatment with the hydroxy-Al pillaring solution was 343 m^2/g. Calcination at 500°C reduced the surface area to 237 m^2/g. The surface areas of the calcined Si/Al PILMont(2) and Ni/Al PILMont were similar to that of calcined Al PILMont, being 227 and 253 m^2/g respectively.

The estimated surface area of calcined beidellite was 117 m^2/g, which is considerably higher than that of calcined montmorillonite. The surface area of beidellite treated with the hydroxy-Al solution was 198 m^2/g. Calcination of Al PILBeid decreased the measured surface area to 163

m^2/g.

The surface areas of the Ni-SMM samples were larger than that of SMM. This is in agreement with results reported by Swift and Black (1974). Calcination of the SMM, Ni-SMM(7), and Ni-SMM(21) samples at 500°C resulted in a decrease in surface area in all cases. The surface area of calcined SMM was smaller than that of calcined beidellite.

Treating SMM with the hydroxy-Al pillaring solution resulted in a significant increase in surface area after calcination, larger, in fact, than that observed upon pillaring beidellite. The surface area of calcined Al PILSMM according to the Langmuir isotherm, which was the more linear of the two isotherms, was 215 m^2/g, while that according to the BET isotherm was 163 m^2/g. If both monolayer (or limited layer) and multilayer adsorption were occurring in this clay, which would be the case if treatment with the pillaring solution resulted in the partial generation of a microporous pillared structure in the essentially macroporous SMM structure, the BET estimate would be lower than the actual surface area, while the Langmuir estimate would be higher. It seems likely, therefore, that a representative surface area would lie somewhere between these two estimates.

Treatment of the two Ni-SMM clays with the pillaring solution did not appear to have a marked effect on the surface areas of these clays.

3.1.2.5 Propane Adsorption

Propane adsorption experiments were carried out on the TG-DTA apparatus described earlier. Figure 3.15 shows the weight gain versus time for one of the samples tested. The profile of the curve is typical of the results obtained from all the samples. The rate of adsorption was initially rapid, but decreased steadily. Adsorption was allowed to continue for six hours, after which time propane uptake still appeared to be occurring, but had slowed down considerably.

Table 3.6 summarises the results of the experiments. Weight gain due to propane adsorption is expressed as a percentage of the calcined mass of catalyst.

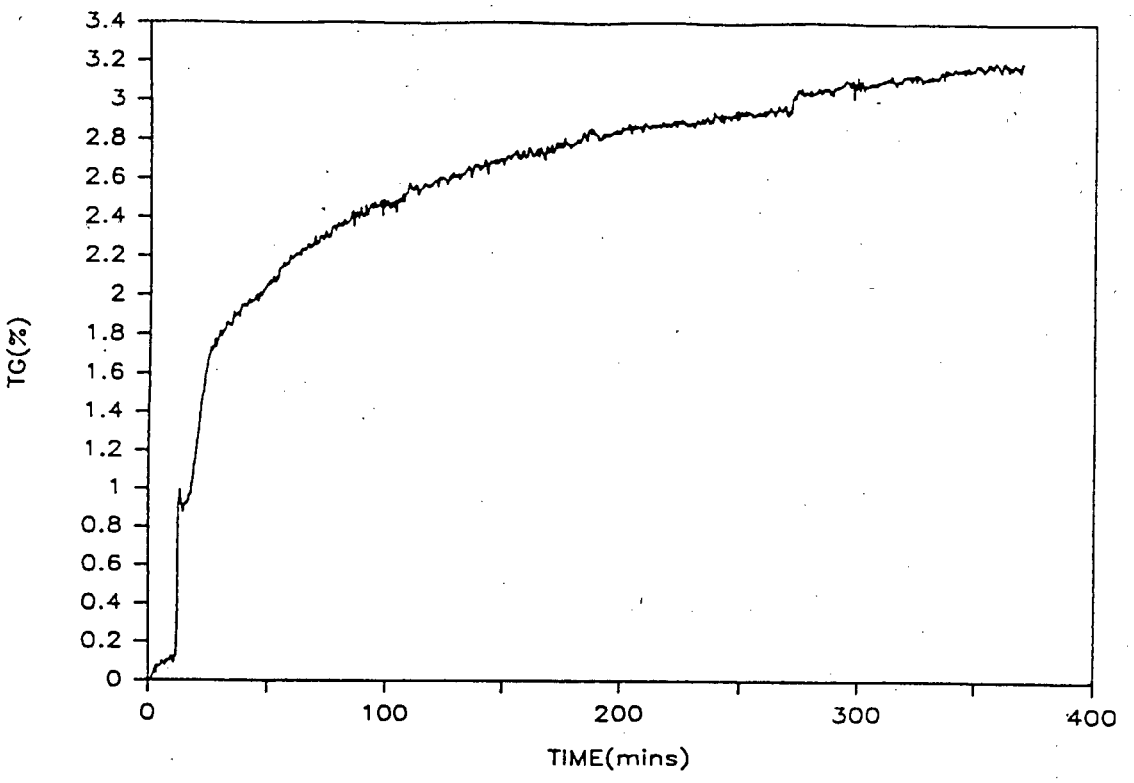

Fig. 3.15. Propane Adsorption: Typical Adsorption Profile

Sample	Weight Gain (%)
Na Mont	0.4
Al PILMont	3.2
Si/Al PILMont(2)	2.9
Ni/Al PILMont	2.0
Na Beid	0.6
Al PILBeid	1.8
SMM	0.5
Al PILSMM	2.2
Ni-SMM(7)	1.1
Al PILNi-SMM(7)	3.3
Ni-SMM(21)	0.9
Al PILNi-SMM(21)	1.7

Table 3.6. Propane Adsorption: 30°C; Duration 6 hours

Treating montmorillonite with the hydroxy-Al pillaring solution increased the weight gain due to propane adsorption from 0.4% to 3.2%. Treating the clay with the Si/Al pillaring solution gave similar results. The increase in propane adsorption on treatment with the Ni/Al pillaring solution was lower. Na Beid and Na Mont adsorbed similar amounts of propane. Al PILBeid adsorbed less propane than Al PILMont. Treating the SMM and Ni-SMM samples with the hydroxy-Al solution resulted in significant increases in propane adsorption in all cases.

3.1.2.6 Ammonia Temperature Programed Desorption

Figures 3.16 - 3.23 show the results of ammonia TPD experiments carried out on the clay catalyst samples. By integrating the areas under the curves, the total amount of ammonia desorbed per gram of catalyst is obtained. These results are contained in Table 3.7, and are compared with the titration values. In general, the values obtained from the titration of the H_2SO_4 solution agreed well with the integrated values. The quantity of ammonia which desorbed from the catalysts may be regarded as being an indication of the number of available acid sites which are sufficiently strong to hold ammonia at temperatures in the range 100 to 500°C. Table 3.7 also shows the temperatures at which the rate of ammonia desorption reached a maximum for the different catalysts.

The TPD profiles in Figures 3.16 - 3.23 all display a sharp drop in the desorption spectrum in the region of 500°C. It should be noted that this is an experimental artefact and does not represent a sudden decrease in the amount of ammonia desorbing from the catalysts as the temperature approaches 500°C. At the end of each run, samples were held at 500°C until the signal from the TCD, detecting the desorbing ammonia, returned to the baseline. When this signal is plotted against temperature, the spectrum gives the appearance of falling sharply at 500°C. It is possible that acid sites will be present on the catalysts which are sufficiently strong to hold ammonia up to temperatures in excess of 500°C. The ammonia TPD procedure used, however, will not detect the presence of such sites. An indication of the amount of ammonia remaining on the catalysts above 500°C may be obtained by subtracting the amount of ammonia which desorbed from the catalyst between 100 and 500°C from

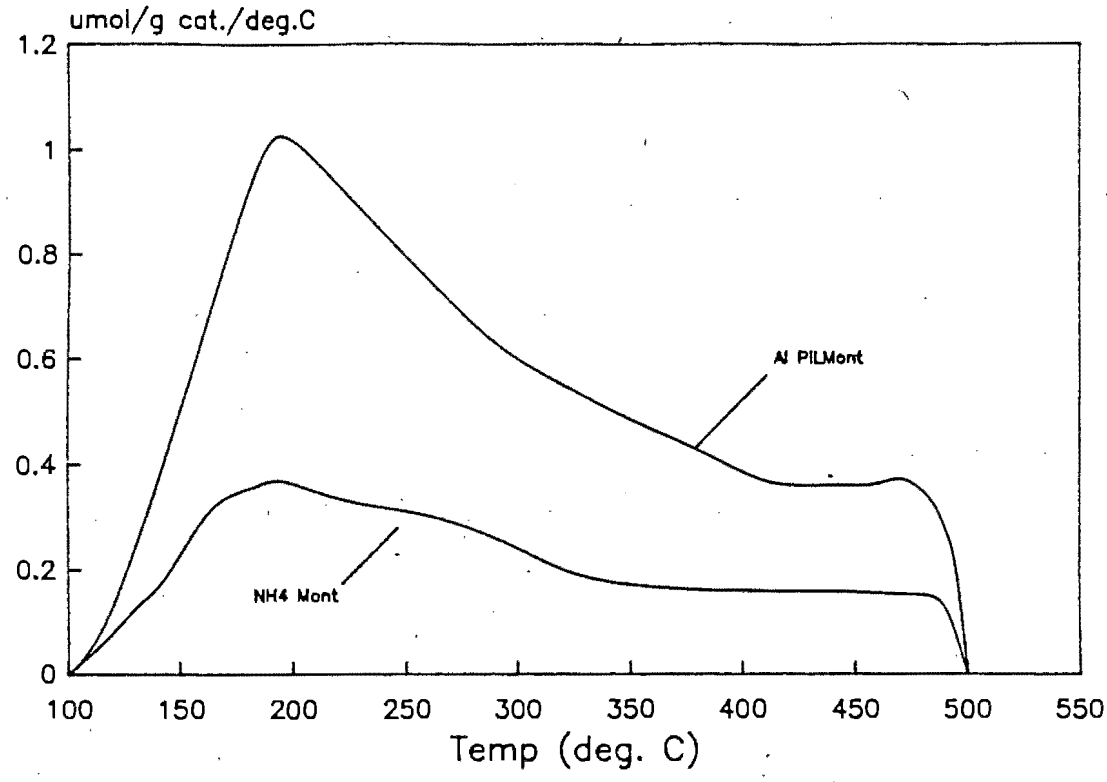

Figure 3.16. Ammonia TPD: NH_4 Mont and Al PILMont

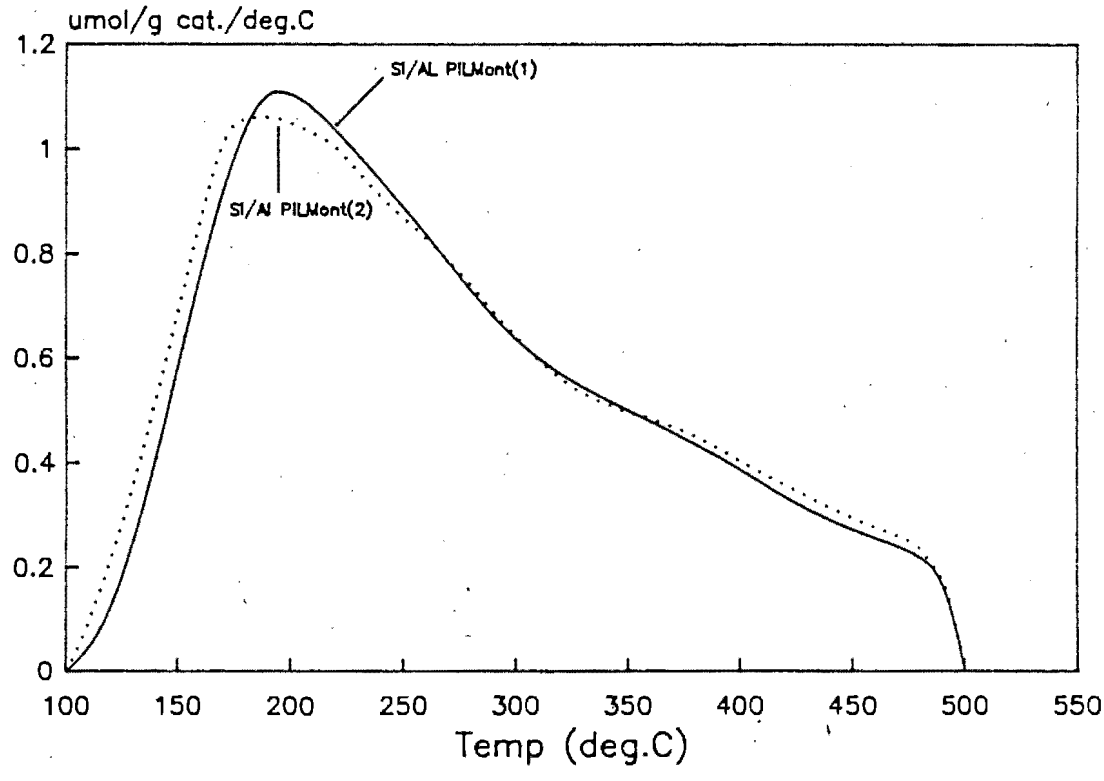

Figure 3.17. Ammonia TPD: Si/Al PILMont(1) and Si/Al PILMont(2)

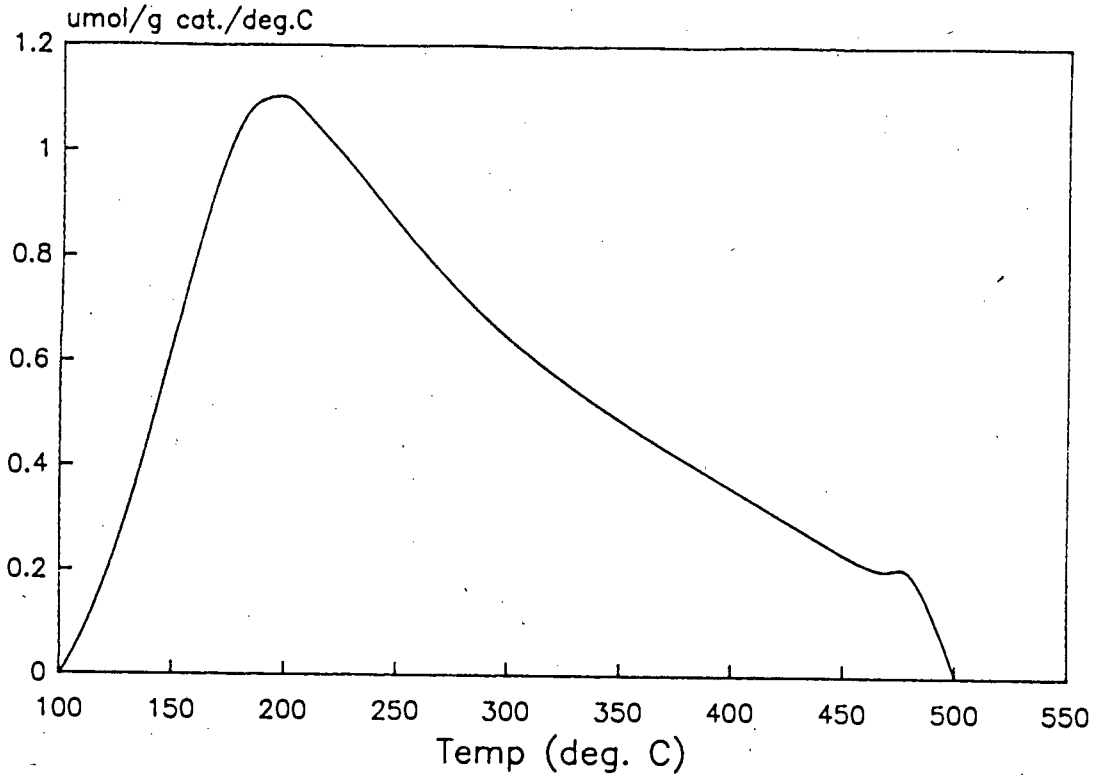

Figure 3.18. Ammonia TPD: Ni/Al PILMont

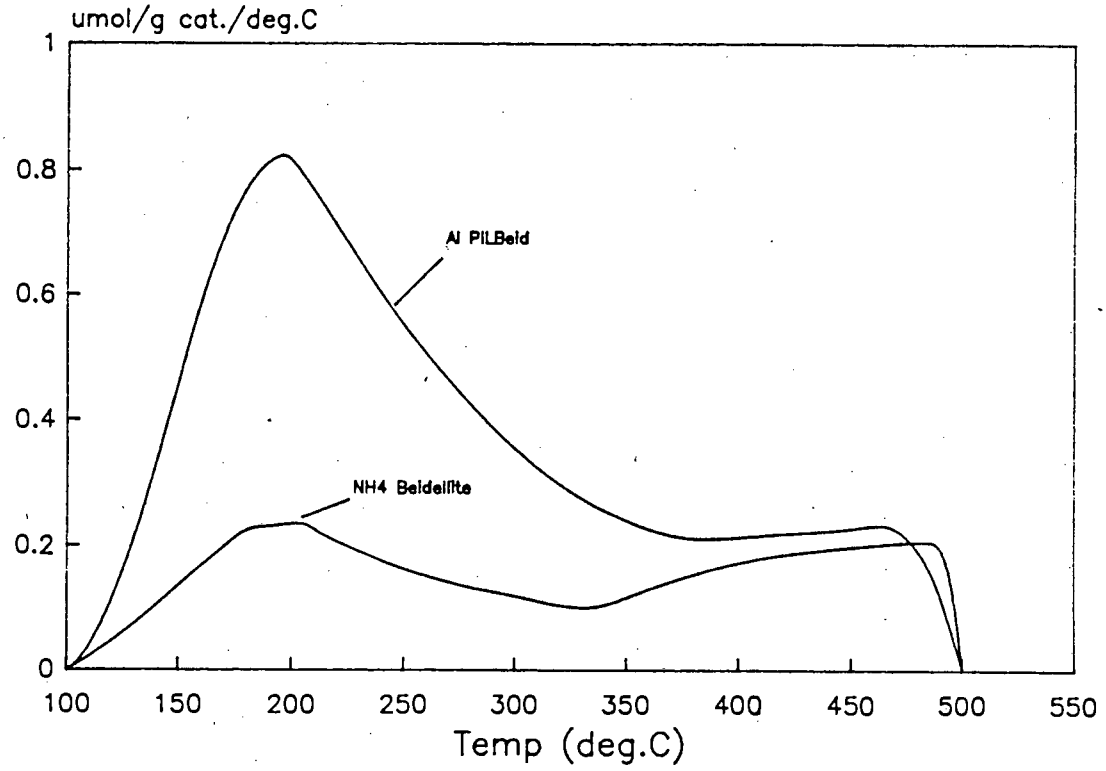

Figure 3.19. Ammonia TPD: NH_4 Beid and Al PILBeid

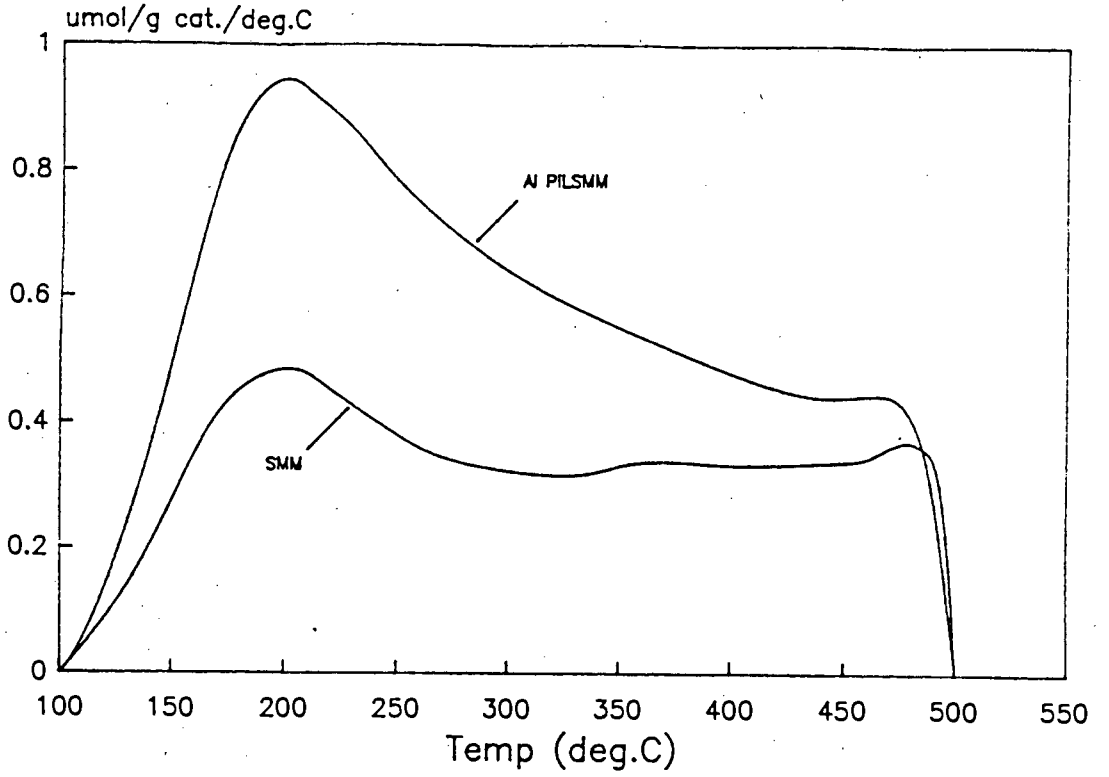

Figure 3.20. Ammonia TPD: SMM and Al PILSMM

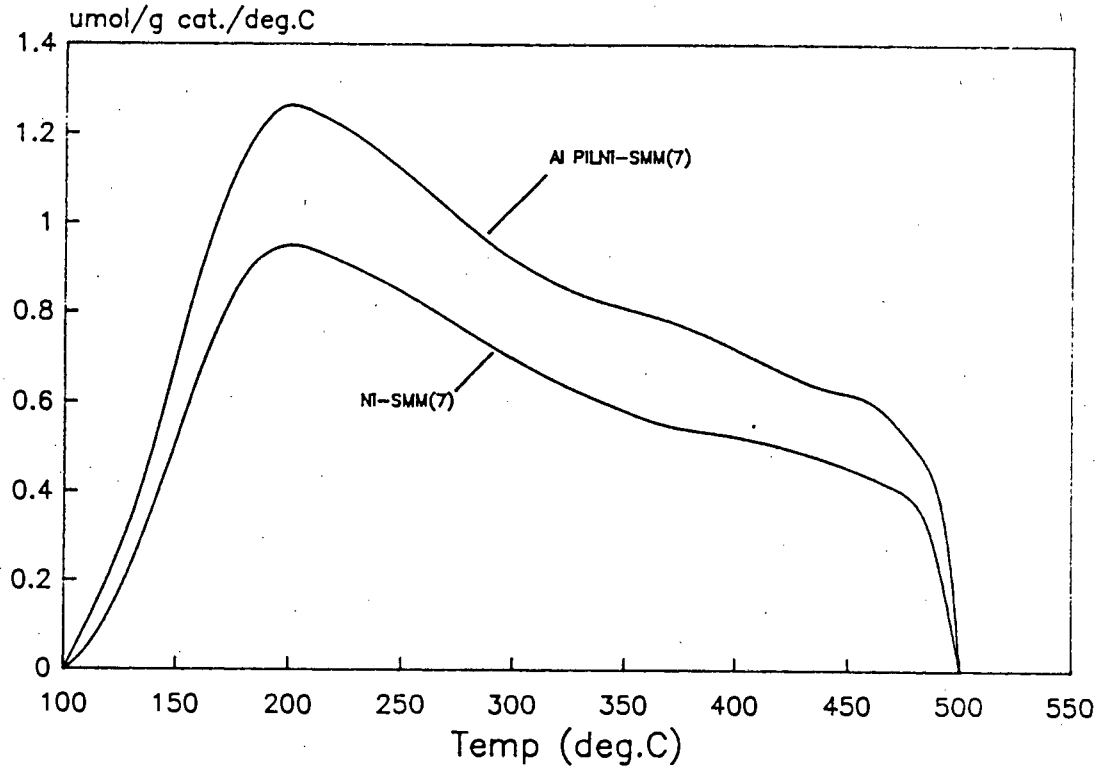

Figure 3.21. Ammonia TPD: Ni-SMM(7) and Al PILNi-SMM(7)

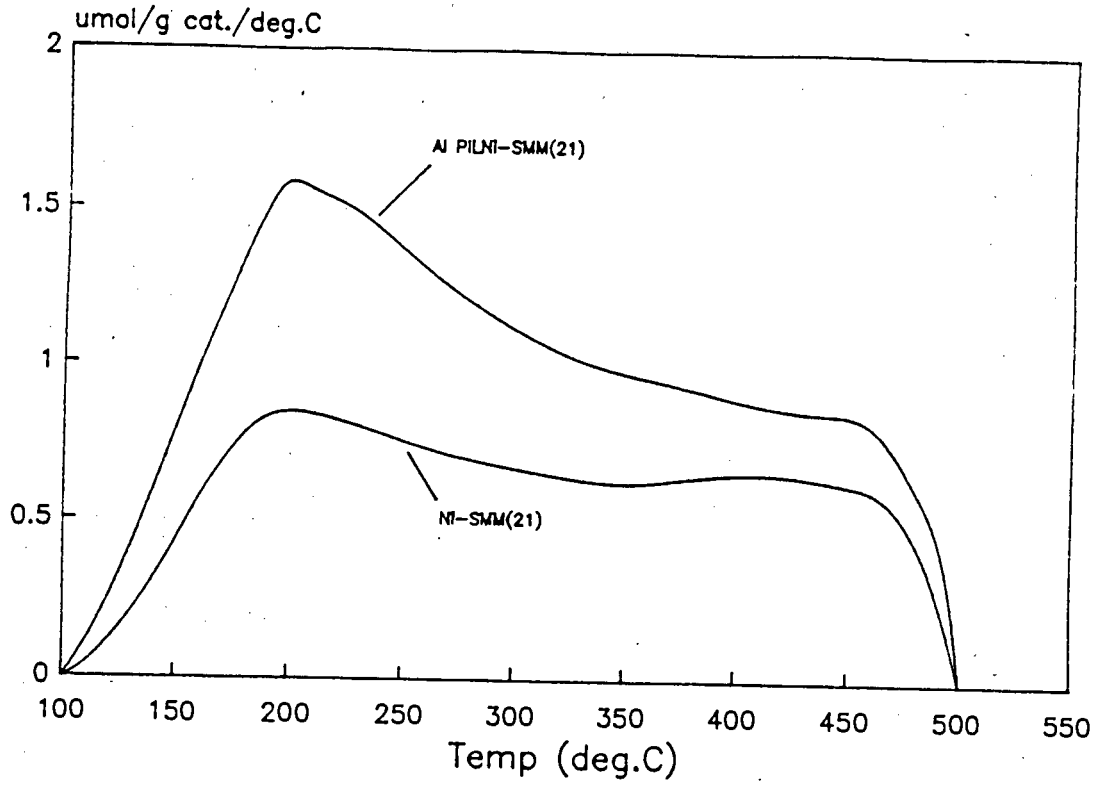

Figure 3.22. Ammonia TPD: Ni-SMM(21) and Al PILNi-SMM(21)

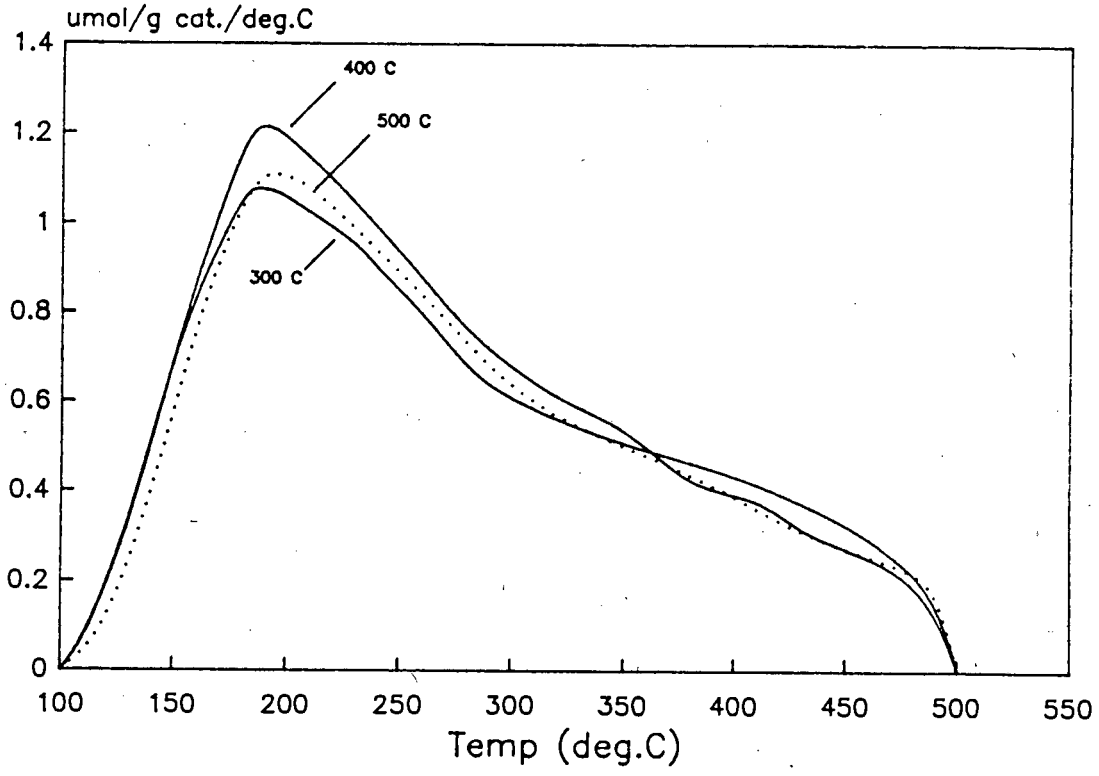

Figure 3.23. Ammonia TPD: Effect of Calcination Temp. on Si/Al PILMont

Clay	NH_3 Desorbed (mmol/g) Integration	Titration	Temp for Max. Desorption (°C)
NH_4^+ Mont.	0.07	0.06	194
Al PILMont	0.22	0.22	194
Si/Al PILMont(1)	0.22	0.23	195
Si/Al PILMont(2)	0.23	0.24	193
Ni/Al PILMont	0.22	0.24	200
NH_4^+ Beidellite	0.04	0.04	205
Al PILBeid	0.14	0.15	195
SMM	0.17	0.16	201
Al PILSMM	0.25	0.28	203
Ni-SMM(7)	0.20	0.20	202
Al PILNi-SMM(7)	0.31	0.33	200
Ni-SMM(21)	0.24	0.23	194
Al PILNi-SMM(21)	0.36	0.36	200

Table 3.7. Ammonia TPD Results

the difference in the amount of ammonia which adsorbed and desorbed at 100°C. Many of the values obtained using this procedure, however, were obviously inaccurate (in some cases ammonia adsorded minus that desorbed at 100°C was smaller than that which desorbed between 100 and 500°C). This is ascibed to inaccuracies in the thermal conductivity readings obtained when the concentration of ammonia in the carrier gas was high, viz., at 100°C. These values are therefore not reported.

From Table 3.7 it can be seen that the desorption maxima of the parent clays are very similar. In all cases, treating the clays with the

pillaring solutions did not result in significant changes in the temperatures at which maximum desorption of ammonia took place.

Figure 3.16 shows the effect of pillaring montmorillonite with the hydroxy-Al solution. The total amount of ammonia which desorbed from NH_4 Mont was very small (0.07 mmol/g) when compared with a catalyst such as H ZSM-5 (Si/Al = 40) (ca. 0.6 mmol/g). The pillaring process increased the amount of ammonia which desorbed from the catalyst above 100°C to 0.22 mmol/g. The TPD profile of the pillared clay was similar to that of the parent clay.

Figure 3.17 shows the TPD spectra of the Si/Al PILMont(1) and Si/Al PILMont(2) samples, while Figure 3.18 shows the TPD spectrum obtained from Ni/Al PILMont. The three catalysts desorbed 0.22, 0.23 and 0.22 mmol NH_3/g, respectively. Their TPD profiles were similar, and similar to that of Al PILMont.

The results obtained from NH_4 Beid and Al PILBeid are shown in Figure 3.19. NH_4 Beid desorbed less ammonia than NH_4 Mont. Upon pillaring with the hydroxy-Al solution, the amount of ammonia which desorbed from the clay between 100 and 500°C increased from 0.04 to 0.14 mmol/g.

Figures 3.20 - 3.22 show the ammonia TPD profiles of SMM and Al PILSMM, Ni-SMM(7) and Al PILNi-SMM(7), and Ni-SMM(21) and AL PILNi-SMM(21), respectively. In all cases, treatment with the pillaring solution resulted in significant increases in the amount of ammonia which desorbed from the clays between 100 and 500°C. The amount of ammonia desorbing increased by 47% in the case of SMM, by 55% in the case of Ni-SMM(7), and by 50% in the case of Ni-SMM(21). SMM in its unpillared form desorbed 0.17 mmol NH_3/g, considerably more than NH_4^+ beidellite (0.04 mmol NH_3/g).

Treating the SMM and Ni-SMM clays with the hydroxy-Al solution resulted in proportionately smaller increases in the amount of ammonia which desorbed from the catalyst than were observed upon pillaring montmorillonite and beidellite (ca. 50% vs. 214% and 250%, respectively).

The TPD profiles obtained from Si/Al PILMont(2) calcined at three different temperatures are shown in Figure 3.23. Decreasing calcination temperature did not appear to have a significant effect on the ammount of ammonia which desorbed from the catalyst between 100 and 500°C. The temperatures at which maximum desorption took place also remained relatively unaffected.

Table 3.8 shows the amount of ammonia which desorbed per square meter of catalyst surface area. The surface areas used are those shown in Table 3.5 for clay samples calcined at 500°C. The Langmuir estimates were used for all pillared montmorillonite and beidellite samples, while BET estimates were used for the parent montmorillonite and beidellite clays and all SMM and Ni-SMM clays.

Clay	umol NH_3/m^2
NH_4^+ Mont	3.04
Al PILMont	0.93
Si/Al PILMont(2)	1.01
Ni/Al PILMont	0.87
NH_4^+ Beid	0.34
Al PILBeid	0.86
SMM	1.68
Al PILSMM	1.53
Ni-SMM(7)	1.08
Al PILNi-SMM(7)	1.63
Ni-SMM(21)	1.59
Al PILNi-SMM(21)	2.40

Table 3.8. Ammonia TPD: NH_3 Desorbed/m^2 of Clay Surface Area

Table 3.9 shows the ratio of the number of moles of ammonia which desorbed from the catalysts between 300 and 500°C to that which desorbed between 100 and 300°C. This ratio may be regarded as being an indication of the ratio of stronger to weaker acid sites on the catalysts. Because the TPD procedure used for this work does not detect the presence of acid sites which are able to hold ammonia at temperatures in excess of 500°C, this ratio represents a lower limit.

Clay	NH_3 (>300°C) / NH_3 (<300°C)
NH_4^+ Mont	0.62
Al PILMont	0.67
Si/Al PILMont(1)	0.57
Si/Al PILMont(2)	0.53
Ni/Al PILMont	0.47
NH_4^+ Beid	1.06
Al PILBeid	0.45
SMM	0.98
Al PILSMM	0.74
Ni-SMM(7)	0.76
Al PILNi-SMM(7)	0.79
Ni-SMM(21)	0.85
Al PILNi-SMM(21)	0.80

Table 3.9. Ammonia TPD: Ratio of ammonia desorbing above 300°C to that desorbing below 300°C

3.1.3 Reaction Studies

3.1.3.1 Propene Oligomerisation

3.1.3.1.1 Catalyst Activities

Reproducibility

Reproducibilty runs were performed using Si/Al PILMont(1) and SMM catalysts. Results are compared with the original runs in Table 3.10 and Figure 3.24. Differences in the results of the two SMM runs may be due to variations in the WHSV, which proved difficult to control accurately, and to possible differences in the water content of the feed (molecular sieves were not replaced for every run); the activity of SMM (Fletcher et al., 1986) and Ni-SMM (O'Connor et al., 1988) has been shown to be very sensitive to the moisture content of the feed.

Overall mass balances were carried out for all propene oligomerisation runs. The mass loss in all cases was less than 5%.

Montmorillonite and Beidellite

As it was not known what reaction temperatures would be most suitable for comparing the propene oligomerisation activities of montmorillonite, beidellite, and their pillared derivatives, preliminary investigations were carried out using Al PILMont and Al PILBeid. The catalysts were run at 100, 150, and 180°C for a period of one hour at each temperature. Both showed signs of activity at 180°C. On the grounds of these results, the run procedure outlined in Section 2.3.1.2 was used to compare the performances of this group of catalysts for propene oligomerisation. The initial reaction temperature used was 200°C and the WHSV based on the total feed was approximately 5 h^{-1} (P = 50 atm).

Table 3.11 shows the conversion levels attained by the catalysts at four different temperatures. The conversion figures represent the average conversion levels over a period of one hour at each temperature.

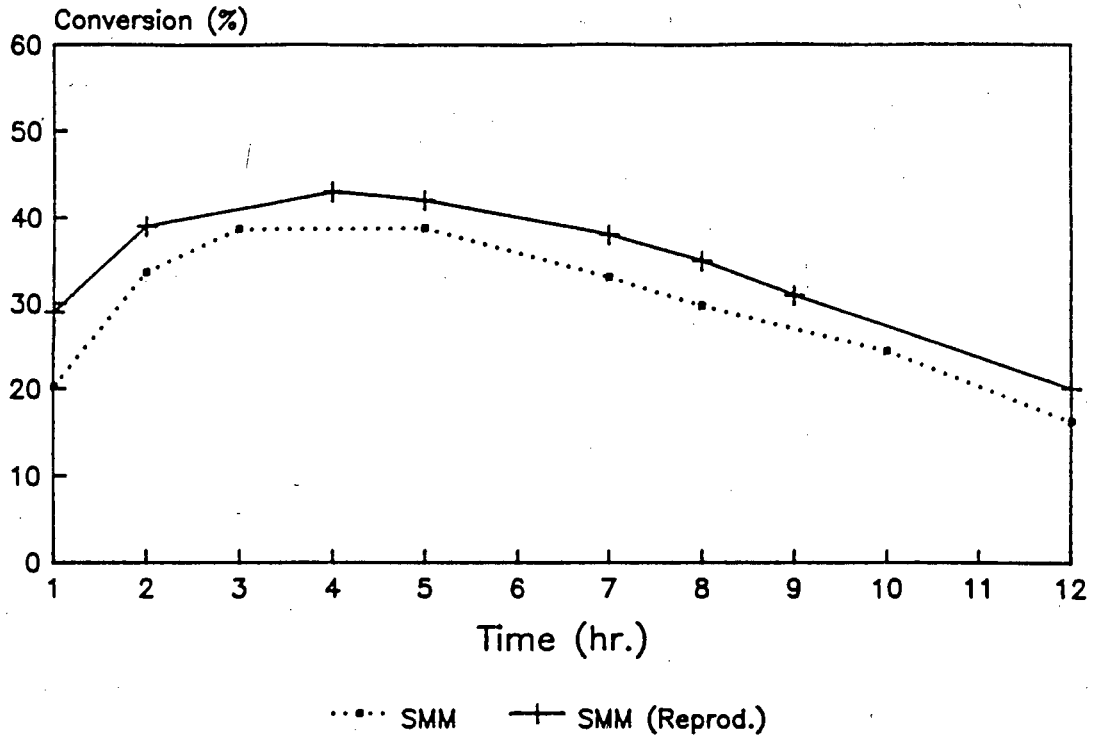

Figure 3.24. Reproducibility of Propene Oligomerisation over SMM

Temp. (°C)	Conversion (%)	
	Run 1	Run 2
200	9	11
250	3	5
300	3	2
350	2	2

Table 3.10. Reproducibility of Propene Olig. over Si/Al PILMont(1)

Catalyst	Conversion (%) 200°C	250°C	300°C	350°C
NH_4^+ Mont	-	-	-	traces
Al PILMont	11	5	5	4
Si/Al PILMont	12	7	4	3
Ni/Al PILMont	10	6	4	2
NH_4^+ Beid	-	-	traces	traces
Al PILBeid	7	4	3	3

Table 3.11. Propene Oligomerisation: Montmorillonite and Beidellite (Pillared and Unpillared)

Na Mont and NH_4^+ Mont showed no activity below 350°C. At this temperature, traces of liquid product appeared in the catchpot. Quantities were too small to be collected and weighed. No conversion figures are therefore reported. At the end of the run both catalysts were visibly coked.

Na Beid and NH_4 Beid showed no signs of activity below 300°C. At 300°C and 350°C, both catalysts produced traces of liquid product. Catalysts were visibily coked at the end of reaction.

Pillaring of montmorillonite resulted in noticeable increases in the conversion of propene. The montmorillonite samples pillared with the Al, Si/Al, and Ni/Al pillaring solutions behaved very similarly. Conversion levels were around 10% at 200°C, between 3 and 7% at 250°C, between 2 and 5% at 300°C, and between 2 and 4% at 350°C. Liquid production appeared to drop off rapidly after the first few minutes of reaction at each temperature. This effect was most noticeable at the higher temperatures. As the conversion levels reported represent an average over a period of one hour, the initial conversion levels at each temperature, particularly those at the higher temperatures, were probably higher than the average values reported. All catalysts were visibily coked when removed from the reactor.

Pillaring of beidellite with the hydroxy-Al pillaring solution resulted in significant increases in the levels of conversion attained by the catalyst. Conversion levels were slightly lower than those attained by the pillared montmorillonite samples. As was observed with Al PILMont, the rate of liquid product formation appeared to decrease rapidly during reaction at each temperature, indicating a high rate of catalyst deactivation.

SMM and Ni-SMM

Figures 3.25 - 3.27 show the results of propene oligomerisation runs performed over SMM and Al PILSMM, Ni-SMM(7) and Al PILNi-SMM(7), and Ni-SMM(21) and Al PILNi-SMM(21), respectively. The reaction temperature used for the SMM samples was 140°C, while that used for the nickel containing samples was 150°C. The WHSV was held at around 5 h^{-1} in all cases (P = 50 atm).

Table 3.12 compares the activities of the catalysts according to the mass of liquid produced per gram of catalyst over a period of 12 hours. Average conversion levels are also shown.

Ni-SMM(7) was the most active unpillared clay, followed by Ni-SMM(21) and SMM. These results are consistent with the findings of O'Connor et al. (1988) who reported that Ni-SMM(7) displayed greater activity for propene oligomerisation than SMM.

A consideration of Figures 3.25 - 3.27 and Table 3.12 shows that treatment with the hydroxy-Al pillaring solution resulted in significant increases in catalyst activity in all cases. The activities of the Ni-SMM samples, as indicated by the mass of liquid produced per gram of catalyst, increased by 47%, while that of SMM increased by 27%.

The reaction profiles of all the catalysts were similar. In all cases maximum conversion levels were only reached after between three and six hours. The rate of catalyst deactivation appeared to be similar in all cases.

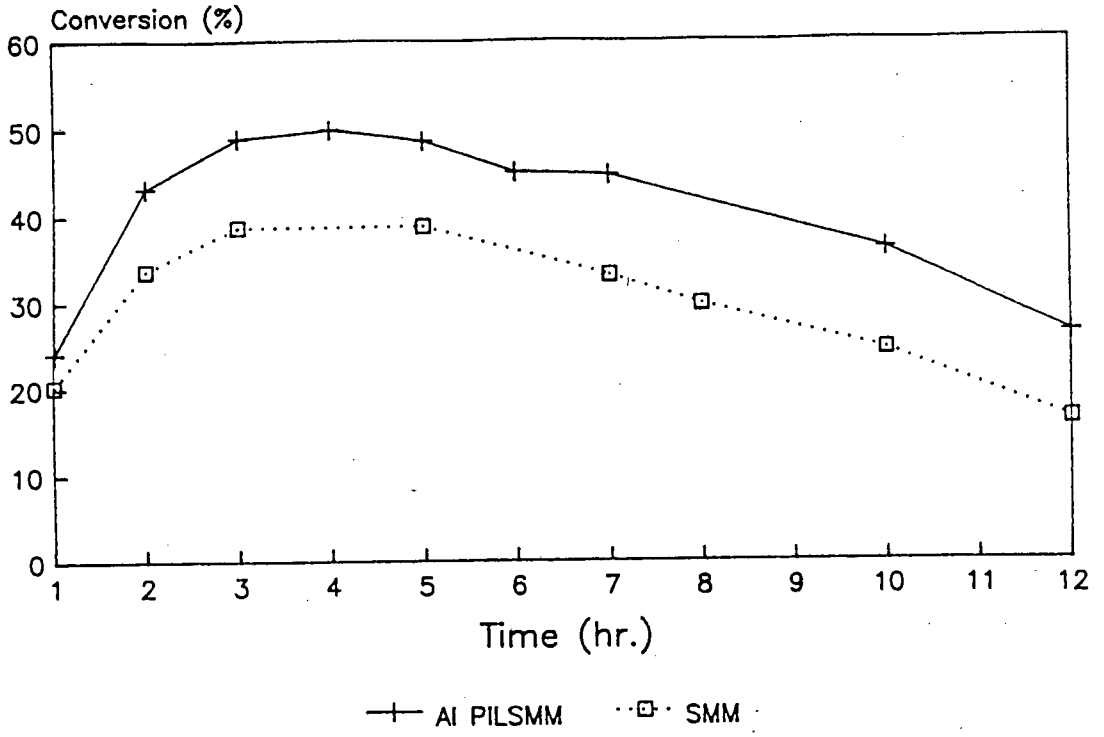

Figure 3.25. Propene oligomerisation: SMM and Al PILSMM
150°C

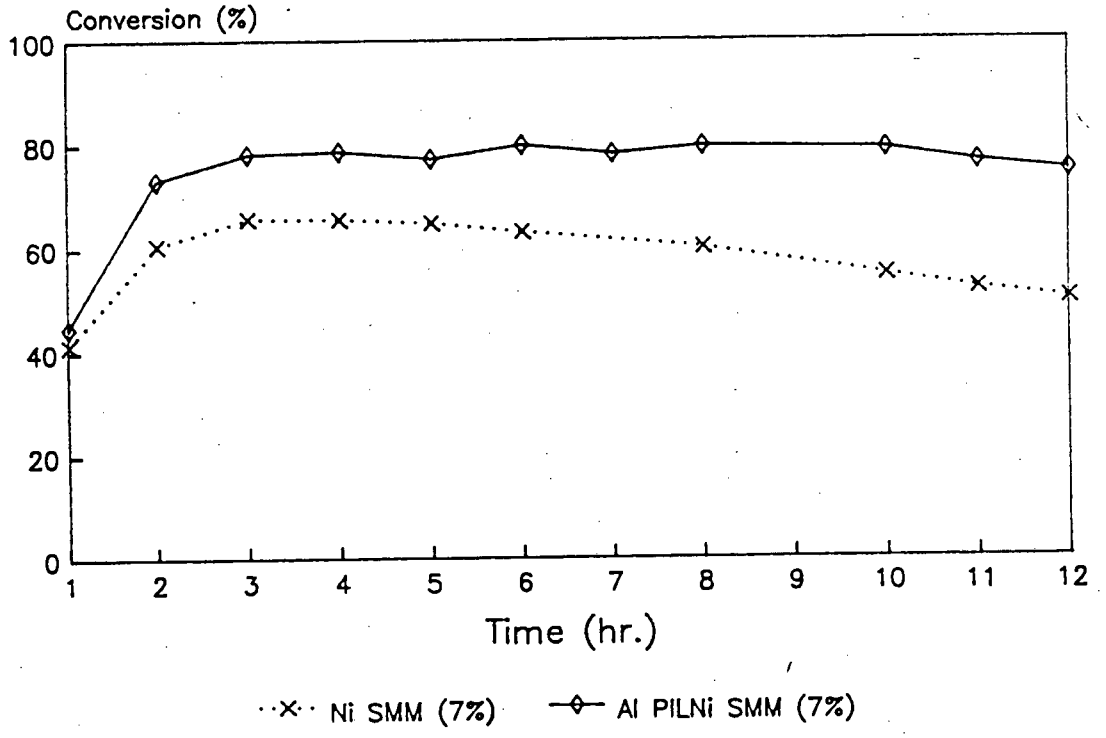

Figure 3.26. Propene Oligomerisation: Ni-SMM(7) and Al PILNi-SMM(7)
150°C

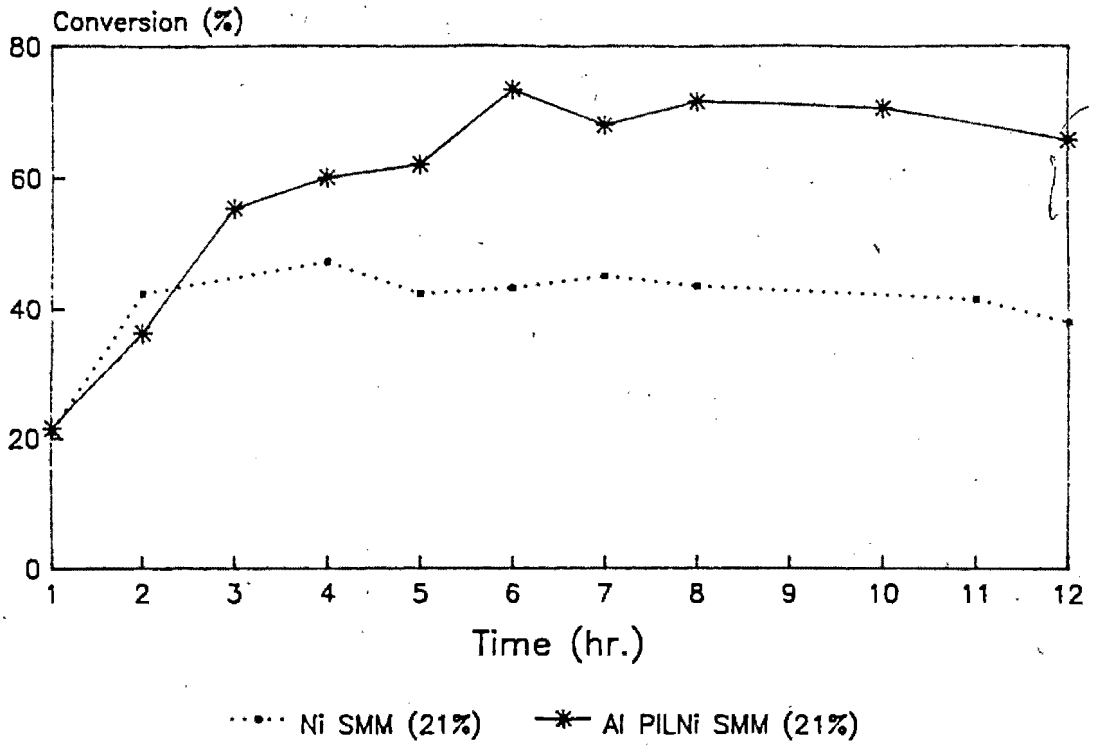

Figure 3.27. Propene Oligomerisation: Ni-SMM(21) and Al PILNi-SMM(21) 150°C

Catalyst	Activity (12 hrs) (g liq. prod./g cat.)	Ave. Conversion (%) (12 hrs)
SMM	16.9	30
Al PILSMM	21.5	39
Ni-SMM	27.6	50
Al PILNi-SMM	40.7	75
Ni-SMM(21)	23.1	42
Al PILNi-SMM(21)	34.1	62

Table 3.12. Propene Oligomerisation: Effect of Pillaring on Catalyst Activity (SMM and Ni-SMM)

3.1.3.1.2 Product Selectivities

Figures 3.28 - 3.31 show the liquid product selectivities, in terms of carbon number distribution, of Al PILMont, Si/Al PILMont(1), Si/Al PILMont(2), and Ni/Al PILMont, respectively, at the four reaction temperatures.

Product distributions appeared to be similar, irrespective of the type of pillaring solution which was used. Selectivities to the C_{21+} fraction increased markedly with increasing reaction temperature (C_{21+} selectivities at 200 and 350°C were ca. 10% and 25%, respectively).

Fig. 3.32 shows the product distribution obtained from Al PILBeid at the different reaction temperatures. Selectivities were initially similar to those of the pillared montmorillonite samples (ca. 60% C_{12+} at 200°C in both cases). Unlike the pillared montmorillonite samples, however, selectivity to the C_{21+} fraction decreased with increasing temperature (C_{21+} selectivities at 200 and 350°C were 18% and 8%, respectively).

As the reaction temperatures were increased for the pillared montmorillonite and beidellite catalysts, resolution of the GC oligomer peaks, particularly the high molecular weight oligomers, deteriorated, indicating the generation of more uniform carbon number distributions.

Due to the low conversion levels attained by the unpillared montmorillonite and beidellite samples, insufficient product was available for analysis. A comparison of the selectivities of the pillared and unpillared versions of these clays is, therefore, not possible.

Figures 3.33 - 3.35 show the average liquid product distributions obtained from SMM and Al PILSMM, Ni-SMM(7) and Al PILNi-SMM(7), and Ni-SMM(21) and Al PILNi-SMM(21), respectively. The selectivities of the unpillared SMM and Ni-SMM samples were very similar. This is in agreement with results reported by O'Connor et al. (1988). Treating these clays with the hydroxy-Al pillaring solution did not appear to have a significant effect on the product distribution obtained. The selectivities of these clays, in both the pillared and unpillared forms,

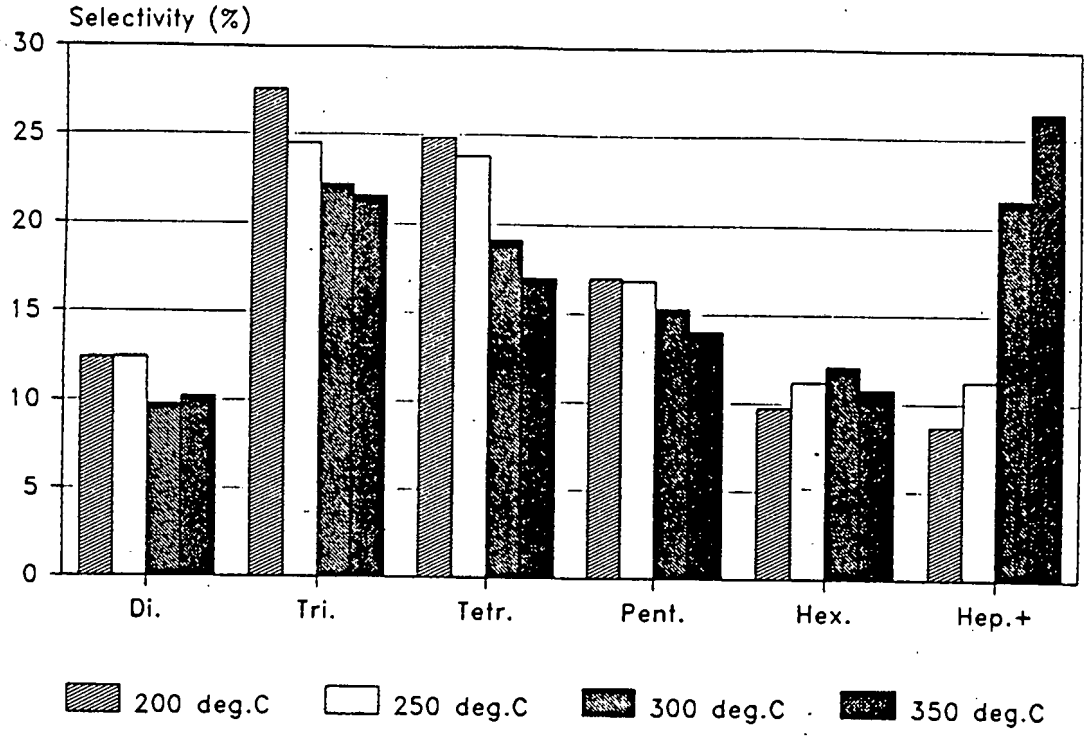

Figure 3.28. Propene Olig.: Product Selectivity of Al PILMont

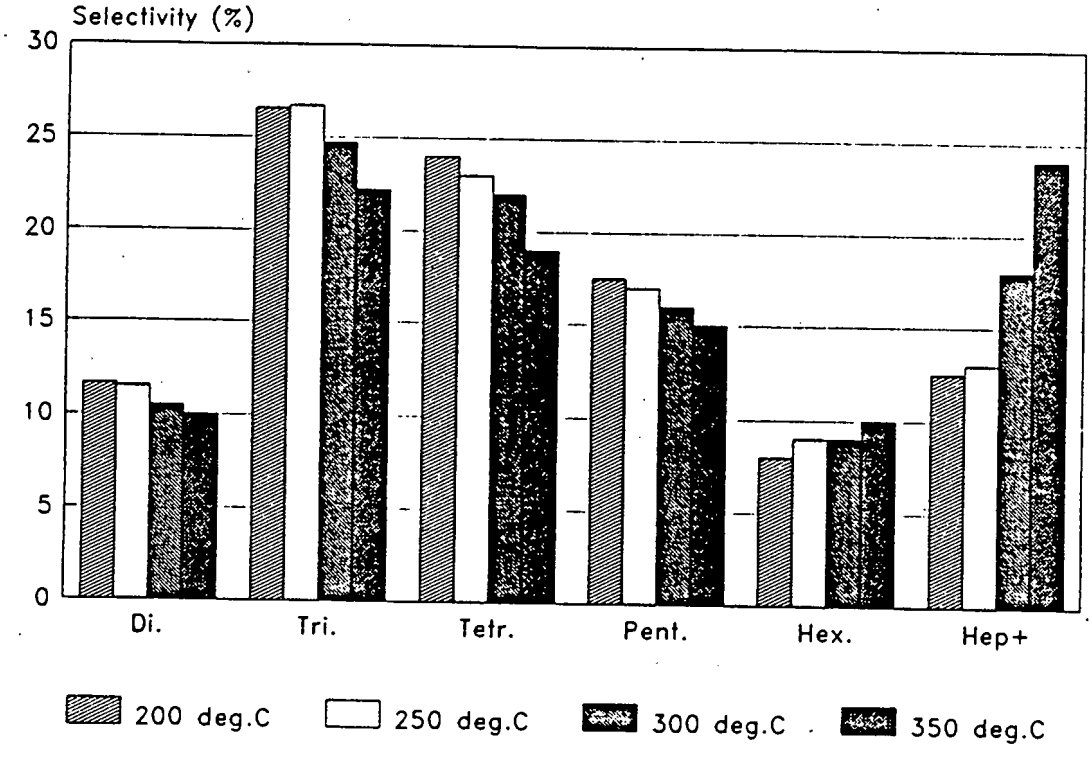

Figure 3.29. Propene Olig.: Product Selectivity of Si/Al PILMont(1)

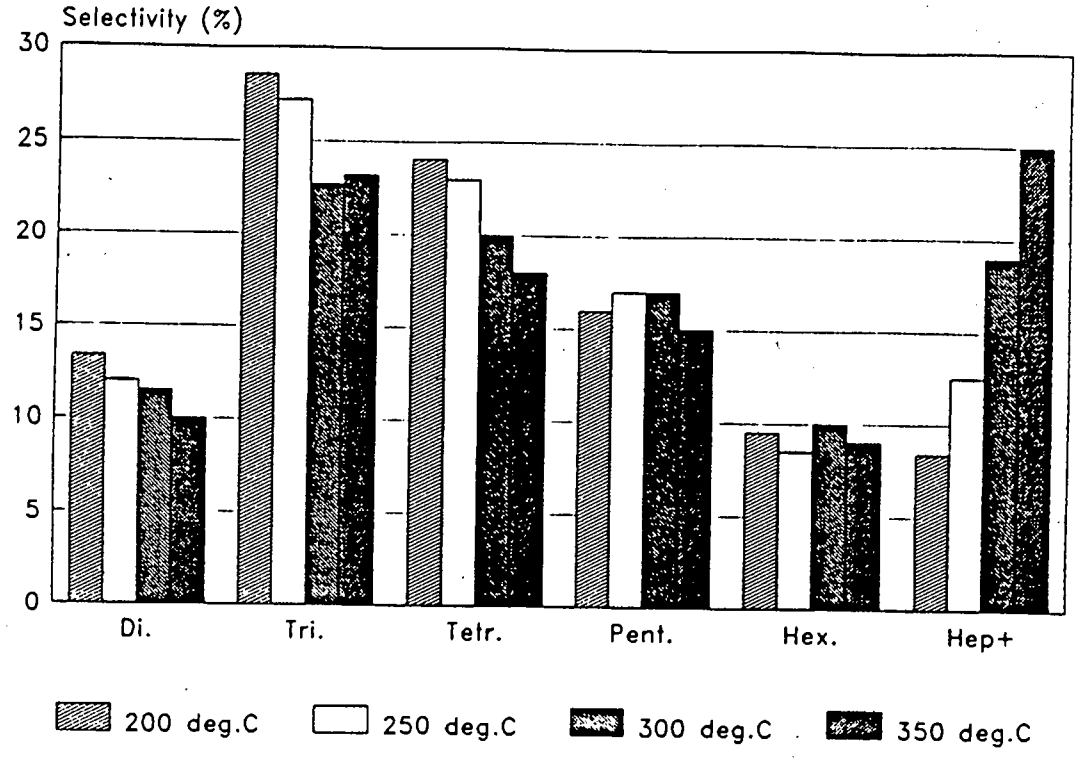

Figure 3.30. Propene Olig.: Product Selectivity of Si/Al PILMont(2)

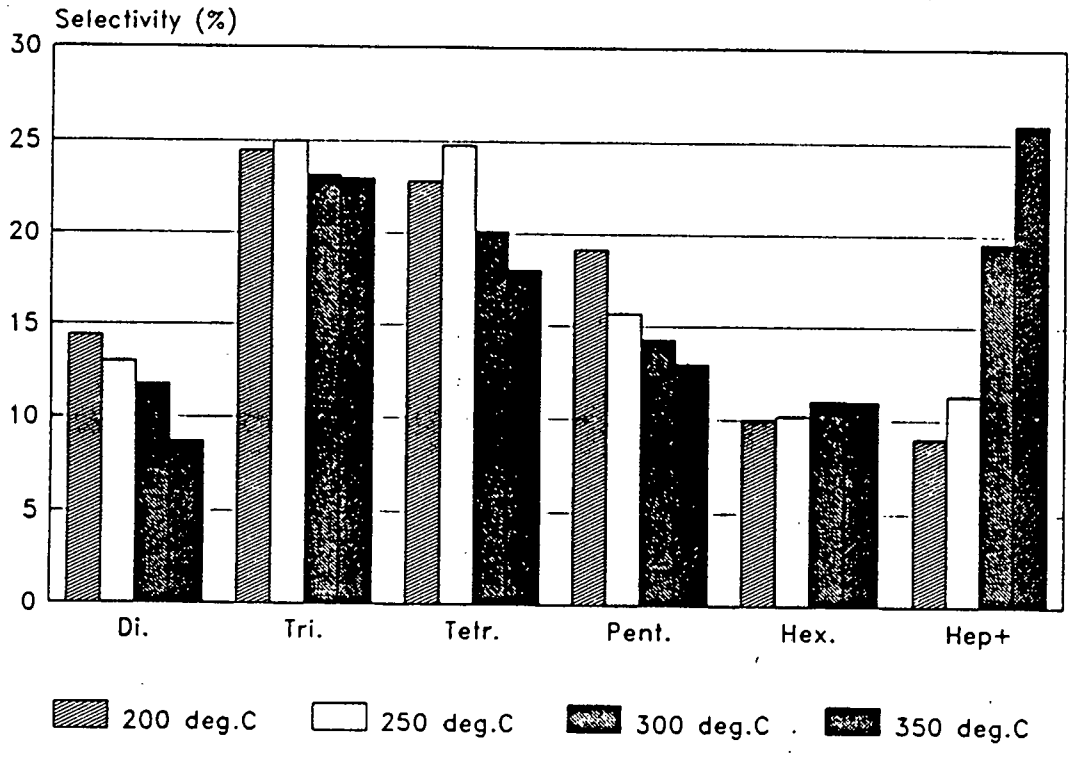

Figure 3.31. Propene Olig.: Product Selectivity of Ni/Al PILMont

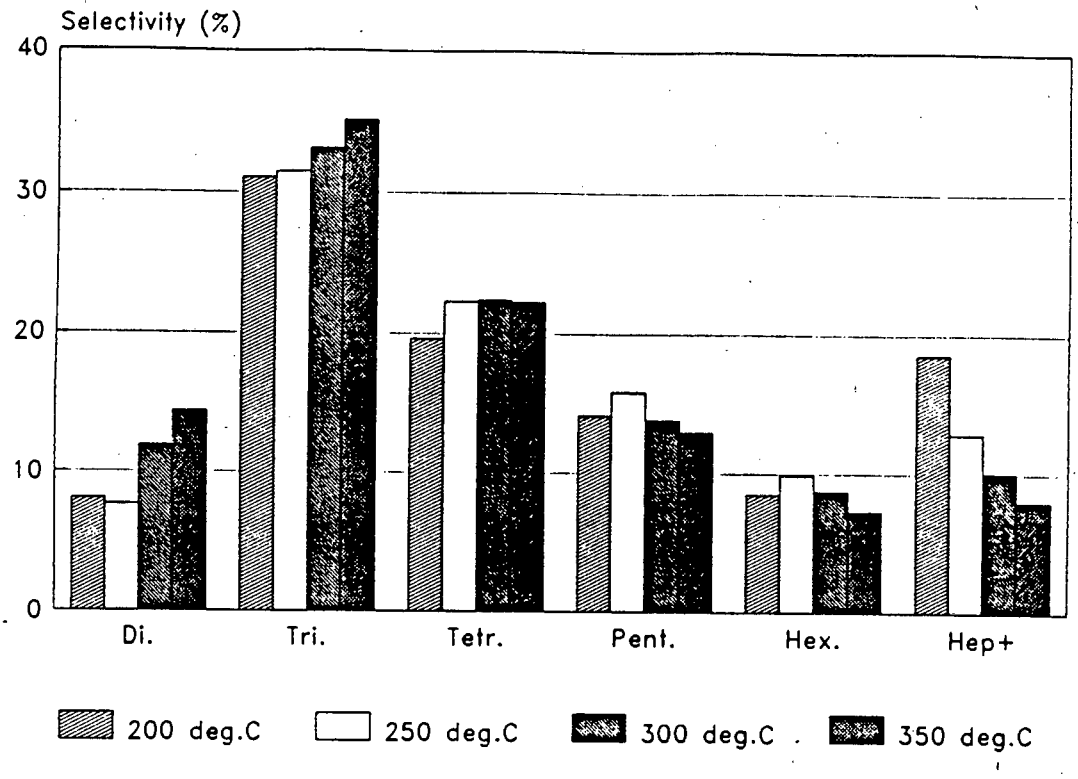

Figure 3.32. Propene Olig.: Product Selectivity of Al PILBeid

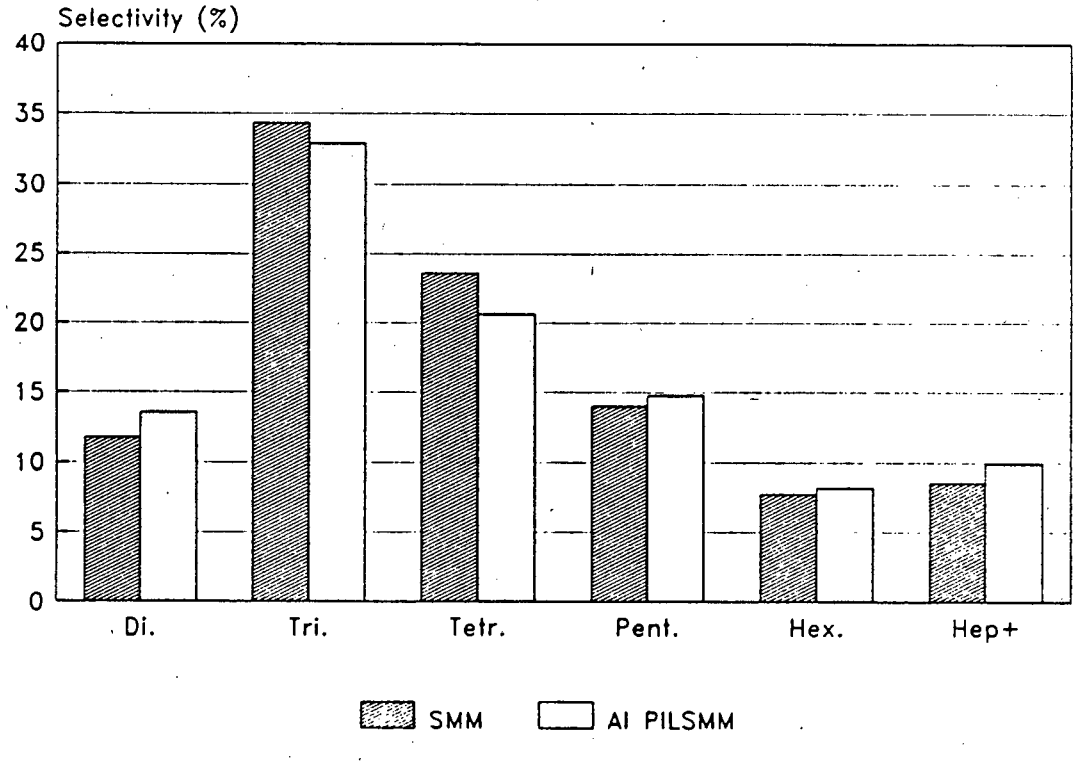

Figure 3.33. Propene Olig.: Product Selectivity of SMM and Al PILSMM (140°C)

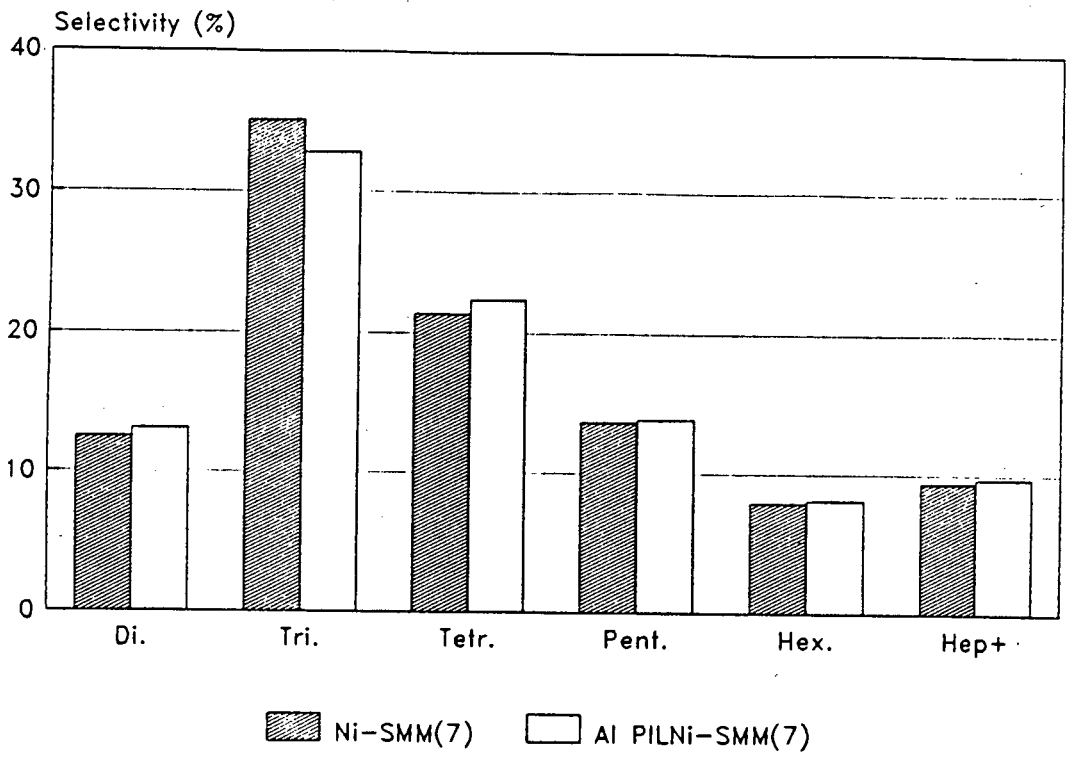

Figure 3.34. Propene Olig.: Product Selectivity of Ni-SMM(7) and Al PILNi-SMM(7) (150°C)

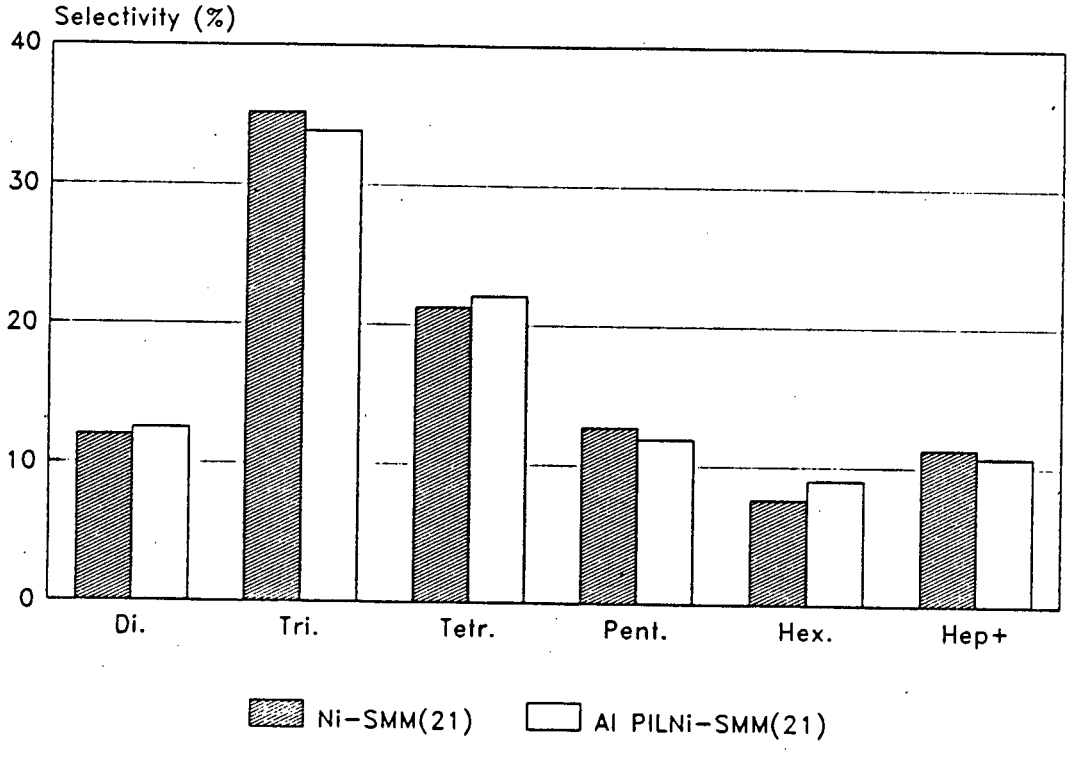

Figure 3.35. Propene Olig.: Product Selectivity of Ni-SMM(21) and Al PILNi-SMM(21) (150 °C)

did not vary noticeably with time on stream.

3.1.3.1.3 Coke Studies

The removal of coke deposited in the clay catalysts used for propene oligomerisation was monitored using TG-DTA, as described earlier.

Typical TG and DTA curves are shown in Figure 3.36. The TG curve indicated the presence of two types of coke. Heating the sample to 500°C under flowing N_2 resulted in a noticeable mass loss. Shortly after reaching 500°C, the sample mass stabilised. This mass loss is attributed largely to the volatilisation of high boiling point hydrocarbons which are either occluded in the catalyst structure, or strongly adsorbed on active sites. The DTA curve indicated that this volatilisation is an exothermic process. Although desorption of hydrocarbons would be expected to be an endothermic process, cracking of high molecular weight hydrocarbons at the elevated temperatures in the presence of acid sites, facilitating diffusion of cracked molecules out of the catalyst structure, is an exothermic process. The introduction of air after 180 minutes resulted in a further mass loss. This mass loss was accompanied initially by a strong exotherm and is attributed to the combustion of carbonaceous deposits present on the catalyst, referred to as "graphitic" coke hereafter. As the mass losses resulting from the removal of the two different types of coke are clearly discernible, it is possible to compare the relative amounts of high boiling point hydrocarbons and graphitic coke, as defined above, which are present on the different catalysts.

Table 3.13 summarises the results of the TG runs performed on selected coked catalysts. The percentage of the total high boiling point hydrocarbons which desorbed below 400°C is shown in the last column. This should give an indication of the ease of diffusion out of the clays.

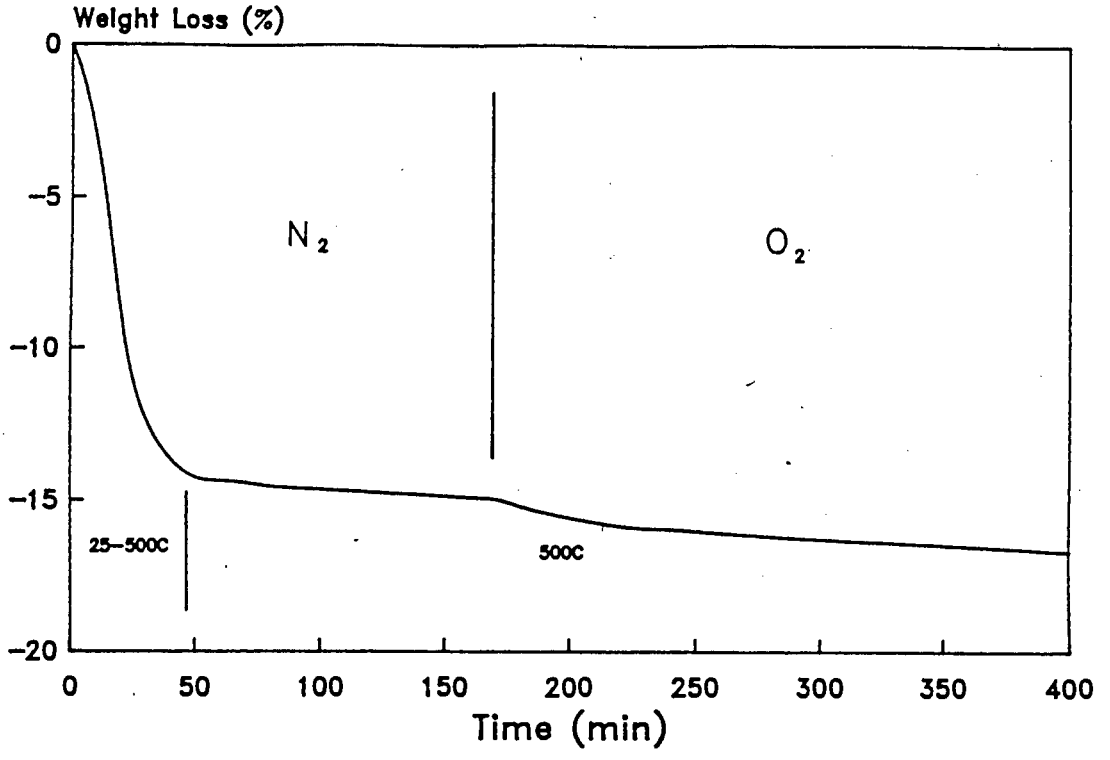

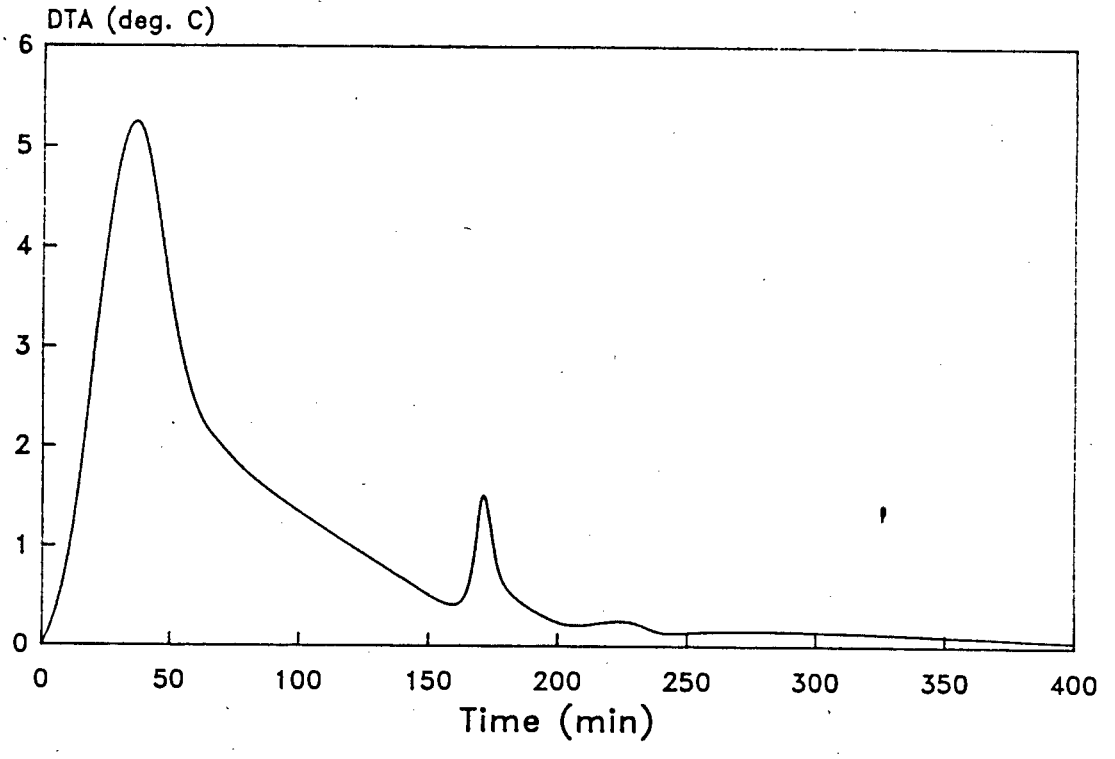

Figure 3.36. Coke Studies: Typical TG - DTA Profiles

Catalyst	Tot Mass Loss (%)	High b.p. (%)	Graphitic (%)	* (%)
Al PILMont	14.3	54	46	39
Al PILBeid	10.1	50	50	49
SMM	11.8	90	10	80
Al PILSMM	10.9	93	7	83
Ni-SMM(7)	17.3	95	5	92
Al PILNi-SMM(7)	15.3	92	8	91
Ni-SMM(21)	17.2	92	8	89
Al PILNi-SMM(21)	12.6	86	14	81

* Percentage of total high boiling point hydrocarbons which desorbed below 400°C

Table 3.13. Coke content of Deactivated Samples from Propene Olig.

After the propene oligomerisation runs, the reactor was allowed to cool down to room temperature whilst in contact with the feed. This cooling period would facilitate the adsorption of light hydrocarbons present in the feed onto the catalysts. Transfer of the coked samples into storage bottles for subsequent thermal analysis would result in the adsorption of a certain amount of water by the catalysts. It is likely that the desorption of physisorbed water and light hydrocarbons are contributing to the mass losses observed below temperatures of around 200°C.

After thermal analysis, the dark appearance of the catalyst samples persisted, suggesting that coke removal in air was incomplete at 500°C. The temperature could not be increased beyond this point without introducing additional mass losses which occur as a result of clay lattice dehydroxylation. Although the total coke content of the catalysts can therefore not be conclusively established using this method, it is adequate for comparative purposes.

The extent to which coke formation occurred on the Ni-SMM samples was greater than that on SMM. This is probably due to the higher activities of the Ni-SMM catalysts. The slightly higher reaction temperature used for the Ni-SMM runs could also contribute to the observed differences. The proportion of graphitic coke present on these catalysts was similar, being less than 10% in all cases. Treatment with the pillaring solution appeared to reduce the extent of coke formation on these catalysts. The decrease is most noticeable in the Ni-SMM(21) sample. The proportion of graphitic coke did not change significantly after pillaring.

Coke formation appeared to be more extensive on Al PILMont than Al PILBeid. Comparing the extent of coke formation on Al PILMont and Al PILBeid with that on SMM and Ni-SMM catalysts seems unjustified in view of the very different reaction conditions used. The percentage of graphitic coke present on Al PILMont and Al PILBeid was similar, being 46 and 50%, respectively. This was considerably higher than that on any of the SMM and Ni-SMM samples.

3.1.3.2 Reaction of 124 Trimethylbenzene

3.1.3.2.1 Catalyst Activities

Unless otherwise indicated, all experiments were performed at atmospheric pressure using a WHSV of 2.4 h^{-1}. Conversion levels were calculated from the results of the gas chromatogram product analyses according to the formula

$$\% \text{ conversion} = 100 \times (124\text{TMB fed} - 124\text{TMB unreacted})/124\text{TMB fed}.$$

Figure 3.37 compares the activities of NH_4^+ Mont and Al PILMont. Pillaring resulted in a noticeable increase in catalyst activity. Both catalysts showed significant signs of deactivation during the course of the run. Regeneration of the Al PILMont sample in air at 500°C for four hours fully restored the activity of the catalyst, indicating that coke formation was the sole cause of deactivation.

Fig. 3.38 shows the conversion levels attained by the montmorillonite samples treated with the Al, Si/Al, and Ni/Al pillaring solutions. Other than the Ni/Al PILMont sample, which appeared to be slightly less

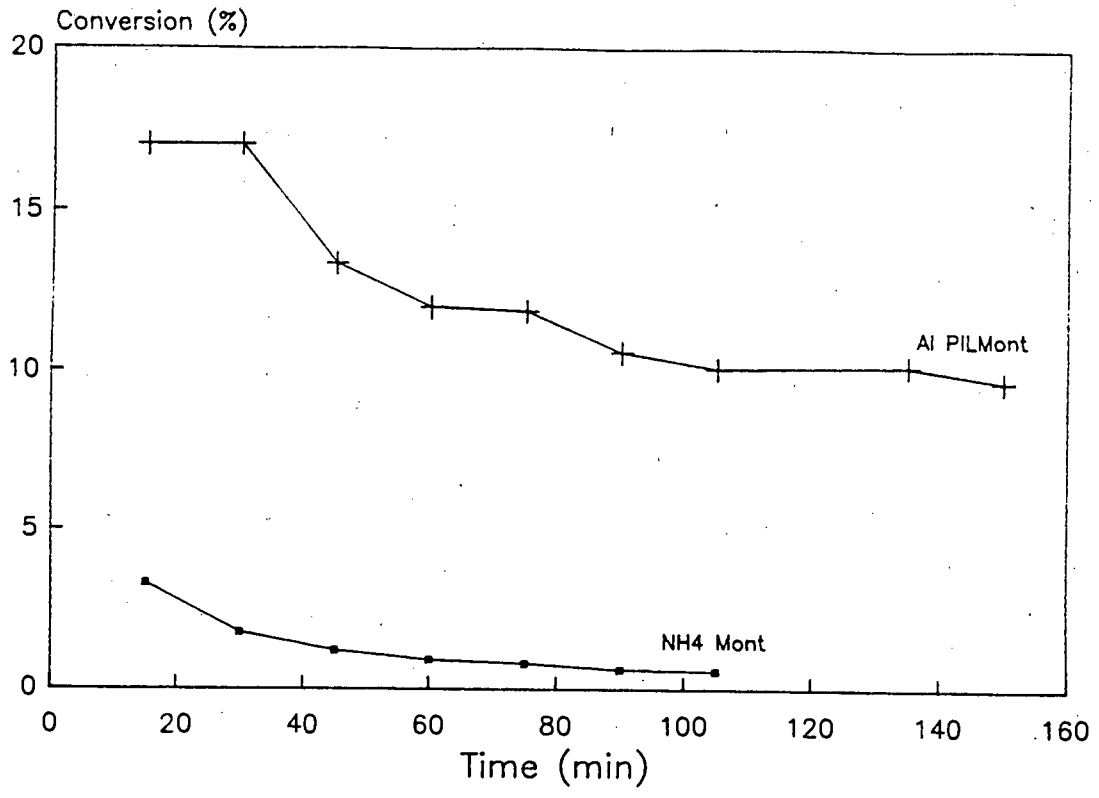

Figure 3.37. Reaction of TMB: NH_4^+ Mont and Al PILMont

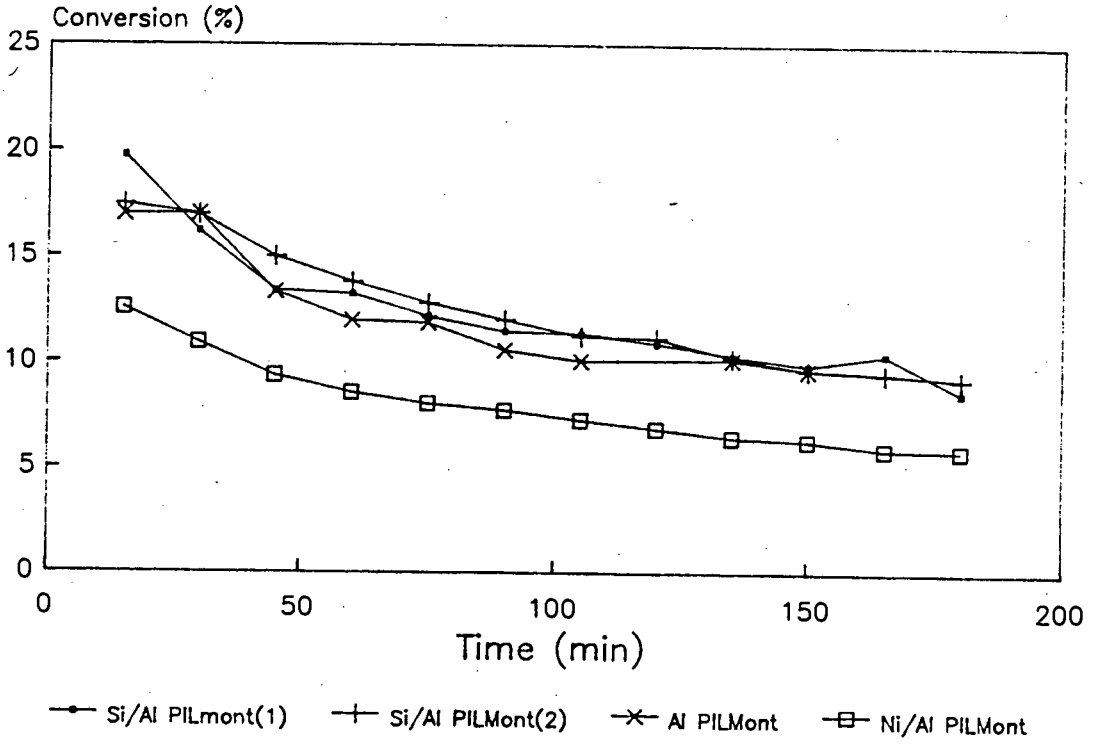

Figure 3.38. Reaction of TMB: Al, Si/Al, and Ni/Al PILMont

active, the activities of these catalysts were very similar, as were the rates at which they deactivated.

The activities of NH_4^+ Mont and NH_4^+ Beid were very similar. Pillaring beidellite with the hydroxy-Al solution resulted in a significant increase in activity, as shown in Figure 3.39. The increase was not as large as that observed on pillaring montmorillonite.

Figures 3.40 - 3.42 show the effect that treating SMM, Ni-SMM(7), and Ni-SMM(21), respectively, with the hydroxy-Al solution has on the 124TMB conversion levels of these catalysts. In all cases, catalyst activity increased.

SMM was the most active of the three clays, followed by Ni-SMM(7), and Ni-SMM(21). Treatment with the pillaring solution did not significantly alter the rates at which these clays deactivated. Surprisingly, the rate of deactivation of the largely macroporous unpillared SMM and Ni-SMM samples was not noticeably lower than that of the more microporous Al PILMont and Al PILBeid catalysts.

An amorphous silica-alumina sample gave an initial conversion of 27%. The rate of deactivation of this catalyst was lower than that of any of the clay samples. Table 3.14 summarises the conversion levels attained by the different catalysts.

In order to investigate the effect that intial conversion levels had on the reaction selectivity of the catalysts, the WHSV's used for the Al PILMont and SMM samples were increased to 5 and 8 h^{-1}, respectively. This resulted in a decrease in the initial conversion levels from 17 to 10% in the case of Al PILMont, and from 24 to 13% in the case of SMM.

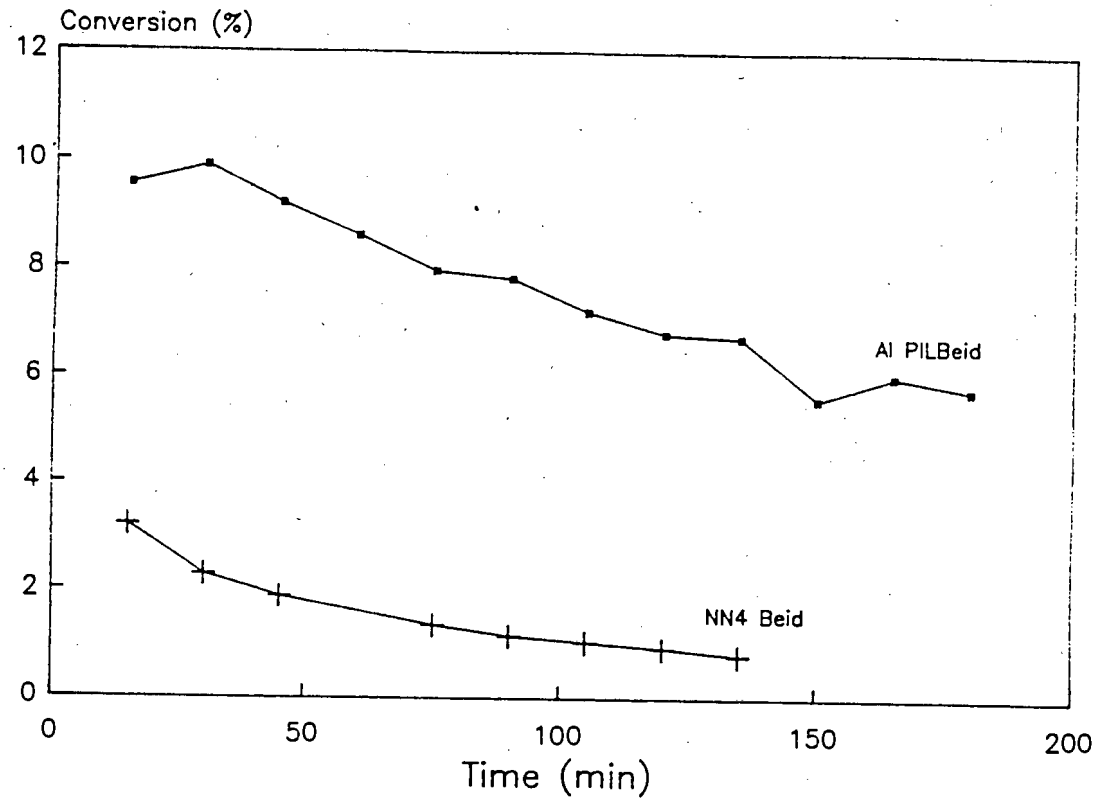

Figure 3.39. Reaction of TMB: NH_4^+ Beid and Al PILBeid

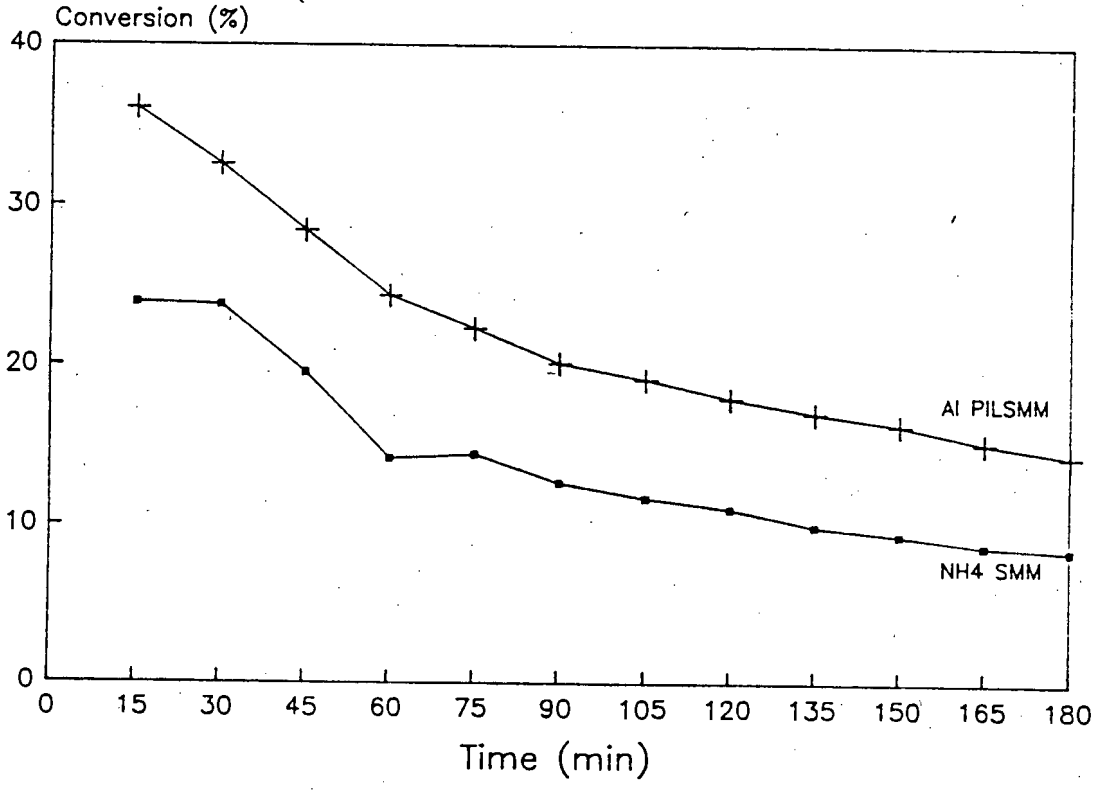

Figure 3.40. Reaction of TMB: SMM and Al PILSMM

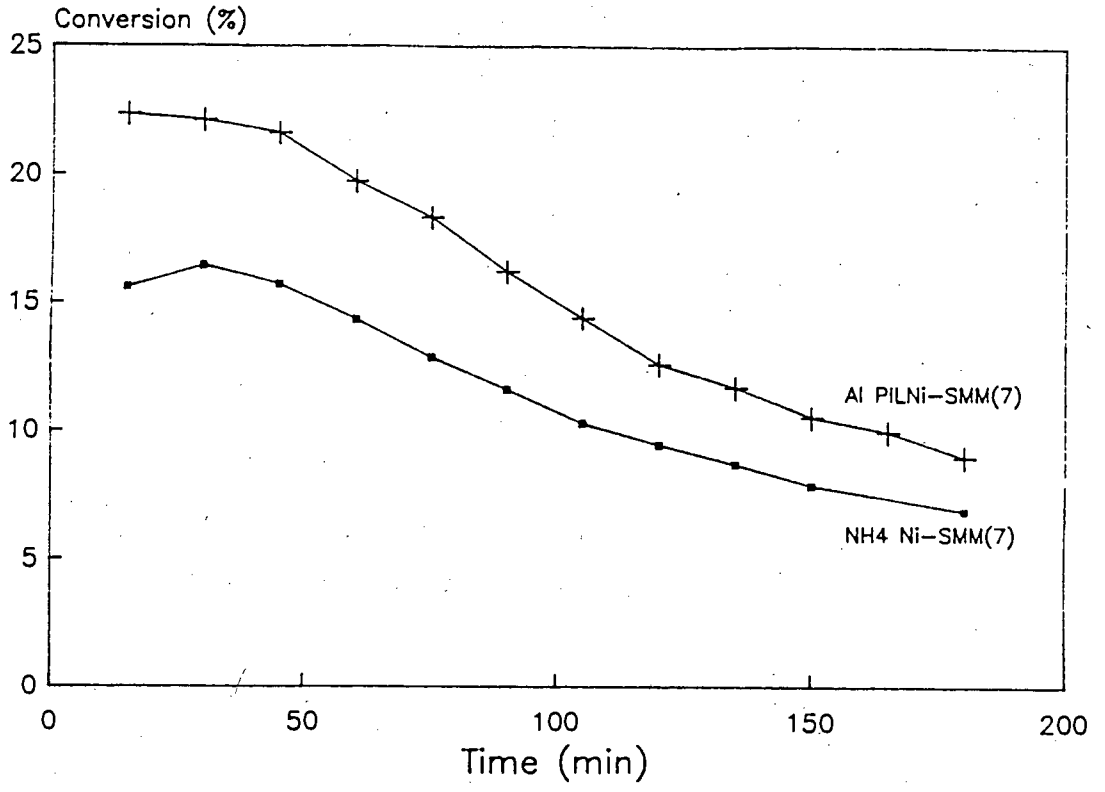

Figure 3.41. Reaction of TMB: Ni-SMM(7) and Al PILNi-SMM(7)

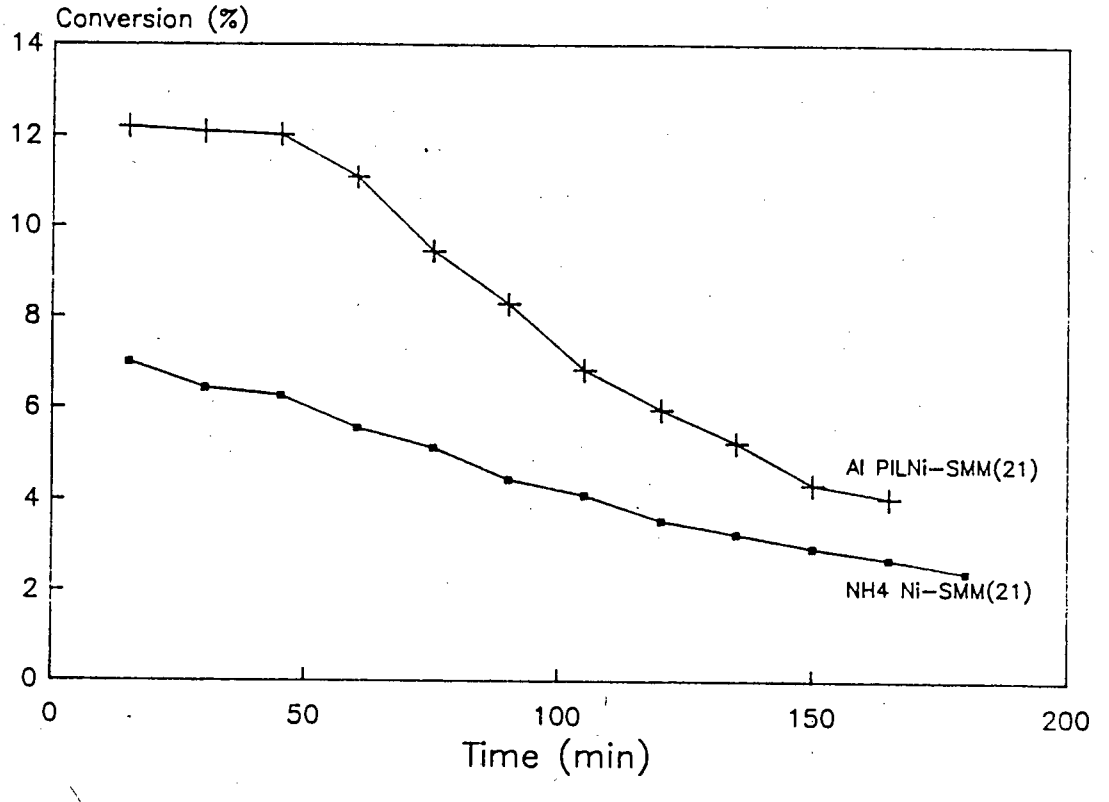

Figure 3.42. Reaction of TMB: Ni-SMM(21) and Al PILNi-SMM(21)

Catalyst	Conversion Range (%)	Ave. Selectivity to Isom. Reaction (%)	1245 TetMB Selectivity (%) *
NH_4^+ Mont	3.3 - 0.6	5.9	72 - 74
Al PILMont	17 - 9.7	12.1	59 - 64
Si/Al PILMont(1)	20 - 8.6	14.3	57 - 62
Si/Al PILMont(2)	17.5 - 9.3	13.9	57 - 62
Ni/Al PILMont	12.5 - 8.3	8.3	65 - 71
NH_4^+ Beid	3.2 - 0.8	9.9	68
Al PILBeid	9.6 - 5.8	9.8	66 - 68
SMM	24 - 8.4	30.7	45 - 50
Al PILSMM	36 - 15	21.3	45 - 52
Ni-SMM(7)	16.5 - 6.9	17.3	57 - 62
Al PILNi-SMM(7)	22 - 9	17.7	55 - 60
Ni-SMM(21)	7 - 2.5	8.4	69 - 72
Al PILNi-SMM(21)	12 - 2.4	11.3	61 - 67
Silica Alumina	27.5 - 20	35.9	45 - 46

* The two values reported represent the initial and final TetMB selectivities, respectively.

Table 3.14. Reaction of 124 TMB: Summarised Conversion Levels, Selectivity to Isomerisation Reaction, and 1245 TetMB Selectivity.

Table 3.15 compares the reactivities of the 123, 135, and 124 TMB isomers over SMM and Si/Al PILMont(1). Initial conversion levels, as well as conversion levels after 90 minutes on stream, are reported. A WHSV of 2.4 h^{-1} was used in all cases. 124 TMB was the most reactive isomer over Si/Al PILMont(1), followed by 123 TMB and 135 TMB. Over the SMM catalyst, 123 TMB appeared to be slightly more reactive than the 124 TMB isomer, while 135 TMB was, once again, the least reactive isomer.

Catalyst	Reactant Isomer	Conversion (%)	
		Initial	90 min
SMM	123	35	18
SMM	135	22	7
SMM	124	24	13
Si/Al PILMont(1)	123	15	7
Si/Al PILMont(1)	135	9	2
Si/Al PILMont(1)	124	20	11

Table 3.15. Reactivity of TMB Isomers Over Two Catalysts

3.1.3.2.2 Catalyst Selectivities

Conversion of 124 TMB occurs via three competing reactions, viz., disproportionation, isomerisation, and dealkylation. The selectivities of the catalysts to these three reactions were calculated as follows (all figures, in mass%, were obtained from the results of GC product analysis):

$$\text{Isomerisation}(\%) = 100 \times (123\ \text{TMB} + 135\ \text{TMB}) / 124\ \text{TMB reacted}$$

$$\text{Disprop.}(\%) = 100 \times (\text{xylene from disprop.} + \text{TetMB}) / 124\ \text{TMB reacted}$$

$$= 100 \times 1.79 \times \text{TetMB} / 124\ \text{TMB reacted}$$

$$\text{Dealkylation}(\%) = 100 \times (\text{benz.} + \text{toluene} + \text{xylene} - .79 \times \text{TetMB}) / 124\ \text{TMB reacted}$$

It is unlikely that calculating selectivity to the isomerisation reaction by using the concentrations of 123 and 135 TMB present in the products will give an accurate estimate of the actual extent to which 124 TMB isomerisation takes place, as the 123 and 135 isomers would, themselves, be expected to disproportionate and isomerise. However, it seems a reasonable way of comparing the extent to which reactant

isomerisation takes place on different catalysts.

At the reaction temperature used for this work, viz. 300°C, dealkylation did not take place to an appreciable extent. For all the catalysts tested, an average of less than 3% of the 124 TMB which reacted was converted via this reaction. In all cases, disproportionation was the dominant reaction, although the extent to which isomerisation took place did vary significantly from catalyst to catalyst. Fig. 3.43 shows the reaction selectivities vs. time on stream for Al PILMont. Selectivities remained fairly constant during the course of the run. This was found to be the case for most of the catalysts tested. In some cases, however, selectivity to the isomerisation reaction appeared to increase slightly with time on stream. Table 3.14 shows the average selectivities of the various catalysts to the isomerisation reaction. In general, the more active catalysts displayed higher selectivities to the isomerisation reaction. When the initial conversion level of Al PILMont was decreased from 18% to 11%, and that of SMM was decreased from 24% to 13%, by increasing the WHSV's to 5 and 8 h^{-1}, respectively, the initial selectivities of these catalysts to the isomerisation reaction decreased from 13% to 10% in the case of Al PILMont, and from 24% to 22% in the case of SMM.

124 TMB and its two isomers, 123 and 135 TMB, disproportionate to form 1245, 1235, and 1234 TetMB, and o-, m-, and p-xylene. The 1235 isomer is thermodynamically most stable among the tetramethylbenzenes. Kikuchi et al. (1984) report that the equilibrium composition is roughly 52% 1235, 35% 1245, and 13% 1234 TetMB. The equilibrium composition of the TMB isomers at 300°C is 13% 123, 62% 124, and 25% 135 TMB (PROCESS manual, Simulation Sciences Inc., Fullerton California, 1986). The equilibrium composition of the xylene isomers, at 300°C, is 23% o-xylene, 53% m-xylene, and 24% p-xylene (Taylor et al., 1946). Figure 3.44 shows the TetMB selectivities of Al PILMont as a function of time on stream. The results indicate selective disproportionation to the 1245 isomer. This was found to be the case for all the catalysts tested. In general, selectivities to 1245 TetMB increased with time on stream, while those to 1235 TetMB decreased. 1234 TetMB slectivities remained essentially constant with run time. Appendix 3(a) contains the TetMB selectivities as a function of run time for all the catalysts tested.

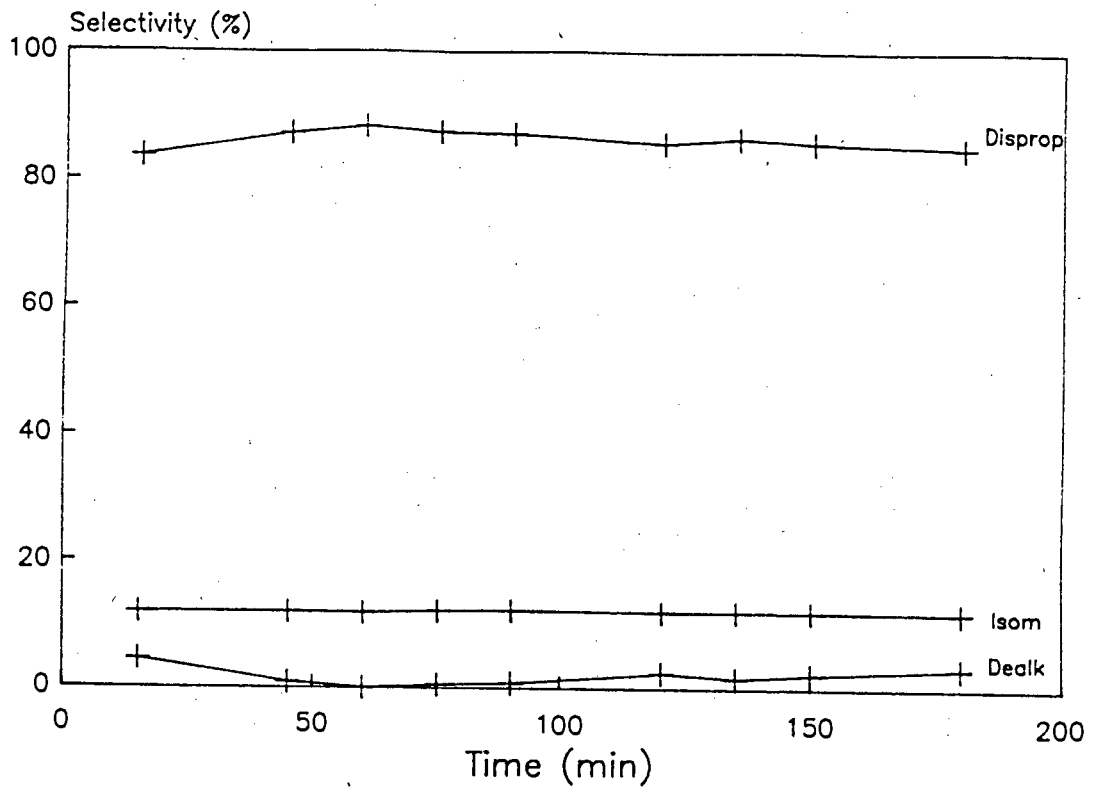

Figure 3.43. Reaction of 124 TMB: Reaction Selectivity of Al PILMont

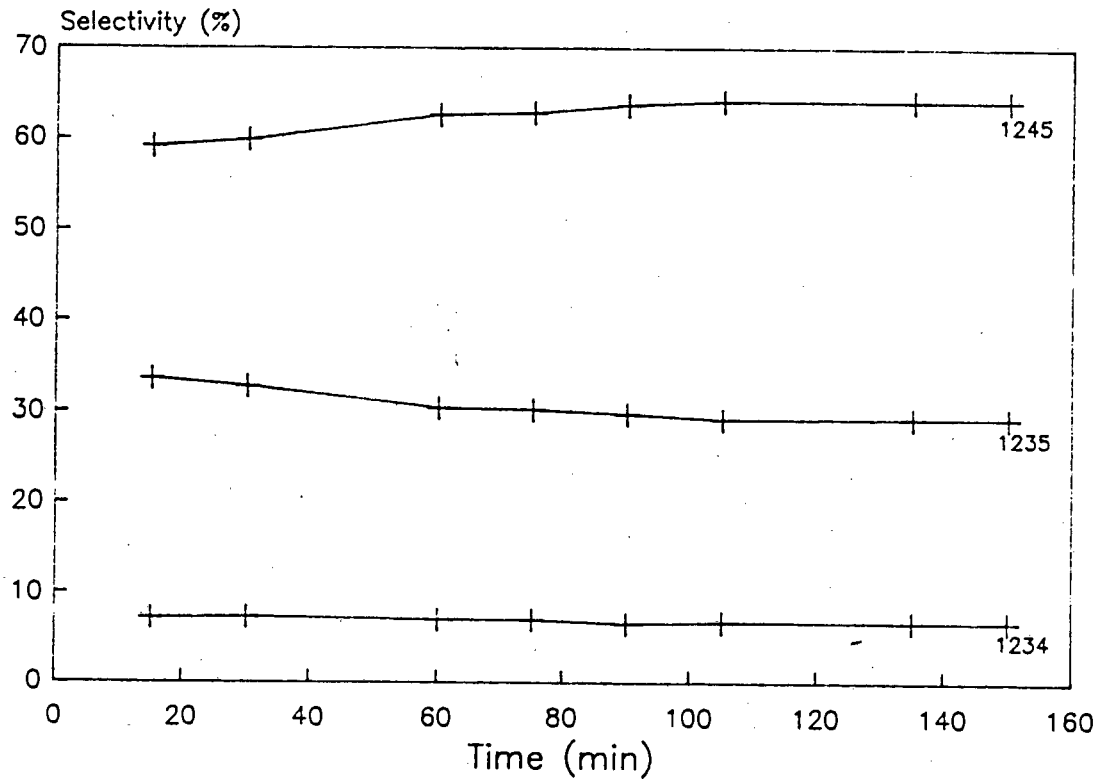

Figure 3.44. Reaction of 124 TMB: TetMB Selectivity of Al PILMont

Table 3.14 shows the 1245 selectivities of all the catalysts at the start and at the end of reaction. From this table it can be seen that there appears to be a strong correlation between the selectivity to the isomerisation reaction, and the 1245 selectivities of the different catalysts.

Figure 3.45 shows 1245 selectivities of the four pillared montmorillonite catalysts and pillared beidellite as a function of 124 TMB conversion levels. The figure facilitates comparison of the 1245 selectivities of these catalysts at similar conversion levels. A consideration of this figure and Table 3.14, which shows the average selectivities of these catalysts to the isomerisation reaction, indicates that selectivities to the 1245 isomer decreased with increasing reactant isomerisation activity. In general, increased levels of reactant isomerisation were accompanied by decreased 1245 TetMB selectivities, increased 1235 selectivities, and moderately increased 1234 selectivities.

Figure 3.46 shows the xylene selectivities of Al PILMont. O-xylene selectivities were higher than would be expected from thermodynamic equilibrium levels. This was found to be the case for all the catalysts tested. Appendix 3(b) contains the xylene selectivities as a function of run time for all the catalysts. In general, o-xylene selectivities increased with decreasing conversion levels during the course of the runs. Selectivities to m-xylene decreased, while p-xylene selectivities remained essentially unchanged. Table 3.16 shows the m- and o-xylene selectivities of the catalysts averaged over the course of the runs. In all cases, o-xylene selectivity was around 40%, while that of m-xylene was in the region of 45%. Xylene selectivities appeared to be independent of catalyst fomulation.

Table 3.16 also shows the 135 and 123 TMB selectivities of the different catalysts averaged over the course of the runs. Selectivities to these isomers were fairly similar in all cases. 135 TMB was produced in greater quantities than 123 TMB. This is consistent with the fact that 135 isomer is more favoured thermodynamically.

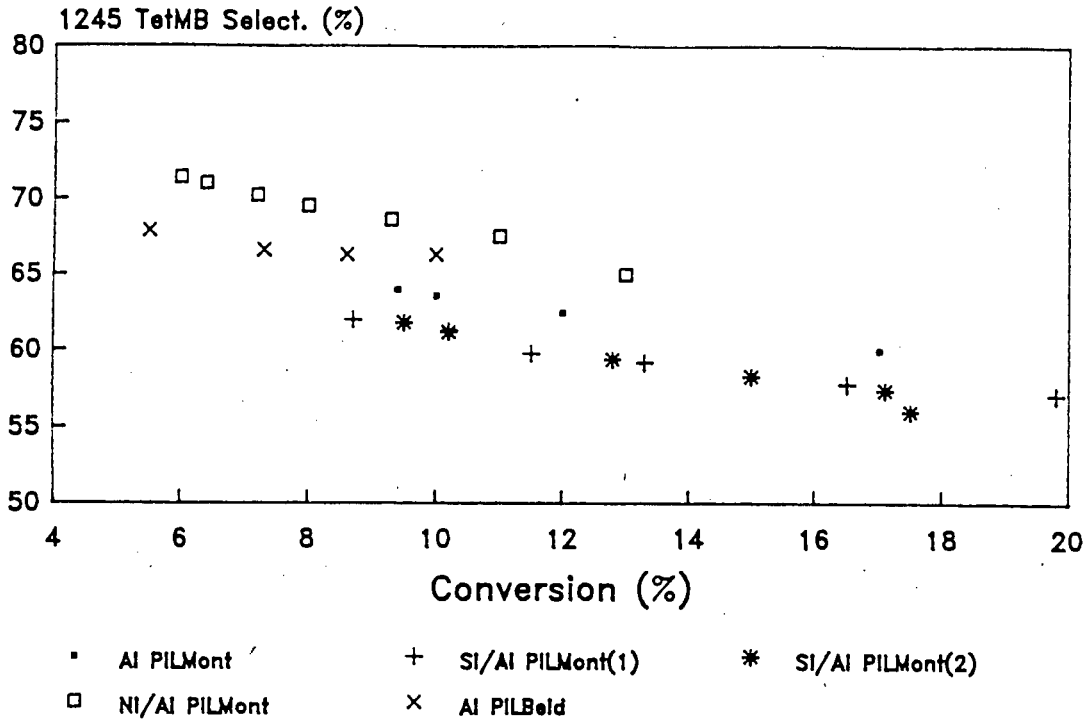

Figure 3.45. Reaction of 124 TMB: 1245 TetMB Selectivity vs. Conversion

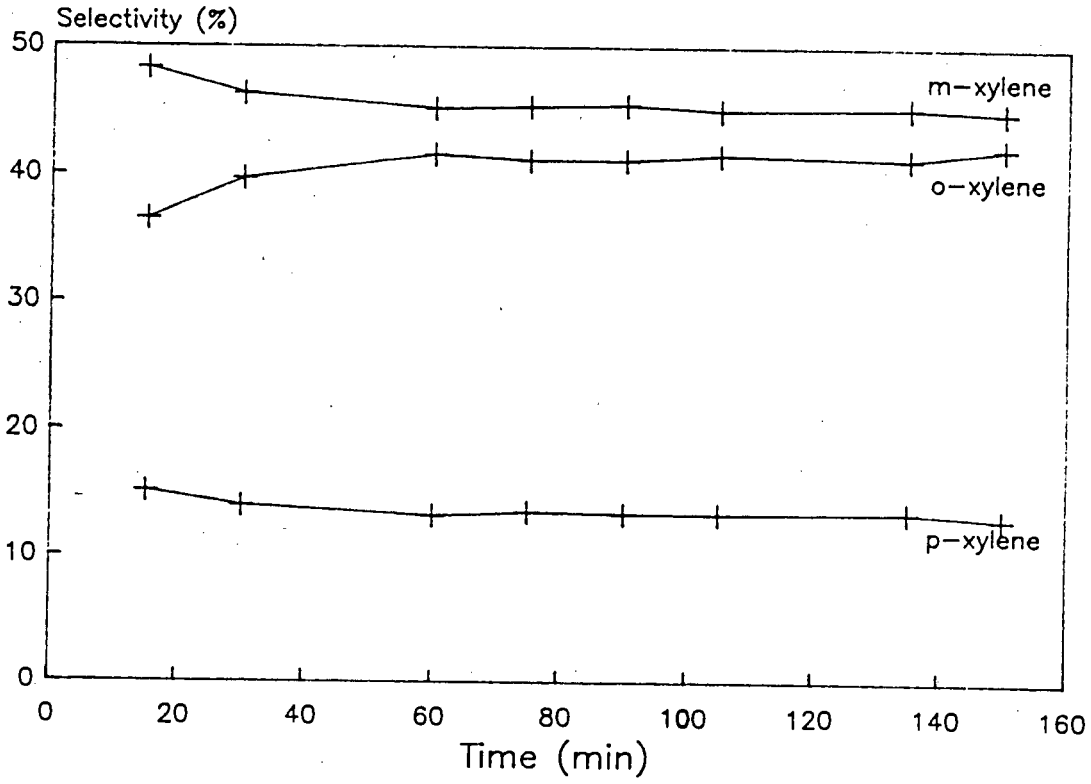

Figure 3.46. Reaction of 124 TMB: Xylene Selectivities of Al PILMont

Catalyst	Ave. Xylene Selectivities		Ave. TMB Selectivities	
	M-Xylene (%)	O-Xylene (%)	135	123
NH_4 Mont	46	38	59	41
Al PILMont	45	41	54	46
Si/Al PILMont(1)	46	40	56	44
Si/Al PILMont(2)	46	40	54	46
Ni/Al PILMont	45	41	53	47
NH_4 Beid	45	41	55	44
Al PILBeid	45	42	53	47
SMM	46	40	63	37
Al PILSMM	46	40	62	39
Ni-SMM(7)	44	40	56	44
Al PILNi-SMM(7)	45	40	57	43
Ni-SMM(21)	43	39	55	45
Al PILNi-SMM(21)	44	39	55	45
Silica Alumina	45	40	62	38

Table 3.16. Reaction of 124 TMB: O- and M-Xylene Selectivities, and 135 and 123 TMB Selectivities

Tables 3.17(a) and (b) show the products obtained from the reaction of 123, 135, and 124 TMB over Si/Al PILMont(1) and SMM. Selectivities to the reactant isomerisation reaction are also shown. The selectivities listed in the table are an average of the values recorded over a period of 90 minutes.

When compared with the products obtained from the reaction of 124 TMB, reaction of 123 TMB over both catalysts resulted in a decrease in selectivity to 1245 TetMB, an increase in selectivity to 1235 TetMB, and an increase in 1234 TetMB selectivity. Selectivities to the p- and m-xylene isomers decreased, while the o-xylene concentration increased. Reaction of 135 TMB over both catalysts resulted in a decrease in

selectivity to 1245 TetMB and an increase in selectivity to the 1235 isomer. Selectivity to 1234 TetMB remained unchanged. Xylene selectivities resulting from the reaction of 135 TMB are not reported

Catalyst	Reactant	Select. to Isom. (%)	TetMB Selectivity (%)		
			1245	1235	1234
SMM	123	68	32.7	54.1	13.2
SMM	135	75	34.5	56.7	8.9
SMM	124	28	47.2	43.6	9.2
Si/Al PILMont(1)	123	50	19.3	61.1	19.5
Si/Al PILMont(1)	135	68	22.7	69.6	7.5
Si/Al PILMont(1)	124	14	58.7	33.9	7.4

Table 3.17(a). Reaction of 123, 135, and 124 TMB Over Two Catalysts: Selectivities to Isomerisation Reaction and TetMB Selectivities.

Catalyst	Reactant	Xylene Selectivity (%)		
		P-xy	M-xy	O-xy
SMM	123	6.2	40.5	53.3
SMM	135	*	*	*
SMM	124	14.8	48.1	37.1
Si/Al PILMont(1)	123	2.7	36.9	60.4
Si/Al PILMont(1)	135	*	*	*
Si/Al PILMont(1)	124	13.8	46.8	39.4

* O-xylene present as feed impurity (4% by mass)

Table 3.17(b). Reaction of 123, 135, and 124 TMB Over Two Catalysts: Xylene Selectivities

due to the fact that o-xylene was present as a feed impurity (ca. 4% by mass). 123 TMB and, particularly, 135 TMB showed a greater tendency to isomerise than 124 TMB. Reactant isomerisation levels were higher over SMM than over the pillared montmorillonte catalyst.

3.2 LANTHANUM EXCHANGED H ZSM-5

3.2.1 Catalyst Characterisation

3.2.1.1 X-Ray Diffraction

Table 3.18 shows the XRD peak positions of the synthesised ZSM-5 sample. The spectrum agrees well with that reported by Argauer and Landolt (1972) and confirms that the sample has the ZSM-5 structure. There was no appreciable difference in the spectrum of the catalyst after exchange with lanthanum ions.

Peak Position (A)	
Argauer and Landolt (1972)	Synthesised
11.1	11.2
10.0	10.0
7.4	7.46
7.1	7.07
6.3	6.39
6.04	6.06
5.97	5.98
5.56	5.57
5.01	5.0
4.60	4.61
4.25	4.25
3.85	3.85
3.71	3.70

Table 3.18. XRD Peak Positions: ZSM-5

3.2.1.2 SEM and KEVEX Analysis

Figure 3.47 shows the normalised crystallite size distribution of the ZSM-5 sample. The results were obtained from SEM micrographs taken of the catalyst. The crystals were predominantly in the 1 - 3 micron size range.

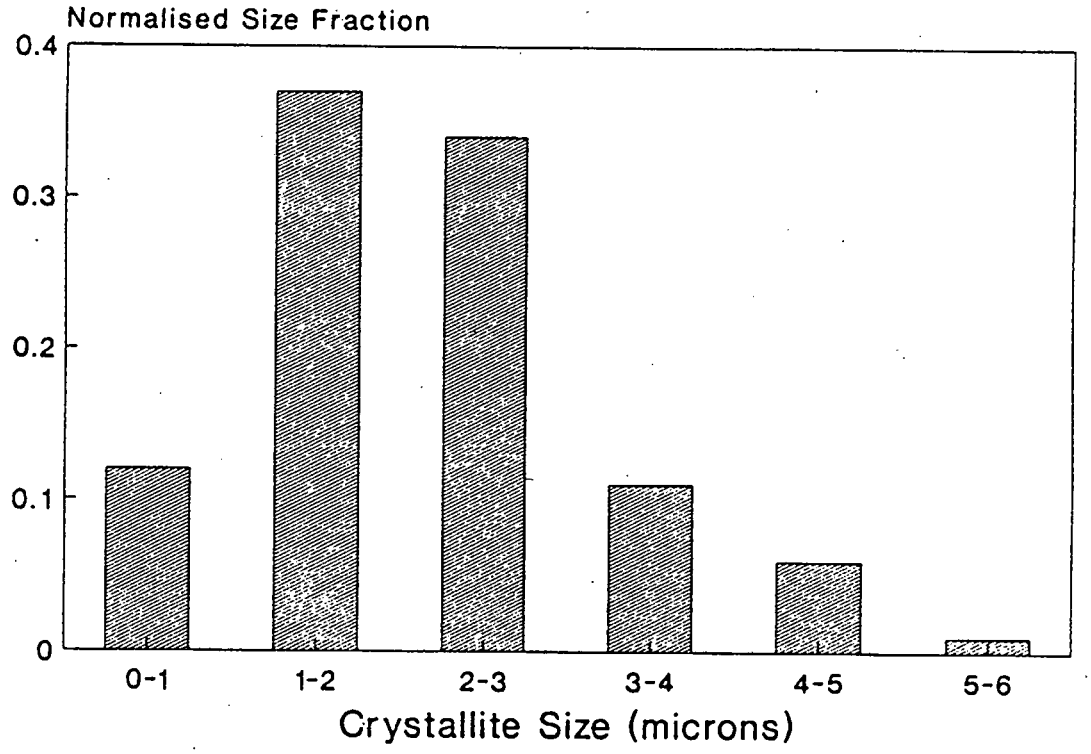

Figure 3.47. Normalised Crystallite Size Distribution of ZSM-5

KEVEX analysis of the pre-ion exchanged catalyst indicated an as charged Si/Al ratio of 40. Similar analysis of the lanthanum exchanged catalyst which had been calcined repeatedly indicated that no dealumination had taken place during the long calcinations required to effect the ion exchange.

3.2.1.3 Lanthanum and Sodium Analysis

Lanthanum analysis of the La^{3+} exchanged ZSM-5 samples prepared according to methods (i) and (ii) described in Section 2.1.2.1 indicated that the catalysts contained 0.13% and 0.6% w/w lanthanum, respectively. If it is assumed that a stoichiometric exchange takes place, with three monovalent ammonium ions being replaced by one trivalent lanthanum ion,

these masses correspond to a lanthanum - ammonium exchange of 5% and 25%, respectively. This assumption may not be valid as it is possible that La ions will undergo hydrolysis to form various La oxide-hydroxide complexes on the surface of the catalyst. However, in the absence of additional information regarding the overall charges of the La complexes, the maximum degree of exchange, viz. 5% and 25%, will be used to designate the zeolite samples hereafter.

Ammonium ZSM-5 was contacted with a NaCl solution to effect a 5% and 25% exchange of sodium for ammonia. The degree of exchange was established by comparing the sodium content of the two catalysts with that of the as synthesised ZSM-5 sample, which is in the sodium form. Sodium content was established using atomic absorption analysis. These two catalyst will be designated as 5% Na ZSM-5 and 25% Na ZSM-5 hereafter.

3.2.1.4 Hexane Adsorption

Hexane adsorption experiments were carried out on the four ZSM-5 catalysts using the TG-DTA apparatus described earlier. Figure 3.48 shows the weight changes versus time for one of the samples tested. The profile of the curve is typical of the results obtained from all the samples.

The weight loss taking place during the first 120 minutes is a result of calcination at 500°C. After this time, the sample was allowed to cool down to 35°C before hexane adsorption commenced. During this cooling period there was a gradual weight gain which was attributed to the adsorption of nitrogen or water onto the catalyst. Hexane adsorption took place rapidly, being 95% complete in less than five minutes.

Table 3.19 summarises the results of the experiments. Weight gain due to hexane adsorption is expressed as a percentage of the calcined mass of catalyst. N_2/H_2O uptake is included in the values presented in the table, as it is likely that at least part of these adsorbed species will be replaced by hexane molecules.

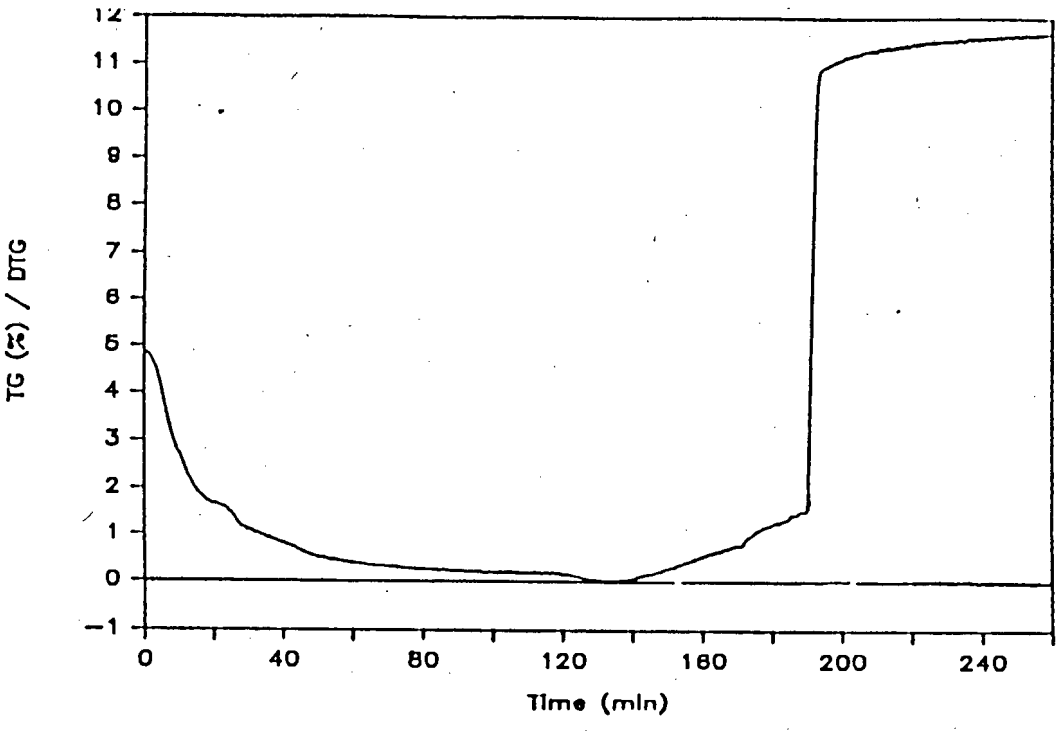

Figure 3.48. Hexane Adsorption on ZSM-5 Catalysts: Typical TG Profile (weight gain is recorded as a percentage of the mass of the uncalcined sample).

Catalyst	Mass gain (%)
5% Na	12.2
5% La	12.2
25% Na	12.2
25% La	12.1

Table 3.19. Hexane Adsorption Results: ZSM-5 Catalysts

The weight gain due to hexane adsorption was virtually identical on all four catalysts and similar to values reported for H ZSM-5 by Hill et al. (1987). The rates at which adsorption took place were also very similar.

3.2.1.5 Ammonia Temperature Programed Desorption

Figures 3.49 and 3.50 show the ammonia TPD profiles of the four catalysts. In all cases, two peaks were present, one at ca. 230°C and the other in the vicinity of 450°C. The low temperature peak represents sites on the catalyst where ammonia molecules are weakly adsorbed (weak acid sites). Similarly, the peak at ca. 450°C corresponds to strong acid sites present on the catalyst. Table 3.20 presents the results obtained by integrating the TPD profiles.

Catalyst	Weak acid TPD peak mmol NH_3/g cat.	Strong acid TPD peak mmol NH_3/g cat.	Total acidity mmol NH_3/g cat.
5% Na	.33	.31	.64
5% La	.35	.31	.66
25% Na	.37	.25	.62
25% La	.38	.24	.62

Table 3.20. Ammonia TPD: ZSM-5 Catalysts

Table 3.20 shows that increasing the La or Na content of the catalyst causes a decrease in the number of strong acid sites, and a slight increase in the number of weak acid sites. Increasing the La or Na metal loadings on the catalyst did not significantly affect the positions of the two TPD peaks.

3.2.2 Reaction Studies

3.2.2.1 Propene Oligomerisation

3.2.2.1.1 Catalysts Activities

Figures 3.51 and 3.52 show the conversion levels attained by the sodium and lanthanum modified H ZSM-5 catalysts. Increasing the degree of sodium exchange led to a decrease in the conversion levels attained by the catalyst. The rate at which the 25% Na ZSM-5 sample deactivated,

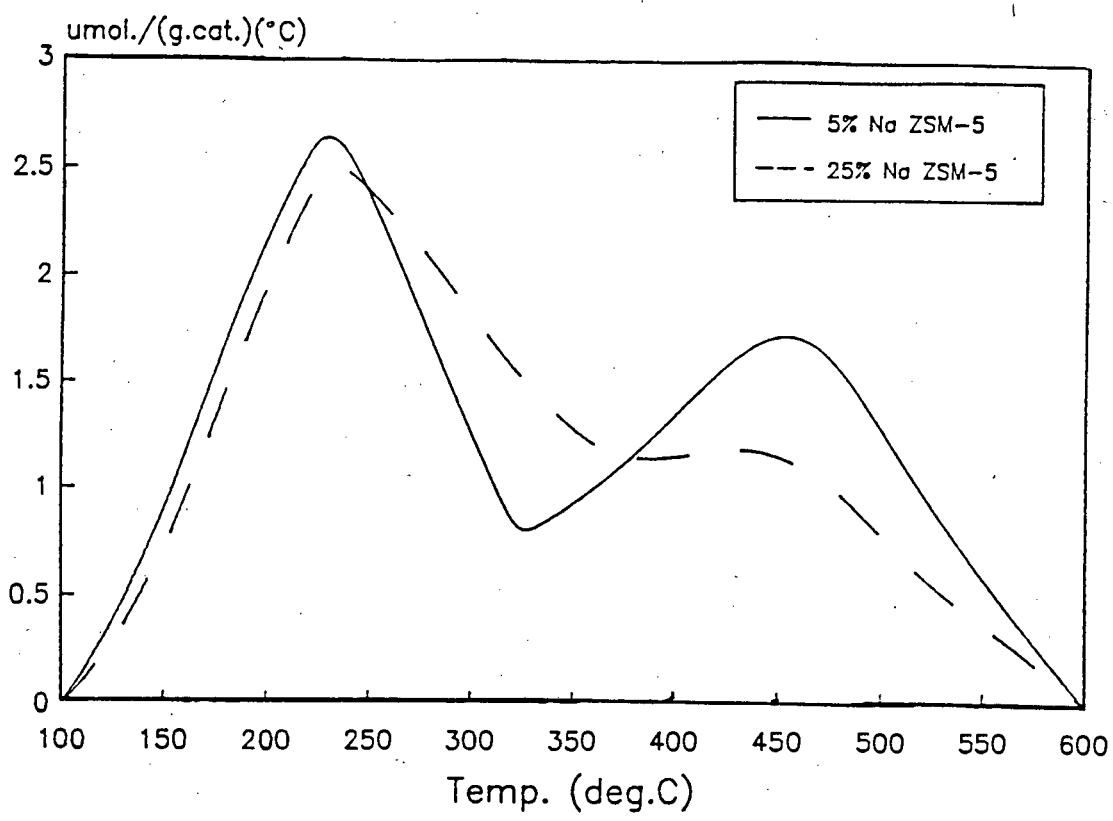

Figure 3.49. Ammonia TPD: 5% Na and 25% Na ZSM-5

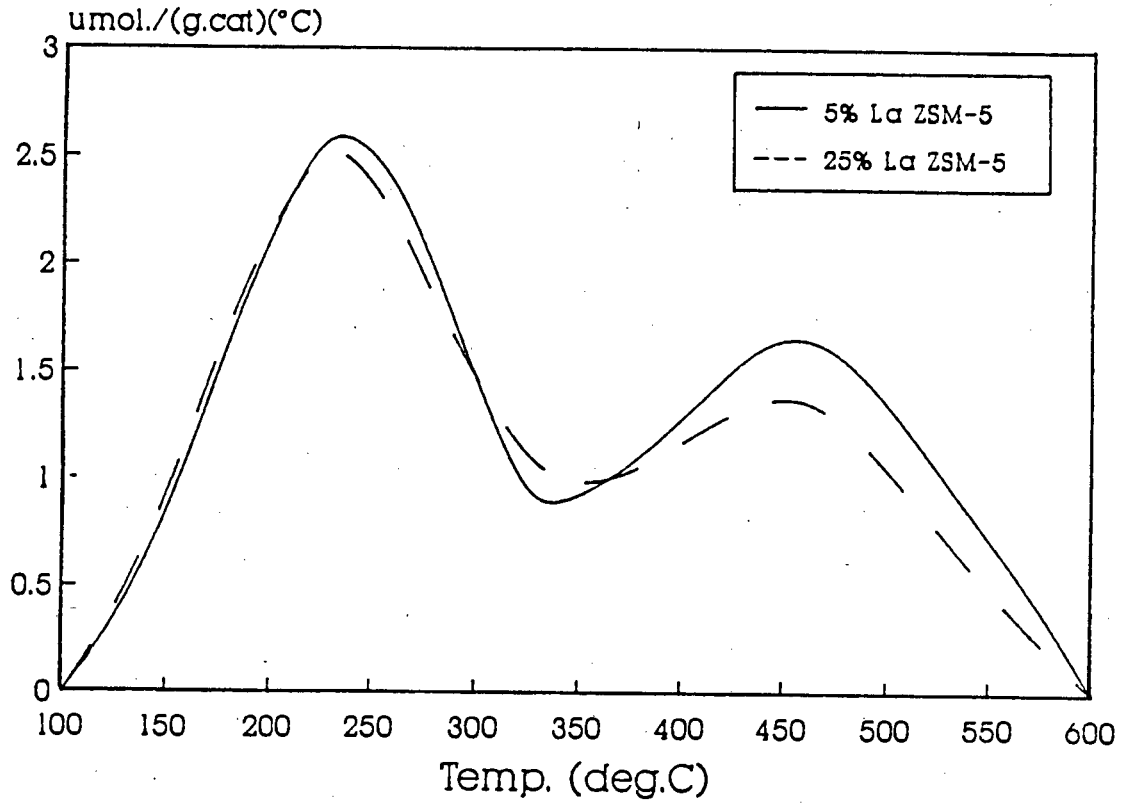

Figure 3.50. Ammonia TPD: 5% La and 25% La ZSM-5

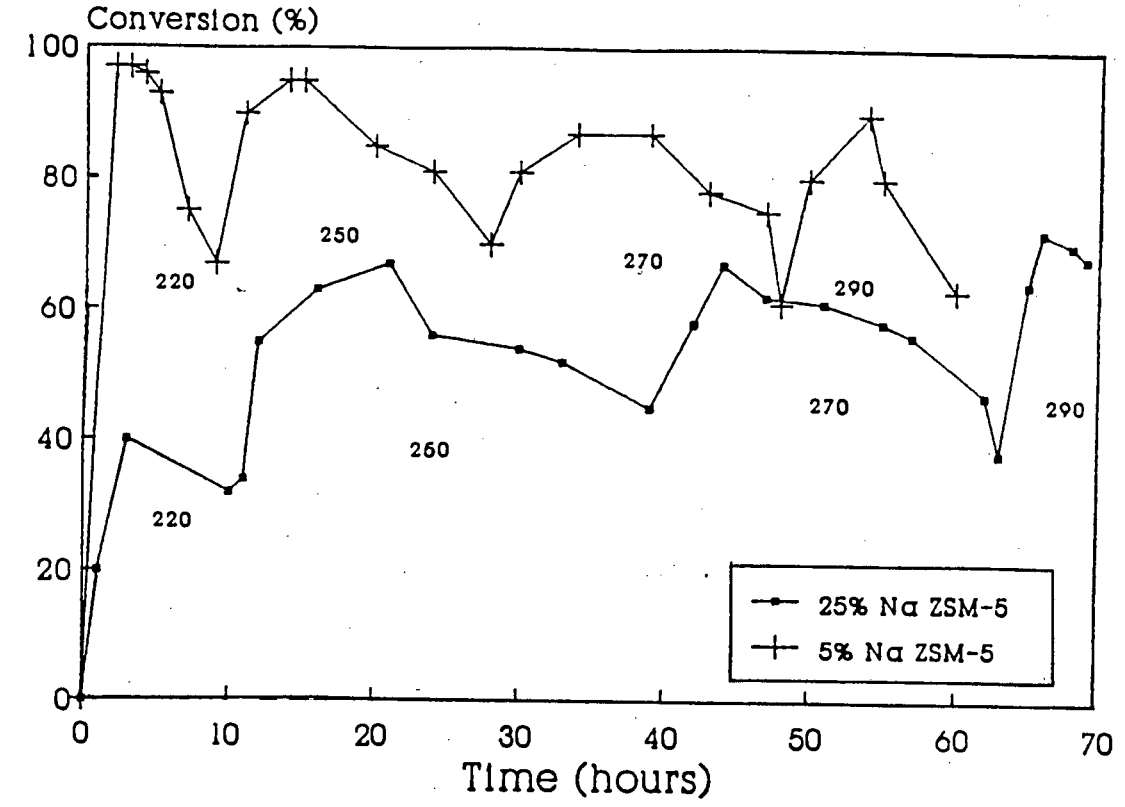

Figure 3.51. Propene Oligomerisation over 5% Na and 25% Na ZSM-5

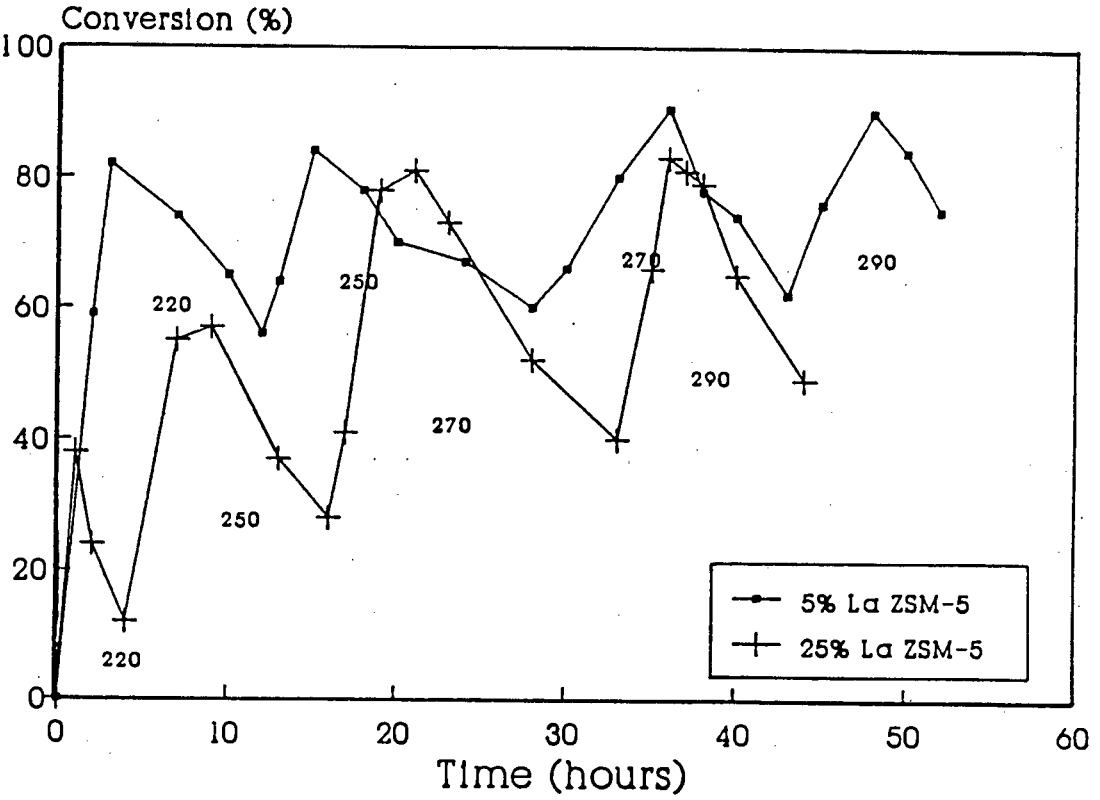

Figure 3.52. Propene Oligomerisation over 5% La and 25% La ZSM-5

however, was slower than that of the 5% Na sample. As was observed with sodium, increasing the La content of H ZSM-5 led to lower conversion levels for the propene oligomerisation reaction. Unlike the sodium catalysts, however, the rate of catalyst deactivation appeared to increase with increasing La content.

3.2.2.1.2 Product Selectivity

Figures 3.53 and 3.54 show the average liquid product selectivities of the 5% Na and 5% La, and 25% Na and 25% La ZSM-5 samples, respectively. The cumulative C_{12}^{+} selectivities of 5% Na and 5% La ZSM-5 were both 58%, while that of 25% Na and 25% La ZSM-5 were 48% and 51%, respectively. Table 3.21 shows the fraction of liquid product which boiled above 165°C. The results were obtained from ASTM D86 distillations.

Catalyst	Fraction of product with b.p. > 165°C
5% Na	65 %
5% La	65 %
25% Na	56 %
25% La	57 %

Table 3.21. Propene Oligomerisation over ZSM-5 Catalysts: Fraction of Liquid Product Boiling above 165°C

Figures 3.53 and 3.54 and Table 3.21 indicate that the selectivities of the Na and La catalysts were very similar. As the extent of exchange was increased, selectivity towards the heavier, diesel products decreased slightly in both cases. No significant differences were found in the off gas analyses from the four catalysts.

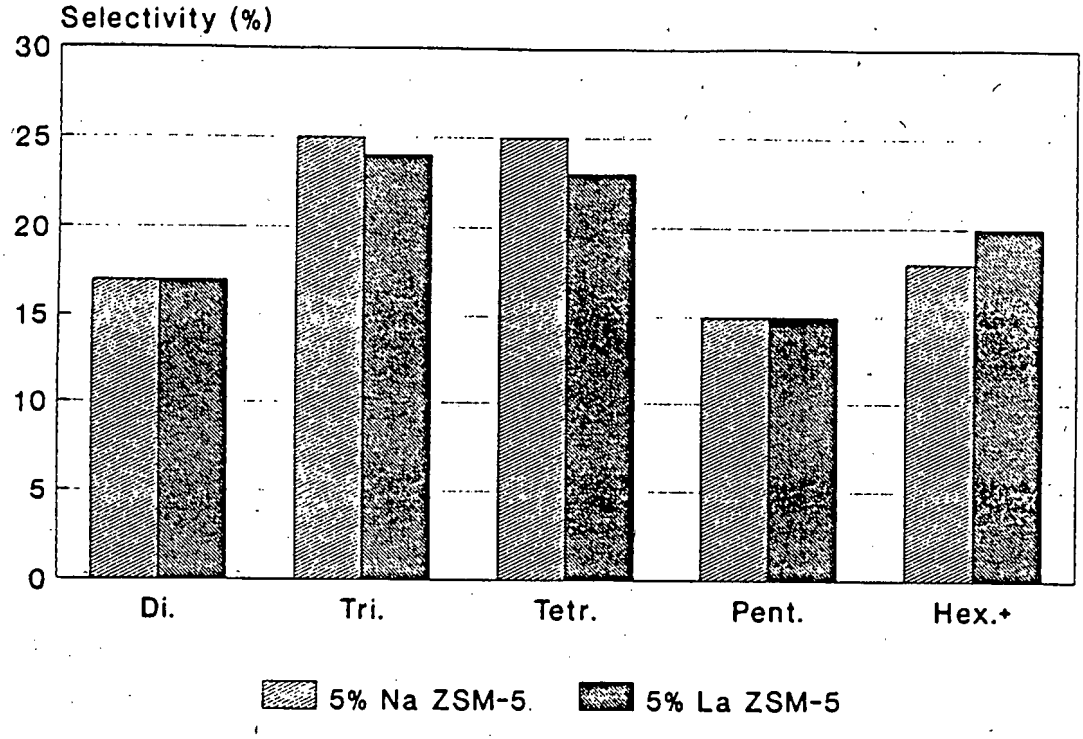

Figure 3.53. Propene Oligomerisation Liquid Product Selectivities: 5% Na and 5% La ZSM-5

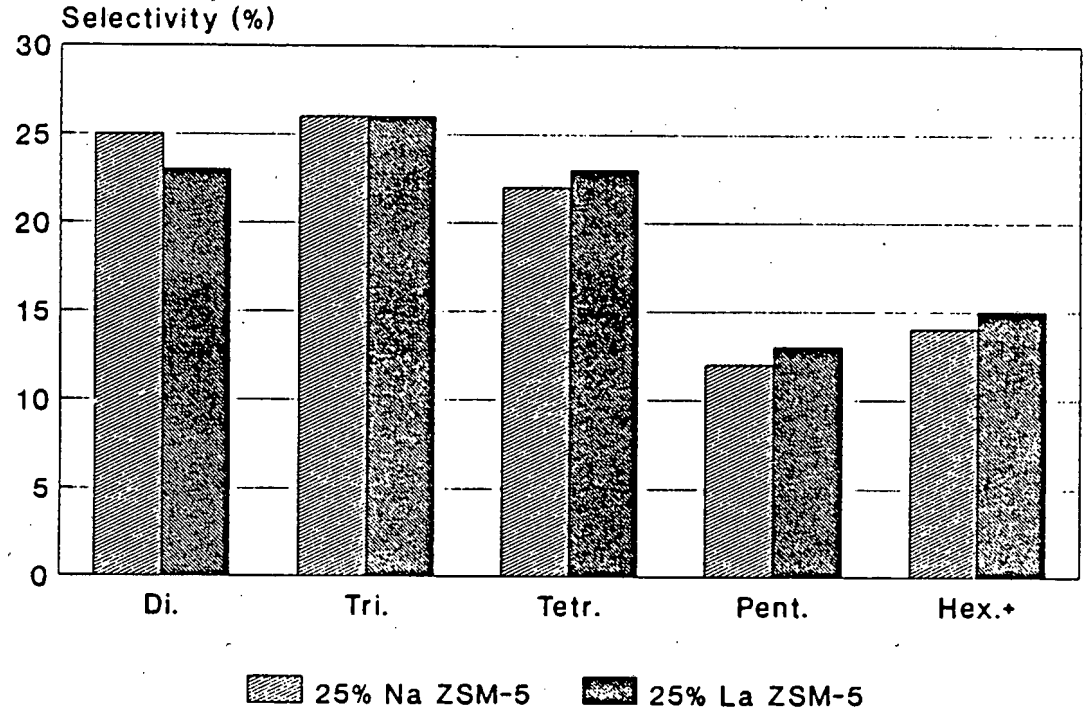

Figure 3.54. Propene Oligomerisation Liquid Product Selectivities: 25% Na and 25% La ZSM-5

3.2.2.2 Hexane Cracking

3.2.2.2.1 Catalyst Activity

Figures 3.55 and 3.56 show the conversion levels attained by the four ZSM-5 catalysts during hexane cracking at 400 and 500°C, respectively. The 5% exchanged samples were more active than the 25% exchanged samples, with the La exchanged catalysts having similar activities to those of the corresponding Na catalysts. In all cases, the catalysts showed only limited signs of deactivation after three hours on stream. The results of a "blank" run, performed at 500°C in the absence of any catalyst, indicated that essentially no thermal cracking was taking place in the reactor.

3.2.2.2.2 Product Selectivity

Table 3.22 shows the cumulative C_1 - C_3 selectivities of the four catalysts, while Table 3.23 shows the C_3 and C_4 paraffin/olefin ratio of the products. The La exchanged samples appeared to show slightly greater selectivities towards the lower molecular weight compounds than the sodium samples. However, this difference did not increase with increasing degree of exchange. As might be expected, the C_1 - C_3 selectivities were greater at the higher reaction temperature. As compared with Na, the presence of La resulted in lower paraffin/olefin ratios in the product. Increasing the degree of Na and La exchange, however, did not significantly affect these ratios.

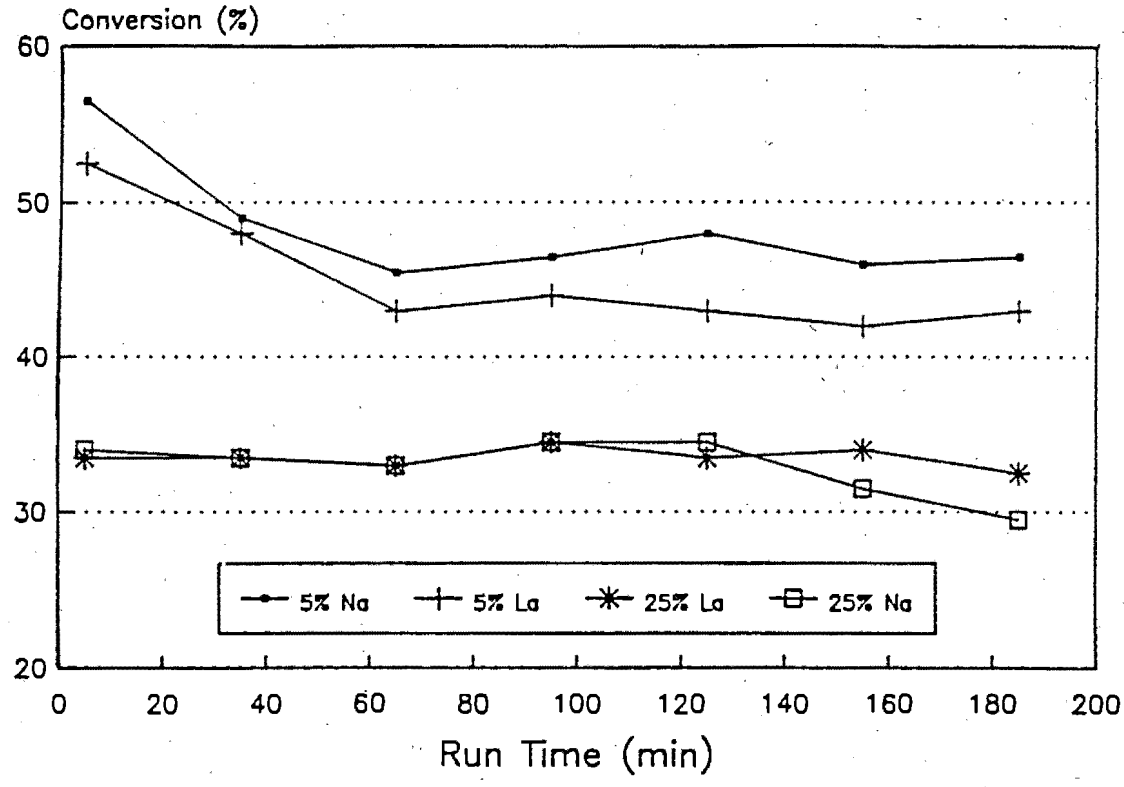

Figure 3.55. Conversion of Hexane over ZSM-5 Catalysts: 400°C

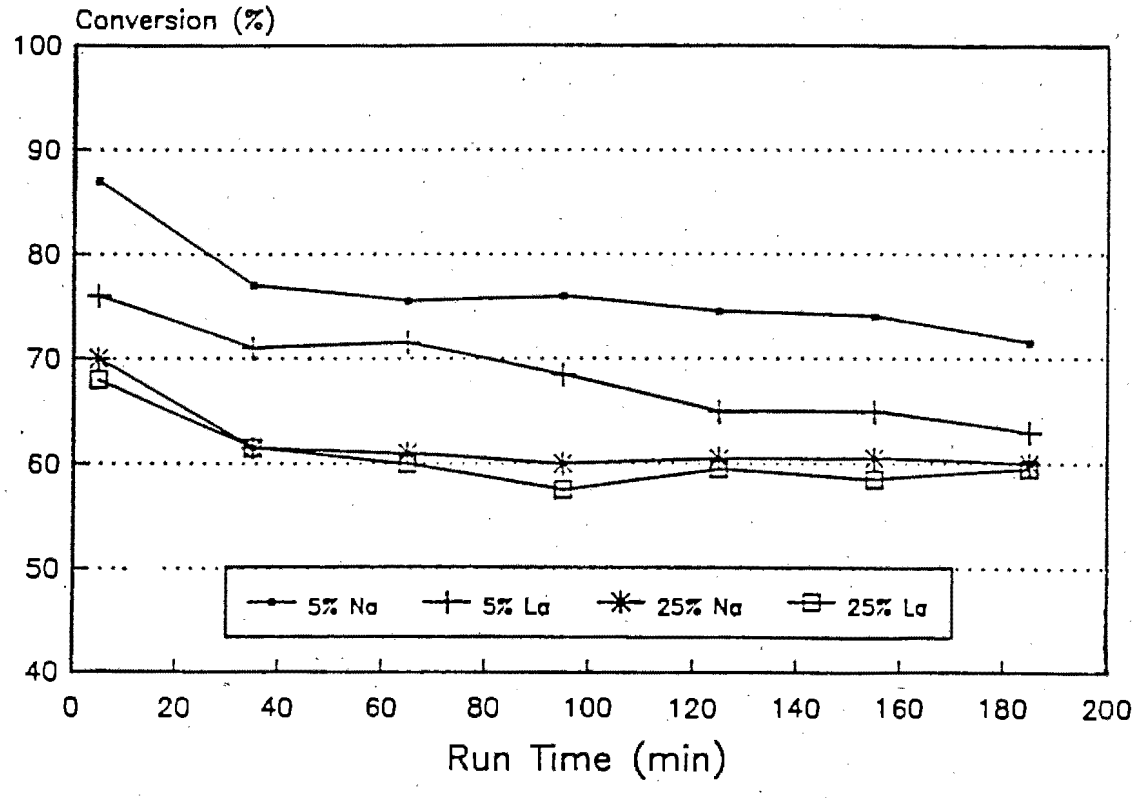

Figure 3.56. Conversion of Hexane over ZSM-5 Catalysts: 500°C

Catalyst	400°C	500°C
5% Na	58	78
5% La	66	81
25% Na	59	76
25% La	63	78

Table 3.22. Hexane Cracking over ZSM-5 catalysts: Cumulative C_1 - C_3 Selectivities.

	400°C		500°C	
Catalyst	$C_3/C_3^=$	$C_4/C_4^=$	$C_3/C_3^=$	$C_4/C_4^=$
5% Na	2.7	2.5	1.2	0.9
5% La	1.7	1.6	0.8	0.7
25% Na	2.6	2.3	1.1	0.8
25% La	1.7	1.6	0.8	0.7

Table 3.23. Hexane Cracking over ZSM-5 Catalysts: Paraffin/Olefin Ratio in Products.

4 DISCUSSION

4.1 Pillared Clays

The idealised unit cell formula for montmorillonite may be written

$$M_{x/n}^{n+}[Al_{4-x}Mg_x][Si_8]O_{20}(OH)_4^{x-}$$

where M is the charge balancing cation. In naturally occurring montmorillonites, however, a certain amount of Al does substitute for Si in the tetrahedral layer. In addition, Fe is usually present in the octahedral layer, either in the 2^+ or 3^+ form. M usually consists of mixtures of cations such as Na^+, K^+, Ca^{2+} and Mg^{2+}. From the chemical analysis of the montmorillonite sample (see Section 2.1.1.1), it is possible to estimate the structural formula of the clay. In order to do this, the following assumptions were made: Fe is present only in the 3^+ form in the octahedral sheet. The presence of this element, therefore, does not contribute to the lattice charge deficit. All Mg present, as indicated by the chemical analysis, is situated in the octahedral layer. No magnesium performs a charge balancing role. All calcium, potassium and sodium present is located in the interlayer spaces. Thus, the lattice charge deficit, as indicated by the quantities of Na^+, K^+, and Ca^{2+} present, is representitive of the total amount of isomorphous substitution taking place in the clay. This, together with the Mg assay, enables an estimation of the extent to which Al substitutes in the tetrahedral layer. Accordingly, the unit cell formula may be written

$$Na_{0.7}K_{0.06}Ca_{0.29}[Mg_{0.86}Fe_{0.48}Al_{2.66}][Al_{0.48}Si_{7.52}]O_{20}OH_4^{1.34-}\cdot 5.8H_2O.$$

The suppliers of the clay indicated that the sample may contain a small amount of an SiO_2 impurity. The SiO_2 content, as calculated from the proposed unit cell formula, is slightly smaller than that indicated by the suppliers. The presence of such an impurity may be contributing to this difference.

The theoretical CEC of the clay, as calculated from the unit cell formula, is 1.54 meq/g. The measured CEC, reported by the suppliers of the clay, is 0.96 meq/g. Davidtz (1976) found similar differences between the theoretical CEC's and the measured CEC's of a number of different montmorillonite samples. If the measured value is taken to be the maximum useful CEC of the clay, an estimate of the average

interpillar spacing which will result from treating the clay with the hydroxy-Al pillaring solution can be made. It is assumed, in so doing, that a complete exchange takes place between the charge balancing cations and the pillaring species. This assumption seems reasonable in view of the fact that Shabtai (1980) and Shabtai and Lahav (1980) found that smectite clays in the Na exchanged forms can be crosslinked to a stoichiometric extent by using an equivalent amount or excess of hydroxy-Al oligocations. From the CEC and the unit cell mass, the charge per unit cell is calculated to be 0.731 units. The dimensions of the surface of the unit cell are estimated to be 5.2 x 9.0 A (Yamanaka and Brindley, 1979). As each unit cell has two faces, the surface area per unit cell is calculated to be 93.6 A^2. The very small contribution to the area from the edges of the lamella is ignored. This would give the clay a total interlayer surface area of 741 m^2/g. Mott (1988) report that a figure of between 750 and 800 m^2/g for the total surface area of all the lamella faces is used quite widely as a benchmark for clay minerals. From the charge and the surface area of the unit cell, surface charge density is calculated to be one negative charge per 128 A^2. A lattice area of 896 A^2 would therefore be required to satisfy the charge on one Al_{13}^{7+} pillaring cation. As the pillaring cations will be located predominantly in the interlayer spaces, with lattice surface area both above and below the pillar, the pillar density should be one pillar every 449 A^2. This corresponds to a centre to centre pillar spacing of 21.2 A. Brindley and Sempels (1977) report that the diameter of the Al_{13}^{7+} oligocation is ca. 11.7 A. This would mean that the interpillar spacing, or lateral pore size in Al PILMont should be ca. 9.5 A.

Occelli et al. (1984) reported that the average interpillar spacing in Al PILMont is 14 A, while Tsai (1983) reported that the predominant lateral pore sizes in Al pillared La^{3+} exchanged montmorillonite are in the range 11 - 15 A. These results indicate that montmorillonite has a lower pillar density than is predicted theoretically.

The idealized unit cell formula for beidellite is

$$Na_x[Al_4][Al_xSi_{8-x}]O_{20}(OH)_4^{x-}$$

The exact value of x is not known in the case of the synthesised beidellite in the present study, although it will be less than 1 (Granquist and Pollack, 1967; Brown, 1961). Brown (1961) reports that a

typical value of x for beidellite is around 0.7. The theoretical CEC of this clay, therefore, is smaller than that of the montmorillonite sample. It seems reasonable to assume that the useful CEC of the beidellite sample will also be smaller than that of the montmorillonite clay. The unit cell dimensions of beidellite are very similar to those of montmorillonite (Brown, 1961). It might be expected, therefore, that the interpillar spacing in Al PILBeid would be greater than that in Al PILMont.

The value of x in the unit cell formula of the swellable material present in the SMM clay is not exactly known, although it is expected to lie in the same range as that of beidellite, i.e., $x < 1$ (Granquist and Pollack, 1967). Pillar density in SMM should therefore be fairly similar to that in beidellite.

Values of x in the unit cell formula of the swellable material present in Ni-SMM clays have been proposed by van Santen et al. (1984). These researchers found that an analysis of the energetics of swelling shows two regions where the clays are expected to be non-swellable. One region is found at high Al_{tetra}/Si_{tetra} ratios ($x > 1.8$), where the negative charges on the layers stabilise the cations between the layers better than the solvation energy of the water. The other region is found at low Al_{tetra}/Si_{tetra} ratios ($x < 1$), where the number of cations per layer area is so low that the attractive Van de Waals energy per unit layer area is larger than the gain in solvation energy. Van Santen et al. (1984) did not indicate that the presence of different quantities of nickel in the clay had any effect on the values of x which give rise to swellable material. This is not surprising as the presence of nickel in the octahedral positions does not affect the lattice charge deficit of the clay. It seems reasonable to assume, therefore, that the energetics of swelling in Ni-SMM and SMM clays should be similar. In view of this, the results reported by van Santen et al. do not appear to be consistent with those reported by Granquist and Pollack (1967) and Brown (1961). If it is valid to assume that the concentration of tetrahedrally co-ordinated Al is the only factor determining swellability, then the pillar density in pillared Ni-SMM should be fairly similar to that in SMM.

The complete disappearance of the original 001 XRD peak, and the appearance of a well defined peak corresponding to an interlayer spacing of ca. 9.9 A on treatment of the 100% swellable montmorillonite and beidellite clays with the hydroxy-Al solution suggests that pillaring is extensive in both these clays. Calcination of Al PILMont and Al PILBeid decreased the interlayer spacing to 7.9 and 8.5 A, respectively. This difference may be due to the formation of different bonds between the pillars and the clay layers in the two samples. From MAS NMR studies of calcined pillared beidellite, Plee et al. (1985) concluded that bonding occurs between the tetrahedral sheet of the clay and the Al_{13}^{7+} pillaring cation. In contrast, from the results of a similar examination of Al PILMont, Tennakoon et al. (1987) suggested that calcination causes condensation of residual hydroxyl groups on the Al_{13}^{7+} cation with the octahedral lattice hydroxyls in montmorillonite, resulting in the formation of bonds which anchor the pillar to the octahedral sheet.

It is not surprising that treating montmorillonite with the three different pillaring solutions (Al, Si/Al, and Ni/Al) resulted in very similar changes in the basal spacings of the clay, as the basic structure of all three pillaring species is essentially the same. In all cases, contacting montmorillonite with the pillaring solution resulted in the formation of an interlayer spacing of around 9.9 A. Calcination of these pillared clays which, it is proposed, gives rise to alumina, silica-alumina, and mixed nickel oxide-alumina pillars respectively, resulted in the formation of an interlayer spacing of about 8 A. It should be noted, however, that there is no direct evidence in this work to indicate that the addition of tetraethyl orthosilicate to the hydroxy-Al pillaring solution resulted in the incorporation of Si into the pillaring species.

Scott and Reed (1966) reported a 10.4 A basal spacing for ammonium exchanged mica, while the basal spacing of ammonium exchanged beidellite is about 12.6 A (Brown, 1961; Granquist, 1966). Due to the proximity of the XRD peaks corresponding to these two basal spacings, the peaks appear as a single broad peak in SMM, situated in a position corresponding to a basal spacing intermediate between 10.4 and 12.6 A. In the case of the sample used for this work, the 001 peak was positioned at 11.4 A. This 11.4 A peak shifted to 9.8 A on calcination,

a spacing which agrees well with the thickness of the 2:1 layers (ca. 9.6 A). This indicates that heat treatment effectively eliminates interlayer spaces in both phases of the clay. Granquist (1966) suggested that the percentage of mica-like material present in uncalcined SMM can be obtained from the position of the 001 peak by a simple consideration of additivity relationships. Hence

$$\% \text{ mica-like material} = (d_{001}\text{beid} - d_{001}\text{SMM})/(d_{001}\text{beid} - d_{001}\text{mica}) \times 100.$$

Substituting 11.4 A for d_{001}SMM gives a value of 59%. This value should be regarded simply as an estimate, as changes in relative humidity can affect the basal spacing of the beidellite phase in the clay slightly.

Pillaring of SMM resulted in the appearance of two 001 peaks. This is readily explained by the fact that this clay is only partially swellable. The above calculation suggests that only about 40% of the clay layers should take part in the ion exchange process which leads to the generation of a pillared structure. The original 11.4 A peak shifted to a value of 10.4 A and a new peak appeared at around 20.5 A. The 10.4 A peak is attributed to the basal spacing of the mica-like material, which should remain unaffected by the pillaring process, and agrees well with the value reported by Scott and Reed (1966) for ammonium exchanged mica. The 20.5 A peak appears as a result of an increase in the basal spacings of the beidellite-like material and is attributed to the generation of a pillared structure in this phase of the clay. Calcination of Al PILSMM resulted in a shift of the 10.4 A peak to around 9.8 A, corresponding to the elimination of the interlayer spacings of the mica-like material. The 20.5 A peak shifted to a value of ca. 19 A as a result of dehydroxylation of the pillaring species. This corresponds to a stable interlayer spacing of 9.4 A. The fact that this spacing is a little larger than that observed in the calcined Al PILBeid sample is probably due to experimental error resulting from the relatively poor 001 XRD peak resolution obtained with the pillared SMM samples.

As the 001 basal spacings of swellable and non-swellable smectites with monovalent cations are around 12.6 and 10.4 A, respectively, it seems reasonable to expect that, as was the case with SMM, the 001 peak of Ni-

SMM would lie somewhere between these two values. Swift et al. (1976) reported the 001 peak positions for Ni-SMM clays with different metal loadings. They found that some of the samples had basal spacings of over 13 A. They felt that these high values may be a result of intercalated acetate since nickel acetate was used as the nickel source in the synthesis mixture. The Ni-SMM(21) sample used in this work was also synthesised using nickel acetate as the source of nickel. It is possible, therefore, that the position of the 001 peak (12.1 A) may be affected by the presence of intercalated acetate. As it is not known what nickel source was used in the synthesis of the Ni-SMM(7) sample supplied by Harshaw/Filtrol, no attempt is made to estimate the percentage of swellable material present in either of these two clays using the position of the 001 XRD peak. The synthesised Ni-SMM(21) clay appeared to contain a significant quantity of a two layered clay material which should have no swellable property. The proportion of swellable material present in this clay should therefore be relatively small.

As with SMM, calcination of the two Ni-SMM clays eliminated interlayer spacings, as indicated by the shift in the position of the 001 XRD peak from 12.1 to 9.8 A. No peaks appeared to be present in the XRD spectra of the Al PILNi-SMM(7) and Al PILNI-SMM(21) samples in the region where the 001 basal peaks are situated. XRD analysis of the montmorillonite samples pillared as references for the SMM and Ni-SMM clays showed the characteristic 001 peak at around 19.5 A, indicating that the absence of a low angle 001 peak in the XRD spectra of the Ni-SMM samples was not a result of the nature of the pillaring solution used. One possible explanation for the absence of any clearly defined 001 peaks in the Al PILNi-SMM(7) and Al PILNi-SMM(21) samples (other than the 7.2 A peak of Ni-serpentine which appeared to be unaffected by the pillaring solution) could be that the pillaring solution somehow induced delamination of the clay layers. This would result in the generation of a so called "house of cards" structure in the layers of the clay. Smectite clays with this type of layer configuration (such as laponite) have very weak 001 basal peaks as a result of limited layer stacking in the basal direction.

The absence of any well defined 001 peaks in the XRD spectra of the pillared Ni-SMM clays does not necessarily mean that no pillaring has

taken place. It does however suggest that if pillaring has taken place, the extent to which a pillared structure is generated in the Ni-SMM clays is more limited than was the case in SMM or beidellite.

Thermal analysis indicated that treating Na Mont and Na Beid with the hydroxy-Al pillaring solution resulted in an increase in the water content of the clays, and a decrease in the rate of diffusion of water molecules out of the clay structure. The treated clays incurred a greater weight loss between 300 and 400°C, the temperature range in which dehydroxylation of the Al_{13}^{7+} pillaring cations takes place. These changes are attributed to the generation of microporous pillared structures in the clays.

The increase in the water content and in the weight loss between 300 and 400°C on pillaring montmorillonite was greater than that observed on pillaring beidellite. This suggests that the extent to which microporous pillared structures were generated in these clays was greater in montmorillonite than in beidellite. It is possible, however, that differences in the increase in weight loss between 300 and 400°C observed upon pillaring montmorillonite and beidellite may be a result of differences in the CEC's of the two parent clays. The theoretical CEC of beidellite is lower than that of montmorillonite (see Chapter 4). This may give rise to a lower pillar density in Al PILBeid.

The TG curves of Na Mont and Na Beid both exhibited shoulders in the region of 500°C, representative of the onset of extensive lattice dehydroxylation. These shoulders were essentially absent in the pillared versions of these clays. Instead, gradual weight losses took place in the temperature range 400 - 600°C. This suggests that lattice dehydroxylation takes place at lower temperatures in the pillared clays.

Ming-Yuan et al. (1988) investigated the effect of heat treatment on structural OH groups of Na Mont and Al PILMont. They found that the pillared clay lost its structural OH groups on heating more easily than the parent clay. Since the negative charge and also the structural OH groups of the octahedral sheet are located mostly towards the six membered rings formed by Si tetrahedra in the tetrahedral sheet, Na^+ cations in the interlayer spaces of Na Mont are correspondingly located

opposite to, and very possibly blocking, those six membered rings. Hence, most structural groups are rather stable during thermal treatment. The pillaring process releases quite a number of Na^+ cations from blocked six membered rings and facilitates the dehydroxylation of structural OH groups (Ming-Yuan et al., 1988). In addition, protons liberated during the dehydroxylation of the pillars can migrate to the origins of the lattice charge deficit, namely, the octahedral layers, where they may interact with OH groups. These interactions may lower the temperature at which the clay layers dehydroxylate.

Wright et al. (1972) suggest that dehydroxylation in tetrahedrally substituted clays is proton catalysed, since metal cation exchanged clays showed greater thermal stability than ammonium exchanged clays. The proton liberation accompanying pillar dehydroxylation in Al PILBeid could therefore be responsible for the lower temperatures at which structural hydroxyls were removed from this clay.

The thermal analysis results obtained from montmorillonite samples treated with the Al, Si/Al, and Ni/Al pillaring solutions were similar. If the decreased charge on the Ni/Al pillaring species were to result in an appreciable increase in pillar density, it might be expected that Ni/Al PILMont would exhibit a greater mass loss than Al PILMont in the temperature range where pillar dehydroxylation occurs, namely 300-400°C. In addition, a significant increase in pillar density might result in a decrease in the rate of the diffusion of water molecules out of the pillared structure. Neither of these effects was observed.

Treating the SMM and Ni-SMM samples with the hydroxy-Al pillaring solution also resulted in an increase in the amount of water held by these clays, as indicated by the results of thermal analysis. In the case of the Ni-SMM(7) and SMM samples, weight losses incurred on heating to 200°C increased, on pillaring, by 4% and by 7.9%, respectively. These increases, particularly that of SMM, were significantly greater than those resulting from the pillaring of Na Mont and Na Beid which were 2.4 and 1.2%, respectively. If the increases in water content, resulting from treatment with the Al pillaring solution, are attributed to the generation of microporous pillared structures in these clays, this result is unexpected. The partially swellable nature of SMM and Ni-SMM

should ensure that the generation of a microporous structure in these clays on treatment with the pillaring solution is less extensive than in montmorillonite and beidellite. These results suggest, therefore, that, besides generating a limited microporous structure, contacting SMM and Ni-SMM clays with the pillaring solution may cause changes in the layer morphologies of these clays which increase their capacities to hold water. It should be borne in mind, however, that changes in relative humidity can affect the water content of the clays.

In the unpillared SMM and Ni-SMM clays, weight losses taking place in the temperature region 200 to 750°C are attributed to deammoniation (the unpillared clays are in the ammonium exchanged form), and to structural dehydroxylation. Wright et al. (1972) and Kojima et al. (1986) found that deammoniation and dehydroxylation take place simultaneously on mixed mica-motmorillonite clays. It is therefore not possible to differentiate between the two processes from the TG curves. Mass losses incurred by the pillared clays in this region are also ascribed to deammoniation (it is unlikely that the exchange of the Al_{13}^{7+} cations with NH_4^+ cations would be complete due to the partially swellable nature of these clays), and to lattice dehydroxylation. The presence of pillaring cations would be expected to increase weight loss in the 300 to 400°C temperature range, as dehydroxylation of one Al_{13}^{7+} ion results in a greater weight loss than the removal of seven NH_3 molecules. This effect was not noticeable on any of the clays, suggesting that the extent to which pillaring took place in the SMM and Ni-SMM samples was more limited than was the case in montmorillonite and beidellite.

Protons liberated during deammoniation should be equally effective in catalysing structural dehydroxylation as protons liberated during pillar dehydroxylation. Pillaring would therefore not be expected to decrease the temperatures at which structural OH groups are removed from SMM and Ni-SMM clays.

The results of N_2 adsorption experiments indicated that treating montmorillonite with the hydroxy-Al pillaring solution increased the surface area of the clay from 23 m^2/g to 343 m^2/g. Calcination at 500°C, which resulted in a decrease in interlayer spacing from 9.9 to 7.9 A, reduced the surface area to 237 m^2/g. This value is in good agreement

with that reported by Plee et al. (1987). These researchers found that pillaring a naturally occurring montmorillonite sample, with a measured CEC of 92 meq/g (very similar to the CEC of the clay used for this work), using a similar hydroxy-Al solution, resulted in a surface area of 229 m^2/g after calcination at 300°C. In general, values reported in the literature for the surface area of AL PILMont vary between 150 and 400 m^2/g. Differences in the nature of the naturally occurring clays and slight differences in the procedures used to prepare the hydroxy-Al pillaring solutions are probably responsible for the wide range of reported values.

The Langmuir adsorption isotherms of the calcined and uncalcined Al PILMont samples were significantly more linear than the BET isotherms, which suggested that the surface area of the clay was due predominantly to micropores in the interlayer spaces where the number of layers of N_2 adsorbing would be limited.

There appear to be two possible causes for the observed decrease in surface area of Al PILMont on calcination, these being a complete collapse of some of the interlayer spaces, and a decrease in the available surface area on the pillars resulting from the reduced interlayer spacing.

A decrease in the interlayer spacing would not be expected to reduce the available surface area on the clay layers themselves. If, however, calcination caused a total collapse of some of the pillars, surface area would decrease. If this collapse was sufficiently extensive to result in the observed decrease in surface area, it might be expected that an additional first order XRD peak would appear at around 10 A, corresponding to the presence of a collapsed layered structure. This was not observed.

The diameter of the Al_{13}^{7+} pillaring cation is around 11.7 A (Brindley and Sempels, 1977) while the height is around 9.9 A. This corresponds to an available surface area of 364 A^2 per pillar. Calcination reduces the pillar height to around 7.9 A. Assuming that the diameter of the pillar does not change significantly during dehydroxylation, this reduces the exposed surface area on the pillar by 74 A^2. If the exchange of ions

during the pillaring process is complete, and assuming that this exchange corresponds to the measured CEC of the clay (0.96 meq/g), calcination would result in the loss of 61 m^2/g of surface area due to the decreased pillar height.

If either of the two assumptions made in calculating this value were dropped, namely, that pillar diameter does not change during dehydroxylation, and that the number of pillaring species present fully satisfies the CEC of the clay, it would have the effect of reducing the calculated decrease in the surface area of the clay on calcination.

The observed decrease in surface area (103 m^2/g), therefore, seems high when compared with the calculated maximum value of 61 m^2/g, and is probably a result of the method used to estimate surface area. The surface area was calculated from the slope of a line obtained from a linear regression analysis of the N_2 adsorption data plotted according to the Langmuir equation. This equation assumes monolayer adsorption on the sample surface. While it is true that the number of layers of N_2 adsorbing on the interlayer surfaces of the clay will be limited by the interlayer spacing, it is unlikely that monolayer adsorption will occur. The surface area estimates made using the Langmuir equation will therefore be artificially high, as will the decreases in surface area resulting from a decrease in interlayer spacing on calcination.

Introducing one of the Al_{13}^{7+} pillaring cations into the interlamellar space would result in the loss of around 215 A^2 of surface area on the layer surfaces. The available surface area on the pillar (height = 9.9 A) is ca. 364 A^2. Similarly, after calcination (pillar height = 7.9 A, max. pillar diameter = 11.7 A), the available surface area on the pillar will be greater than the area which the pillar occupies on the clay layers above and below. Increasing pillar density would therefore be expected to result in an increase in surface area. Shabtai et al. (1984) reported the surface areas of montmorillonite pillared with different quantities of the Al_{13}^{7+} cation and found that surface area increased with increasing Al_{13}^{7+}/mont ratios up to the point where the quantity of Al_{13}^{7+} cations fully satisfied the lattice charge deficit. It seems likely that these observed increases in surface area are a result of increases in pillar density, although it is possible that, while the

quantity of Al_{13} cations used is lower than than that required to satisfy the lattice charge deficit, some interlayer spaces may remain unpillared. Increasing the Al_{13}^{7+}/mont ratio would then increase the extent of pillaring, not the pillar density. This would also result in an increase in surface area.

The presence of nickel in the hydroxy-Al pillaring cation reduces the charge on this ion. The Ni/Al PILMont sample was prepared with a hydroxy-Al solution containing enough nickel to replace an average of 3.73 aluminium atoms in each Al_{13}^{7+} cation, thereby reducing the charge to +3.27. Subsequent analysis of the Ni/Al PILMont clay indicated that the sample contained enough nickel to replace an average of 1.82 aluminium atoms per pillar, giving the pillaring cation an average charge of ca. +5.18. This figure, however, should be regarded as being an estimate. The size of the pillaring cation should not change significantly as a result of modification with nickel. The surface area of calcined Ni/Al PILMont was slightly higher than that of calcined Al PILMont (253 vs. 237 m^2/g, respectively). This could be an indication of an increased pillar density in the nickel containing sample, although the observed difference may simply be within the limits of experimental accuracy.

Treatment with the hydroxy-Al pillaring solution increased the the measured surface area of beidellite from 117 m^2/g to 198 m^2/g. Calcination of the pillared clay decreased the surface area to 163 m^2/g. The linearity of the Langmuir adsorption isotherm suggested that, as in the case of Al PILMont, the surface area is due predominantly to micropores in the interlayer spaces generated by pillaring. Brindley and Sempels (1977) reported a Langmuir surface area of 214 m^2/g for a naturally occurring beidellite clay pillared with a hydroxy-Al solution. The OH/Al ratio in the pillaring solution was 2.4 and the sample was outgassed at 110°C prior to argon adsorption. Outgassing at 325°C reduced the surface area to 195 m^2/g.

The surface area of Al PILBeid was lower than that of Al PILMont in both the calcined and uncalcined form. This suggests that the generation of an expanded-layer structure is less extensive in beidellite than in montmorillonite. It is not clear why this should be the case as both

clays should be essentially 100% swellable. It is possible that differences in the clay particle size range used during the pillaring process could be playing a role here. The much larger beidellite particles (<75 um vs. <2 um) may have a greater proportion of interlayer space which is inaccessible to the pillaring ions. It is also possible that subtle differences in the pillar solution preparation procedure used, in particular, the rate of addition of NaOH to $AlCl_3$, may be contributing to the observed differences in the surface areas of the two pillared clays.

Differences in layer morphologies are solely responsible for differences in the surface areas of smectite minerals. Montmorillonite is typically characterised by extensive layer stacking in the basal direction. This particular layer configuration gives rise to relatively low surface areas. Mixed mica-montmorillonite clays, such as SMM and Ni-SMM, typically consist of aggregates of layers or "platelets" which orient themselves randomly, giving rise to a larger exposed layer area. The surface area of montmorillonite might therefore be expected to be lower than that of the SMM and Ni-SMM clays. The results of the N_2 adsorption experiments indicated that this was the case. The estimated surface area of calcined beidellite was five times that of calcined montmorillonite (117 m^2/g and 23 m^2/g, respectively), and was in fact higher than that of SMM (101 m^2/g). This result suggests that the layers of the unpillared beidellite clay are considerably more delaminated than those of the unpillared montmorillonite sample.

Calcination of the unpillared SMM and Ni-SMM samples resulted in a decrease in the measured surface areas of the clays. This decrease may not be ascribed to the elimination of interlayer spaces during heat treatment, as outgassing of uncalcined samples prior to N_2 adsorption also results in the collapse of the interlayer spaces (Mott, 1988). Wright et al. (1972) observed a similar decrease in the surface area of SMM after calcination at 650°C and attributed this to increased platelet-to-platelet association in the clay. It seems likely that a similar explanation would hold for the Ni-SMM samples.

Treating the SMM and Ni-SMM samples with the hydroxy-Al pillaring solution decreased the linearity of the BET N_2 adsorption isotherms and

increased the linearity of the Langmuir isotherms. This effect was most pronounced in the case of SMM. The observed changes in the linearity of the two isotherms may be regarded as being an indication of an increase in the proportion of surface area present on which the number of layers of N_2 adsorbing are limited. The result suggests that microporous structures are generated in all these clays and that pillaring is more extensive in SMM than in the Ni-SMM samples.

Calcined Al PILSMM had a significantly higher surface area than calcined SMM. This is consistent with the XRD results which indicated the presence of an expanded-layer structure in the pillared clay. Pillaring of SMM appeared to result in a greater increase in surface area than was observed upon pillaring beidellite. This is unexpected in view of the different swellable properties of the two clays. The relatively high surface area of unpillared beidellite indicated that layer delamination in the clay was extensive. The generation of an extensive pillared structure in this clay would therefore increase face-to-face layer aggregation. This would have the effect of reducing the contribution of exposed layer faces to the surface area of the clay. The increase in surface area observed upon pillaring beidellite may therefore not be representative of the amount of pillared interlayer area present in Al PILBeid. In the case of SMM, it seems likely that pillaring would take place within the five-layered platelets. If this was the case, the contribution of exposed layer faces to the surface area of SMM would not be expected to decrease on pillaring. The larger increase in surface area observed on pillaring SMM may therefore not be indicative of the generation of a more extensive pillared structure in this clay than in beidellite. A technique such as TEM would be required to investigate this hypothesis.

Treating the two Ni-SMM samples with the pillaring solution did not appear to have a marked effect on the surface areas of these clays. This result is surprising in view of the fact that XRD analysis suggested that treatment with the pillaring solution increased the extent of layer delamination in both clays. In addition, NH_3 TPD and propane adsorption experiments indicated that the number of available acid sites and the pore volume of the two clays increased noticeably after treatment with the pillaring solution. It is not clear how such changes in the

properties of these clays can be accompanied by essentially no change in surface area.

Propane adsorption experiments indicated that the pore volumes of all the clays treated with pillaring solutions increased significantly. The pore volumes of Al PILMont and Si/Al PILMont(2) were similar, but the weight gain due to propane adsorption on Ni/Al PILMont appeared to be smaller than that on Al PILMont (2% vs. 3.2%, respectively). This suggests that the sample treated with the Ni/Al pillaring solution has a smaller pore volume and may be an indication of a higher pillar density resulting from the lower charge on the pillaring species.

Unpillared montmorillonite and beidellite adsorbed similar amounts of propane. This result is surprising in view of the fact that the surface area measurements indicated that the beidellite clay was considerably more delaminated. The macroporous pore volume of this clay would therefore be expected to be greater than that of montmorillonite. Pillaring beidellite did not result in as large an increase in the amount of propane adsorbed as pillaring montmorillonite. This result is consistent with the surface area measurements in suggesting that pillaring is not as extensive in the beidellite clay.

The amount of propane adsorbed onto SMM was similar to that adsorbed onto Na Mont. This is unexpected as the macroporous pore volume of SMM should be greater than that of montmorillonite. No explanation is offered for this result.

Treating the SMM and Ni-SMM samples with the hydroxy-Al pillaring solution increased the amount of propane adsorbed in all cases. In the SMM and Ni-SMM(7) samples, the increases were greater than that observed on pillaring beidellite. It seems possible, therefore, that these increases do not arise solely due to the generation of microporous pillared structures in these clays.

The number of ammonia molecules desorbing from a catalyst during ammonia TPD may be regarded as being a measure of the number of acid sites present on the catalyst which are accessible to a molecule with dimensions similar to that of ammonia. The temperature at which

desorption takes place is an indication of the strength of the acid sites.

Treating the clay samples used for this work with pillaring solutions resulted in an increase in the total number of available acid sites present, as indicated by ammonia TPD. This increase in acidity can occur as a result of two factors. Firstly, the increase in the accessible layer surface area increases the number of clay lattice acid sites which are available for adsorption. Secondly, acid sites may be present on the pillars.

Ocelli et al. (1983) reported that Al PILMont contained both Lewis and Bronsted acid sites according to the IR spectra of adsorbed pyridine. At a temperature of 400°C acidity was found to be mostly of the Lewis type. The proton donating ability of structural hydroxyl groups has been reported for clay minerals by Hall (1985). Ming-Yuan et al. (1988) compared the IR spectra of Al PILMont and the parent montmorillonite in the OH stretching region. Their results suggested that the OH groups present on the pillars do not make a significant contribution to the IR adsorption, especially for samples pretreated at higher temperatures. It seems reasonable, in light of the above findings, that after calcination at 500°C, any acidic contributions from the Al pillars themselves would be of the Lewis type.

Plee et al. (1985) reported the possible bonding between the tetrahedral sheet of the clay and Al_{13} pillars, through MAS NMR examination of pillared beidellite calcined at 300 - 400°C. The existence of Si-O-Al(IV) linkages in the tetrahedral sheet is a prerequisite for this type of bonding. Since the Al_{13} ion is acidic, it transfers protons to the layers upon calcination. The most likely point of attack is at an Si-O-Al(IV) linkage with the formation of a silanol group. The protonated Si-(OH)-Al(IV) structure in the tetrahedral sheet may react with the pillar to form either Si-O-Al_p or Al(IV)-O-Al_p linkages, where Al_p represents aluminium present in the pillar. Plee et al. (1985) reported that the MAS NMR spectral changes accompanying this process pointed to the latter type linkage. This Al(IV)-O-Al_p linkage induces an inversion of an aluminium tetrahedron of the tetrahedral sheet. This leads to a different Si-O-Al(IV) linkage in the tetrahedral sheet in which the

negative charge of the Al tetrahedron is no longer buried in a continuous tetrahedral network, but is exposed in the interlamellar space. This should induce a large number of strong acid sites as compared with those in Al PILMont.

As both SMM and Ni-SMM are tetrahedrally substituted clays, calcination of the Al PILSMM and Al PILNi-SMM samples should result in the formation of similar linkages between the pillars and the clay structure.

Calcination of montmorillonite pillared with hydroxy-Si/Al oligocations should result in the formation of stable SiO_2-Al_2O_3 pillars. These pillars would be expected to be more acidic than the alumina pillars.

Calcination of Ni/Al PILMont should result in the formation of stable NiO-Al_2O_3 pillars. The acidic properties of these pillars should be similar to those of the Al_2O_3 pillars, their acid sites being predominantly of the Lewis type.

In the discussion which follows, the phrases "the number of acid sites", and "acid site density" refer to those accessible acid sites present on the various clay samples which hold ammonia up to temperatures in the range 100 to 500°C, as indicated by ammonia TPD.

The increases in the number of acid sites present on the essentially 100% swellable montmorillonite and beidellite samples on treatment with the hydroxy-Al solution were 214% and 250%, respectively. The corresponding increases for the SMM and Ni-SMM samples were noticeably lower, being in the region of 50% in all three cases. This would seem to reflect the partially swellable nature of these clays. However, the mixed mica-montmorillonite samples consist of two clay phases with different concentrations of tetrahedrally co-ordinated Al and, consequently, different acid site densities. The generation of pillared structures would be expected to take place only in the swellable phases of these clays, which have the lower acid site density. Therefore, if a similar number of layers were pillared in the partially swellable and fully swellable clays, the proportional increase in the number of acid sites on the partially swellable clays would be expected to be lower than that on the fully swellable clays, as the relative contribution of

the phase with the lower acid site density to the total available surface area of the partially swellable clay should increase upon pillaring.

XRD analysis of the SMM sample indicated that the clay comprised approximately 40% swellable material. While the amount of swellable material present in the Ni-SMM samples is uncertain, the presence of a significant quantity of a two layered clay in the Ni-SMM(21) sample should ensure that the proportion of non-swellable material present in this clay is relatively small. The actual increase in the number of acid sites observed upon pillaring SMM was 0.08 mmol/g as compared with 0.1 mmol/g in the case of beidellite, while that of the Ni-SMM(7) and Ni-SMM(21) samples were 0.11 and 0.12 mmol/g, respectively. If the increases in acidity observed on pillaring the SMM and Ni-SMM clays arise solely due to the generation of pillared structures in these clays, these results suggest that the acid site density of the swellable material present in the partially swellable clays is significantly greater than that of the beidellite sample. If this is not the case, the observed increases in acidity on the SMM and Ni-SMM clays would have to be attributed, at least partly, to changes in layer morphology, other than the generation of pillared structures, which increase the number of accessible acid sites on the clays. Layer delamination would have such an effect.

The liberation of protons resulting from the dehydroxylation of the pillaring species present in pillared clays would not be expected to result in an increased acidity when compared with the deammoniation process which takes place on the NH_4^+ exchanged parent clays. As mentioned previously, the increases in the number of acid sites observed on pillaring may be a result of two factors, namely, an increase in the accessible clay layer surface area, and the presence of additional Lewis acid sites on the pillars. No attempt is made to asses the contribution of Lewis sites on the pillars to the increases in the number of available acid sites observed on pillaring from the results of this study.

Table 3.8 shows the amount of ammonia desorbed from the pillared and unpillared clays per square meter of surface area. These figures may be

regarded as being indications of the acid site densities on the clays. When considering these values it should be borne in mind that surface area estimates were made using N_2 as a probe molecule, whereas ammonia was used to estimate the number of acid sites present.

The acid site density of Si/Al PILMont(2) did not appear to be significantly higher than that of Al PILMont. This result is not in agreement with the findings of Shabtai et al. (1989) who pillared montmorillonite with similar pillaring solutions and found that the sample treated with the Si/Al solution had a noticeably higher acid site density than Al PILMont (a microbalance was used to measure the amount of adsorbed ammonia present on the pillared catalysts at different temperatures). If the additional acid sites arising from the presence of Si in the pillars were very weak, it is possible that ammonia molecules held by these sites would desorb below 100°C. If this was the case, the ammonia TPD procedure used for this work would not detect the presence of such sites. Similarly, the TPD procedure would not detect the presence of acid sites which are capable of holding ammonia at temperatures greater than 500°C.

Pillaring montmorillonite appeared to result in a large decrease in acid site density. In contrast, pillaring beidellite increased acid site density. Treating SMM with the hydroxy-Al solution decreased the apparent acid site density of the clay slightly, while that of the two Ni-SMM samples increased. There appears to be no obvious explanation for these results.

It is widely accepted that peak positions in ammonia TPD spectra are affected by the ratio of the gas flowrate to the number of sites which adsorb ammonia. Comparing the ratios of strong to weak acid sites on catalysts with different acidities using TPD spectra may therefore be misleading. In addition, differences in porous structures can alter TPD peak positions by affecting the rates at which ammonia molecules diffuse out of the catalysts. In the dicussion which follows, comparisons of the acid site strength distributions of different catalysts are made only in cases where it is felt that differences in the number of acid sites present and in the porous structure are sufficiently small so as to have a negligible effect on the position of the TPD peak.

The results in Table 3.10 indicate that NH_4 Beid had a greater proportion of strong acid sites than NH_4 Mont (strong/weak = 1.06 and 0.62, respectively). This is probably due to the differences in the isomorphous substitutions taking place in the two clays. Plee et al. (1985) found that pyridine chemisorbed on Bronsted acid sites in montmorillonite was rapidly removed by evacuation at 300°C. In contrast, beidellite retained pyridine chemisorbed on Bronsted acid sites after evacuation at 400°C. In NH_4 Beid, substitution of Al for Si in the tetrahedral layers gives a net negative charge to the silicate layer. Protons liberated during deammoniation accompanying calcination will be captured by tetrahedral Si-O-Al linkages and, consequently, Si-OH-Al linkages similar to those on zeolites will be generated. The strong Bronsted acidity of NH_4 Beid may be associated with these linkages. In contrast, NH_4 Mont is an octahedrally charged smectite and contains no tetrahedral Si-O-Al linkages. The negative charge on this clay is somewhat homogenously distributed in the silicate layers, whereas that of beidellite is localised. Isomorphous replacement in octahedral layers will probably therefore generate weak Bronsted acidity compared with that in tetrahedral layers. The presence of strong Bronsted acid sites may be contributing to the observed higher proportion of strong acid sites in NH_4 Beid. It is also likely that the strength of Lewis acid sites arising from the tetrahedral Si-O-Al(IV) and octahedral Al(VI)-O-Mg linkages will differ.

The ratios of stronger to weaker acid sites on the SMM, Ni-SMM(7), and Ni-SMM(21) were 0.98, 0.76, and 0.85, respectively. The differences in these values may be a result of differing acid site densities on the three clays. Differences in the proximity of acid sites, resulting from different concentrations of tetrahedrally co-ordinated Al, can alter the extent of acid site interactions and hence affect acid site strength. It is interesting to note that, of the three clays, the sample with the highest strong/weak acid site ratio (SMM) also had the highest acid site density, while that with the lowest strong/weak ratio (Ni-SMM(7)) had the lowest acid site density. This result suggests that increasing acid site density on these clays enhances acid site strength. It is also possible that the presence of varying amounts of nickel in the octahedral positions of the clays could influence acid site strength.

The observed differences in the acid site strengths of the three catalysts, however, were small, and may be within the limits of experimental accuracy.

The strong/weak acid site ratios for the Al, Si/Al, and Ni/Al PILMont samples varied in the range 0.47 to 0.67. As was the case with the SMM and Ni-SMM clays, these observed differences may be within the limits of experimental accuracy. It seems difficult, therefore, to attach significance to them.

A somewhat unexpected result is that, according to ammonia TPD results, treating montmorillonite with the hydroxy-Al solution resulted in very little change in the acid site strength distribution of the clay, whereas similar treatment of beidellite appeared to result in a significant decrease in the strong/weak acid site ratio. This is at variance with the proposal of Plee et al. (1985) that bonding between the Al pillars and the tetrahedral sheet in Al PILBeid, as compared with pillar-lattice bonding in Al PILMont, should induce a large number of strong acid sites due to the formation of different Si-O-Al(IV) linkages which are exposed in the interlayer space.

It could be expected that unpillared SMM would exhibit greater acidity than unpillared beidellite due to the greater acid site density of the non-swellable material present in the former clay. This was found to be the case. It is conceivable, however, that, in spite of having a lower average acid site density, pillared beidellite could have a greater number of accessible acid sites than pillared SMM due to the fact that ca. 60% of the material present in SMM should remain unaffected by the pillaring process. This was not found to be the case. The relative difference in the number of accessible acid sites on the two clays, however, was seen to diminish.

Zhinqun (1987) used Al PILMont for ammonia adsorption-IR examination. They studied the intensities of the band at 1430 cm^{-1}, which corresponds to the presence of Bronsted acid sites, at different pretreatment temperatures. They found that Bronsted acidity decreased with increasing temperature, especially above 300°C. The same researchers studied the dependence of the amount of Lewis acidity on temperature using IR

measurements from adsorbed pyridine. Their results indicated that the amount of Lewis acidity gradually decreased with pretreatment temperature. The TPD profiles of Si/Al PILMont(2) calcined at 300, 400, and 500°C do not indicate that the total acidity of this clay increased with decreasing pretreatment temperature. Changes in pretreatment temperature also did not appear to affect the acid site strength distribution of the clay.

In the above discussion, a comparison of the acidic properties of the different clays used for this work was made from the results of the ammonia TPD experiments. It should be noted that this comparison did not take into account the possible presence of acid sites which are sufficiently strong to hold ammonia up to temperatures in excess of 500°C.

Unpillared montmorillonite and beidellite showed very limited activity for propene oligomerisation in both the Na^+ and NH_4^+ exchanged forms. This is not surprising in view of the fact that the number of available acid sites present on these catalysts, as indicated by ammonia TPD, are very small. The NH_4^+ exchanged versions of these clays would be expected to be much more active than their Na^+ exchanged counterparts due to the presence of protons liberated during the deammoniation process accompanying calcination. These protons are known to give rise to Bronsted acidity and, through lattice dehydroxylation, Lewis acidity. Na^+ cations, on the other hand, probably function as very weak Lewis acid sites. As conversion levels were so low, it was not possible to compare the activities of the NH_4^+ and Na^+ exchanged forms of these clays.

Both Na^+ and NH_4^+ beidellite showed signs of activity at 300°C, whereas their montmorillonite equivalents appeared to start reacting at only 350°C. It is difficult to attach significance to this result, however, in view of the extremely low levels of conversion attained by these catalysts.

Pillaring of montmorillonite with the Al, Si/Al, and Ni/Al pillaring solutions resulted in significant increases in propene oligomerisation activity in all cases. Occelli et al. (1985) reported that Al PILMont

converted 17% of the propene present in a feed containing 25% propane and 75% propene at a temperature of 200°C. The pressure used was 41 atm and the WHSV was 1 h^{-1}. The higher level of conversion reported by these researchers is probably largely due to the lower WHSV which was used. As the montmorillonite samples used in this work and in the work reported by Occelli et al. were both naturally occurring minerals, possible differences in chemical compositions could also account for the differences in the observed propene oligomerisation activity.

Treating montmorillonite with hydroxy-Al and hydroxy-Si/Al pillaring solutions resulted in the generation of microporous structures with similar surface areas and acidities. As the charge on these two pillaring species is the same, pillar densities would be expected to be similar. Increasing the Si/Al ratio in the pillaring solution from 1 to 2 did not appear to affect the properties of the pillared clay. It is not surprising, therefore, that Al PILMont, Si/Al PILMont(1), and Si/Al PILMont(2) showed similar activities for propene oligomerisation.

As with montmorillonite, pillaring beidellite with the hydroxy-Al solution resulted in a significant increase in the propene oligomerisation activity of the catalyst. The activity of Al PILBeid was, however, slightly lower than that of Al PILMont. This is consistent with the results of ammonia TPD and N_2 adsorption experiments which indicated that the number of accessible acid sites and the surface area of Al PILBeid were smaller than that of Al PILMont.

The propene oligomerisation activities of the SMM and Ni-SMM clays were considerably greater than those of the montmorillonite and beidellite samples in their pillared or unpillared forms. The Ni-SMM catalysts were more active than SMM, a result consistent with the ammonia TPD results which indicated that the Ni containing samples had a greater number of accessible acid sites. Ni-SMM(21), however, was less active than Ni-SMM(7), in spite of having a slightly greater number of acid sites. Possible differences in layer morphology, and the different Ni loadings in the two clays could be playing a role here.

The lattice structures of beidellite and SMM are identical. The very large differences in the propene oligomerisation activities of Al

PILBeid and NH_4^+ SMM are unexpected in view of the ammonia TPD results. These results indicated that the total number of available acid sites present on the two clays was fairly similar (0.14 and 0.17 mmol/g, respectively). Although it was found that the average acid site density of SMM is greater than that of Al PILBeid (Table 3.8), and that the acid site strength of the two clays differed (Table 3.9), it seems unlikely that this alone would account for such large differences in propene oligomerisation activity.

The results of ammonia TPD experiments indicated that the number of accessible acid sites present on the pillared montmorillonite samples was greater than that on SMM and Ni-SMM(7) (0.22 vs. 0.17 and 0.20 mmol/g, respectively), and slightly smaller than that on Ni-SMM(21) (0.24 mmol/g). Although the nature of acidity in the montmorillonite and mixed mica-montmorillonite clays could differ as a result of the different types of isomorphous substitution taking place in their clay structures, the much greater propene oligomerisation activity demonstrated by the SMM and Ni-SMM samples cannot be explained by the ammonia TPD results.

It seems likely, therefore, that the oligomerisation rates over the catalysts used for this work are not a function of catalyst surface area, acid site strength and acid site density alone. Diffusion limitations, induced by reaction products held in the microporous structures generated by pillaring, could be limiting the reaction rate in the pillared montmorillonite and beidellite clays. Such limitations should be essentially absent in the case of the unpillared SMM and Ni-SMM catalysts where reaction takes place only on exposed layer edges and faces. The SMM and Ni-SMM clays showed signs of activity at temperatures as low as 100°C, whereas the pillared montmorillonite and beidellite samples became active only at around 180°C. This could also be a result of diffusional constraints resulting in reaction products being unable to leave the microporous pillared structures at low temperatures.

The presence of nickel in the pillars of Ni/Al PILMont could affect the activity of the pillared clay. In addition, an increase in pillar density, resulting from the reduced charge on the Ni substituted pillaring species and supported by the results of the propane adsorption

experiments, could affect the rate at which oligomerised products diffuse out of the catalyst. If the rate of oligomerisation in pillared montmorillonite is controlled by the rate of diffusion of product molecules out of the microporous pillared structure of the clay, this would affect catalyst activity. The reduced pore size could also alter the concentration of reactant molecules around acid sites, which may also affect catalyst activity. However, the reaction data indicated that the catalytic activity of the Ni/Al PILMont and Al PILMont samples was very similar.

Unlike the SMM and Ni-SMM samples, which showed only limited signs of deactivation after twelve hours on stream, the pillared montmorillonite and beidellite catalysts deactivated rapidly. Liquid hydrocarbon occlusion in the microporous pillared structures of the pillared montmorillonite and beidellite samples are probably responsible for the higher rate of catalyst deactivation.

Thermal analysis indicated that coke formation on Al PILMont was greater than that on Al PILBeid. This might be expected in view of the moderately higher activity of the former clay, and in view of the fact that pillaring of montmorillonite appears to have generated a more extensive microporous structure in this clay. The high iron content of the montmorillonite sample (4.4%), however, could also contribute to the greater coke content of this catalyst by catalysing dehydrocyclisation reactions which lead to more aromatics and coke formation. Lussier et al. (1980) found that montmorillonite samples in which iron was partially removed gave reduced coke levels during the cracking of gas oil fractions. The treatment used to remove iron, however, reduced the surface area and acidity of the clay.

The percentage of "graphitic" coke present on Al PILMont and Al PILBeid was similar, being 46 and 50%, respectively. This was considerably higher than that on any of the SMM and Ni-SMM samples. The higher reaction temperatures used for the pillared montmorillonite and beidellite samples are an obvious explanation for this large difference. It is also possible, however, that the experimental technique used to estimate the relative amounts of "graphitic" and "high boiling point hydrocarbon" coke present on the catalysts could be contributing to this

difference. The extensive microporous pillared structures present in Al PILMont and Al PILBeid may restrict the diffusion of the high boiling point hydrocarbon coke molecules out of the catalyst structure during heating to 500°C in nitrogen. At the higher temperatures, viz., 400 - 500°C, these hyrocarbons could be converted into graphitic coke before they are removed. This would increase the observed proportion of this type of coke. The effect of the extensive presence of these microporous structures on the rate of diffusion of the long chain length hydrocarbon molecules out of the coked catalysts is evident from Table 3.13. In the case of Al PILMont and Al PILBeid, only 39 and 49%, respectively, of the total high boiling point hydrocarbons which desorbed from the catalysts on heating to 500°C in N_2 desorbed below 400°C. This figure was between 80 and 92% for the pillared and unpillared SMM and Ni-SMM samples.

Treating the SMM and Ni-SMM clays with the hydroxy-Al pillaring solution resulted in significant increases in propene oligomerisation activities. This is consistent with the observed increases in the number of available acid sites accompanying the pillaring process. Liquid production per gram of catalyst (over a period of twelve hours) increased by 27% in the case of SMM, 47.5% in Ni-SMM(7), and 47.6% for Ni-SMM(21).

The concentrations of tetrahedrally coordinated aluminium in beidellite, SMM and Ni-SMM clays which give rise to swellable material are relatively low and lie in a fairly narrow range. As this range should be similar for all three clays, as discussed earlier, the acidic properties of any pillared structures generated in these clays should not be vastly different. Hence, if the changes in propene oligomerisation activity observed on pillaring the SMM and Ni-SMM samples are ascribed to the generation of microporous pillared structures, it should be possible to explain these changes by considering the activity of the microporous pillared structure of Al PILBeid for the same reaction. This was not the case.

The microporous structure of Al PILBeid started converting propene only at ca. 180°C, whereas pillaring of SMM and Ni-SMM resulted in noticeable increases in conversion at 140 and 150°C, respectively. Pillaring the partially swellable SMM and Ni-SMM clays, which can generate a

microporous structure only to a limited extent due to the presence of non-swellable material, increased the average conversion levels from 30 to 39% in SMM, from 42 to 62% in Ni SMM(21), and from 50 to 75% in Ni-SMM(7). The more extensive microporous pillared structure in Al PILBeid converted only 7% of the propene at 200°C. Furthermore, the microporous structure in Al PILBeid deactivated rapidly, whereas the increased activity resulting from the pillaring of the SMM and Ni-SMM clays was not significantly reduced after twelve hours on stream. In view of this, it seems unlikely that any microporous pillared structures present in the pillared SMM and Ni-SMM samples are solely responsible for the observed increases in oligomerisation activity.

It was proposed earlier that, besides generating a microporous structure in the swellable phases of the clays, pillaring of SMM and Ni-SMM clays may result in an increase in layer delamination. This proposal is consistent with the results of propene oligomerisation runs performed with these catalysts. This delamination process would increase the number of accessible acid sites present on the clays. Unlike the microporous pillared structure, the lack of structural constraints in the macroporous structures resulting from layer delamination caused by treatment with the pillaring solution would not be expected to promote hydrocarbon occlusion which, it is proposed, was primarily responsible for the rapid deactivation of the pillared structures present in the montmorillonite and beidellite clays. It would therefore be expected that the rates of deactivation of the pillared SMM and Ni-SMM samples would not be greater than those of their unpillared analogues. This was, in fact, the case.

Thermal analysis of the coked catalysts from propene oligomerisation runs indicated that, after twelve hours on stream, the amount of coke present on the SMM and Ni-SMM samples was slightly reduced if the clay had been treated with the hydroxy-Al pillaring solution. This was in spite of the fact that pillaring increased the activities of the catalysts. This reduction in coke formation was more pronounced in the case of the Ni-SMM samples than in SMM, as was the increase in catalyst activity accompanying pillaring. It is most unlikely that the limited presence of pillared structures in the pillared versions of these clays was responsible for the decrease in coke formation, as it is likely that

hydrocarbon occlusion and coke formation were responsible for the rapid deactivation of Al PILBeid and Al PILMont. Changes in layer morphology, however, due to the proposed delamination accompanying pillaring, could result in reduced coke formation by increasing effective pore sizes, thereby reducing physical constraints which slow down the diffusion of coke precursors out of the catalyst structure.

The generation of zeolite-like microporosity by pillaring might be expected to affect the product selectivities of these clays during propene oligomerisation. Shape selectivity arising from their channel openings (approximately 8 x 14 A for Al PILMont) could increase selectivities to lower molecular weight oligomers. It is, unfortunately, not possible to observe the effect that pillaring has on the propene oligomerisation selectivities of montmorillonite and beidellite from the results of this study due to the extremely low levels of conversion attained by the parent clays.

The liquid product selectivities, in terms of carbon number distribution, of the montmorillonite samples treated with the Al, Si/Al, and Ni/Al pillaring solutions were very similar. If the use of the Ni/Al pillaring species does result in a greater pillar density in pillared montmorillonite, this does not appear to affect the product selectivity of the pillared clay appreciably. As the reaction temperature was increased, selectivities of the pillared montmorillonite samples to the C_{21+} fraction increased significantly. This could be due to the fact that the higher temperatures facilitate more rapid diffusion of high molecular oligomers out of the catalyst. Some of these high molecular weight oligomers may have been formed at the lower reaction temperatures.

The product selectivity of Al PILBeid was initially similar to that of Al PILMont. Unlike the pillared montmorillonite samples, however, selectivity to the C_{21+} fraction appeared to decrease with increasing reaction temperature. This decrease could occur as a result of increases in steric constraints in the microporous structure resulting from increased coke formation at the higher temperatures. The different effect that increasing reaction temperature had on the product selectivities of Al PILMont and Al PILBeid may be a result of different

extents of coke formation on the two clays.

The more uniform carbon number distributions generated by the pillared montmorillonite and beidellite clays at the higher reaction temperatures are ascibed to increases in cracking and copolymerisation reactions.

Pillaring of the SMM and Ni-SMM clays resulted in no observed changes in liquid product carbon number distributions of these catalysts during propene oligomerisation. This is not surprising in view of the proposal that any microporous pillared structures present in these clays are probably not contributing significantly to catalyst activity.

The effect that the pillaring process had on the activities of the clays for the reaction of 124 TMB was similar to that observed for propene oligomerisation. Conversion levels increased noticeably in all cases.

The activities of the montmorillonite samples treated with the Al and Si/Al pillaring solutions were very similar. These results are consistent with the ammonia TPD results, XRD results, and N_2 adsorption measurements which indicated that the acidities, surface areas and pillared structures of these clays were similar. The montmorillonite sample treated with the Ni/Al pillaring solution, however, appeared to be less active than the Al PILMont and Si/Al PILMont samples for this reaction. This result is at variance with the ammonia TPD results and surface area measurements which suggested that the acidic properties of the Al, Si/Al, and Ni/Al PILMont samples were very similar. The result can, however, be explained in terms of an increased pillar density in Ni/Al PILMont, although this, and the results of the propane adsorption experiments, constitute the only experimental evidence to suggest that Ni/Al PILMont may have a higher pillar density. The increased pillar density could reduce catalyst activity by slowing down the passage of reactant and product molecules through the pores of the catalyst. The fact that this effect was not observed during propene oligomerisation could be due to the more linear nature of the products formed and the smaller size of the transition state species during this reaction.

The activity of Al PILBeid was lower than that of Al PILMont, which is consistent with the ammonia TPD results and surface area measurements.

Both Ni-SMM samples were noticeably more active than SMM for the propene oligomerisation reaction. SMM, however, was significantly more active than either of the Ni-SMM clays for the reaction of 124 TMB. Similarly, the increases in the propene oligomerisation activities of the clays, on treatment with the pillaring solution, were greater in the case of the Ni-SMM samples than in SMM, whereas the converse was true for the increase in the activities of these clays for the reaction of 124 TMB. No explanation can be offered for these differences at this stage.

The rates of catalyst deactivation during the reaction of 124 TMB over the pillared montmorillonite and pillared beidellite catalysts did not appear to be greater than those of the unpillared SMM and Ni-SMM samples. This result is surprising in view of the fact that hydrocarbon occlusion and subsequent coke formation would be expected to be more extensive in the microporous pillared structures of the montmorillonite and beidellite samples than in the macroporous structures of the partially swellable clays.

There are two widely accepted mechanisms for the acid catalysed disproportionation of aromatic hydrocarbons. One is a consecutive dealkylation-alkylation process, while the other involves the formation of large bimolecular aromatic compounds as intermediates. The former mechanism has been found to take place at higher temperatures and leads to unselective disproportionation.

The reaction of trimethylbenzene (TMB) over catalysts used for this work resulted largely in selective disproportionation when compared to the thermodynamic equilibrium concentrations of the xylenes and tertramethylbenzenes (TetMB). The reaction temperature used for the work was 300°C, which is not particularly high, and there were only limited quantities of dealkylation products present. It follows that the most likely mechanism for TMB disproportionation over these catalysts is the bi-molecular intermediate type. The results of similar work by Kikuchi et al. (1984) using Al PILMont and Zr PILMont led these researchers to similar conclusions.

TMB can be converted via three competing reactions over acid catalysts,

viz., disproportionation, isomerisation, and dealkylation. In order to gain an indication of the reaction selectivities of the catalysts used in this work, it has been assumed that increased quantities of 123 and 135 TMB isomers present in the products are indicative of an increased selectivity to the isomerisation reaction. Table 3.15 shows the conversion levels attained by SMM and Si/Al PILMont(1) during the reaction of 123, 135, and 124 TMB. The assumption seems reasonable in view of the fact that the reactivities of the 123 and 135 isomers over these catalysts were fairly similar to those of the 124 isomer.

All the catalysts tested for this reaction were more selective to o-xylene and 1245 TetMB during the reaction of 124 TMB than would be expected from thermodynamic equilibrium concentrations. There are three possible factors which may be contributing to this result.

(i) Stabilities of the resonating structures of the bimolecular intermediates: The ring structures of TMB molecules in the proposed bimolecular intermediates are linked through a penta-coordinated carbon atom. The resulting positive charge is shared between the two rings. The intermediates may be depicted as follows (methyl groups are not shown):

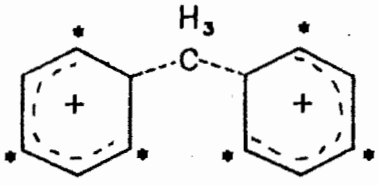

There are three possible positions in each ring where the positive charge may become localised. These are denoted by *. Since methyl groups are electron releasing in nature, differences in the positions of the five unshared methyl groups will be responsible for differences in the stabilities of the different intermediates. Increasing the number of methyl groups located at positions where positive charge can become localised will increase the stability of the intermediate. Figure 4.1 shows all the possible bimolecular intermediates which can be formed between 124 TMB molecules. The number appearing in each ring represents the number of methyl groups located at positions where positive charge may become localised and may therefore be regarded as being an indication of ring stability.

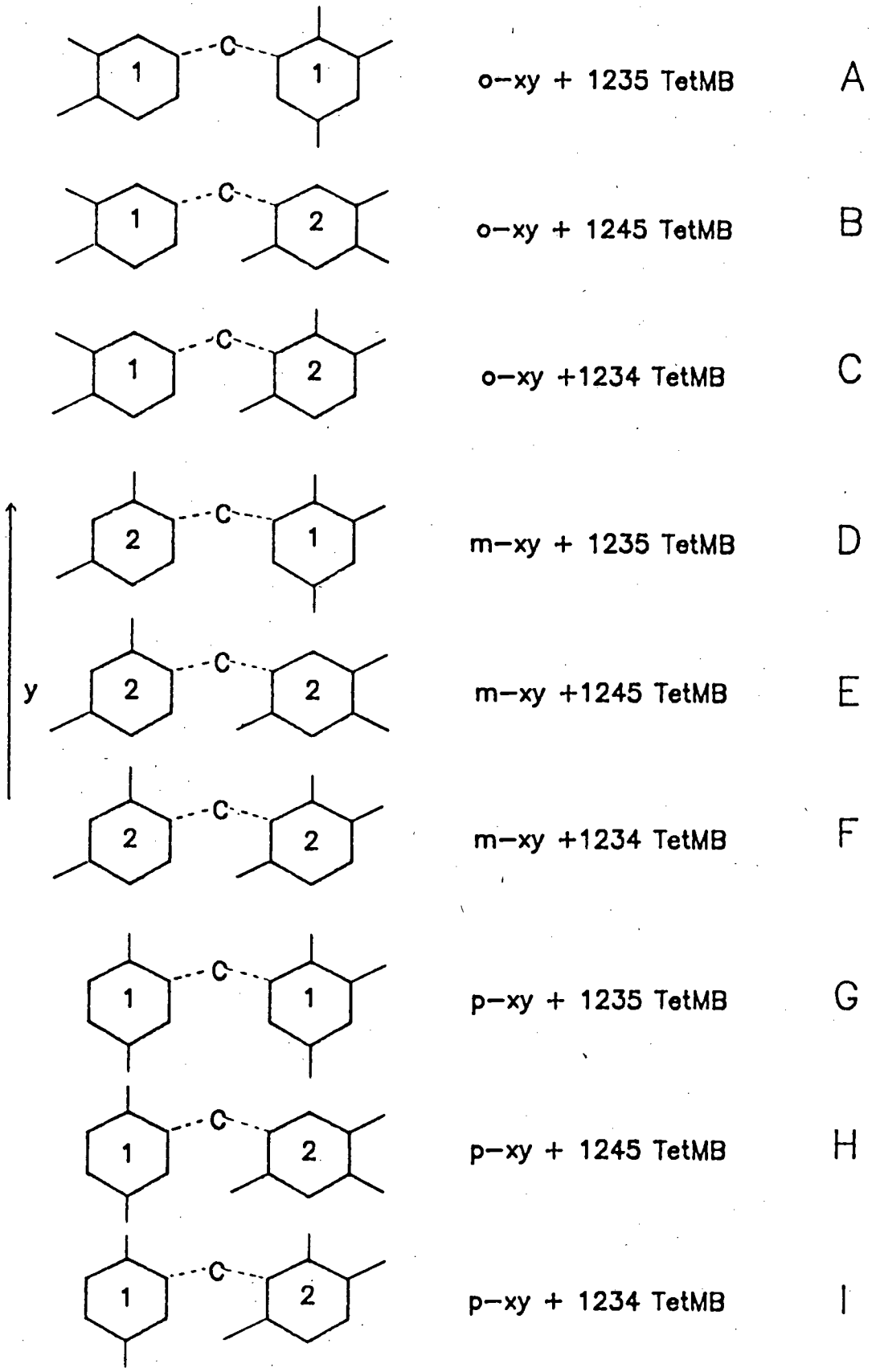

Figure 4.1. Bimolecular Intermediates formed from 124 TMB

(ii) Size of intermediates: If shape selectivity is playing a role in the unexpected xylene and TetMB selectivities, the sizes of the intermediates which give rise to the different xylene and TetMB isomers need to be considered.

(iii) "Methyl group crowding effect": On any bimolecular intermediate formed between TMB molecules, there are four sites located adjacent to the shared penta-coordinated carbon atom where methyl groups may be located (denoted by *).

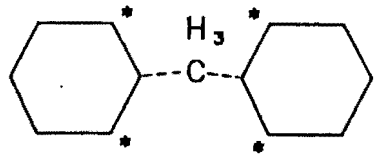

It is proposed that as the occupancy of these sites by methyl groups increases, the probabilty of an intermediate forming decreases owing to steric hindrance. This effect will be referred to as the "methyl group crowding effect".

Kikuchi et al. (1984, 1985) attributed the high o-xylene and 1245 TetMB selectivities of Al and Zr pillared montmorillonite to shape selective properties of the pillared interlayers. Their reasons for doing this were as follows: the stability of the intermediate giving rise to m-xylene and 1235 TetMB (D in Fig. 4.1) is greater than that which gives rise to o-xylene and 1235 TetMB (A). Similarly, intermediates E and F, which give rise to m-xylene, may be considered to be more stable than B and C, which give rise to o-xylene, respectively. They concluded, therefore, that formation of the transition states was not controlled by the stability of these complexes. They pointed out that intermediate B, which leads to the formation of o-xylene and 1245 TetMB, is the smallest of the intermediates and proposed that shape selectivity was responsible for the unexpected selectivities demonstrated by their catalysts. It should be noted that, in interpreting their results, these researchers did not take into account the possibility of "mixed" intermediates forming between 124 TMB and 123 or 135 TMB molecules which will be present as a result of reactant isomerisation. In addition, they did not consider the possible effects of "methyl group crowding" on the formation of intermediates.

All four pillared montmorillonite catalysts and the pillared beidellite catalyst used in this work were more selective to o-xylene and 1245 TetMB than would be expected from thermodynamic equilibrium levels. Amorphous silica alumina and SMM, which has a macroporous structure, were noticeably less selective to the 1245 isomer than the pillared montmorillonite and beidellite clays. The absence of any shape selective properties in SMM and silica alumina is indeed consistent with Kikuchi's proposal that shape selectivity is responsible for the high 1245 TetMB selectivities demonstrated by the pillared clays.

Unpillared montmorillonite, however, displayed a higher selectivity to 1245 TetMB than any of the pillared montmorillonite clays. Due to the absence of any porous structure, this catalyst should not possess any shape selective properties. This result suggests that the unexpectedly high 1245 TetMB selectivities demonstrated by the pillared clays may not be a result of shape selectivity. Similarly, beidellite and pillared beidellite showed very similar selectivities to 1245 TetMB.

The o-xylene selectivities of the silica alumina, SMM, and parent montmorillonite and beidellite catalysts were all very similar to those of the pillared montmorillonite and beidellite clays. In view of this, it seems difficult to ascribe the unexpectedly high o-xylene selectivities of the pillared clays to shape selective properties of the pillared interlayers.

If the possible shape selective properties of the microporous pillared structures of Al PILMont and Al PILBeid for the reaction of 124 TMB are considered, the following points arise. If the bimolecular intermediates present in the microporous structures orient themselves with their benzene rings in the same plane as the clay surface, which seems likely, the only source of shape selectivity would arise from the pillar density. The interpillar spacing in Al PILMont has been estimated to be around 14 A, and is probably larger in Al PILBeid due to its lower cation exchange capacity. The differences in the sizes of the proposed bimolecular reaction intermediates shown in Figure 4.1 arise primarily due to differences in the "heights" of the molecules (size of molecules, as shown in Figure 4.1, when measured in the direction of the y-axis).

The heights of all possible intermediates, however, are considerably smaller than the proposed interpillar spacing. It is unlikely, therefore, that the interpillar spacings would selectively retard the formation of any of the intermediates as a result of differences in their heights.

In view of the results of this study, it is proposed that the high 1245 TetMB selectivities demonstrated by all the catalysts tested occur primarily as a result of differences in the stabilities of the transition state complexes. A consideration of Fig. 4.1 shows that intermediates B, E and H, which give rise to 1245 TetMB, are more stable than intermediates A, D and G, respectively, which give rise to 1235 TetMB, due to a greater number of methyl groups located at positions where positive charge may become localised. The "methyl group crowding effect" does not appear to favour the formation of 1245 TetMB over 1235 TetMB. The stabilities of intermediates giving rise to 1234 and 1245 TetMB are essentially the same. There appear to be three possible reasons for the low 1234 TetMB selectivities. Firstly, the decrease in free energy accompanying the formation of 1235 or 1245 isomers is greater than that accompanying the formation of the 1234 isomer (1245 and 1235 are considerably more favoured thermodynamically). Secondly, 1234 is by far the least stable TetMB isomer. It would therefore be expected to isomerise more rapidly than the 1245 or 1235 isomers. Thirdly, the extent of "methyl group crowding" is greater on the intermediates which give rise to 1234 TetMB.

The high o-xylene selectivities demonstrated by all the catalysts can be explained in terms of the "methyl group crowding effect". Three carbonium ions can be formed as a result of protonation of 124 TMB:

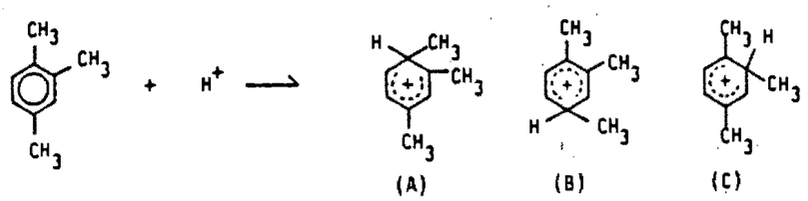

(A) (B) (C)

Carbonium ions A, B and C will give rise to m-, o- and p-xylene, respectively. Both A and C have methyl groups located adjacent to the protonated site. These methyl groups may hinder or prevent the formation bimolecular intermediates. B, which gives rise to o-xylene, is the only carbonium ion which has no methyl groups located adjacent to the

protonated site.

It is further proposed that differences in the 1245 TetMB selectivities of the catalysts tested arise as a result of two factors:

(i) Differences in the extent of reactant isomerisation;

(ii) Differences in the extent of TetMB product isomerisation.

It can be seen from Table 3.14 that catalysts with a greater selectivity towards the isomerisation reaction demonstrated lower selectivities to the 1245 TetMB isomer. (1235 TetMB selectivities increased significantly with reactant isomerisation activity, while 1234 TetMB selectivities increased slightly: see Appendix 3(a)). The following explanation is offered for this result: Bimolecular intermediates comprised exclusively of 124 TMB molecules are, collectively, able to produce all three TetMB isomers. An increase in the reactant isomerisation activity will increase the extent to which disproportionation occurs via the formation of bimolecular intermediates comprised, at least partly, of 123 and 135 TMB isomers, and in particular, intermediates formed between 124 and 123, and between 124 and 135. A consideration of the possible products which can be formed from intermediates comprised of a protonated 124 TMB molecule and a 123 or 135 TMB molecule indicates that 1245 TetMB cannot be formed. (1245 TetMB cannot be formed by adding a methyl group to 123 or 135 TMB). An increase in the extent to which such intermediates are formed would therefore be expected to reduce selectivity to 1245 TetMB. The fact that intermediates comprised of 124 TMB and protonated 123 or 135 TMB molecules will also be formed has not been overlooked. Such intermediates, which result in the addition of a methyl group to the 124 TMB molecule, can give rise to all three TetMB isomers. The complexes formed between protonated 135 and 124, however, are considerably less stable than those formed between 135 and protonated 124 and are therefore probably less likely to form. Of the six complexes formed between 124 and protonated 123 TMB, stability favours the formation of intermediates which give rise to 1245 TetMB over those which give rise to 1235 TetMB. The two least "crowded" forms give rise to 1245 and 1235 TetMB, respectively. Of these the most stable is the former. It is worth noting that none of the possible bimolecular intermediates which can be formed between two 123 TMB molecules, two 135 TMB molecules, or 123 and 135 TMB can produce 1245 TetMB.

It was noticeable that, unlike selectivity to the TetMB isomers, xylene selectivities were essentially unaffected by an increase in the extent of reactant isomerisation. Of the twelve possible bimolecular intermediates which can form between 123 and 124 TMB isomers, the most stable forms give rise to m-xylene. Similarly, of the six intermediates which can form between 135 and 124 TMB, the most stable form gives rise to m-xylene. The fact that catalysts which showed high reactant isomerisation activities did not demonstrate lower o-xylene selectivities suggests that the formation of the above intermediates is not controlled by the stabilities of these complexes. As the "heights" of the above intermediates are all the same (other than two which give rise to 1234 TetMB and o- and m-xylene, respectively), it is most unlikely that shape selectivity is playing a role here. If the "methyl group crowding effect" is considered, the following points arise: of the twelve 124-123 intermediates, the least "crowded" are those formed between a protonated 124 TMB and a 123 TMB molecule which give rise to o-xylene and 1234 or 1235 TetMB. Of the six 124-135 intermediates, the only complex which gives rise to o-xylene is the third least "crowded" intermediate (this intermediate forms 1235 TetMB). The two least "crowded" intermediates, which give rise to m-xylene and 1235 and 1234 TetMB, respectively, are, however, considerably less stable. The "crowding effect", and a combination of intermediate stability and the "crowding effect" may therefore be used to explain the high o-xylene concentrations resulting from intermediates formed between 124 and 123, and 124 and 135 TMB isomers, respectively.

Table 3.14 shows that catalysts with high initial activities demonstrated low 1245 TetMB selectivities. It is possible that TetMB products show a greater tendency to isomerise over the more active catalysts and that this is contributing to the observed differences in TetMB selectivities. This postulate seems to be supported by the fact that 1245 TetMB selectivity increased with decreasing conversion levels accompanying catalyst deactivation in all cases.

In general, over the catalysts tested for this reaction (WHSV = 2.4/hr) it was found that higher initial conversion levels led to increased selectivity to the reactant isomerisation reaction. However, reactant isomerisation activity did not appear to decrease as conversion levels

fell with time on stream. In addition, decreases in the initial activities of SMM and Al PILMont, achieved by increasing the WHSV, resulted in relatively small decreases in the extent of reactant isomerisation activity (decreasing initial conversion levels of SMM from 24% to 13 % and that of Al PILMont from 18% to 11% decreased selectivity to the reactant isomerisation reaction from 24% to 22%, and from 13% to 10%, respectively). It seems unlikely, therefore, that conversion levels themselves are primarily responsible for the differences in reactant isomerisation activities among the catalysts tested.

Isomerisation and disproportionation are common reactions of alkylaromatic hydrocarbons over acid catalysts and are generally competitive. Haag and Olson (1974) have reported that transalkylation of xylene and ethylbenzene over ZSM-5 is prohibited by the pore volume of this catalyst, because transalkylation of these hydrocarbons requires a large space. A similar explanation for xylene isomerisation over ZSM-5 has been given by Collins and Medina (1982). Pillaring of montmorillonite, which has essentially no pore structure, generates a microporous catalyst. Accompanying the pillaring process is an increase in selectivity towards the isomerisation reaction. This could suggest the introduction of a shape selective effect. However, Kikuchi et al. (1985) found that Al PILMont catalysts with decreasing interlayer spacings and hence more constricted channels showed increasing selectivity to the disproportionation reaction. The generation of a microporous structure arising from the pillaring of beidellite resulted in no change in selectivity towards the isomerisation reaction. These results indicate that the microporous structures generated by pillaring do not themselves affect the selectivities of these clays to the isomerisation reaction. The fact that unpillared montmorillonite and silica alumina, neither of which has a porous structure, demonstrate very different selectivities to the isomerisation reaction (average of 6 and 36%, respectively) also suggests that differences in selectivity to this reaction are not a result of differences in the shape selective properties of these catalysts.

It is possible that differences in the acidic properties of these catalysts account for the differences in selectivity to the

isomerisation reaction. It has been suggested that isomerisation and disproportionation occur on different acidic sites. Csicsery and Hickson (1970) and Gnep et al. (1983) suggested that isomerisation required only Bronsted acid sites, whereas disproportionation occurred on Lewis acid sites or Bronsted Lewis acid site pairs. Nayak et al. (1982), on the other hand, have proposed that only Bronsted acid sites are able to catalyse disproportionation.

Kikuchi et al. (1984) found that in the reaction of 124 TMB over Al PILMont calcined at 400°C, selectivity to the isomerisation reaction increased from 8% at 200°C to 25% at 400°C. Ming-Yuàn et al. (1988), on the other hand, found that selectivity to the isomerisation reaction decreased with increasing reaction temperature if Al PILMont was pretreated at 120°C. Occelli et al. (1983) reported that Al PILMont contained both Lewis and Bronsted acid sites according to the IR spectra of adsorbed pyridine. The Lewis/Bronsted site ratio increased with increasing temperature. In the experiment reported by Kikuchi et al., the ratio of Lewis to Bronsted acid sites on the Al PILMont sample calcined at 400°C would not be expected to change significantly with increasing reaction temperature up to 400°C. In the case of the Al PILMont sample pretreated at 120°C, the Lewis/Bronsted site ratio would increase with increasing reaction temperature. The different effect that reaction temperature had on the reaction selectivity of Al PILMont in these two experiments suggests that isomerisation and disproportionation of 124 TMB over this catalyst take place on different acid sites. The decrease in selectivity to the isomerisation reaction accompanying the decrease in Bronsted acidity, observed by Ming-Yuan et al., suggests that the isomerisation reaction is catalysed by Bronsted acid sites.

It is conceivable that the changes in acidity accompanying pillaring of montmorillonite could account for the increase in selectivity to the isomerisation reaction. If this is the case, the increase would have to be attributed to the acidic properties of the pillars, since the nature and density of the acid sites present on the clay layers of NH_4^+ montmorillonite and Al PILMont should be the same (protons liberated upon deammoniation should be equally effective in promoting lattice dehydroxylation as protons liberated during dehydroxylation of the pillaring species). It is not clear from the results of this study,

however, whether the contribution of the pillars to the acidity of these clays is significant.

Similarly, any changes in reactant isomerisation activity of the tetrahedrally substituted clays as a result of pillaring could be attributed to changes in acidic property.

Differences in acid site density, and the possible effect of the presence of nickel in the octahedral positions, on acidic properties, could be contributing to the differences in selectivity to the isomerisation reaction observed in the SMM, Ni-SMM, and beidellite clays.

There is one other factor which perhaps needs to be mentioned in this discussion of what could be responsible for the apparent differences in the isomerisation activity of these catalysts. Kikuchi et al. (1984) showed that the disproportionation of 124 TMB over Al PILMont at 200°C followed second order kinetics, while the isomerisation reaction followed first order kinetics. Differences in the catalyst structures could conceivably affect the concentration of reactant molecules around acid sites, thereby altering reaction selectivity. If this effect were a dominant one, the generation of a microporous structure resulting from the pillaring of the layered clays, montmorillonite and beidellite, should have resulted in similar shifts in reaction selectivities. This was not the case. Pillaring of montmorillonite resulted in an increase in isomerisation activity, while pillaring of beidellite resulted in no apparent change. However, differences in the layer morphologies of the clays used for this work could be contributing to differences in isomerisation activities in this way.

Lanthanum Exchange on H ZSM-5

When a sample of NH_4^+ ZSM-5 is contacted with an aqueous solution of lanthanum chloride under reflux at 80°C for 24 hours, only 5% of the ammonium ions are exchanged with La, assuming a stoichiometric exchange of one La for three ammonium ions. The reason for this very low degree of exchange is probably due to the relative sizes of the ZSM-5 pores and of the exchanging species. An aqueous $LaCl_3$ solution probably contains the following La complexes: $[LaCl_x.(H_2O)_{6-x}]^{(3-x)+}$ where x = 0,1,2,3. Assuming a hard sphere model and typical ionic radii, (d_{La} = 1.04 A , d_{Cl} = 3.6 A and d_{H2O} = 2.8 A (Bloss, 1971)), ionic lanthanum species with x = 1 or 2 have diameters of approximately 7.4 A. The hexa-aquo ion, $La(H_2O)_6^{3+}$, formed when x = 0, would be the smallest of the ionic lanthanum species (d approx. = 6.6 A). On the basis of its smaller size, it is suggested that the hexa-aquo ion constitutes the main exchange species. Work by Shannon et al. (1984) would seem to support this postulate. They found that exchange of the trivalent Rh ion onto various zeolites was achieved by contacting the catalysts with an aqueous $RhCl_3$ solution. Subsequent XPS analyses of the catalysts indicated Cl/Rh ratios not appreciably greater than 0.1. This suggested that very few of the exchanging ionic complexes in the $RhCl_3$ (aq) solutions contained Cl atoms.

The concept of the hexa-aquo ions constituting the main ion exchange species, however, still presents problems. ZSM-5 crystallographic pore sizes are 5.4 x 5.6 A and 5.1 x 5.5 A (Olson et al., 1980). Although it is known that effective pore sizes are somewhat larger than this (Wu et al., 1986), it is probable that in order to achieve a high degree of exchange within the pores of the catalyst, the size of the exchanging ion (approx. 6.6 A) must be reduced. This can occur only if water molecules are stripped from the ion during the exchange process. The 5% exchange achieved after 24 hours at 80°C suggests that this stripping process does not occur to any appreciable extent at that temperature. Subjecting the unwashed catalyst to a temperature of 500°C would drive off at least some of the water molecules from the lanthanum ions located on the catalyst outer surface. In addition, the higher temperature would increase the thermal vibrations of the atoms defining the pore openings of the catalyst, as well as the kinetic energy of the exchanging

cations. This would enable these ions to enter into the catalyst pores more easily and effect an exchange. Further contacting of the catalyst with a $LaCl_3$ (aq) solution would then lead to partial rehydration of the exchanged La ions, effectively locking them into the zeolite pores. The degree of exchange may be increased by repeating this process.

A linear molecule such as n-hexane is able to fill the entire ZSM-5 pore volume by achieving an end-to-end configuration. For this reason, adsorption of such a molecule may be used to monitor changes in the free pore volume of modified ZSM-5 catalysts (Gabelica et al., 1984).

The mass gain due to hexane adsorption was virtually identical on all the Na and La exchanged ZSM-5 catalysts. This indicates that neither the La nor the Na has appreciably altered the effective free pore volume of the catalyst available to linear molecules. Perhaps more important is the fact that the rates of adsorption were virtually identical for all the samples. This suggests that, as is the case with sodium ions (Anderson et al., 1979), the presence of La ions or ionic complexes on the 5% and 25% La catalysts do not introduce any additional steric hindrances for the adsorption of linear molecules.

The results of ammonia TPD experiments indicated that increasing the La or Na content of H ZSM-5 caused a decrease in the number of strong acid sites present. This is due to the fact that during the ion exchange process the ammonium ions, which give rise to strong Bronsted and Lewis acid sites on the catalyst during calcination, are replaced by Na and La ions. The presence of both metals also gives rise to a slight increase in the number of weak acid sites. Sodium cations act as weak Lewis acid sites when present on ZSM-5 (Topsoe et al., 1981). The very similar shifts in acidity resulting from the La and Na exchanges suggest that La ions also function as weak acid sites on the catalyst.

The results of the hexane adsorption experiments demonstrated that sodium and lanthanum ions present on the H ZSM-5 do not restrict the diffusion of molecules such as propene and hexane through the pores of the catalyst. For this reason, any changes in the activity and selectivity of H ZSM-5 in the propene oligomerisation and hexane cracking reactions due to the presence of lanthanum (or sodium) must

almost certainly be attributed to changes in acidity.

Increasing the Na and La content of H ZSM-5 led to significant decreases in the conversion levels attained by the catalyst during the propene oligomerisation reaction. This is ascribed to the decrease in the number of strong acid sites resulting from the exchange of sodium and lanthanum ions with ammonia. The rate of deactivation of 25% Na ZSM-5 was noticeably lower than that of 5% Na ZSM-5. This is also attributed to the reduced number of strong acid sites, which are known to play a significant role in coke formation.

Unlike the Na exchanged samples, the rate at which H ZSM-5 deactivated appeared to increase with increasing La content, suggesting that the presence of lanthanum may affect the mechanism of coke formation on the catalyst.

The results of off-gas analyses from the four catalysts did not indicate that the La exchanged samples produced a greater quantity of light hydrocarbon gases. This suggests thet the presence of lanthanum does not promote cracking of the oligomerised products or coke precursors. The very similar selectivities of the 25% Na and 25% La ZSM-5 samples towards the C_{12}^{+} liquid product fraction also indicated that the lanthanum ions do not increase the extent to which oligomerised products are cracked during this reaction.

Borade et al. (1984) found that the hexane cracking activity of ZSM-5 catalysts is strongly dependent on the number of strong acid sites present. The results of this study are consistent with this finding. Increasing the La and Na content of H ZSM-5 had similar effects on the hexane cracking activity of the catalyst. In both cases, conversion levels decreased noticeably at reaction temperatures of 400°C and 500°C. As all the catalysts showed comparable levels of deactivation after three hours on stream, the results suggest that lanthanum ions do not lower the extent of coke formation on H ZSM-5 any more than sodium ions.

5 CONCLUSIONS

The following conclusions were drawn from the results of this study:

Pillared Clays

Treating montmorillonite with a hydroxy-Al solution results in the generation of an expanded-layer structure which significantly increases the surface area, pore volume and the number of accessible acid sites on the clay.

The addition of tetraethyl orthosilicate to the hydroxy-Al solution prior to pillaring did not increase the acidity of pillared montmorillonite noticeably.

No conclusion is drawn from the results of this study as to whether the incorporation of nickel into the Al_{13}^{+} pillaring species, which reduces the charge on this cation, increases the pillar density in pillared montmorillonite. Although the pore volume of the Ni/Al PILMont clay appeared to be noticeably lower than that of Al PILMont, the acidity and surface area of the two clays were very similar.

Treating beidellite with a hydroxy-Al solution resulted in the generation of a less extensive pillared structure in the clay than in montmorillonite, as indicated by the results of surface area and pore volume measurements. This is unexpected as both clays are essentially 100% swellable. Differences in clay particle size, and possible differences in the pillar solution preparation procedure used, may have contributed to this result.

Contacting SMM with the Al pillaring solution generated an expanded-layer structure in the swellable phase of the clay. The surface area, pore volume and the number of accessible acid sites increased significantly on pillaring.

No well defined 001 basal peaks were present in the XRD spectra of the Ni-SMM samples treated with the Al solution. It is proposed that contact with the pillaring solution induces layer delamination in these clays,

and generates an expanded-layer structure to a more limited extent than is the case in SMM. The observed increases in the pore volume and the number of accessible acid sites on treatment with the pillaring solution are attributed primarily to the delamination process proposed to be taking place. The measured surface areas of the Ni-SMM clays, however, did not appear to change as a result of pillaring. It is not clear how the observed increases in pore volume and the number of accessible acid sites may be accompanied by essentially no change in surface area.

Unpillared montmorillonite and beidellite show very limited activity for propene oligomerisation. Pillaring results in significant increases in the activities of both clays. The propene oligomerisation activities of pillared montmorillonite and pillared beidellite are very similar. Catalyst deactivation occurs rapidly and is ascribed to hydrocarbon occlusion and subsequent coke formation in the microporous pillared structures.

Treating the SMM and Ni-SMM clays with the hydroxy-Al solution results in noticeable increases in propene oligomerisation activity. It is proposed that these increases do not arise solely due to the generation of microporous pillared structures in these clays, but may be a result of changes in layer morphology, such as layer delamination, induced by contact with the pillaring solution.

The propene oligomerisation product selectivities of the SMM and Ni-SMM clays, in terms of carbon number distribution, do not change after contact with the pillaring solution.

The microporous structures present in Al pillared clays are less effective in catalysing the oligomerisation of propene than exposed layer edges and faces in H^+ exchanged smectite minerals.

It seems unlikely that the unexpectedly high concentrations of 1245 tetramethylbenzene and o-xylene formed during the reaction of 124 trimethylbenzene over pillared montmorillonite catalysts are a result of shape selective properties of the pillared clays, as proposed by Kikuchi et al. (1984, 1985). A comparison of the product selectivities of the pillared and unpillared montmorilonite, beidellite, SMM and Ni-SMM

catalysts during this reaction suggests that differences in the selectivities of these catalysts to the 1245 TetMB isomer occur primarily as a result of differences in the extent to which reactant and tetramethylbenzene isomerisation takes place. The unexpectedly high selectivity to the 1245 isomer, observed in all cases, may be a result of the fact that the stabilities of the bimolecular intermediates leading to the formation of this isomer are greater than those leading to the formation of the 1235 isomer. The high o-xylene selectivities demonstrated by all the catalysts may be explained by considering the "crowding effect" of methyl groups located adjacent to the shared penta-coordinated carbon atom in the bimolecular intermediates.

Lanthanum Exchange on H ZSM-5

The large hydration energies of the La^{3+} ion makes the exchange of lanthanum ions with the acidic protons of ZSM-5 far more difficult than the exchange of monovalent sodium ions.

Hexane adsorption experiments showed that, as with sodium exchange, lanthanum exchange does not decrease the effective free pore volume of the catalyst, nor does it increase steric hindrances for the passage of linear molecules.

Ammonia TPD showed that the presence of lanthanum ions leads to a decrease in the number of strong acid sites on the catalyst. This decrease is accompanied by an increase in the number of weak acid sites, suggesting that these ions function as weak acid sites when present on ZSM-5. Sodium exchange was shown to affect acidity in a similar way.

The propene oligomerisation and hexane cracking activity of H ZSM-5 decreased with increasing degree of lanthanum exchange. This is due to the decrease in strong acidity resulting from the exchange. In the former reaction, the presence of lanthanum ions reduced the selectivity towards heavier products. Similar trends were observed for sodium exchanged catalysts. The rate of catalyst deactivation during propene oligomerisation was not reduced by the presence of lanthanum.

6 REFERENCES

Akitt, J.W. and Farthing, A.J., Magn. Resonance., 1978, 32, 345.

Akitt, J.W. and Farthing, A.J., J. Chem. Soc., Dalton Trans., 1981, 1617.

Anderson, J.R., Foger, K., Mole, T., Rajadhyaksha, R.A. and Sanders, J.V., J. Catal., 1979, 58, 114.

Argauer, R.J. and Landolt, G.R., US Pat. 3,702,886, 1972.

Bailey, S.W., in Crystal Structures of Clay Minerals and their X-Ray Identification, (eds. G.W. Brindley and G. Brown), Mineral Soc., London, 1980.

Barrer, R.M., Zeolites and Clay Minerals as Sorbents and Molecular Sieves, Academic Press, New York, 1978.

Bartley, G.J. and Burch, R.R., Appl. Catal., 1986, 28, 209.

Bercick, P.G., Metzger, K.J. and Swift, H.E., Ind. Eng. Chem. Prod. Res. Dev., 1978, 17 (3), 214.

Bertsch, P.M., Thomas, G.W. and Barnhisel, R.I., Soil Sci. Soc. Amer. J., 1986, 50, 825.

Beson, G., Mifsud, A., Tchoubar, C. and Mering, J., Clays and Clay Minerals, 1974, 22, 379.

Black, E., Montagna, A. and Swift, H., US Pat. 3,966,642, 1976.

Bloss, F.D., "Crystallography and Crystal Chemistry", Holt, Rinehart and Winston, 1971.

Borade, R.B., Hedge, S.B., Kulkarni, S.B. and Ratnasamy, P., Appl. Catal., 1984, 13, 27.

Bottero, J.Y., Cases, J.M., Fiessinger, F. and Poirer, J.E., J. Phys. Chem., 1980, 84, 2933.

Brindley, G. and Sempels, R., Clay Minerals, 1977, 12, 229.

Brown, G., "The X-Ray Identification and Crystal Structure of Clay Minerals", Mineralogical Society, London, 1961.

Brunauer, S., Deming, L.S., Deming, W.E. and Teller, E., J. Amer. Chem. Soc., 1940, 62, 1723.

Buckley, R.G. and Tallon, J.L., Chemistry in New Zealand, 1986, Feb., 11.

Burch, R.R, and Warburton, C.I., J. Catal., 1986, 97, 511.

Capell, R.G. and Granquist, W., US Pat. 3,252,889, 1966.

Carrado, K.A., Suib, S.L., Skoularikis, N.D. and Coughlan, R.W., Inorg. Chem., 1986, 25, 4217.

Chang, C.D. and Silvestri, A.J., J. Catal., 1977, 47, 249.

Chang, C.D., Chu, C. and Socha, R.F., J. Catal., 1984, 86, 289.

Chen, N.Y. and Lucki, S.J., Appl. Catal., 1988, 42, 169.

Chiang, R.L. and Staniulis, M.T., PCT B01-J, 29/06, C10G, 11/05, 1986.

Clearfield, A. and Vaughn, P.A., Acta. Cryst., 1956, 9, 555.

Coleman, N.J. and Mc Auliffe, C., Clays and Clay Minerals, 1954, 3rd Natl. Conf., 282.

Collins, D. and Medina, R., Cana. J. Chem. Eng., 1982, 61, 29.

Csicsery, S. and Hickson, D., J. Catal., 1970, 19, 386.

Davitz, J., J. Catal., 1976, 43, 260.

Diddams, P., private communication, 1989.

Dietz, W. A., Journal of Gas Chromatography, 1967, Feb, 68.

Derouane, E.G., Nagy, B., Dejaifve, P., van Hoof, J.H.C., Spekman, B.P., Vedrine, J.C. and Naccache, C., J. Catal., 1978, 53, 40.

Dhar, G.M., Vittal, N. and Babu, T.G.N., Proc. 7th Int. Zeolite Conf., Aug, 1986, 17.

Feitknecht, W. and Berger, A., Helv. Chim. Acta., 1942, 25, 1543.

Flanigen, E.M., Proc. 5th Int. Conf. on Zeolites, (ed. L.V. Rees), Heyden, London, 1980.

Fletcher, J.C.Q., Kojima, M. and O'Connor, C.T., Appl. Catal., 1986, 28, 169.

Flory, P.J., "Priciples of Polymer Chemistry", Cornell University Press, 1964, 222.

Gaaf, J., van Santen, R., European Patent No. 0 090 442, 1983.

Gaaf, J., van Santen, R., Knoester, A. and van Wingerden, B., J. Chem. Soc., Chem. Commun., 1983, 655.

Gabelica, Z., Nagy, B., Derouane, E.G. and Gilson, J.P., Clay Minerals, 1984, 19, 803.

Garwood, W.E., Stucky, G.D. and Dwyer, F.D., ACS Symposium Series 218; American Chemical Soc.: Washington D.C., 1983, 383.

Garwood, W.E., Caesar, P.D. and Brennan, J.A., US Pat. 4,150,062, 1972.

Garwood, W.E. and Lee, W, US Pat. 4,227,992, 1980.

Gary, J.H., Handwerk, G.E., Petroleum Refining: Technology and Economics, (eds. L.F. Albright, R.N. Maddox and J.J. McKetta), Marcel Dekker, Inc., New york, 1975.

Germain, J.E., "Catalytic Conversion of Hydrocarbons", Chapter 4, Academic Press, London, 1969.

Gnep, N., de Aromand, M. and Guisnet, M., Spillover of Adsorbed Species, 1983.

Granquist, W., US Pat. 3,252,757, 1966.

Granquist, W and Pollack, S., The American Mineralogist, 1967, 52, 212.

Granquist, W., Hoffman, G.W. and Boteler, R.C., Clays and Clay Minerals, 1972, 20, 233.

Granquist, W.J., US Pat. 3,976,744, 1976.

Grim, R.E., "Clay Mineralogy", 2nd ed., McGraw Hill, 1968, 194.

Haag, W. and Olson, D., US Pat. 3,856,871, 1974.

Hall, P.L., Clay Mineral, 1985, 15, 321.

Hassen, S.W., Panchenkov, G.M. and Kuznetsov, O.I., Bull. Chem. Soc. Japan, 1977, 50, 2597.

Hattori, S.W., Milliron, D.L. and Hightower, J.W., Preprints Div. Pet. Chem., 1973, 18, No. 1.

Heinermann, J.J., Freriks, J.L., Gaaf, J., Pott, G.T. and Coolegem, J.G., J. Catal., 1983, 80, 145.

Hem, J.D. and Robertson, C.E., US Geol. Surv. Water Supply Pap. 1827-A, 1967, 55.

Herrera, R. and Peech, M., Soil Sci. Soc. Amer. Proc., 1970, 34, 740.

Hill, S.G., Arbuckle, R. and Seddon, D., Zeolites, 1987, 7, 438.

Hongdu, H., Master Thesis, Research Institute of Petroleum Processing, Beijing, China, 1983.

Hsu, P.H. and Bates, J.F., Soil Science, 1964, 28, 763.

Hughes, J.R. and White, H.M., J. Phys. Chem., 1967, 71, 2192.

Huisheng, L. and Ying, W., Internal report of Research Inst. of Petrol. Processing, Beijing, China, 1985.

Iiyama, J.T. and Roy, R., Clays and Clay Minerals, Proc. Nat. Conf., 1963, 10, 4.

Imai, H., Hasegawa, T. and Uchida, H., Bull. Chem. Soc. Japan, 1968, 41, 45.

Johansson, G., Acta. Chem. Scand., 1960, 14, 771.

Jones, W., Catalysis Today, 1988, 2, 357.

Kaeding, W., Chu, C., Young, L. and Butter, S., J. Catal., 1981, 69, 392.

Kikuchi, E., Hamana, R., Nakano, M., Takehara, M. and Morita, Y., J. Japan Petrol. Inst., 1983, 26, 116.

Kikuchi, E., Matsuda, T., Fujiki, H. and Morita, Y., Appl. Catal., 1984, 11, 331.

Kikuchi, E., Matsuda, T., Ueda, J. and Morita, Y., Appl. Catal., 1985, 16, 401.

Kikuchi, E., Matsuda, T., Rep. Asahi. Glass Found. Ind. Techol., 1985, 46, 11.

Kikuchi, E., Matsuda, T., Catalysis Today, 1988, 2, 297.

Kiyozumi, Y., Suzuki, K., Shin, S., Owaga, K., Saito, K. and Yamanaka, S., Jpn. Kokai Tokyo Koho, 59-216631, 1984.

Kojima, M., Fletcher, J.C.Q. and O'Connor, C.T., Appl. Catal., 1986, 28, 169.

Lahav, N., Shani, U. and Shabtai, J., Clays and Clay Minerals, 1978, 26, 107.

Lindsley, J.F., US Pat. 4,340,465, 1982.

Lussier, R.J., Magee, J.S. and Vaughan, D.E., Proc. 7th Canad. Symp. Catal., eds. S.E. Wanke and S.K. Chakrabarty, Chem. Inst. Canad., 1980, 80.

Matsumoto, M., Bull. Chem. Soc. Japan, 1984, 57, 1795.

Miller, S.J. and Bishop, K.C., US pat. 4,340,465, 1986.

Ming-Yuan, H., Zhonghui, L., Enze, M., Catalysis Today, 1988, 2, 321.

Mortland, M.M., Trans. 9th Int. Congr. Soil Sci., 1968, 1, 691.

Mortland, M.M. and Berkheiser, V., Clays and Clay Minerals, 1976, 24, 60.

Mott, C., Catalysis Today, 1988, 2, 199.

Nayak, U., Choudhary, U., Appl. Catal., 1982, 33.

Noll, W., Chem. Erde., 1930, 10, 129.

Oblad, A.G., Mills, G.A. and Heinemann, in P.H. Emmet, Catalysis, 6, Chapter 4, 1958, Reinholdt Publishing Corp., Baltimore.

Occelli, M.L. and Tindwa, R.M., Clays and Clay Minerals, 1983, 31, 22.

Occelli, M. and Tindwa, R., Clays and Clay Minerals, 1983, Vol 31 No. 1, 22.

Occelli, M., Ind. Eng. Chem. Prod. Res. Dev., 1983, 22, 553.

Occelli, M., Parulekar, V. and Hightower, J., 8th Int. Cong. Catal., 1984, 4, 725.

Occelli, M., Hsu, J. and Galya, L., J. Molec. Catal., 1985, 33, 371.

Occelli, M., Innes, R.A., Hure, F.S.S. and Hightower, J.W., J. Appl. Catal., 1985, 14, 69.

Occelli, M. and Innes, R.A., Appl. Catal., 1985, 14, 69.

Occelli, M., and Lester, J.E., Ind. Eng. Chem. Prod. Res. Dev., 1985, 24, 27.

Occelli, M., Proc. 8th Int. Clay Conf., Denver, 1985.

Occelli, M. and Finseth, D.H., J. Catal., 1986, 99, 316.

O'Connor, C.T., Jacobs, L.L. and Kojima, M., Appl. Catal., 1988, 40, 277.

Olson, D.H., Haag, W.O. and Lago, R.M., J. Catal., 1980, 61, 390.

Owen, H., Marsh, S.K. and Wright, S.B., US Pat. 4,456,779, 1984.

Pinnavia, T.J., Tsou, M.S., Landau, S.D. and Raythatha, R.H., J. Molec. Catal., 1984, 27, 195.

Pinnavia, T.J., Tzou, M.S. and Landau, S.D., J. Amer. Chem. Soc., 1985, 107, 2783.

Plee, D., Borg, F., Gatineau, L. and Fripiat, J., J. Amer. Chem. Soc., 1985, 107, 2362.

Plee, D., Schutz, A., Poncelet, G. and Fripiat, J., in Catalysis by Acids and Bases, Studies in Surface Science and Catalysis, vol. 20, Elsevier, Amsterdam, 1985, 343.

Plee, D., Gatineau, L. and Fripiat, J., Clays and Clay Minerals, 1987, Vol. 35 No. 2, 81.

Robschlager, K.H.W., Emeis, C.A. and van Santen, R.A., J. Catal., 1984, 86, 1.

Ryland, L.B., Tamele, M.W., Wilson, J.N., in Catalysis (ed. P.H. Emmet), Reinhold Publ. Co., New York, 1960.

Schmerling, L., and Impatieff, V., Advances in Catalysis, 1950, 2, 21.

Scott, A. and Reed, M., Clays and Clay Minerals, Proceedings of 13th Conference, 1966, 247.

Schutz, A., Plee, D., Borg, F., Jacobs, P., Poncelet, G. and Fripiat, J., Proc. Int. Clay Conf., Denver, 1985, Eds. Schultz, L., Van Olpen, H., and Mumpton, F.A., The Clay Minerals Society, 1987, 1, 305.

Shabtai, J., Frydmand, N. and Lazar, R., Proc. 6th Int. Congr. Catal. B5, 1, 1976.

Shabtai, J., Lazar, R., Oblad, A.G., Proc. 6th Int. Congr., Tokyo, 1980, 828.

Shabtai, J., US Pat. 4,238,364, 1980.

Shabtai, J. and Lahav, N., US Pat. 4,216,188, 1980.

Shabtai, J., Massoth, F., Tokarz, M., Tsai, M. and McCauley, J., 8th Int. Conf. Cat., 1984, iv, 735.

Shabtai, J. and Fijal, J., US Pat. 4,579,832, 1986.

Shabtai, J. and Sterte, J., "Cross Linked Smectites. V. Synthesis and Properties of Hydroxy-Silicoaluminium Montmorillonites and Fluorhectorites", Dept. of Fuels Engineering, University of Utah, Salt Lake City: submitted for publication, Clays and Clay Minerals, 1988.

Solomon, D.H., Clay and Clay Minerals, 1968, 16, 31-39.

Sterte, J., Catalysis Today, 1988, 2, 219.

Sun Guida, Masters Thesis, Research Institute of Petroleum Processing, Beijing, China, 1982.

Swartzen-Allen, S.L. and Matijevic, E., Chemical Reviews, 1974, 74, 385.

Swift, H.E. and Black, E.R., Ind. and Eng. Chem. Prod. Res. and Develop., 1974, 13 (2), 106.

Tabak, S.A., Thailand - US Natural Gas Utilisation Symposium, Feb., 1984, Bankok, Thailand.

Tabak, S.A., Krambek, F.J. and Garwood, W.E., AIChE J., 1986, 32, 1526.

Tennakoon, B., Tilak, D., Jones, W. and Thomas, J., J. Chem. Soc., Faraday Trans. 1, 1986, 86, 3081.

Tennakoon, D., Jones, W. and Thomas, J., Solid State Ionics, 1987, 24, 205.

Thomas, C.L. and Barmby, D.C., J. Catal., 1968, 12, 341.

Tokarz, M. and Shabtai, J., Clays and Clay Minerals, 1985, 33, 89.

Topsoe, N., Pedersen, K. and Derouane, E.G., J. Catal., 1981, 70.

Tsai, G., MSc Thesis, University of Utah, Salt Lake City, 1983.

Tzou, M.S. and Pinnavia, T.J., Catalysis Today, 1988, 2, 243.

Urabe, K., Sakurai, H. and Izumi, Y., J. Chem. Soc. Chem. Commun., 1986, 1074.

Uytterhoven, J.B., Christner, L.G. and Hall, W.K., J. Phys. Chem., 1965, 69, 2113.

van Santen, R., Robschlager, K-H. and Emeis, C., ACS Proceedings, Role of Solid State Chemistry in Catalysis, 1984.

Vaughan, D.E., Lussier, R.J. and Magee, J.S., US Pat. 4,176,090, 1979.

Vaughan, D.E. and Lussier, R.J., Proc. 5th Int. Conf. Zeolites, 1980, 94.

Vaughan, D.E., US Pat 4,666,877, 1987.

Voge, H.H., in P.H. Emmet (ed.) (1958), Catalysis 6, Chapter 5, Reinhold Publishing Corporation, Waverly Press, Baltimore.

Ward, S., Zeolite Chemistry and Catalysis, 1976, J.A. Rabo, ed., Amer. Chem. Soc., Washington, D.C., 118.

Whitmore, F.C., Ind. Eng. Chem., 1934, 26, 94.

Wright, A., Granquist, W. and Kennedy, J., J. Catal., 1972, 25, 65.

Wu, E.L., Landolt, G.R. and Chester, A.W., in "New Developments in Zeolite Science and Technology", Murakami, Y, Lijima, A., Ward, J.W., Elsevier, 1986, 547.

Yamanaka, S. and Brindley, G., Clays and Clay Minerals, 1979, Vol. 27 No. 2, 119.

Yamanaka, S., Doi, T., Sako, S. and Hattori, M., Mat. Res. Bull., 1984, 19, 161.

Yuehua, L, internal report of Research Institute of Petroleum Processing, Beijing, China, 1985.

Yuying, L., internal report of Research Inst of Petr. Processing, Beijing, China, 1986.

Zhinqun, W., Dissertation for Doctor of Technology, Research Inst. of Petr. Processing, Beijing, China.

Zhinqun, W., Huisheng, L., Yue, Z. and Fengren, L., "On Thermal Stabilty of Pillared Montmorillonite", paper presented at the 3rd National Catalysis Conference of China, 1986, Shanghai, China.

Zhinqun, W., Enze, M. and Qin, X., Acta. Petrolei Sinica (Petroleum Proc. Section), 1987, 3, 72.

APPENDICES

APPENDIX 1

Appendix 1(a)

Response factors for hydrocarbon compounds present in the exit gases from propene oligomerisation runs:

Compound	Response Factor
methane	1.058
ethane	1.024
propane	1.000
propene	0.971
i-butane	0.889
n-butane	1.028
n-butene	1.056
i-butene	1.002
t-2-butene	0.994
c-2-butene	1.029
pentane	1.000
n-pentane	1.000

Appendix 1(b)

Gas Chromatograph Settings

Gawmac Series 750P GC (fitted with a 3 m x 6 mm stainless steel column packed with n-octane/Poracil C).

Detector : Flame ionisation
N_2 flowrate : 41.2 ml/min
H_2 flowrate : 30.8 ml/min
Air flowrate : 297 ml/min
Injector temp. : 150°C
Detector temp. : 250°C

Column temp. : Isothermal at 50°C for
program : 20 minutes.
Column pressure : 28 psi
Sample volume : 10 ul

Varian 3400 GC (fitted with a 3 m x 1/8" column packed with OV-101 supported on Chromosorb WHP-SP).

Detector : Flame ionisation
N_2 flowrate : 7.3 ml/min
H_2 flowrate : 30 ml/min
Air flowrate : 300 ml/min
Injector temp. : 250°C
Detector temp. : 310°C
Column temp. : 40°C (5 min); 40 - 180°C at 10°C/min; 180 - 300°C
program : at 20°C/min; 300°C (5 min).
Column pressure : 17 psi
Sample volume : 4 ul

HP 5890 A GC (fitted with a Sepulcowax 10 fused silica capillary column, 30 m x 0.2 mm).

Detector : Flame ionisation
N_2 make-up flowrate : 29.1 ml/min
N_2 column flowrate : 0.9 ml/min
H_2 flowrate : 30 ml/min
Air flowrate : 550 ml/min
Column head pressure : 24 psi
Split vent flowrate : 135 ml/min
Split ratio : 150
Injector temp. : 200°C
Detector temp. : 250°C
Column temp. : 80°C (1 min); 80 - 140°C at
program : 5°C/min
Sample volume : 0.2 ul

APPENDIX 2

Appendix 2(a)

N_2 Sorption Results

N_2 Uptake versus Relative Pressure for Clay Samples:

(u) denotes uncalcined samples.
All other samples calcined at 500°C.

(a) NH_4 Mont;
(b) Al PILMont (u);
(c) Al, Si/Al, Ni/Al PILMont;
(d) NH_4 Beid;
(e) Al PILBeid (u);
(f) Al PILBeid;
(g) SMM (u), Ni-SMM(7) (u) and Ni-SMM(21) (u);
(h) SMM and Al PILSMM;
(i) Ni-SMM(7) and Al PILNi-SMM(7);
(j) Ni-SMM(21) and Al PILNi-SMM(21).

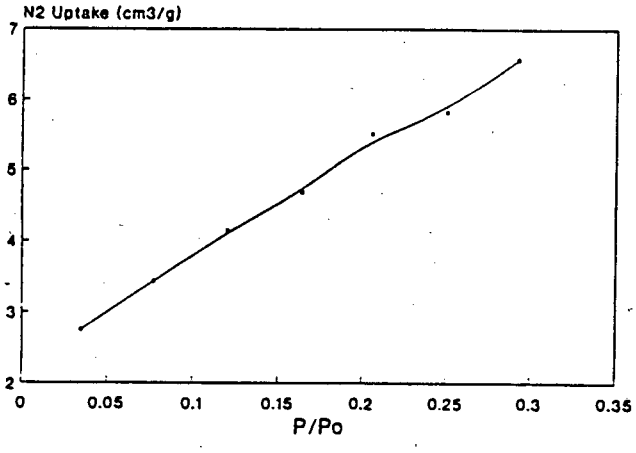

(a)

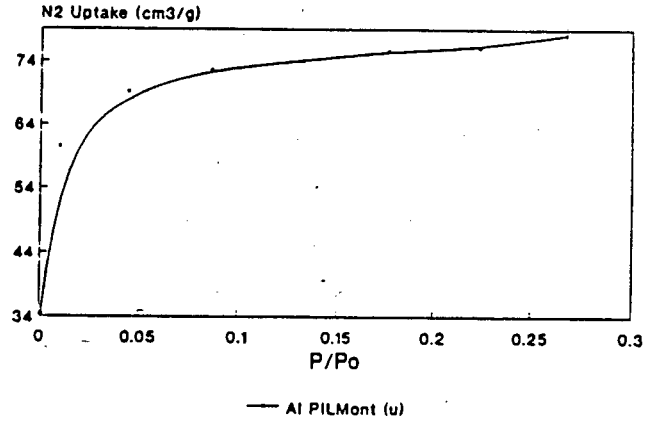

(b)

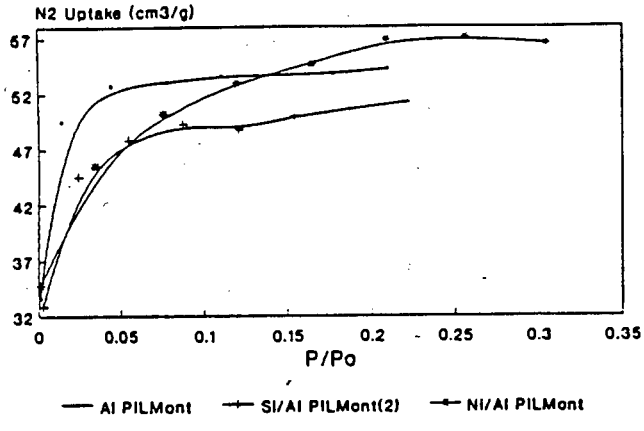
N2 Uptake (cm3/g)
57
52
47
42
37
32
0
0.05
0.1
0.15
0.2
0.25
0.3
0.35
P/Po
Al PILMont
Si/Al PILMont(2)
Ni/Al PILMont

(c)

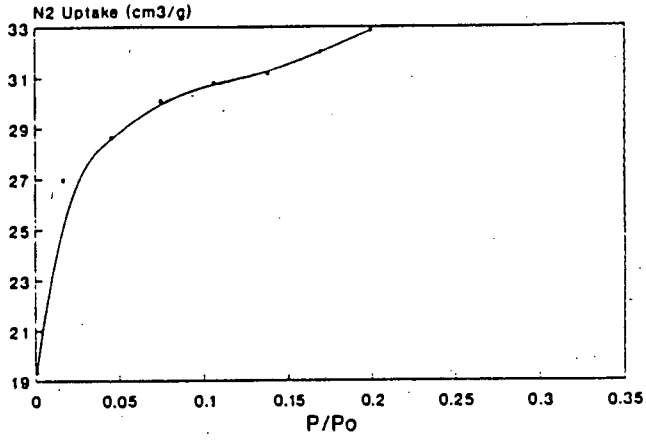
N2 Uptake (cm3/g)
33
31
29
27
25
23
21
19
0
0.05
0.1
0.15
0.2
0.25
0.3
0.35
P/Po

(d)

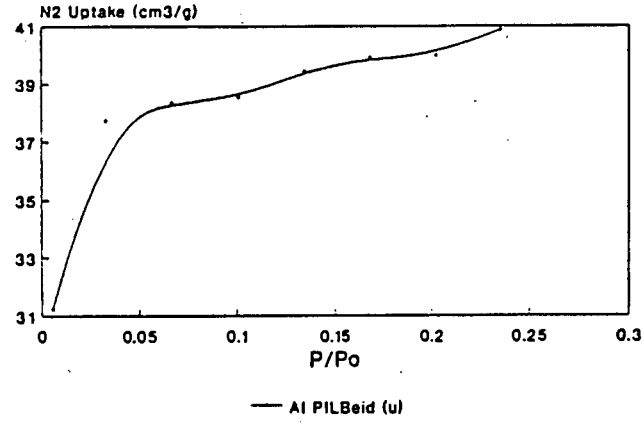
N2 Uptake (cm3/g)
41
39
37
35
33
31
0
0.05
0.1
0.15
0.2
0.25
0.3
P/Po
Al PILBeid (u)

(e)

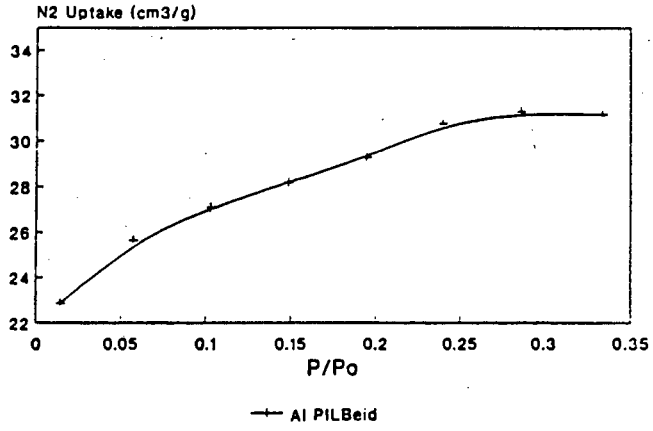
N2 Uptake (cm3/g)
34
32
30
28
26
24
22
0
0.05
0.1
0.15
0.2
0.25
0.3
0.35
P/Po
Al PILBeid

(f)

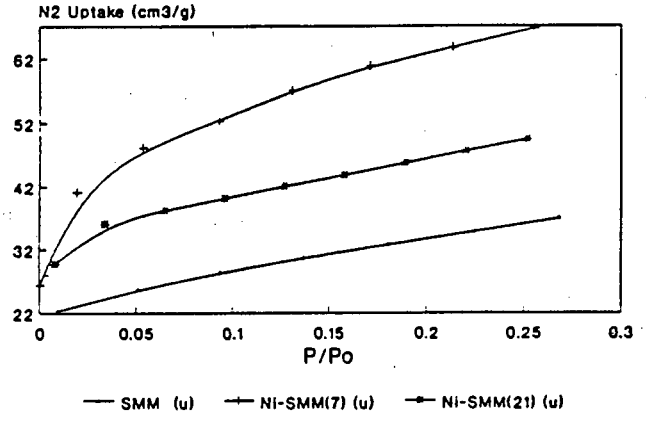
N2 Uptake (cm3/g)
62
52
42
32
22
0
0.05
0.1
0.15
0.2
0.25
0.3
P/Po
SMM (u)
Ni-SMM(7) (u)
Ni-SMM(21) (u)

(g)

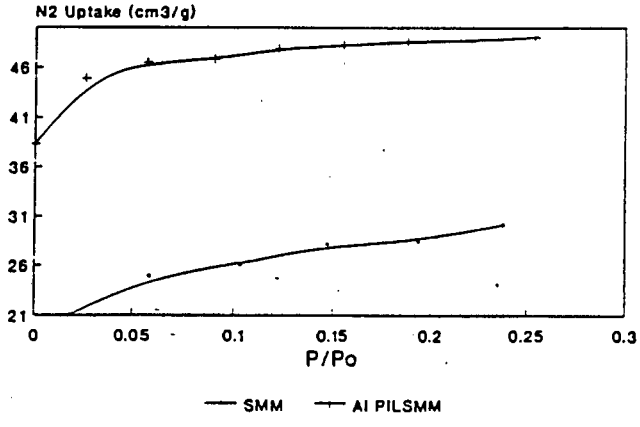
N2 Uptake (cm3/g)
46
41
36
31
26
21
0
0.05
0.1
0.15
0.2
0.25
0.3
P/Po
SMM
Al PILSMM

(h)

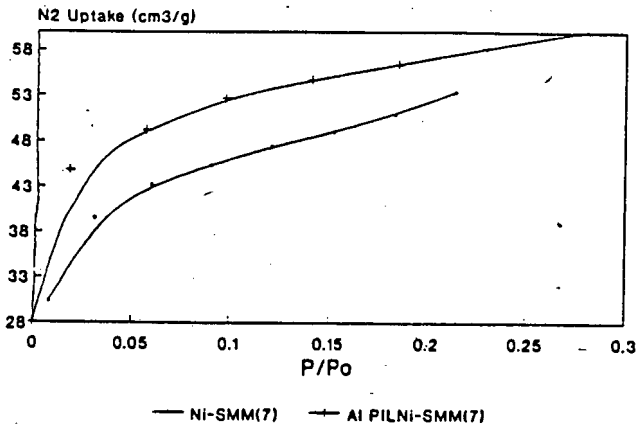
N2 Uptake (cm3/g)
58
53
48
43
38
33
28
0
0.05
0.1
0.15
0.2
0.25
0.3
P/Po
Ni-SMM(7)
Al PILNi-SMM(7)

(i)

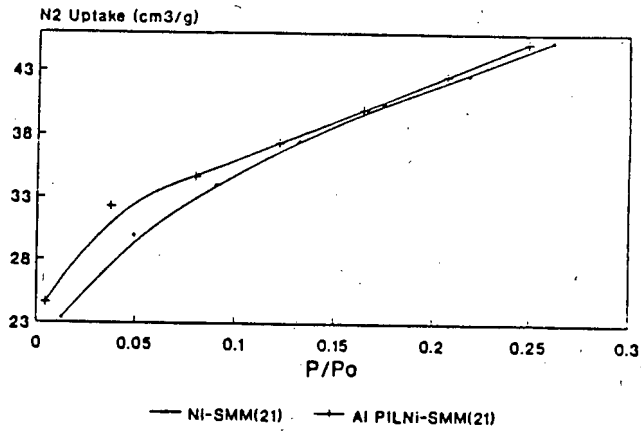
N2 Uptake (cm3/g)
43
38
33
28
23
0
0.05
0.1
0.15
0.2
0.25
0.3
P/Po
Ni-SMM(21)
Al PILNi-SMM(21)

(j)

Appendix 2(b)

N_2 Sorption Results

BET and Langmuir Isotherms of Clay Samples Not Shown in Text:

(a) Al PILMont - calcined;
(b) Si/Al PILMont(2) - calcined;
(c) Ni/Al PILMont - calcined;
(d) Al PILBeid;
(e) Al PILBeid - calcined;
(f) SMM - calcined;
(g) Al PILSMM - calcined;
(h) Ni-SMM(7);
(i) Ni-SMM(7) - calcined;
(j) Al PILNi-SMM(7) - calcined;
(k) Ni-SMM(21);
(l) Ni-SMM(21) - calcined;
(m) Al PILNi-SMM(21) - calcined.

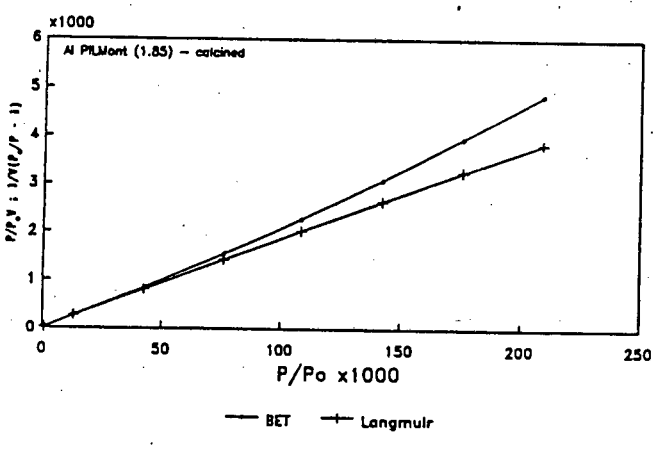

(a)

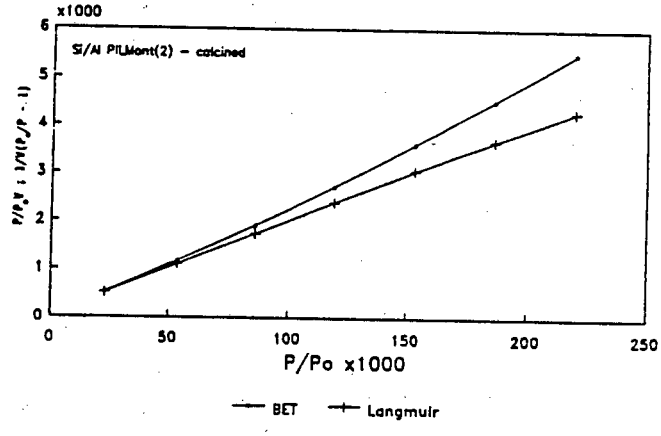

(b)

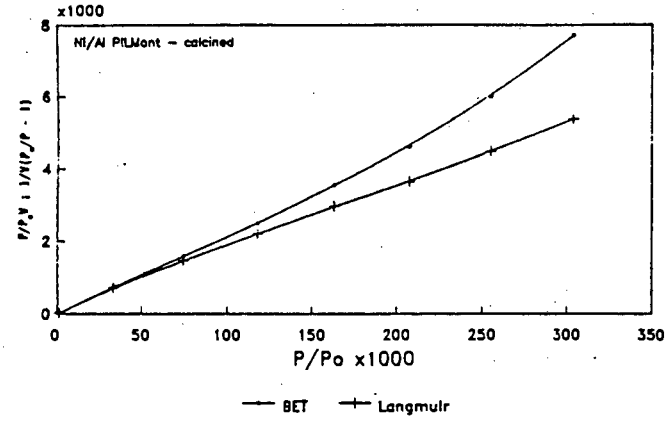
x1000
Ni/Al PILMont – calcined
P/Po x1000
BET
Langmuir

(c)

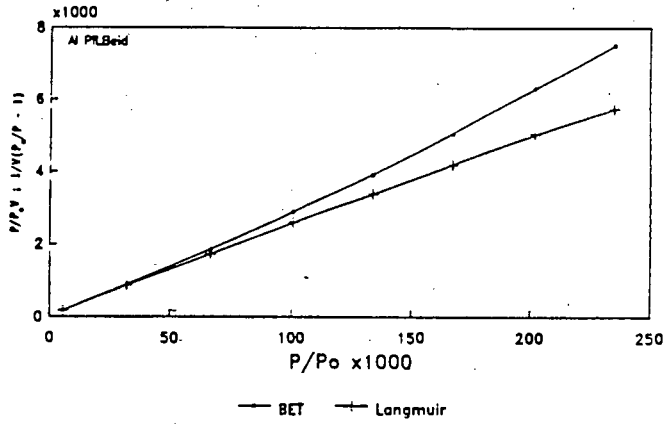
x1000
Al PILBeid
P/Po x1000
BET
Langmuir

(d)

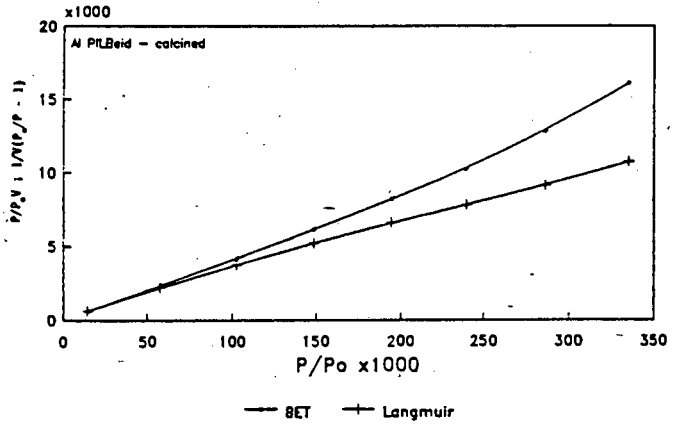
x1000
Al PILBeid – calcined
P/Po x1000
BET
Langmuir

(e)

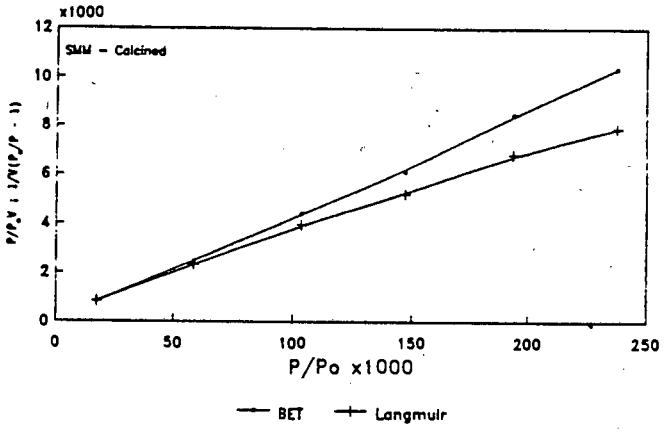
x1000
SMM – Calcined
P/Po x1000
BET
Langmuir

(f)

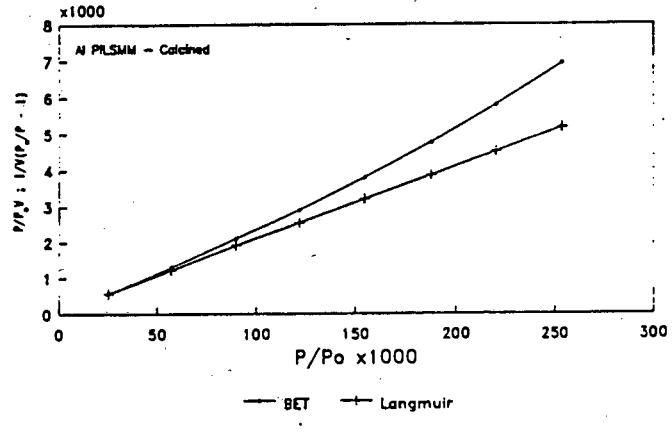
x1000
Al PILSMM – Calcined
P/Po x1000
BET
Langmuir

(g)

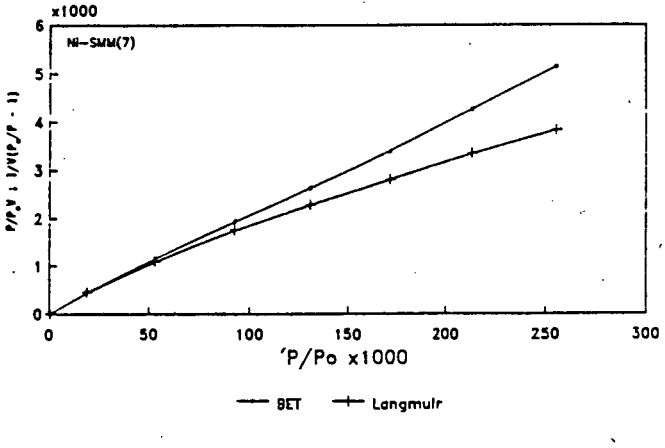
x1000
Ni–SMM(7)
'P/Po x1000
BET
Langmuir

(h)

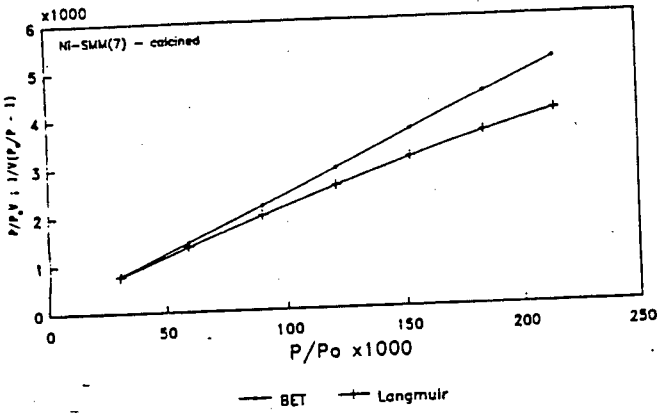
x1000
Ni-SMM(7) - calcined
P/Po x1000
BET
Langmuir

(i)

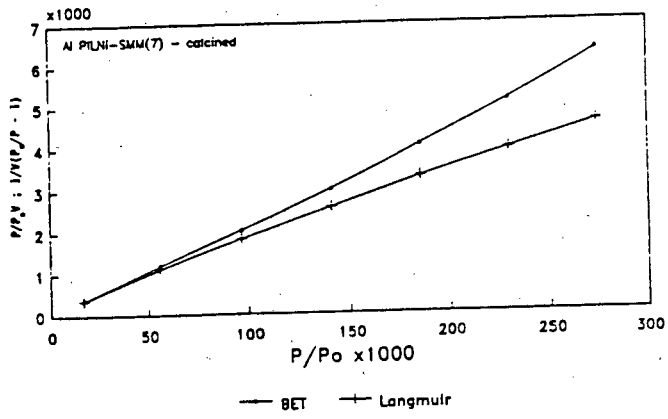
x1000
Al PtLNi-SMM(7) - calcined
P/Po x1000
BET
Langmuir

(j)

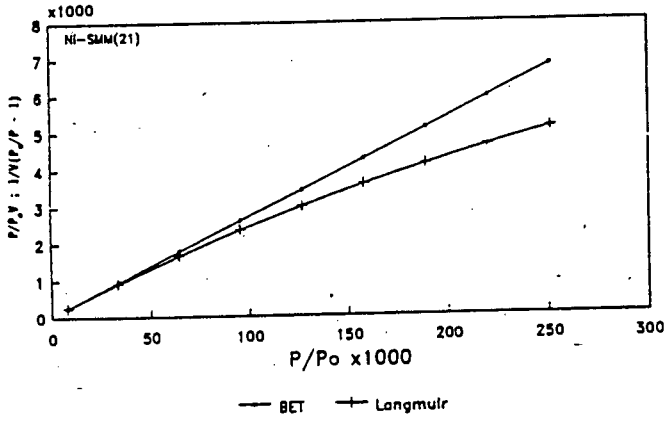
x1000
Ni-SMM(21)
P/Po x1000
BET
Langmuir

(k)

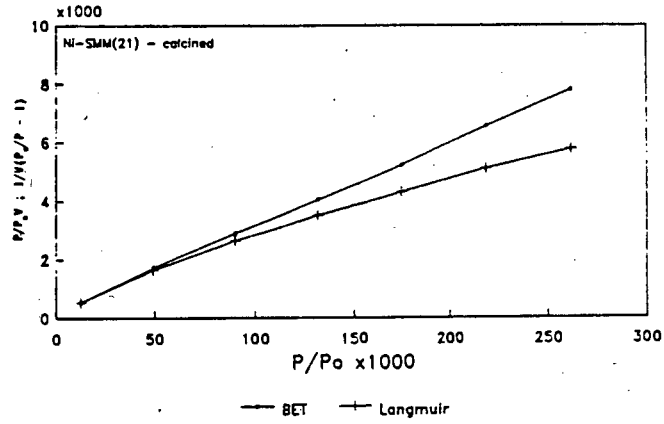
x1000
Ni-SMM(21) - calcined
P/Po x1000
BET
Langmuir

(l)

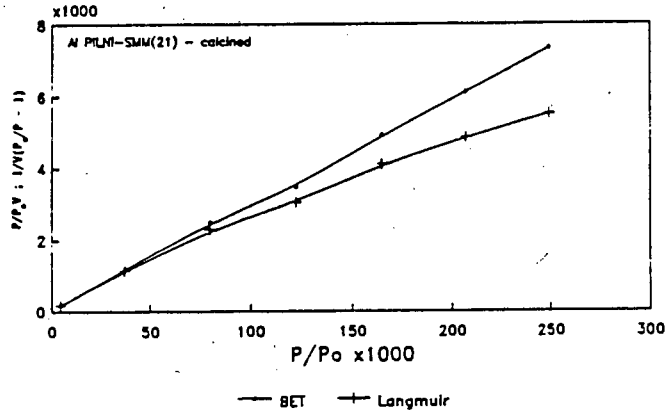
x1000
Al PtLNi-SMM(21) - calcined
P/Po x1000
BET
Langmuir

(m)

APPENDIX 3

Appendix 3(a)

Reaction of 124 Trimethylbenzene over Clay Catalysts

Tetramethylbenzene Selectivity versus Run Time:

(a) NH_3 Mont;
(b) Al PILMont;
(c) Si/Al PILMont(1) and (2);
(d) Ni/Al PILMont;
(e) NH_3 Beid and Al PILBeid;
(f) SMM and Al PILSMM;
(g) Ni-SMM(7) and Al PILNi-SMM(7);
(h) Ni-SMM(21) and Al PILNi-SMM(21);
(i) Silica Alumina.

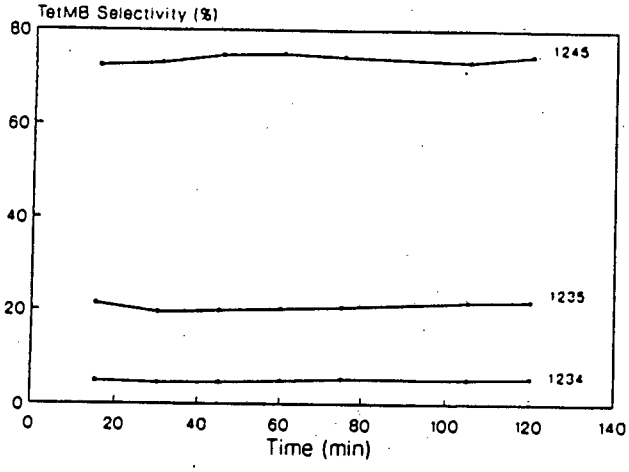

(a)

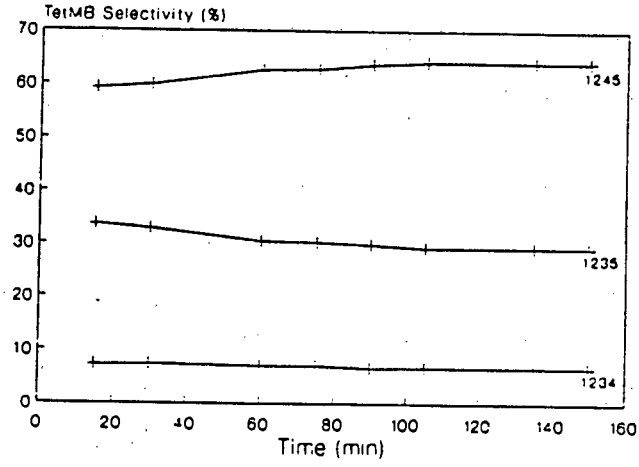

(b)

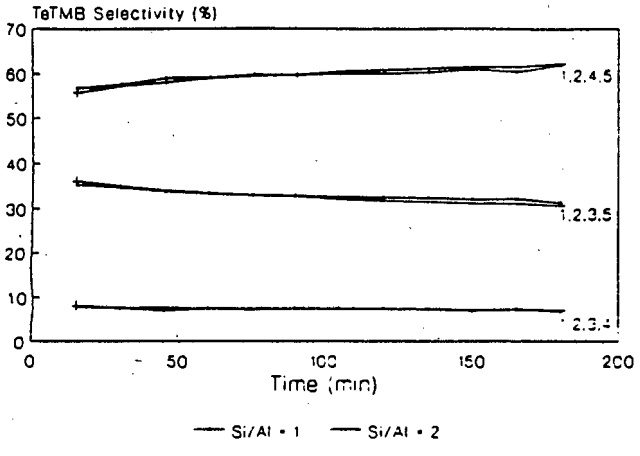
TeTMB Selectivity (%)
70
60
50
40
30
20
10
0
0
50
100
150
200
Time (min)
1,2,4,5
1,2,3,5
2,3,4
Si/Al = 1
Si/Al = 2

(c)

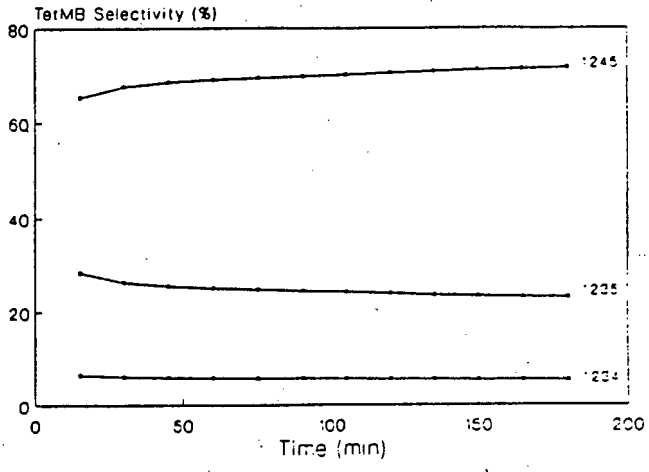
TetMB Selectivity (%)
80
60
40
20
0
0
50
100
150
200
Time (min)
1245
1235
1234

(d)

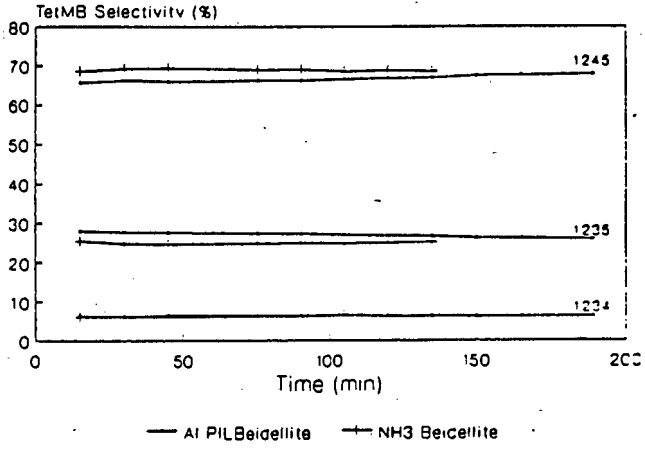
TetMB Selectivity (%)
80
70
60
50
40
30
20
10
0
0
50
100
150
200
Time (min)
1245
1235
1234
Al PILBeidellite
NH3 Beidellite

(e)

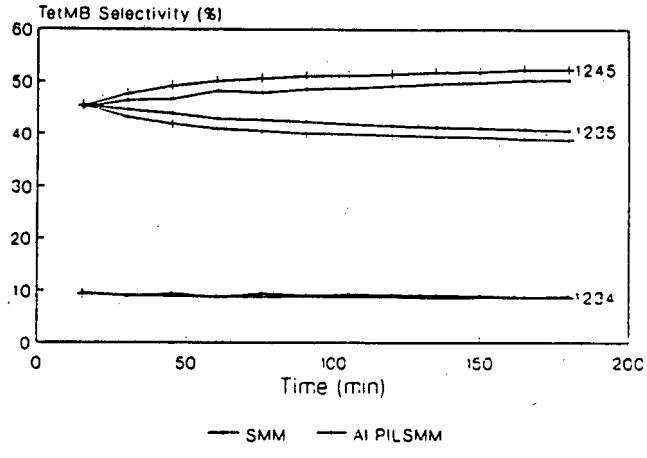
TetMB Selectivity (%)
60
50
40
30
20
10
0
0
50
100
150
200
Time (min)
1245
1235
1234
SMM
Al PILSMM

(f)

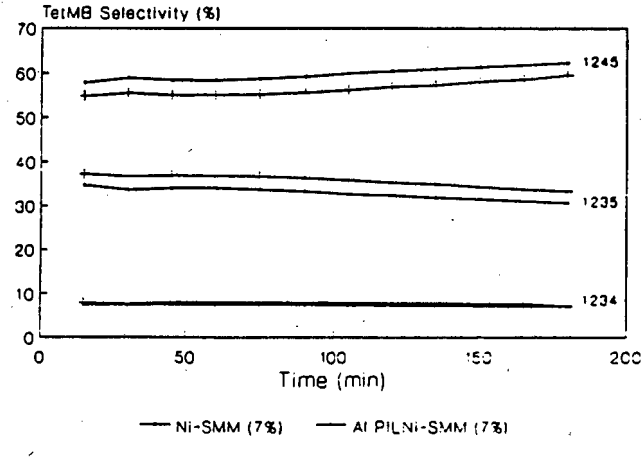
TetMB Selectivity (%)
70
60
50
40
30
20
10
0
0
50
100
150
200
Time (min)
1245
1235
1234
Ni-SMM (7%)
Al PILNi-SMM (7%)

(g)

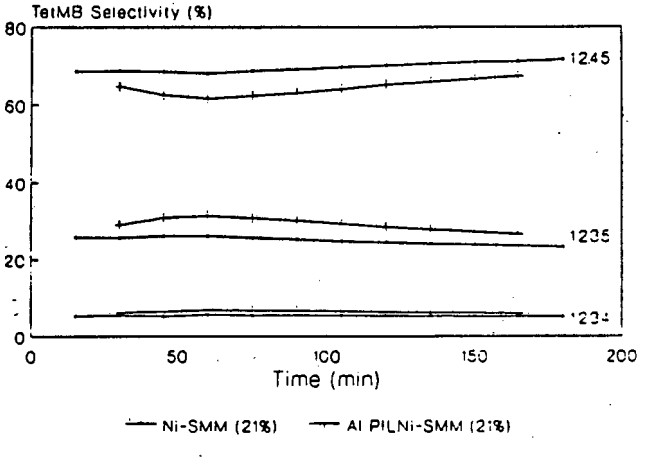
TetMB Selectivity (%)
80
60
40
20
0
0
50
100
150
200
Time (min)
1245
1235
1234
Ni-SMM (21%)
Al PILNi-SMM (21%)

(h)

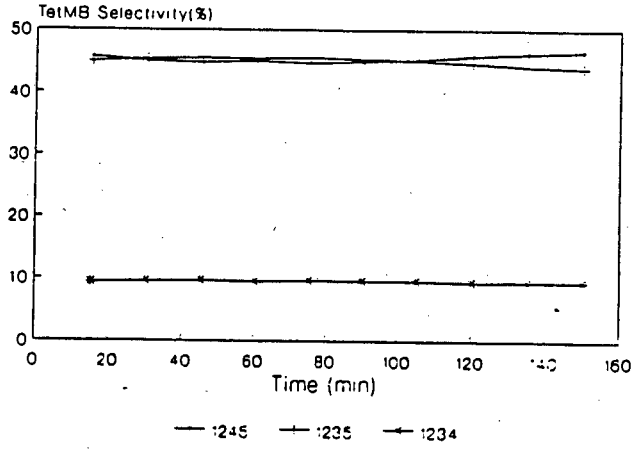
TetMB Selectivity(%)
50
40
30
20
10
0
0
20
40
60
80
100
120
160
Time (min)
1245
1235
1234

(i)

Appendix 3(b)

Reaction of 124 Trimethylbenzene over Clay Catalysts

Xylene Selectivity versus Run Time:

(a) NH_3 Mont;
(b) Al PILMont;
(c) Si/Al PILMont(1) and (2);
(d) Ni/Al PILMont;
(e) NH_3 Beid and Al PILBeid;
(f) SMM and Al PILSMM;
(g) Ni-SMM(7) and Al PILNi-SMM(7);
(h) Ni-SMM(21) and Al PILNi-SMM(21);
(i) Silica Alumina.

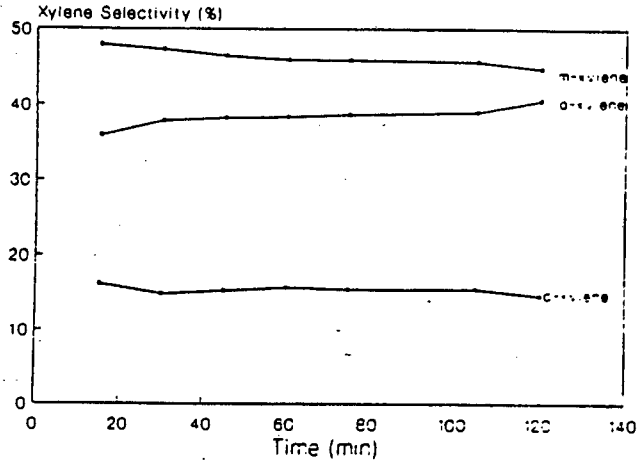

(a)

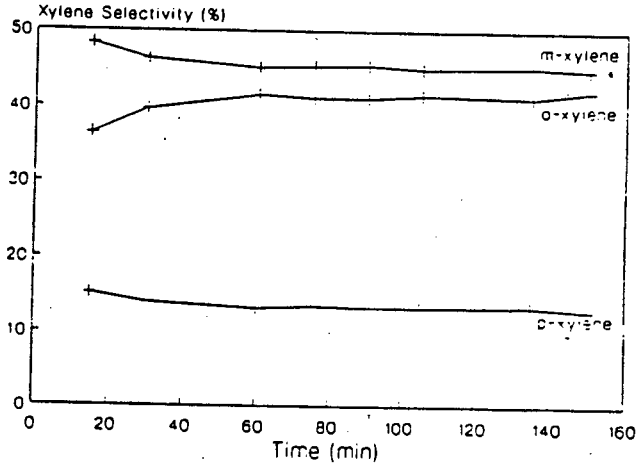

(b)

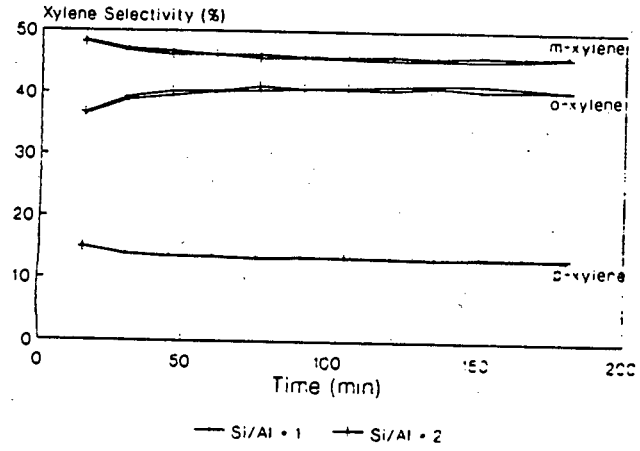
Xylene Selectivity (%)
m-xylene
o-xylene
p-xylene
Time (min)
Si/Al • 1
Si/Al • 2

(c)

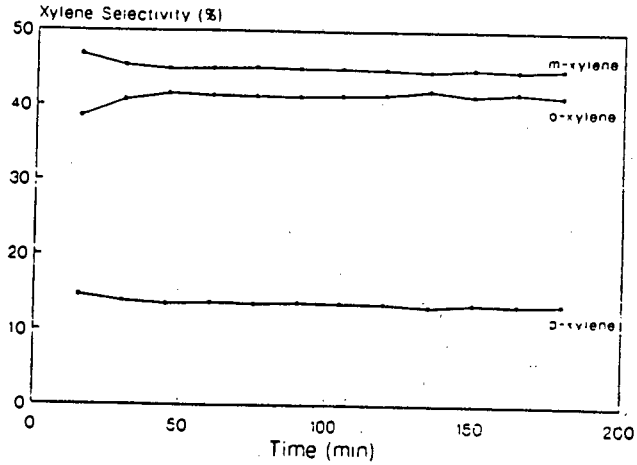
Xylene Selectivity (%)
m-xylene
o-xylene
p-xylene
Time (min)

(d)

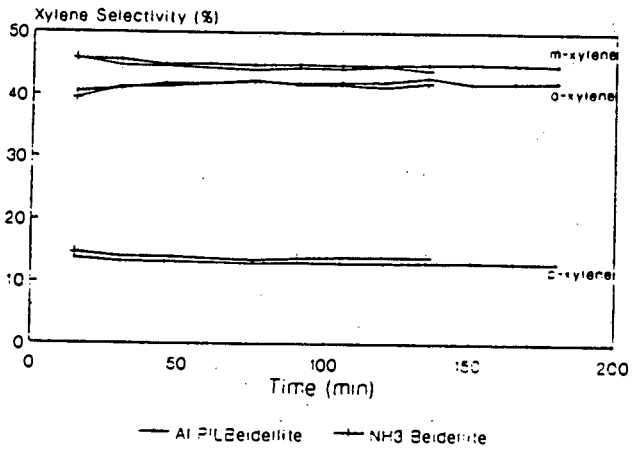
Xylene Selectivity (%)
m-xylene
o-xylene
p-xylene
Time (min)
Al PILBeidellite
NH3 Beidellite

(e)

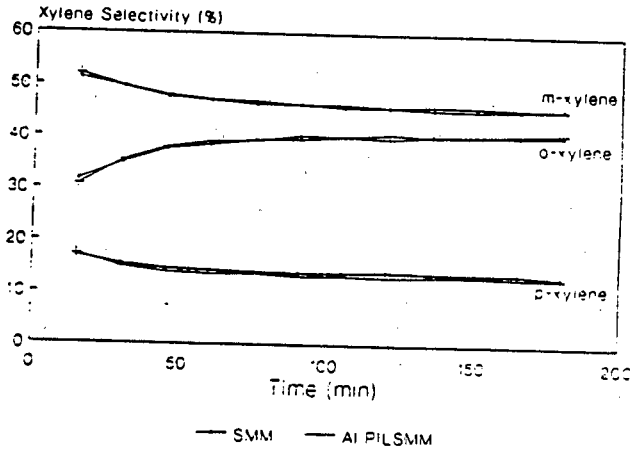
Xylene Selectivity (%)
m-xylene
o-xylene
p-xylene
Time (min)
SMM
Al PILSMM

(f)

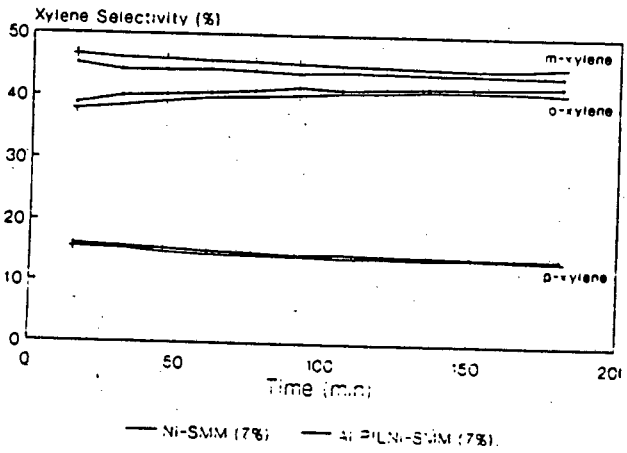
Xylene Selectivity (%)
m-xylene
o-xylene
p-xylene
Time (min)
Ni-SMM (7%)

(g)

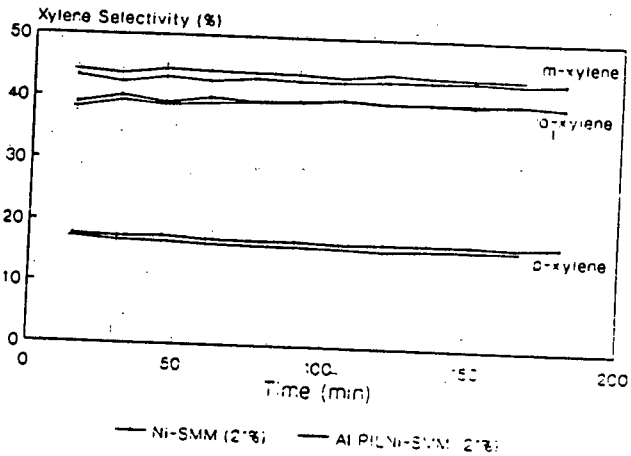
Xylene Selectivity (%)
m-xylene
o-xylene
p-xylene
Time (min)
Ni-SMM (2%)

(h)

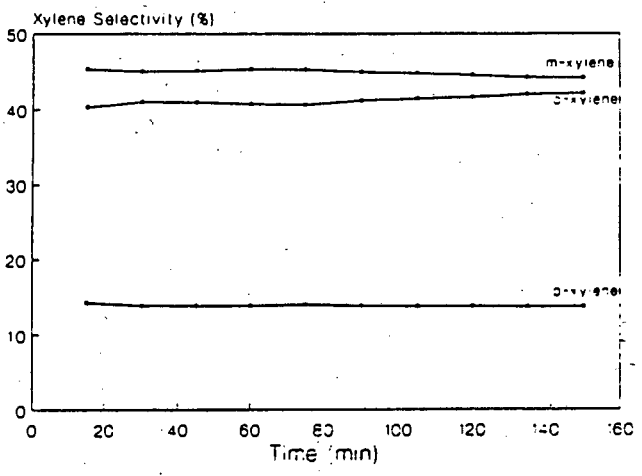
Xylene Selectivity (%)
50
40
30
20
10
0
m-xylene
0
20
40
60
80
100
120
140
160
Time (min)

(i)